THE ROLE OF AMPK IN MEDIATING RADIATON RESPONSES IN CANCER

THE ROLE OF AMP-ACTIVATED PROTEIN KINASE (AMPK) IN MEDIATING RADIATION REPONSES IN CANCER CELLS

By TORAN SANLI, B.Sc., M.Sc.

A Thesis Submitted to the school of Graduate Studies in Partial Fulfillment of the Requirements for the Degree Doctor of Philosophy

McMaster University DOCTOR OF PHILOSPHY (2012) Hamilton, Ontario (Medical Science)

TITLE: The role of AMP-activated protein kinase (AMPK) in mediating radiation responses in cancer cells

AUTHOR: Toran Sanli, B.Sc. (*Honours with 1st Class Standing*) (Brock University), M.Sc. (Brock University)

SUPERVISOR: Professor Gurmit Singh, Ph.D.

NUMBER OF PAGES: v, 273

Abstract

One of the hallmark features of cancer is altered metabolism, whereby rates of glucose and fatty acid turnover are constitutively elevated to support uncontrolled propagation. The key regulator of energy metabolism is the enzyme AMP-activated protein kinase (AMPK), which suppresses anabolic pathways that increase proliferation and enhanced catabolic pathways that liberate energy, all in an attempt to maintain energy homeostasis in the cell. In addition to regulating metabolism, AMPK has also been implicated as a tumour suppressor and we have suggested that it may be a modulator of radiation responses in cancer cells *in vitro*. Moreover, we investigated the molecular mechanisms that facilitate ionizing radiation (IR)-induced AMPK activation, as well as demonstrated that certain AMPK activating drugs can work as radiation sensitizers in a variety of cancer cell lines. Stemming from this framework, we also provided experimental evidence that suggests AMPK is centrally involved in pathways that regulate DNA damage and proliferation at the basal level, and in response to IR. One of the targets involved in these pathways that can also influence AMPK regulation is the stress-activated Sestrin 2 protein. We have provided evidence that Sestrin 2 mediates IR-induced activation and expression of AMPK. Taken together, this work has provided novel insight into the ability of IR to modulate the activity and expression of AMPK, which in turn is required to facilitate the appropriate stress-response in cancer cells. Given its emerging interest in the cancer field, AMPK may become an important biomarker for evaluating clinical outcomes in patients undergoing radiation therapy.

Preface

This doctoral work has been prepared as a "sandwich" Ph.D. thesis, and consists of four manuscripts, all of which have now been published, or accepted for publication. Many of the experimental protocols were oriented around the general focus on AMPK signalling in response to ionizing radiation, and as such, the reader may encounter some repetition in experimental design between articles. Following the introduction and background information, each paper is presented as a separate chapter that highlights a particular theme within the overall framework of the thesis. Supporting, unpublished data may also be included following each paper to strengthen the materials and objectives of each individual study. The figures are denoted so that the chapter number is indicated first, followed by the actual figure number that corresponds to the appropriate paper (e.g. Figure 1 for chapter 2 is labeled as **Figure 2.1**).

The last chapter will contain a conclusion that will summarize the major findings of the author's thesis, as well as provide future directions to expand on this work. References contained within the body of the sandwich thesis are formatted in accordance to the journal in which they were published. Literature cited within the introduction and conclusion of the thesis will adhere to the American Psychological Association (5th edition) style, with the bibliography of references appearing at the end of the dissertation. Additional information pertaining to general methodologies and supporting experiments are provided in Appendix 1 and 2 respectively.

Acknowledgements

I would like to thank my supervisor, Dr. Gurmit Singh, for his guidance and support of my research project throughout the years. I would also like to acknowledge and thank Dr Theodoros Tsakiridis for initially taking me on as a graduate student and exposing me to the translational work with AMPK and radiotherapy at the Juravinski Cancer Centre (JCC). Dr. Tsakiridis has been a long-time mentor throughout my graduate training at both the Master's and Doctoral level. In addition, Dr. Hal Hirte is also a member on my committee and has provided helpful feedback throughout my training.

I would also like to thank the kind and supportive staff and graduate students at the JCC. The input and feedback from the many members of our lab has greatly aided me with my research projects and has contributed to my knowledge and experience as a scientist. I am greatly indebted to Dr. Katja Linher-Melville, who has help train me in many aspects of basic cell biology, as well as contribute to a couple of our published papers. Helpful advice was also given by Dr. Eric Seidlitz, who is knowledgeable in all aspects of research conducted at the JCC. Sarah Hopmans and Yaryna Storozhuk also aided me in conducting experiments, as well as the radiation therapy staff at the JCC.

Importantly, I would like to thank my family for their continued support of my ongoing education. My parents have always encouraged me to have high academic standards, and it is from them where I have gained my strong work ethic. Equally essential is the love and support of my wife, Elizabeth, whom I can confide in and look to for guidance as a fellow graduate student. My goal is to now put this Ph.D degree to good use to benefit society and provide for our future.

Table of Contents

List of Diagrams, Figures, and Tables

List of Abbreviations

4E-BP1	Eukaryotic Initiation Factor 4E Binding Protein 1
ACC	Acetyl Coenzyme-A Carboxylase
ADP	Adenosine diphosphate
AICAR	5-aminoimidazole-4-carboxamide riboside
AIS	Auto-Inhibitory Sequence
ANOVA	Analysis of variance
AMP	Adenosine monophosphate
AMPK	AMP-Activated Protein Kinase
AMPK-/-	AMP-Activated Protein Kinase α1/α2 Knockout
ASC	Associated with SNF1 Kinase
AT	Ataxia Telangiectasia
ATCC	American Type Culture Collection
ATM	Ataxia Telangiectasia Mutated
ATP	Adenosine Triphosphate
ATR	Ataxia Telangiectasia and Rad3 Related
β-SID	Beta Subunit Interacting Domain
BER	Base Excision Repair
Ca^{2+}	Calcium Ion
CaMKK	Calmodulin-Dependent Protein Kinase Kinase
CBM	Carbohydrate Binding Module
CBS	Cystathionine Beta Synthase
CC	Compound C
CC3	Cleaved Caspase 3
CDK	Cyclin-Dependent Kinase
CDKI	Cyclin-Dependent Kinase Inhibitor
Chk 1/2	Check Point Kinases 1/2
CPT-1	Carnitine-Palmitoyl Transferase-1
^{60}Co	Cobalt Radiotherapy Unit
$C0_2$	Carbon Dioxide
DMEM	Dulbecco's Modified Eagle's Medium
DMSO	Dimethyl Sufoxide
DNA	Deoxyribonucleic Acid
DNA-PK	DNA Protein Kinase
DSB	Double Strand Break
dSesn	*Drosophila* sestrin
EEF2K	Eukaryote Elongation Factor 2 Kinase
EGF	Epidermal Growth Factor
EGFR	Epidermal Growth Factor Receptor
ERK	Extracellular Signal-Regulated Kinase
FAS	Fatty Acid Synthase
FBS	Fetal Bovine Serum

FAD	Flavin Adenine Dinucleotide
FoxO	Forkhead Family of Transcription Factor
GADD	Growth Arrest and DNA Damage Gene
Gy	Gray
H2AX	Histone H2A Family Member
H+	Hydrogen Ion
HIF-1α	Hypoxia-Inducible Factor-1α
HR	Homologous Recombination
HMG-CoA	Hydroxy-3-Methyl-Glutaryl-CoA Reductase
IGF-I	Insulin-like Growth Factor-I
IR	Ionizing Radiation
JNK	c-Jun N-terminal Kinase
KIS	Kinase Interaction Sequence
LDH-A	Lactate Dehydrogenase
LDL	Low-Density Lipoproteins
LKB1	Liver Kinase B1
NAD+	Nicotinamide Adenine Dinucleotide
NTCP	Normal Tissue Complication Probability
MAPK	Mitogen-Activated Protein Kinase
MAPKKK	Mitogen-Activated Protein Kinase Kinase Kinase
MEF	Mouse Embryo Fibroblasts
MMR	Mismatch Repair
MO25	Scaffolding Mouse 25 Protein
MRE11	Meiotic Recombination 11
mSIN1	Mammalian Stress-Activated Protein Kinase Interacting Protein 1
mTOR	Mammalian Target of Rapamycin
NBS1	Nijmegen Breakage Syndrome 1
NER	Nucleotide Excision Repair
NHEJ	Non-Homologous End-Joining
PBS	Phosphate Buffered Saline
PFK	Phosphofructokinase
PGC 1α	Peroxisome Proliferator-Activated Receptor Gamma Coactivator 1-Alpha
Pi	Phosphate Group
PI	Propidium Iodide
PI3K	Phosphoinositide-3 Kinase
PIKK	Phosphoinositide 3-Kinase Related Protein Kinase
PIP	Phosphatidylinositol/Phosphoinositide Phosphate
PTEN	Phosphate and Tensin Homolog
PVDF	Polyvinylidene Difluoride
TBS	Tris Buffered Saline
TBS-T	Tris Buffered Saline-Tween 20
Rb	Retinoblastoma Protein

ROS	Reactive Oxygen Species
RPMI	Roswell Park Memorial Institue Media
RT	Radiotherapy
S6K	p70-S6 Kinase
SDS	Sodium Dodecyl Sulfate
SDS-PAGE	SDS-Polyacrylamide Gel Electrophoresis
SESN	Sestrin
Sesn2F	Sestrin2 Flag-Tagged Vector
SF2	Survival Fraction after 2Gy
siRNA	Small Interference RNA
SSB	Single Strand Break
STRAD	Ste20-Related Adaptor Protein
TCA	Tricarboxylic Acid Cycle
TAK1	Transforming Growth Factor β Activated Kinase
TCP	Tumour Control Probability
Tet-OFF SESN2	Tetracycline-Inducible SESN2 Cells
TSC	Tuberous Sclerosis Complex
ULK1	Unc-51-Like Kinase 1
WT	Wild Type

Chapter 1: Introduction

Cellular Energy Metabolism

The sustained survival and function of a living cell is dependent on the dynamic regulation of energy metabolism. Efficient metabolism is comprised of a highly complex series of chemical reactions that are organized into specific metabolic pathways that produce high energy compounds, including nicotinamide adenine dinucleotide (NAD+), flavin adenine dinucleotide (FAD), and adenosine triphosphate (ATP) (Campbell & Farrell, 2011). Energy in the form ATP can be generated from the breakdown of simple and complex sugars (carbohydrates), as well as fats and protein. This process requires that these substrates be broken down into simpler components, where carbohydrates can be hydrolysed into glucose, fats can be converted into glycerol or fatty acids, and protein into amino acids (Campbell & Farrell, 2011).

Glucose is one of the most readily available forms of energy that can be utilized through two distinct metabolic pathways, through glycolysis, which can occur independently of molecular oxygen, or through oxidative phosphorylation via the Krebs cycle, which does require oxygen (Lunt & Vander Heiden, 2011). Glycolysis occurs in the cytoplasm and can metabolize glucose to pyruvate, which can further be reduced to lactate or ethanol, a process known as fermentation. The free energy generated from this process can quickly generate 2 molecules of ATP per molecule of glucose (Campbell & Farrell, 2011). On the other hand, in the presence of oxygen pyruvate can also enter the mitochondria and get converted into Acetyl CoA to initiate the Krebs cycle (also known as the tricarboxylic acid (TCA) or citric acid cycle). The Krebs cycle was initially

described by the German biochemist Hans Krebs as a series of multi-step redox reactions within the mitochondria that generates a high yield of ATP, as well as CO_2 (Lunt & Vander Heiden, 2011). The complete oxidation of one molecule of glucose through the Krebs cycle efficiently produces 36 molecules of ATP (Weinberg & Chandel, 2009).

To a similar extent fatty acids can also be metabolized through the Krebs cycle to generate ATP. This procedure requires that the fatty acids be transported to the mitochondrial membrane by carnitine-palmitoyl transferase-1(CPT-1), which is then shuttled across the inner mitochondrial membrane by carnitine (Campbell & Farrell, 2011). Once the fatty acids have entered the mitochondria they undergo beta oxidation by being converted into acetyl CoA. The rate-limiting step for the beta oxidation of fatty acids is CPT-1, which can be mutated in cancer (Lunt & Vander Heiden, 2011). Conversely, proteins can be broken down into amino acids, which can further be oxidized into urea and CO_2 to generate ATP, or be utilized as intermediate substrates in the Krebs cycle.

Energy Metabolism in Cancer Cells

One of the hallmarks of cancer is that these cells exhibit altered metabolism compared to normal tissue. To support their rapid proliferation, cancer cells utilize nutrients such as glucose and fatty acids at a much higher rate than normal cells (Weinberg & Chandel, 2009). Interestingly, malignant cells also predominantly metabolize glucose through glycolysis rather than oxidative phosphorylation, even in the presence of an oxygen-rich environment. This observation was first made in the 1920's by Otto Warburg, who noted that tumour slices consume glucose at high rates through

aerobic glycolysis, a phenomenon called the "Warburg effect" (Warburg, Wind, & Negelein, 1927). Warburg hypothesized that this shift in glucose metabolism from oxidative phosphorylation to glycolysis was due to a dysfunctional mitochondrial phenotype in the cancer cells (Figure 1). However, recent studies have indicated that most tumour cells have fully functioning mitochondria (Fantin, St-Pierre, & Leder, 2006; Moreno-Sanchez, Rodriguez-Enriquez, Marin-Hernandez, & Saavedra, 2007), pointing to a different role for glycolysis in supporting cancer proliferation.

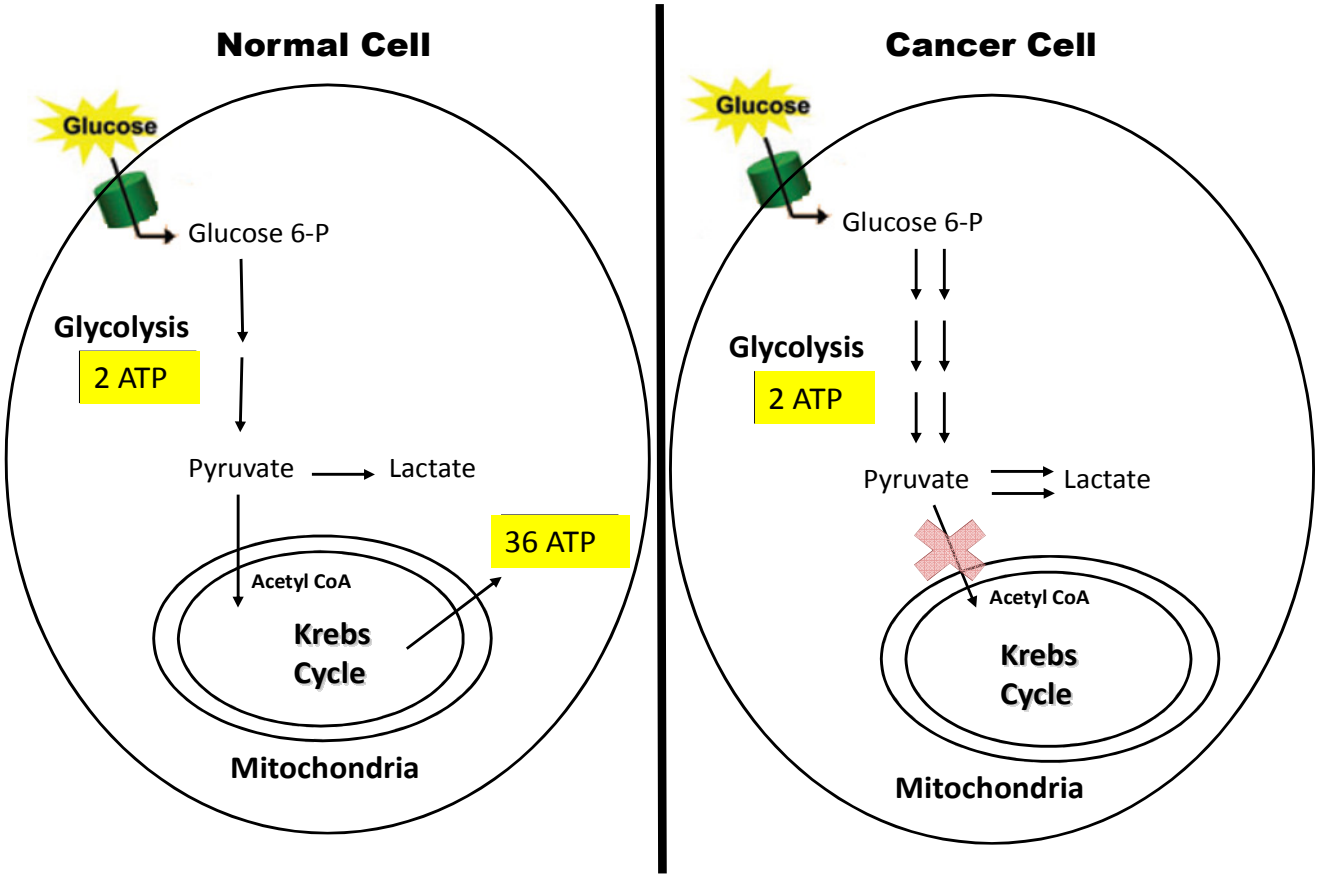

Figure 1.1: Diagrammatic representation of the Warburg effect. The double arrows indicate the preferential pathway for glucose metabolism in cancer cells. The red "X" implies that the mitochondria in cancer cells may be damaged (according to Warburg).

One explanation for the preferential use of glycolysis to obtain energy in cancer cells is the fact that fermentation (pyruvate → lactate + ATP) occurs at a rate of approximately 100 times faster than oxidative phosphorylation (Bartrons & Caro, 2007). On average, this would yield roughly 18 times more ATP per mole of glucose than the Krebs cycle would generate in the same amount of time (Bartrons & Caro, 2007). Additionally, elevated rates of glycolysis in cancer also provide these cells with the glycolytic building-blocks (nucleotides, amino acids, and lipids) required for sustained macromolecule biosynthesis that are essential for cell division (Shaw, 2006).

Another possible explanation for the glycolytic phenotype observed in cancer is that tumours often undergo periods of hypoxia, where their high rates of metabolism outstrip the nutrient supply from the surrounding environment. As such, the transcription factor hypoxia-inducible factor-1α (HIF-1α) is upregulated. HIF-1α is a key regulator of several genes implicated in glycolysis including glucose transporters and lactate dehydrogenase (LDH-A), the enzyme that converts pyruvate into lactate (Gatenby & Gillies, 2004). Thus, glycolysis may be an adaptation to hypoxic conditions in the tumour-environment that may promote a positive-feedback loop of fermentation through enhanced HIF-1α expression. Moreover, metabolic byproducts of lactate formation, such as hydrogen ions (H+), cause a chronic acidification of the surrounding environment that may favor malignant cell survival (Bartrons & Caro, 2007). Whereas extended exposure of normal cells to an acidic microenvironment will trigger apoptosis through a p53-dependent mechanism, most cancer cells have mutated p53 and can withstand lower pH levels, thereby selecting for the malignant transformation of cells.

Cancer cells also rely on high rates of *de novo* lipid synthesis to support their proliferation (Hatzivassiliou et al., 2005). To support this increase in lipid generation, tumours can adapt their metabolism towards the utilization of citrate as a precursor for fatty acid and cholesterol synthesis. Normally, citrate is generated as a Krebs cycle intermediate when pyruvate enters the mitochondria and gets converted to acetyl CoA. Citrate is created by the oxidation of acetyl CoA, which is then converted into oxaloacetate to carry out the full oxidation of glucose through the Krebs cycle (Gatenby & Gillies, 2004). However, citrate can also exit the mitochondria and be exported to the cytosol where it can re-generate acetyl CoA as the rate-limiting step for *de novo* lipid biosynthesis. Malignant cells exploit this process of citrate metabolism, using it as an end-product for lipid synthesis, causing a truncation in the Krebs cycle (Hatzivassiliou et al., 2005). Taken together, cancer cells exhibit multiple alterations in substrate metabolism to support their uncontrolled growth and proliferation.

Regulating Energy Balance and the Identification of AMPK

In light of the multiple pathways that regulate metabolism through various substrates, it should be emphasized that ATP is the major energy currency of the cell. Structurally ATP consists of three phosphate groups attached to an adenine ring and a ribose sugar (adenosine). The phosphate groups bound to ATP are “high energy” bonds that can by hydrolyzed, yielding adenosine diphosphate (ADP) or adenosine monophosphate (AMP), to provide energy for the cell to do work (Hardie & Hawley, 2001). The reactions that interconvert ATP, ADP, and AMP nucleotides and the required

enzymes to facilitate these reactions are as follows (adapted from Hardie & Hawley, 2001):

(1) ATP → ADP + Pi	ATPase
(2) ATP → AMP +PPi	Ligases
(3) ADP + Pi → ATP	ATP synthases
(4) 2ADP + Pi ←→ ATP + AMP	Adenylate kinase

where Pi is equal to a phosphate group and the arrows indicate which way the enzyme drives the chemical reaction (Hardie & Hawley, 2001). The concentrations of these nucleotides in the cell are analogous to the charge on a cell phone battery. The cellular "battery" is charging up when it is undergoing catabolic processes that generate ATP (reaction 3), such as utilizing nutrients following a meal. Conversely, the cell "battery" gets drained when performing the majority of metabolic processes that convert ATP to ADP (reaction 1) or AMP (reaction 2). Given the vital role of the cell to maintain the appropriate ratios of ATP:ADP and ATP:AMP, it comes as no surprise that specific molecular mechanisms have evolved to modulate the levels of these nucleotides. Through intense scientific investigation, AMP-activated protein kinase (AMPK) has emerged as the "master regulator" of the ATP:AMP ratio (Hardie, 2011; Steinberg & Kemp, 2009).

AMPK was initially identified in the 1970's as a molecule that could inhibit 3-hydroxy-3-methyl-glutaryl-CoA reductase (HMG-CoA) and acetyl CoA carboxylase (ACC1 and ACC2), which are molecules important in fatty acid synthesis (Carlson & Kim, 1973). However, the name AMPK was not adopted until the late 1980's when Carling et al. (1987) determined that a single protein kinase was responsible for the

phosphorylation and inactivation of both HMG-CoA and ACC in response to rising AMP levels (Carling, Zammit, & Hardie, 1987). Hence AMPK was branded after its allosteric activator, the nucleotide AMP, which is mainly generated by the adenylate kinase reaction (reaction 4) *in vivo*.

AMPK Structure and Function

AMPK is a heterotrimeric serine/threonine protein kinase that is conserved across all eukaryotes, including fungi, plants, and animals. The only exception is the obligatory intracellular parasite *Encephalitozoon cuniculi*, which relies on host AMPK to regulate energy status (Hardie, Carling, & Gamblin, 2011). AMPK defends cells against physiological and pathological stress stimuli, including starvation, heat shock, hypoxia, and exercise that lowers the ATP:AMP ratio by shifting metabolism to ATP generation, while systematically blocking energy expenditure (Oakhill, Scott, & Kemp, 2009). Since AMPK is the focus of this thesis, an overview of this kinase is provided in the introduction, with similar discussion found throughout subsequent chapters.

The AMPK Subunits

Structurally, AMPK contains multiple subunit isoforms, which include two α-subunits (α1-2), two β-subunits (β1-2), and three γ-subunits (γ1-3), that allow for up to 12 heterotrimeric AMPKαβγ combinations in mammals (Hardie, 2011). The genes that encode each AMPK subunit are named PRKA, followed by its subunit identifier, A1-2 for α-subunits, B1-2 for β-subunits, and G1-3 for γ-subunits. In addition, these genes are dispersed across different chromosomes: α1 (5p12), α2 (1q31), β1 (12q24.1), β2 (1q21.1), γ1 (12q12-14), γ2 (7q35-36), and γ3 (2q35) (Steinberg & Kemp, 2009).

In terms of sequence homology, the AMPK α1 and α2 subunits are very similar (~550 residues). Both α-subunits have conserved NH_2-terminal catalytic domains, followed by an auto-inhibitory domain, and divergent COOH-terminal tails (Figure 2) (Oakhill et al., 2009). The AMPK β1 and β2 subunits consist of approximately 270 residues, and with the exception of the first 65 residues, are also highly conserved. On the other hand, the AMPK γ1, γ2, and γ3 subunits vary in sequence length and NH_2-terminus. Beyond this though, the γ-subunits share a conserved COOH-terminal region of approximately 300 residues that contain four cystathionine beta synthase (CBS) domains that are important in binding nucleotides (ATP, ADP, and AMP) (Oakhill, et al., 2009).

The catalytic α-subunit of AMPK (63kDa) consists of a kinase domain at the N-terminus, followed by a regulatory domain that contains an auto-inhibitory sequence (AIS), and a subunit interacting domain (β-SID) that binds to the β-subunit at the C-terminus (Figure 2) (Hardie & Hawley, 2001). Phosphorylation of AMPKα on its conserved Thr172 residue within the activation loop is required for full enzyme activity. The regulatory β-subunit of AMPK acts as a scaffold on which the α and γ-subunits can bind. There are two conserved regions on the β-subunit known as the kinase interaction sequence (KIS) and the associated with SNF1 kinase (ASC, the yeast orthologue of AMPK), where the subunits can assemble respectively (Steinberg & Kemp, 2009). The β-subunit also contains a mid-molecule glycogen binding domain, known as the carbohydrate binding module (CBM) that metabolizes starch and glycogen. The role of the CBM is still being elucidated, but it may aid in the localization of AMPK to downstream substrates that also bind glycogen, such as glycogen synthase (Jorgensen et

al., 2004). In addition, the AMPK β1-subunit can undergo post-translational modification by myristoylation and phosphorylation of its Ser108 residue, which is required for AMPK localization and activity (Figure 2) (Oakhill et al., 2010). Myristoylation is a frequently used method of post-translational modification via the addition of myristic acid to the N-terminus of proteins, which in turn, acts as a lipid anchor to secure signalling molecules to membranes. In the case of the AMPK, myristoylation of the β-subunit is absolutely essential to initiate AMPK activation in response to AMP (Oakhill et al., 2010).

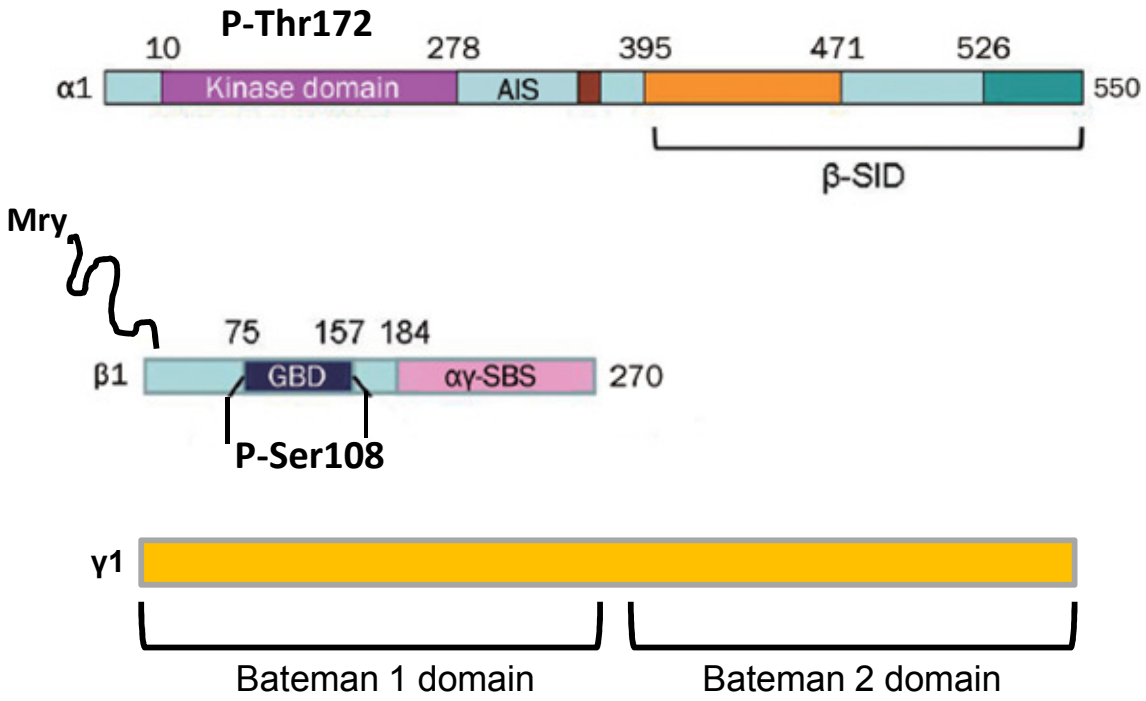

Figure 1.2: The characteristics of the AMPK subunits (modified from Shirwany & Zou, 2010). The numbers associated with the AMPK α1 and β1 subunits indicate the number of residues. P-Thr172 and P-Ser108 highlight the phosphorylation sites on the AMPK subunits that are associated with its activation. ***AIS***: auto inhibitory sequence, ***β-SID***: β-

subunit interacting sequence, ***Mry***: myristoylation ***GBD***: glycogen binding domain, and ***αγ-SBS***: α and γ subunit interacting sequence.

The four tandem CBS repeats of the γ-subunit of AMPK were initially defined by Bateman (1997) who observed that these repeats occur as two pairs of domains, known as Bateman domains (Figure 2) (Bateman, 1997). These domains are congregated together in a pseudosymmetrical manner, such that there are four clefts where adenine nucleotides such as ATP, ADP, and AMP can bind (site 1, site 2, site 3, and site 4). Interestingly, only three of these sites on AMPKγ actually bind adenine nucleotides, with one site (site 2) always remaining unoccupied. Moreover, site 4 of AMPKγ associates with AMP very tightly, and does not exchange with ATP or ADP. Thus, the ability of AMPK to sense cellular energy status is dependent on sites 1 and 3 of the AMPK γ-subunit, which can competitively bind all three adenine nucleotides (ATP, ADP, and AMP) with relatively the same affinity (Hardie et al., 2011).

One intriguing question that arises when addressing the ability of AMPKγ to bind adenine nucleotides is how ADP and AMP effectively compete with ATP when the total ATP concentrations are usually exceedingly higher than those of ADP and AMP. One possibility is that the majority of cellular ATP is bound to magnesium ($Mg.ATP^{2-}$), which has a 10-fold lower affinity then free ATP (Xiao et al., 2011). Therefore, ADP and AMP may only need to compete with free ATP for site 1 and 3 binding to the AMPKγ subunit, which is present at similar concentrations as ADP/AMP.

Modes of AMPK Activation

Adenine Nucleotides

As stated above, a decrease in the cellular ATP detected by increased ADP or AMP levels will trigger approximately a 10-fold increase in AMPK activity. Binding of ADP or AMP will increase AMPK activity by causing a conformational change that promotes α-subunit Thr172 phosphorylation, as well as inhibition of Thr172 de-phosphorylation by protein phosphatases (Hardie, 2011). In addition, AMP but not ADP was also shown to support allosteric activation of AMPK that has already been phosphorylated on Thr172 of the α-subunit (Corton, Gillespie, Hawley, & Hardie, 1995). Since AMP continues to be the only adenine nucleotide that can allosterically activate AMPK it seems appropriate that the name AMPK (after AMP-activated protein kinase) remain valid, despite the recent identification of "ADP sensing" by this kinase (Xiao et al., 2011).

Identification of Upstream AMPK Kinases

Since the early 2000's, it had became evident that phosphorylation events occurred on the AMPKα Thr172 residue that were vital for full AMPK activity. However, many attempts in rodent systems have failed to identify these potential upstream phosphotransferases that were responsible for this mechanism. It wasn't until 2003 that upstream regulators of AMPK were identified using studies in yeast (*S. cervisiae*) (Hardie, 2005). Several groups discovered potential regulators of the yeast orthologues of AMPK α (Snf1) and γ (Snf4), including Pak1 (Nath, McCartney, & Schmidt, 2003), Tos3 (Hong, Leiper, Woods, Carling, & Carlson, 2003), and Elm1 (Sutherland et al., 2003), which were all found to phosphorylate and activate AMPK. Interestingly, two of the closest matches to these three yeast kinases in mammals were

liver kinase B1 (LKB1) and calmodulin-dependent protein kinase kinase β (CaMKKβ) (Hardie, 2005).

It is now known that the major upstream kinase that regulates mammalian AMPK is LKB1 (also referred to as serine/threonine kinase 11). LKB1 is the tumour suppressor that is mutated in Peutz Jeghers syndrome, which is associated with the development of hamartomas (benign intestinal polyps) and an increased risk for developing malignant cancers at other sites within the body (Hardie, 2005). Inactive LKB1 is sequestered in the nucleus, but active LKB1 translocates to the cytoplasm where it forms a heterotrimeric complex with two accessory subunits, Ste20-related adaptor protein (STRAD), and scaffolding mouse 25 protein (MO25) (van Veelen, Korsse, van de Laar, & Peppelenbosch, 2011). STRAD blocks the nuclear re-localization of LKB1, while Mo25 stabilizes the association for the LKB1-STRAD-Mo25 complex. In addition, the LKB1-STRAD interaction also promotes LKB1 auto-phosphorylation at various sites, but the functional relevance of this is still being elucidated (van Veelen et al., 2011).

LKB1 phosphorylates AMPK on its α-Thr172 residue, leading to at least a 100-fold increase in AMPK activity (Hardie, 2011). Interestingly, LKB1 has been suggested to have a basal state of continuous activity, and therefore its ability to increase AMPK activity is mainly dependent on AMP binding and causing a conformational change to AMPK to make it a better substrate for Thr172 phosphorylation (Sakamoto, Goransson, Hardie, & Alessi, 2004). In addition, LKB1 is also responsible for the phosphorylation and activation of 12 other AMPK-related kinases, on residues that are equivalent to Thr172 of AMPKα1/2 (Lizcano et al., 2004). The physiological functions of most of

these kinases are not well understood, but unlike AMPK, they do not appear to be regulated by metabolic stress.

While LKB1 is ubiquitously expressed, some tissues can also mediate α-Thr172 phosphorylation of AMPK through CaMKK. Certain tissues such as the hypothalamus, neurons, and T-lymphocytes can stimulate AMPK through calcium (Ca^{2+}) signalling pathways that activate CaMKK (Hardie, 2011). Studies have shown that CaMKKβ rather than CaMKKα is the principal kinase that phosphorylates AMPK in response to increase intracellular Ca^{2+} levels (Hawley et al., 2005; Woods et al., 2005). Interestingly, activation of AMPK by CaMKKβ can occur without any changes in adenine nucleotide levels, although Ca^{2+} can work synergistically with enhanced AMP or ADP levels to modulate AMPK activity (Hardie, 2011).

Recently, support for a third AMPK kinase that is present in mammals has been recognized. Transforming growth factor β (TGF-β)-activated kinase (TAK1) is a member of the mitogen-activated protein kinase kinase kinase (MAPKKK) family, and has been shown to phosphorylate and activate AMPK *in vitro* (Momcilovic, Hong, & Carlson, 2006). However, the physiological importance of TAK1-mediate AMPK phosphorylation remains ambiguous and studies are still evaluating its ability to regulate AMPK activity *in vivo*.

Pharmacological Activators of AMPK

Numerous pharmacological agents have also been reported to activate AMPK including the nucleoside 5-aminoimidazole-4-carboxamide riboside (AICAR), the anti-diabetic agents metformin and phenformin, and polyphenols such as resveratrol (Fogarty

& Hardie, 2010). AICAR was the first compound identified to enhance AMPK activity both *in vitro* and *in vivo* (Corton et al., 1995; Sullivan et al., 1994). AICAR enters the cell via the adenosine transporters, where it is subsequently converted to the AMP mimetic "ZMP" by adenosine kinase. This ZMP analog of AMP can then bind to the AMPK γ-subunit to trigger the allosteric activation of this kinase (Fogarty & Hardie, 2010).

The oral hyperglycemic agent metformin (N',N'-dimethylbiguanide) is one of the most prescribed type 2 diabetes drugs worldwide (Kourelis & Siegel, 2011). It, along with other biguanides (phenformin and buformin), are derived from the herb *Galega officinalis* (the French lilac) which had reported medicinal uses dating back to medieval times for the treatment of polyuria and halitosis (Dowling, Goodwin, & Stambolic, 2011). While phenformin and buformin were withdrawn from clinical use due to lactic acidosis toxicity, metformin has been found to be very well tolerated, and was approved for the treatment of hyperglycemia in Canada in 1972 (Dowling et al., 2011). The major effect of metformin action has been shown to lower blood glucose levels in human patients by blocking hepatic gluconeogenesis. Furthermore, studies *in vitro* have shown metformin enhances AMPK activity, which in turn decreases fatty acid synthesis, stimulates glucose uptake, and sensitizes cells to insulin (Zang et al., 2004; Zhou et al., 2001).

However, there is still debate as to whether AMPK is the primary target of metformin action, since a recent report found that mice lacking AMPK expression in the liver still maintained the hypoglycemic effect of metformin (Foretz et al., 2010). In addition, some AMPK-activating agents, including metformin, were found to be mitochondrial poisons that either inhibit the respiratory chain (biguanides) or block ATP

synthase (resveratrol), thereby causing indirect activation of AMPK by lowering ATP levels (Gledhill, Montgomery, Leslie, & Walker, 2007; Owen, Doran, & Halestrap, 2000).

It should be noted that following the characterization of AMPK as a target for the treatment of metabolic disease, major investigation into developing specific activators of AMPK has been commenced by pharmaceutical companies. The first direct chemical activator of AMPK was a derivative of theinopyridone named A-769662, developed by Abbott Laboratories (Cool et al., 2006). A-769662 activates AMPK independent of adenine nucleotide levels (AMP), and the upstream kinases LKB1 and CaMKKβ. However, it does require auto-phosphorylation of Ser108 of the AMPK β-subunit. *In vivo* studies of *ob/ob* mice treated with A-769662 found a significant reduction in plasma glucose and triglyceride levels (Cool et al., 2006), but its usefulness in humans is tainted by poor oral absorption.

More recently, a compound identified as PT1 was shown to directly activate AMPK through association and inhibition of its α-subunit auto-inhibitory domain (Pang et al., 2008). Like the Abbott Laboratories compound, treatment with PT1 *in vitro* enhanced AMPKα-Thr172 phosphorylation independently of the AMP/ATP ratio, and upstream regulation by LKB1 or CaMKKβ (Pang et al., 2008). However, the effects of PT1 using *in vivo* models are still being elucidated.

Downstream Targets of AMPK

Once activated, AMPK directly phosphorylates a number of downstream targets that acutely affect energy metabolism and growth, or induce changes in gene expression

that will lead to long-term alterations in metabolic programming (Mihaylova & Shaw, 2011). AMPK has a vast number of substrates on which it can act (Figure 3), but in general this enzyme upregulates catabolic pathways and suppresses anabolic pathways to restore energy balance to the cells.

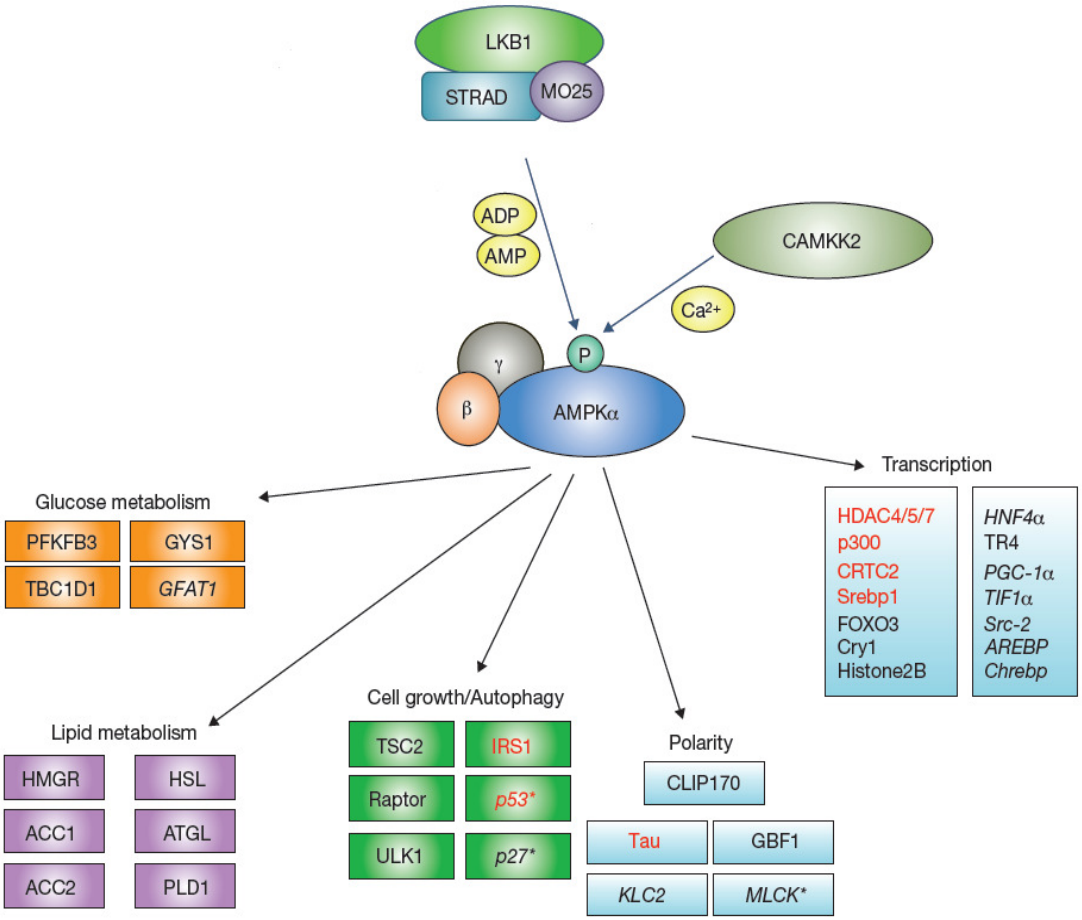

Figure 1.3: Downstream targets of AMPK (modified from Mihaylova & Shaw, 2011). The targets shown in red have been shown to be regulated by other AMPK-like kinases.

Glucose Uptake

Specific examples of catabolic pathways that are enhanced by AMPK include glucose uptake and fatty acid oxidation. AMPK can stimulate glycolysis through the

direct phosphorylation of phosphofructokinase (PFK). Furthermore, AMPK activation stimulates translocation of the glucose transporter GLUT4, to the plasma membrane to enhance glucose entry into the cell (Steinberg & Kemp, 2009). AMPK can also further increase glucose uptake by elevating the transporter activity of GLUT1 at the plasma membrane (Barnes et al., 2002). Notably, these effects of AMPK on glucose uptake can occur independently of insulin action, which is beneficial in insulin-resistant individuals. At the transcriptional level AMPK can also increase GLUT4 gene expression through the phosphorylation and regulation of the transcription factor peroxisome proliferator-activated receptor gamma coactivator 1-alpha (PGC 1α), or GLUT4 enhancer factor (GEF). Moreover, through a similar mechanism involving PGC 1α, AMPK can also increase mitochondrial biogenesis (Fogarty & Hardie, 2010).

Fatty Acid Oxidation

As stated previously, AMPK was initially characterized as a kinase that could inhibit ACC and HMG-CoA, which are the rate limiting steps for fatty-acid and sterol synthesis. Early studies identified that AMPK phosphorylated ACC at three different serine residues, Ser79, Ser1200, and Ser1215 (Davies, Sim, & Hardie, 1990). Of these multiple serine residues, it was found that Ser79 is the major site responsible for AMPK-mediated inhibition of ACC activity (Davies et al., 1990).

AMPK is capable of stimulating fatty acid oxidation by decreasing malonyl-CoA levels through inhibition of ACC2, and subsequent increasing CPT-1 activity. To a similar extent, AMPK blocks anabolic fatty acid synthesis by inhibiting HMG-CoA and fatty acid synthase (FAS) through reduction of ACC1 activity (Steinberg & Kemp, 2009).

Thus, by lowering energy-consuming process such as lipid synthesis on one hand, and increasing ATP producing pathways such as glycolysis and beta oxidation of fatty acids in the other, AMPK activation restores energy homeostasis to the cell.

Protein Synthesis and mTOR Signalling

Another significant contributor to energy expenditure in the cell is protein synthesis. Thus, an important mechanism to conserve energy under metabolic stress is to inhibit protein production. AMPK blocks protein synthesis through multiple points. It phosphorylates and activates eukaryote elongation factor 2 kinase (EEF2K), which in turn phosphorylates and inhibits eEF2, a chief promoter of peptide elongation and protein production (Browne, Finn, & Proud, 2004). In addition, AMPK is a potent inhibitor of the mammalian target of rapamycin (mTOR), a protein kinase that promotes cell growth, proliferation, protein synthesis, and has been implicated in the progression of cancer.

mTOR is a member of the phosphatidylinositol 3-kinase related kinases (PIKK) superfamily, which can exists as two different protein complexes mTORC1 and mTORC2 (van Veelen et al., 2011). The mTORC1 complex consists of mTOR, the regulatory associated protein of mTOR (raptor), and mLST8, and is sensitive to inhibition by the chemical drug rapamycin. mTORC1 phosphorylates p70-S6 kinase (S6K) and eukaryotic initiation factor 4E (eIF4E) binding protein 1 (4E-BP1) to initiate protein synthesis, as well as regulates cell proliferation and survival (van Veelen et al., 2011). On the other hand, mTORC2 exists as a protein complex containing mTOR, rapamycin-insensitive companion of mTOR (rictor), and mammalian stress-activated protein kinase interacting protein 1 (mSIN1) (Bhagwat & Crew, 2010). mTORC2 was recently

discovered to be the long sought after protein kinase that phosphorylates Akt on Ser473, which was previously given the alias PDK2 (Sarbassov, Guertin, Ali, & Sabatini, 2005). In addition, mTORC2 plays a role in cell size and regulates the actin cytoskeleton (Bhagwat & Crew, 2010).

AMPK inhibits the activity of the mTORC1 complex through multiple mechanisms to conserve energy. One mechanism by which AMPK blocks mTOR is through modulation of the tuberous sclerosis complex (TSC) proteins (TSC1:TSC2). TSC1:TSC2 have GTPase activity towards the small G-protein Rheb, which promotes mTORC1 activity when it is GTP-bound. AMPK activates TSC2 by direct phosphorylation on its Thr1227 and Ser1345 residues, which in turn converts Rheb into its inactive GDP-bound state (van Veelen et al., 2011). An alternative mechanism for AMPK to inhibit mTORC1 is through direct phosphorylation and inhibition of the mTOR binding partner raptor, which blocks the ability of mTOR to phosphorylate its downstream substrates (Gwinn et al., 2008).

Interestingly, AMPK and mTOR are known to converge on unc-51-like kinase 1 (ULK1), a protein kinase that regulates autophagy. Autophagy is a process of "self-engulfment" where cells dissolves their own organelles (macroautophagy) and cytoplasmic machinery (microautophagy) to provide adequate nutrients under low-energy conditions (Mizushima, 2010). AMPK can directly phosphorylate and activate ULK1, which is important to initiate autophagy, sustain energy balance, and maintain mitochondrial homeostasis. Conversely, mTOR exhibits inhibitory phosphorylation on

ULK1, thereby promoting energy expenditure and cell proliferation (Mihaylova & Shaw, 2011).

Modulation of Gene Transcription

Finally, AMPK is known to phosphorylate and regulate a wide range of transcription factors, their co-activators, as well as directly interact with histones. For example, in response to metabolic stress AMPK can phosphorylate p53 on its Ser15 residue and cause cell cycle arrest (Jones et al., 2005). Furthermore, recent evidence has demonstrated that AMPK can provoke transcriptional regulation through the direct phosphorylation of histone H2B on Ser36 (Bungard et al., 2010). In addition, AMPK may be recruited to the promoters of stress-induced genes such as p21 and CPT1 by transcription factors such as p53 (Bungard et al., 2010). Taken together, AMPK can target multiple signalling pathways by acute phosphorylation or alterations in gene transcription in an attempt to attenuate metabolic stress.

Pharmaceutical Modulators of AMPK Activity as Anti-Cancer Agents

AMPK is a known regulator of metabolism that has also been implicated in controlling cell growth and proliferation. The increasing interest in AMPK as a target for cancer has come about, in part from the realization that this kinase is sandwiched between multiple tumour suppressors, including LKB1, p53, and TSC1/2. Moreover, all of these proteins are part of a signalling cascade that negatively regulates the mTOR pro-survival pathway. Thus, it stands to reason that drugs that modulate AMPK activity may work as anti-cancer agents that can slow down or block uncontrolled proliferation through induction of cell cycle checkpoints or through suppression of mTOR. Furthermore,

pharmaceutical agents that increase AMPK activity may be beneficial as adjuvants for chemo or radiation therapy, the latter which is discussed in more detail in later sections.

AICAR

Early reports using AICAR demonstrated that it can inhibit cell growth through regulation of AMPK or *de novo* purine synthesis (Imamura, Ogura, Kishimoto, Kaminishi, & Esumi, 2001; Thomas, Meade, & Holmes, 1981). In cultured cancer cells, AICAR treatment activates AMPK, which in turn leads to Ser15 phosphorylation of p53 and subsequent G1 cell cycle arrest (Imamura et al., 2001). In addition, AICAR has been shown to inhibit tumour growth in colon cancer xenografts *in vivo* (Buzzai et al., 2007).

Furthermore, studies have indicated that AICAR can be an adjuvant to radiation therapy. AICAR treatment in prostate cancer cells sensitized them to the cytotoxic effects of ionizing radiation (Isebaert, Swinnen, McBride, Begg, & Haustermans, 2011). However, the authors of this study suggested that the radiosensitizing effects of AICAR are AMPK-independent, and require ZMP accumulation (Isebaert et al., 2011).

Metformin

Prolonged administration of metformin was found to reduce the incidence of spontaneous tumour formation in mouse models of cancer (Anisimov et al., 2005). Given the fact that there are millions of patients that are chronically administered metformin, epidemiologists have initiated studies to see if the results of metformin treatment in mice were recapitulated in the human incidence of cancer development. Strikingly, two independent reports have found that patients with type 2 diabetes taking metformin rather than other anti-diabetic medications were significantly at a lower risk of developing

cancer (Bowker, Majumdar, Veugelers, & Johnson, 2006; Evans, Donnelly, Emslie-Smith, Alessi, & Morris, 2005). This finding sparked wide-spread interest in metformin as an anti-cancer target, which became the focus of investigation for many basic scientists.

An initial report from Michael Pollak's laboratory (Zakikhani, Dowling, Fantus, Sonenberg, & Pollak, 2006) demonstrated that metformin could inhibit breast cancer cell proliferation *in vitro*, through an AMPK-dependent mechanism. Later it was shown that metformin targets and inhibits mTOR-dependent protein translation in breast cancer cells through a mechanism that involves the LKB1/AMPK signalling pathway (Dowling, Zakikhani, Fantus, Pollak, & Sonenberg, 2007). Since then, numerous studies have found that metformin can inhibit the proliferation of a wide range of cancer cell lines, including prostate (Ben Sahra et al., 2008), lung (Antonoff & D'Cunha, 2010), gliomal (Isakovic et al., 2007), and ovarian cancer cells (Bodmer, Becker, Meier, Jick, & Meier, 2011). It should be noted that all of these studies use relatively high (1-20mM) concentrations of metformin to activate AMPK in these cell cultures, which are several fold higher levels than can be achieved in human plasma (5-40μM). However, this difference may be attributed to the lack of the organic cation transporter-1 (OCT1) in many of these cell cultures, which are required for the selective uptake of metformin into the cell (Fogarty & Hardie, 2010).

In addition to metformin working as a cancer monotherapy it has also been used as an adjuvant to chemotherapy (Rocha et al., 2011) and as shown in this thesis, radiation therapy (Sanli et al., 2010). Interestingly, both the combined effect of metformin with

chemo- or radiotherapy potentiated cell cycle arrest and AMPK signalling greater than the individual treatments alone. Overall, this observation reinforces the role of AMPK activation as a means of suppressing cancer survival.

Resveratrol

The polyphenol resveratrol (3,5,4'-trihydroxystilbene) is a naturally occurring phytoalexin that is present in many plants, including grapes, mulberries, peanuts, and pine trees (Aggarwal et al., 2004). Resveratrol has been reported to have many favorable biological effects (reviewed in Fogarty & Hardie, 2010) and can activate AMPK *in vitro* and *in vivo* (Baur & Sinclair, 2006). Several studies have indicated that resveratrol has anti-proliferative effects in cancers of breast, prostate, colon, thyroid, pancreas, lung, and lymphoid origin (reviewed in Aggarwal et al., 2004). These effects are generally believed to be mediated through resveratrol-induced cell cycle arrest and apoptosis. In addition, resveratrol has also been utilized as a sensitizer of cancer cells to chemotherapy and radiation therapy (Hsieh & Wu, 2010; Rashid et al., 2011).

Statins

The 3-hydroxy-3-methylglutaryl-CoA reductase inhibitors, or statins are widely used drugs given to cardiovascular disease patients for the management of hypercholesterolemia (Goldstein, 2007). Statins reduce the levels of low-density lipoproteins (LDL) by effectively blocking HMG-CoA reductase, a molecule required for the conversion of HMG-CoA into mevalonate, which is the rate-limiting step in cholesterol synthesis (Hindler, Cleeland, Rivera, & Collard, 2006). By depleting precursors of the mevalonate pathway, statins also alter the structural components of cell

membranes, which rely on cholesterol. In addition, the post-translational modification of intracellular G-proteins, including Rac, Rho, and Ras, are block by statins because they require mevalonic acid to aid in signal transduction (Goldstein, 2007). Furthermore, some statin members including simvastatin (Rossoni et al., 2011), atorvastatin (P. M. Yang et al., 2010), and as we have indicated (in this thesis) lovastatin, have been shown to activate AMPK signalling.

The family of statins, including lovastatin, cerivastatin, atorvastatin, simvastatin, and pravastatin, have all been implicated in reducing cancer cell proliferation by blocking G1-S phase cell cycle transition and inducing apoptosis (Graaf, Richel, van Noorden, & Guchelaar, 2004). However, studies have indicated that all statins may not be equal in their potency in inducing cancer cell death. Cerivastatin was shown to be ten times more effective than other statins in inducing apoptosis in acute myeloid leukemia (AML) cells (Wong et al., 2001). In addition, numerous reports have demonstrated that statins can block tumour development *in vivo* (reviewed in Graaf et al., 2004).

Perhaps the most studied statin in cancer therapy is lovastatin, which has been examined as both a single anti-cancer agent and as a sensitizer for chemo and radiotherapy (Agarwal et al., 1999; Fritz, Brachetti, & Kaina, 2003). An added benefit of lovastatin in patients undergoing radiotherapy is its ability to reduce IR-induced pro-inflammation and cell death in normal tissue (Ostrau et al., 2009), while potentially sensitizing cancer cells to IR-induced apoptosis. Chapter 3 of this thesis highlights the ability of lovastatin to act as a radiation sensitizer in lung cancer cells.

The Stress-Responsive Sestrin Proteins

Sestrins (SESNs) are a family of stress-regulated proteins that function to protect normal cells from oxidative damage through redox and cell signalling pathways (Budanov, Lee, & Karin, 2010). In addition, SESNs have been reported to active AMPK and suppress mTOR in both flies and mammals that are exposed to genotoxic stress. *Drosophila melanogaster* have a single orthologue of SESN (dSesn), while mammals express three different SESNs (SESN1, SENS2, and SESN3) (Lee et al., 2010).

The Identification of Sestrins

The discovery of mammalian SESNs was initiated by studies that attempted to distinguish novel genes that are regulated by the tumour suppressor p53. In the 1990's the Kley's laboratory identified a new p53 target gene known as p53-activated gene 26 (PA26), which had similar properties to the growth arrest and DNA damage (GADD) genes (Velasco-Miguel et al., 1999). PA26 (now known as SESN1) was shown to be regulated by genotoxic stimuli, including UV radiation, IR, and chemotherapy. Interestingly, the PA26 gene can be transcribed into three different mRNAs from different promoter regions, which allows for three separate proteins to be encoded: PA26-T1 (68kDa), PA26-T2 (55kDa), and PA26-T3 (48kDa) (Velasco-Miguel et al., 1999). Of these protein isoforms, only T2 and T3 of PA26 are induced by p53, with T2 being predominantly expressed isoform *in vitro*.

A few years later a close homologue of the PA26 gene was discovered by Feinstein's group that was characterized as hypoxia-inducible gene 95 (Hi95), based on its ability to be regulated by hypoxia and other stress conditions (Budanov et al., 2002). As opposed to PA26, Hi95 (SESN2) is transcribed into a single mRNA species that

encodes a 60kDa protein. In addition, Hi95's induction by hypoxia was shown to be p53-independent, but its regulation by DNA damaging agents including UV radiation and IR occurs in a p53-dependent fashion (Budanov et al., 2002).

Shortly after Hi95 was characterized, a third member of this family was found through *in silico* analysis and named SESN3 (Peeters et al., 2003). SESN3 has two different splice variants that can encode two separate proteins products of 57.3kDa and 36kDa respectively (Budanov et al., 2010). In addition, unlike PA26 and Hi95, SESN3 appears to operate independently of p53, but is positively regulated by the forkhead family of transcription factors (FoxO) (Chen et al., 2010).

All three of these proteins make up the family of SESNs, whose name is derived from a small Italian town called Sestri Levante, where scientists uncovered their amino acid sequence homology (Budanov et al., 2010). Structurally, the predicted organization of SESNs suggests that they are globular proteins comprised of mostly α-helical regions, although obvious structural folds or motifs are lacking. However, there are numerous putative serine/threonine and tyrosine phosphorylation sites present on SESNs, where predicted protein kinases including, protein kinase C and casein kinase 2 can act (Budanov et al., 2010).

Antioxidant Function of Sestrins

SESNs were recently found to be structurally similar to the *Mycobacterium tuberculosis* AhpD protein, which is part of the alkyl-hydroperoxidereductase system that defends against reactive oxygen species (ROS) (Budanov, Sablina, Feinstein, Koonin, & Chumakov, 2004). Both AhpD and SESNs were established to be responsible for the

regeneration and rescue of thiol-specific peroxidase that become over-oxidized following their interaction with ROS, which leads to their inactivation. Indeed, knockdown of SESN1 or SESN2 by gene silencing *in vitro* led to enhanced ROS production (Budanov et al., 2004). In addition, a recent report has indicated that oncogenic Ras activation promotes the suppression of SESN1 and SESN3, and this may play a role in Ras-induced ROS accumulation (Kopnin, Agapova, Kopnin, & Chumakov, 2007).

Sestrins and Suppression of mTOR Signalling

Completely independent of their redox function, SESNs were recently shown to have importing physiological function by regulating the AMPK and mTOR pathway. An initial report from Karin's laboratory demonstrated that transient overexpression of SESN1 and SESN2 resulted in strong suppression of mTORC1 complex *in vitro* (Budanov & Karin, 2008). The mechanism by which SESN1/2 accomplished this was through direct association and activation of AMPK and TSC2, two negative regulators of mTOR signalling. Importantly, they also observed that SESN2-deficent mice fail to block mTORC1 activation in response to genotoxic challenge (Budanov & Karin, 2008). On the other hand, SESN3 can also suppress mTORC1 through TSC2 via enhanced activity of FoxO1 (Chen et al., 2010). Taken together, the SESNs play an important role in suppressing growth and proliferation in response to stress through TSC2-mediated inhibition of mTORC1.

Furthermore, the same group of researchers observed that deletion of the *Drosophila* SESN (dSESN) gene caused flies to acquire age-associated pathologies including mitochondrial dysfunction, sarcopenia, and triglyceride accumulation that were

consistent to chronic TOR activity (Lee et al., 2010). Indeed western blotting analysis of dSESN-null flies showed increased TOR expression and reduced levels of AMPK. Interestingly, when these flies were treated with AMPK activators such as metformin or AICAR, the accumulation of triglycerides and loss of muscle mass was largely attenuated, indicating that dSESN is an important upstream regulator of AMPK that is required to keep TOR levels in check (Lee et al., 2010).

Overview of Radiobiology and its Application in Cancer

All living things are continually exposed to background ionizing radiation (IR) from natural sources, including cosmic and terrestrial radiation. Another potential exposure to IR is through man-made sources, which occurs mainly though medical diagnostics, occupational use, and power generation (Podgorsak, 2005). Approximately 90% of all radiation exposure to humans is generated from natural sources, while exposure to man-made sources has a much higher propensity for causing cell injury. However, uses of man-made IR for medical therapy and diagnosis are becoming more widespread due to the recent advances in radiation oncology, medical physics, and the implementation of adequate safety measures. The branch of science that studies the effect of IR on biological tissue and living organisms is known as radiation biology (Tannock & Hill, 1998). This following section will provide background information on IR and its relevance as a targeted treatment for cancer.

Types and Classifications of IR

Based on its biological effect, IR can be classified into two different categories, direct and indirect. Direct forms of IR are charged particles such as alpha particles,

electrons, and heavy ions with enough energy to directly disturb the atoms of the medium that they pass through (Suntharaling, Podgorsak, & Hendry, 2009). Conversely, γ-rays and x-rays are indirect forms of IR that do not cause direct biological damage themselves, but rather, produce secondary charged ions after passing through a medium.

Ionization is the mechanism by which one or more electrons are removed from the nucleus of an atom once they are exposed to IR. This process causes the affected atom to leave behind a positive charge (ion) that may go on to produced damaging effects in the irradiated biological material (Suntharaling et al., 2009). Ionization of living tissue can include disruption of biological material such as DNA, lipids, and proteins, or inorganic compounds like minerals and water. Direct IR can cause cell damage to biological material (mainly DNA), while indirect IR mainly interacts with inorganic molecules like water, which makes up approximately 80% of the cell composition. This indirect action of radiation with water is called water-radiolysis and can produce free radicals such as OH^- (hydroxyl radicals), that can in turn cause cellular damage (Hall et al., 1988).

Cellular and Molecular Events in Response to Ionizing Radiation

IR-induced DNA damage and Repair

IR is known to cause a variety of lesions to the physical structure of DNA, including single strand breaks (SSB) in the phosphodiester linkage, double strand breaks (DSB), base damage, protein-DNA cross-linkage, and protein-protein cross-linkage (Steel, 2002). The quantity of DNA lesions that are generated in response to IR is large, but these lesions translate into only a small number of killed cells. For examples, an IR dose between 1-2Gy is estimated to give rise to ~1000 SSB, ~40 DSB, and >1000 bases

damaged (Bristow & Hill, 1998). Although the number of DSB is low, experimental evidence has shown that these DSB play a critical role in IR-induced cell killing and correlate with cellular radiosensitivity (Hall et al., 1988).

There are various cellular mechanisms in place to repair DNA damage that are specific to the type of DNA lesion. The vast majority of DNA repair pathways have evolved under the premise that DNA damage will only disrupt a single strand of DNA (Mladenov & Iliakis, 2011). Therefore, after the lesion is removed from the damaged DNA strand, it can be fully restored by using information from the complementary, non-injured DNA strand. The types of repair processes used to fix this type of SSB include base excision repair (BER), nucleotide excision repair (NER), and mismatch repair (MMR) (Mladenov & Iliakis, 2011). BER can repair single base DNA damage by using DNA glycosylase to remove the injured base, which is then reinserted by DNA ligase (Sancar, Lindsey-Boltz, Unsal-Kacmaz, & Linn, 2004). On the other hand, NER is well situated to recognize large DNA lesions and is the major repair system for SSB breaks. In this case, damaged bases are isolated by excision nuclease, an enzyme that makes dual incisions that flank the area of DNA damage in the strand, which can then be removed to make way for repair resynthesis (Sancar et al., 2004). MMR is a system that may also be used for the detection and repair of erroneous insertions, deletions, or translocations that can arise in SSB due to DNA damage (Podgorsak, 2005).

Higher order eukaryotes have also developed mechanisms to detect and repair DSB. The two different pathways used to mend DSB are non-homologous end joining (NHEJ) and homologous recombination (HR) (Powell & Kachnic, 2003). The NHEJ

pathway is an error-prone mechanism of DNA repair that is able to link two DNA ends together without any regard for sequence homology. Since IR-induced DSB are often associated with damage to the phosphodiester bonds that make up the DNA backbone or to the bases of the terminal nucleotides, prerequisites for NHEJ include extensive removal/addition of many nucleotides that may change the DNA sequence of the repaired fragment (Mladenov & Iliakis, 2011). Conversely, HR provides a high-fidelity mechanism of DNA repair that utilizes the sequence homology of an undamaged copy of the broken region from a homologous chromosome. The process takes place in three steps: strand invasion, branch migration, and Holliday junction (Sancar et al., 2004). Strand invasion and branch migration of a sister chromatid is initiated by the Rad51 protein following DNA damage. The formation of Holliday junction acts as a mobile cross-bridge between the two complementary DNA double stands, where the exchange of genetic material required for error-free homologous repair occurs (Sancar et al., 2004).

Cell Cycle and Checkpoints

In living cells that undergo cell division, there is a homeostatic regulation that occurs between cell proliferation, differentiation, growth arrest, and apoptosis. The temporal framework that balances these events is known as the cell cycle (Figure 4), which was described more than 50 years ago by the radiation biologists Howard and Pelc (Howard & Pelc, 1953). Four stages of the cell cycle were characterized based on observations with microscopy and autoradiography techniques (Howard & Pelc, 1953). Cell cytokinesis and segregation of chromosomes were easily visualized under a light microscope, which is referred to as mitosis (M-phase). The rest of the cell cycle stages

were classified using radioactive labelling of DNA (Rudoltz, Kao, Blank, Muschel, & McKenna, 1996). The period where DNA synthesis occurs is known as S-phase, while the gap (G-phase) between M and S is G1-phase. There is also a gap phase that takes place between S and M, which is called G2-phase. In addition, fully differentiated mammalian cells are capable of exiting the cell cycle and subsist in a quiescent state known as G0-phase (Figure 4) (Rudoltz et al., 1996).

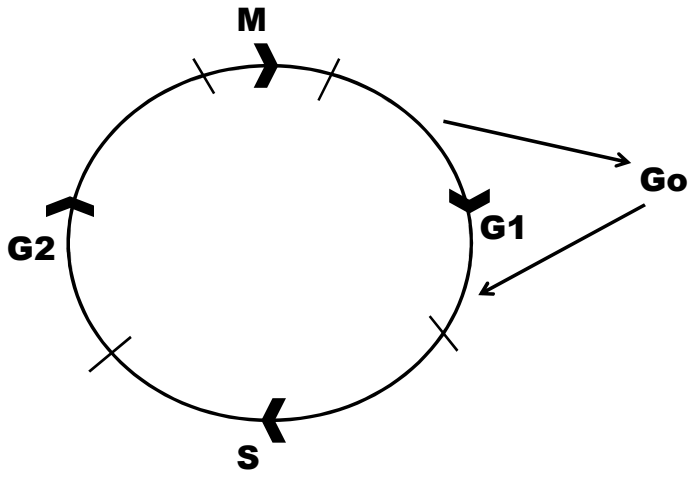

Figure 1.4: The proposed model of cell cycle as portrayed by Howard and Pelc.

The class of signalling molecules that drive cells through the different stages of the cell cycle are called cyclin dependent kinases (CDKs) (Walworth, 2000). The CDKs have kinase activity that remains inactive until it has bound an accessory protein, termed cyclin. Thus, an active CDK consists of a CDK-cyclin complex, which can then phosphorylate downstream proteins to drive cell cycle progression (Rudoltz et al., 1996). Each CDK-cyclin complex becomes active at distinct points along the phase boundaries of the cell cycle. For example, the D family of cyclins binds to CDK4 or CDK6, while

cyclin E can bind CDK2 to propel cells through the G1-phase and into S-phase (Tyson, Csikasz-Nagy, & Novak, 2002). The length of time that CDK-cyclin complexes remain associated varies, with levels of cyclin D increasing in early G1-phase and terminating into S-phase, while cyclin E levels are enhanced later in G1-phase and are maintained through much of S-phase (Walworth, 2000). Similarly, CDK1 (also known as cdc2) regulates progression of the cell cycle in later phases by forming a complex with cyclin B during the G2-to-M phase transition, allowing cells to exit interphase and enter mitosis (Tyson et al., 2002). Levels of cyclin B usually increase in later S-phase, peak in G2/M-phase, and subsequently decrease in early G1-phase.

To protect the integrity of the genome the cell cycle is subjected to multiple checkpoints, which become active upon DNA damage events, such as IR, and prevent further cycle cell progression (Tyson et al., 2002). Defined checkpoints are stepped up near the end of G1-phase (also known as the restriction point) before the cells are committed to enter DNA synthesis, mid-S-phase, and at the end of G2-phase before cells enter mitosis. Many signalling molecules that are responsible for maintenance of these checkpoints are mutated in cancer, thus providing a strategy for cancer cells to exhibit uncontrolled proliferation (Bristow & Hill, 1998).

A well defined regulator of the G1 checkpoint is the retinoblastoma (Rb) family of proteins (Masciullo, Khalili, & Giordano, 2000). When Rb is in a hypophosphorylated state, it binds and prevents the activity of the transcription factor E2F, which in turn is required for the transcription of many genes required for S-phase progression. However, once Rb is phosphorylated by CDKs, particularly CDK4, it releases E2F and transcription

of S-phase genes ensues (Masciullo et al., 2000). A group of small molecule CDK inhibitors (CDKIs) are also important for G1 checkpoint regulation, and include p21, p15, p16, p27, and p58 (Reed et al., 1994). p21, which is part of the Cip/Kip family ($p21^{WAF1/CIP1}$), was the first of the CDKIs characterized, and was initially identified as the novel protein associated with CDK2 and the product of p53-mediated transcription. All members of this family can bind to and block a wide range of CDKs, thereby blocking cell progression at various phases of the cell cycle (Reed et al., 1994). However, only p21 has been directly implicated in DNA damage-induced cell cycle arrest and is well established to be upregulated by IR (Pawlik & Keyomarsi, 2004).

DNA Damage Recognition and Signalling in Response to IR

The primary transducer of DSB-induced DNA damage is the serine-threonine protein kinase ataxia telangiectasia mutated (ATM) (Lavin & Kozlov, 2007). Structurally, ATM is a 350kDa protein that belongs to the PIKK family, which also includes DNA-dependent protein kinase (DNA-PK) that can also sense DSB, as well as ATM and Rad3-related protein (ATR) which detects SSB (Ditch & Paull, 2011). Mutation of this gene gives rise to ataxia telangiectasia (AT), an autosomal recessive disorder that arises in young children (Pawlik & Keyomarsi, 2004). These patients show signs of ataxia that is strongly associated with progressive loss of motor function. Hypersensitivity to ionizing radiation, as well as increased risk of developing malignancies and type 2 diabetes are also hallmarks of AT (Ditch & Paull, 2011). In addition, patients with AT show defects in G1, S, and G2 cell cycle arrest in response to IR (Bensimon, Aebersold, & Shiloh, 2011).

Activation of ATM by autophosphorylation of its Ser1981 residue occurs in response to IR-induced DNA damage. Activated ATM then initiates a complex network of signalling events that lead to cell cycle arrest and DNA repair (Bensimon et al., 2011). To facilitate the repair of DNA lesions, ATM phosphorylates a member of the histone H2A family, known as H2AX on its serine 139 residue. Phosphorylated H2AX (γH2AX) is visible as nuclear foci using immunofluorescence and it leads to the recruitment of repair complexes at the site of DNA damage (Fernandez-Capetillo, Lee, Nussenzweig, & Nussenzweig, 2004). Constituents of this DNA repair complex includes meiotic recombination 11 (MRE11), RAD50, and Nijmegen breakage syndrome 1 (NBS1), which together comprise the MRE11 complex. Formation of the MRE11 complex then facilitates DNA repair through NHEJ or HR, (Lavin & Kozlov, 2007). Surprisingly, the MRE11 complex has also recently been reported to catalyze the activation of ATM, suggesting that there is a positive feedback loop between the initiation of DNA damage recognition and repair (Stracker & Petrini, 2011).

In addition to DNA repair signalling, ATM as well as its related family member ATR, phosphorylate and activates the check point kinases 1/2 (Chk1 and Chk2), which are critical for cell cycle regulation in response to DNA damage (Lavin & Kozlov, 2007). ATM is also a well established regulator of the tumour suppressor p53 (Lavin & Kozlov, 2007). Phosphorylation of p53 on multiple serine residues (Ser6, Ser15, Ser20, Ser37, Ser46, and Ser392) by upstream stress-kinases including ATM and Chk1/2 are required for its stabilization and induction of G1-phase cell cycle arrest (Rodier, Campisi, & Bhaumik, 2007). Stable p53 also enhances p21 transcription, which acts as a potent

inhibitor of CDKs that drive cell cycle progression through the G1 phase (Bristow & Hill, 1998).

Moreover, ATM is also important for cell cycle arrest in the later phases of the cell cycle. ATM-mediated phosphorylation of NBS1 is required for intra-S-phase cell cycle arrest in response to IR (Stracker & Petrini, 2011). To a similar extent, ATM can regulate BRCA1 to activate the S-phase checkpoint (Pawlik & Keyomarsi, 2004). In addition, G2 cell cycle arrest following irradiation can be facilitated by ATM through multiple pathways. One possibility is that ATM can phosphorylate Chk2 on Thr68, which is required for activation of the dual-specificity phosphatases Cdc25A/C, which in turn inhibits CDK1 activation (Pawlik & Keyomarsi, 2004). On the other hand, ATM-induced p53 activation can enhance the transcription of 14-3-3σ, a signalling protein that blocks G2-phase progression by sequestering CDK1 in the cytoplasm (Pawlik & Keyomarsi, 2004). Furthermore, p21 has also been implicated in blocking the CDK1/cyclin B complex, thereby preventing G2-phase progression in response to DNA damage (Woo & Poon, 2003).

Radiotherapy and Fractionation of Tumours

Radiation therapy (or radiotherapy) is the medical use of IR to treat cancer by delivering a localized dose of IR to the tumour to prevent cell proliferation and metastasis (Bristow & Hill, 1998). The goal of radiotherapy is to effectively deliver enough IR to kill the tumour without irradiating normal tissue to an extent that it will lead to serious side-effects. This principle of deciding on a radiation dose that is effective enough to damage the tumour without significantly harming normal tissue is known as the

therapeutic ratio (Suntharaling et al., 2009). Conceptually the therapeutic ratio is based on two different outcomes, one is represented as the tumour control probability (TCP), and the other is the normal tissue complication probability (NTCP) (Suntharaling et al., 2009). Radiotherapy targets the tumour in a way that maximizes the TCP (>0.5 probability of tumour control) and at the same time, minimizes the NTCP (< 0.05 probability of complications) (Steel, 2002).

The therapeutic ratio can vary by numerous factors, including dose rate, the quality of IR beam, the use of drugs that work as radiosensitizers or radioprotectors, and the type of tissue being affected by IR (Bristow & Hill, 1998). One way to enhance the therapeutic ratio is to deliver a series of low doses of IR over an extended period of time. This is a commonly used treatment modality for radiotherapy and is known as fractionation (Tannock & Hill, 1998). Traditionally, clinical radiotherapy is given up to 5 days per week over a period of 5-7 weeks, with a daily fraction of ~2Gy (Bristow & Hill, 1998).

The foundation of fractionating the doses of IR is based upon five basic biological principles, known as the five Rs of radiotherapy (Steel, McMillan, & Peacock, 1989). The first principle is radiosensitivity, where a group of cells may have different degrees of sensitivity to radiation therapy. Often tumours consist of a heterogeneous population of cells that may have different intrinsic radiosensitivities (Steel et al., 1989). Another important aspect of fractionation that was discussed earlier is repair following IR. Depending on how damaging the IR fraction was, cells may undergo repair or cell death (Suntharaling et al., 2009). Over the course of IR treatment both tumour and normal cells

may also increase their rate of proliferation. This effect is known as repopulation, and may represent a significant cause of treatment failure in cancer (Kim & Tannock, 2005). Redistribution of proliferating cell populations throughout the cell cycle also occurs in response to fractionated IR. In general some of the surviving cells will be blocked in the G2-phase, which is the most radiosensitive phase of cell cycle. Furthermore, a population of these cells may also redistribute into early G1-phase, which may also be sensitive to IR treatment, whereas S-phase cells are the most radiation resistant (Kim & Tannock, 2005). Overall, fractionation will tend to make a whole population of cells more sensitive to IR compared with a single dose of radiation. Finally, reoxygenation of hypoxic cells occurs during fractionated radiotherapy. Over a long period of time this enhanced oxygenation of cells will make tumours more radiosensitive to IR (Bristow & Hill, 1998).

Another framework for fractionation that has gained significant attention is hyperfractionation (Suntharaling et al., 2009). This is an approach that utilizes more than one fraction of IR per day with smaller doses per treatment (<1.8Gy). The benefits to this mode of fractionation are still being examined, but it is speculated to reduce the long-term side effects and allow for delivery of an overall higher total dose of IR to the tumour (Suntharaling et al., 2009).

Measuring Irradiated Cell Survival and Sensitivity

The gold standard in measuring the radiosensitivity of a population of irradiated cells is to assess their ability to undergo multiple cell divisions (between 5-6 replications), to produce a viable colony of >50 cells (Hall et al., 1988). This type of measurement of individual cell survival *in vitro* is known as the clonogenic survival. The

most common method used to illustrate clonogenic survival in response to a radiation dose-response is the linear quadratic model, which plots the survival of cells against the radiation dose on a logarithmic scale. This model is based on the premise that multiple lesions induced by IR interact within the cell to cause cell death (Tannock & Hill, 1998). Although the linear quadratic model is the most widely used model to measure cell survival following irradiation, it is not always reliable at low doses of IR (<3 Gy). Thus, for practical purposes many researchers measure the survival of cells following a dose of 2Gy IR (Podgorsak, 2005). The survival fraction after 2Gy (SF2) is a variation of the linear quadratic survival curve that is useful because it mimics the majority of clinically relevant doses of IR given in radiotherapy. In general, the larger the SF2 value, the less sensitive the cell line is to IR (Tannock & Hill, 1998).

Often cancer cells from various tumours can display intrinsic radiation resistance through the accumulation of genetic mutations (such as mutations in tumour suppressors like LKB1 or p53) and upregulation of pro-survival pathways (such as EGFR, Akt and mTOR). As stated above, the *in vitro* radiosensitivity of cancer cells can be measured using the conventional clonogenic survival assay. While this assay is convenient to use, *in vitro* measurements have certain restriction in predicting clinical outcomes for patients, including not accurately assessing the tumour microenvironment, accounting for tumour heterogeneity, and the radiosensitivity of stem cells *in vivo* (Bristow & Hill, 1998).

In research, certain cancer cell lines have been characterized as having varying degrees of radiosensitivity. Table 1 indicates the extent of sensitivity for some of the most extensively used cancer cell lines of lung, breast, and prostate origin, as well as their

LKB1 and p53 status. In addition, many of these same cell lines have been utilized for the research conducted in this thesis, which will be encountered in later chapters.

Table 1: The intrinsic radiation sensitivity of established lung, breast, and prostate cancer cell lines.

Cell Line	**LKB1 Status**	**p53 Status**	**Cancer Type**	**Radiation Resistance**	**References**
A549	-	+	Lung	High	(Carmichael et al., 1989) (Sharma et al., 2009)
NCI-H23	-	+	Lung	Low	(Carmichael et al., 1989)
NCI-H1299	+	-	Lung	Intermediate	(Nagata et al., 2010)
SK-MES-1	+	-	Lung	Intermediate	(Sharma et al., 2009)
MCF7	+	+	Breast	Intermediate	(Toulany et al., 2011)
MDA-MB-231	-	+	Breast	High	(Chaachouay et al., 2011) (Toulany et al., 2011)
SK-BR-3	+	+	Breast	High	(Toulany et al., 2011)
PC-3	+	-	Prostate	High	(Rudner et al., 2010) (Skvortsova et al., 2008)
DU-145	-	+	Prostate	Intermediate	(Rudner et al., 2010)
LNCaP	+	+	Prostate	Low	(Scott, Gumerlock, Beckett, Li, & Goldberg, 2004)

Hypothesis and Objectives

"*AMP-activated protein kinase (AMPK) is a signalling molecule that regulates radiation responses in cancer cells. Ionizing radiation (IR) enhances AMPK activity and expression to modulate cell cycle and survival. In addition, agents that potentiate AMPK activity are synergistic with IR to decrease cancer cell survival.*"

Specific objectives:

i) To investigate the role of AMPK responses to ionizing radiation in cancer cells.

ii) To evaluate the ability of drugs that activate AMPK as radiation sensitizers in cancer cells.

iii) To examine the impact of AMPK on cell signalling pathways that regulate (a) DNA repair, and (b) survival in response to IR.

iv) To identify the role of SESN2 in (a) modulating AMPK expression and activity, as well as (b) regulate pathways that are stimulated by IR.

Each of these objectives is addressed in the subsequent chapters of my thesis, which are comprised of papers that address the key points of my hypothesis. To better understand the organization of the manuscripts that make up each of these chapters, the following is a list of the titles of each paper and a brief explanation of its content.

- **Chapter 2:** Ionizing radiation activates AMP-activated kinase (AMPK): A target for radiosensitization of cancer cells.

  This paper identified that ionizing radiation (IR) increased AMPK activity in numerous epithelial cancer cell lines. Furthermore, the mechanism by which IR induces AMPK is dependent on ATM, but independent of LKB1. AMPK was also shown to be a central mediator of IR-induced cell cycle arrest. Finally, using metformin (an AMPK activator) or compound C (inhibitor), I implicated AMPK as an important target for the radiation sensitization in cancer cells.

- **Chapter 3:** Lovastatin sensitizes lung cancer cells to ionizing radiation. Modulation of molecular pathways of radioresistance and tumour suppression.

  In this manuscript, the potential of lovastatin to sensitize lung cancer cells to IR was evaluated. Lovastatin inhibited the EGFR pro-survival pathway, blocked IR-induced Akt and Erk signalling, and potentiated IR-induced AMPK activity. In addition, lovastatin induced apoptosis and sensitized lung cancer cells to the cytotoxic action of IR.

- **Chapter 4:** Ionizing radiation regulates the expression of AMP-activated protein kinase (AMPK) in epithelial cancer cells. *Modulation of cellular signals regulating cell cycle and survival.*

This manuscript explored the regulation of AMPK subunit expression 24-48h following IR in cancer cells. In addition, the role of AMPK expression (using wildtype and AMPKα1/2 -/- MEFs) on signalling pathways that regulate cell cycle, DNA repair, and survival were also examined. I also suggested that AMPK is an important regulator of genomic stability.

- **Chapter 5:** Sestrin2 modulates AMPK subunit expression and its response to ionizing radiation in breast cancer cells.

  This paper aimed to better understand the mechanism by which IR can modulate AMPK activity and survival. I evaluated the role of the stress-activated protein sestrin2, and its ability to regulate the expression and activity of AMPK in breast cancer cells. Furthermore, sestrin2 was found to be required for IR-induced AMPK expression and activation, as well as act as a radiation sensitizer that inhibited cancer cell survival through AMPK signalling.

Chapter 2: Ionizing Radiation Activates AMPK

In this chapter, an author generated version is provided of the paper "Ionizing radiation activates AMP-activated kinase (AMPK): A target for radiosensitization of cancer cells", published in the *International Journal of Radiation Oncology Biology and Physics* in September 2010. Permission was kindly given by Elsevier Limited (licence # 2753680830643). Please see appendix 3 for an attached copyright license.

In this paper, I performed all of the cell culture, western blotting, immunofluorescence, cell cycle, and cell proliferation experiments for the lung cancer cell lines. I generated all of the figures and wrote the paper in collaboration with Dr. Theodoros Tsakiridis, and also received critical feedback from the other listed authors. Supporting cell culture and western blotting for prostate and breast cancer cells were carried out by a Master's student, Ayesha Rashid, and a lab technician Caiqiong Liu. These supporting data were incorporated into the manuscript to demonstrate that activation of AMPK by ionizing radiation is a universal effect among different cancer cell types.

Context and Background Information

AMPK is activated by numerous stress stimuli including hypoxia, heat shock, and starvation in order to regulate cellular energy levels, induce cell cycle arrest, and modulate cell survival (Hardie, 2008). However, very little is known about the effect of ionizing radiation on the regulation of the AMPK signalling pathway in cancer cells. When I began my Ph.D studies at McMaster University (September 2008), initial observations from Dr. Tsakiridis laboratory demonstrated that ionizing radiation (IR)

rapidly phosphorylated and activated AMPK in lung cancer cells. This observation led me to address the mechanism by which IR activates AMPK, as well as the potential for AMPK activators to act as radiation sensitizer in cancer cells *in vitro*. The latter objective has great clinical relevance as many tumours of lung, prostate, or breast origin display radiation-resistance and poor survival outcome in advanced stages of the disease.

I first sought to understand the temporal and dose-dependent relationship of IR on AMPK activation in lung cancer cells, and where this activation occurs. To address this, A549 and SK-MES lung cancer cells were grown in culture and treated with a single dose of 2-8Gy IR using a colbalt (^{60}Co) clinical radiation unit. I then used western blotting to measure the levels of phosphorylated AMPKα on Thr172 on lung cancer cells treated with different time-points or doses of IR. AMPK appeared to be rapidly phosphorylated within 15min following 8Gy IR treatment, with sustained activity for up to 24h. In addition, I observed a dose-dependent increase in AMPK phosphorylation in response to 2-8Gy IR, with no changes in the total protein levels of AMPKα. Moreover, immunofluorescence microscopy was performed using the phosphorylated AMPK antibody to determine the subcellular distribution of activated AMPK in response to IR. I observed that AMPK is rapidly phosphorylated in the nucleus (15min) in response to 8Gy IR, and later (1h) translocates into the cytoplasm of A549 lung cancer cells. An antibody against phosphorylated histone H2Ax (γH2Ax) (a marker of DNA damage) was also used to demonstrate that IR indeed caused DNA-double stranded breaks, but there was little evidence of co-localization for phosphorylated AMPKα and γH2Ax.

Once I established that IR activates AMPK in lung cancer cells, I addressed the molecular mechanism by which this event occurs. An appealing explanation is that IR modulates the activity of LKB1, the major upstream kinase of AMPK, which in turn enhances AMPK phosphorylation. However, lung cancer cells that are LKB1-null (A549 and NCI-H23) still demonstrated increased AMPK activity following IR treatment, suggesting that this is an LKB1-independent phenomenon. Another kinase that has been proposed to regulate both LKB1 and AMPK is ataxia-telangiectasia mutated (ATM), a vital sensor of DNA damage and facilitator of DNA repair machinery and cell cycle checkpoints (Alexander & Walker, 2010; Jones et al., 2005). To address to role of ATM in mediating IR-induced AMPK activity I measured the phosphorylation levels of ATM and AMPK by western blotting in radiated A549 cells there we pre-treated in the absence or presence of KU55933, a specific chemical inhibitor of ATM. Treatment with KU55933 abolished the effect of IR to induce ATM and AMPK phosphorylation, as well as downstream p53 and p21 expression, indicating that ATM is a required effector for IR-induced AMPK induction.

Although AMPK is known to facilitate p53-dependent G1/S cell cycle checkpoint under metabolic stress (Jones et al., 2005), its ability to modulate cell cycle arrest in response to IR-induced DNA damage is still being elucidated. To examine the importance of AMPK in regulating IR-induced cell cycle arrest I used chemical (compound C) and molecular (siRNA against AMPKα) inhibition of AMPK activity in A549 cells treated with IR. Compound C is a widely used, cell-permeable, competitive inhibitor of ATP binding to the catalytic AMPKα subunit that provides inhibition of AMPK at micromolar

concentrations (IC_{50} = 0.04μM) (Machrouhi et al., 2010). However, compound C has also been implicated in inhibiting other potential protein kinases at lower IC_{50} values than AMPK, suggesting that it may have some "off target" effects (Bain et al., 2007). A549 and H1299 cells that were treated with compound C 1h prior to 8Gy IR exhibited blocked AMPK phosphorylation, as well as downstream inhibition of IR-induced p53 (in A549 cells that are 53 positive) and p21.

To recapitulate the finding of chemical inhibition with compound C, I also used small interference siRNA (siRNA) against the α1 and α2 subunits of AMPK to selectively block its expression, and subsequent activity. The specific siRNA sequences for mammalian AMPKα1 and AMPKα2 were obtained through the Qiagen Gene Globe database, and cells were transfected with these siRNA per the manufactures protocol found in Appendix 1. Similar to compound C, siRNA against AMPKα1/2 completely abolished AMPK activity and downstream p53 and p21 signalling, indicating that AMPK plays an important role in mediating the effects of IR on cell cycle checkpoint regulation.

To see if these changes in AMPK/p21 protein levels corresponded with function changes in the cell cycle, I performed cell cycle analysis in H1299 cells that were treated with IR alone, or in combination with knockdown of AMPKα1/2. Cells that were treated with 8Gy IR were fixed and analyzed 24h later using propidium iodide staining and cell cycle analysis software from a flow cytometer (appendix 1). IR alone induced G2/M cell cycle arrest, which is a well documented effect of radiation (Rudoltz et al., 1996). However, in cells that were pre-treated with AMPKα siRNA the IR-induced G2/M arrest

was attenuated, indicating that AMPK plays a functional role in instigating cell cycle checkpoint regulation in response to IR.

Ultimately, the ability of AMPK to regulate IR-induced cell cycle arrest would also likely have effects on cancer cell survival. To examine if modulation of AMPK activity would alter cell viability, I performed clonogenic survival assays in A549 and H1299 cells that were treated with the AMPK inhibitor compound C or the AMPK activator metformin alone, or in combination 2Gy IR. The survival fraction after 2Gy (SF2) is a dose commonly used in clinical radiotherapy (Carmichael et al., 1989), and was the reason I chose to utilize this amount in combination with compound C or metformin to measure clonogenic survival. Compound C alone did not significantly affect cell survival, but it did contribute to radiation resistance. On the other hand, metformin alone activated AMPK and significantly decreased cell survival. Furthermore, metformin combined with 2Gy IR further potentiated AMPK phosphorylation and sensitized both A549 and H1299 cells to the cytotoxic effect of IR.

Based on these findings, I generated a model on the molecular pathways that converge on AMPK to regulate radiation responses in cancer cells. In response to IR, ATM is rapidly phosphorylated, which in turn activates AMPK to regulate cell cycle and survival through induction of p21. In addition, pharmaceutical inhibition (compound C) or activation (metformin) of AMPK can alter radiation sensitivity, whereby blockade of AMPK promotes radiation-resistance, or activation enhances radio-sensitization. Thus, drugs that activate AMPK may be an attractive adjuvant with combined radiotherapy.

Paper: Ionizing Radiation Activates AMP-Activated Kinase (AMPK): A Target for Radiosensitization of Human Cancer Cells.

Toran Sanli[*] M.Sc., Ayesha Rashid[*] B.Sc., Caiqiong Liu[*]M.Sc., Shane Harding[†] B.Sc., Robert G. Bristow[†,‡] M.D., Ph.D., Jean-Claude Cutz[§] M.D., Gurmit Singh[§], Ph.D., **James Wright[*] M.D. and Theodoros Tsakiridis[*] M.D., Ph.D.**

Departments of [*]Oncology and [§]Pathology and Molecular Medicine, Juravinski Cancer Center and McMaster University, Hamilton and Departments of [†]Medical Biophysics and [‡]Radiation Oncology, University of Toronto, Toronto, Ontario, Canada

Running Title: Ionizing radiation activates AMPK in cancer cells.

Address Correspondence to: Theodoros Tsakiridis, M.D., Ph.D., Department of Oncology, McMaster University and Juravinski Cancer Center, 699 Concession Street, Hamilton, Ontario, Canada L8V 5C2; Tel.: 905-387-9495x64704, Fax: (905) 575-6362, Email: theos.tsakiridis@jcc.hhsc.ca

Conflicts of Interest Notification: There are no conflicts of interest to be report.

Abstract

Purpose: Adenosine monophosphate (AMP)-activated kinase (AMPK) is a molecular energy sensor regulated by the tumor suppressor LKB1. Starvation and growth factors activate AMPK through the DNA damage sensor Ataxia Telengiectasia Mutated (ATM). We explored the regulation of AMPK by ionizing radiation (IR) and its role as target for radiosensitization of human cancer cells.

Methods and Materials: Lung, prostate and breast cancer cells where treated with IR (2-8 Gy) after incubation with either ATM or AMPK inhibitors or the AMPK activator metformin. Then, cells were subjected to lysis and immunoblotting, immunofluorescence microscopy, clonogenic survival assays, or cell cycle analysis.

Results: IR induced a robust phosphorylation and activation of AMPK in all tumour cells, independent of LKB1. IR activated AMPK first in the nucleus and this extended later into cytoplasm. The ATM inhibitor KU55933 blocked IR-activation of AMPK. AMPK inhibition with Compound C (CC) or anti-AMPK α-subunit siRNA blocked IR-induction of the cell cycle regulators p53 and $p21^{waf/cip}$ as well as the IR-induced G2/M arrest. Compound C caused resistance to IR, increasing the surviving fraction after 2Gy, but the anti-diabetic drug metformin enhanced IR-activation of AMPK and lowered the survival fraction after 2 Gy further.

Conclusions: We provide evidence that IR activates AMPK in human cancer cells in an LKB1-independent manner leading to induction of $p21^{waf/cip}$ and regulation of the cell cycle and survival. AMPK appears to (1) participate in an ATM-AMPK-$p21^{waf/cip}$

pathway, (2) be involved in regulation of the IR-induced G2/M checkpoint and (3) may be targeted by metformin to enhance IR responses.

Key Words: Ionizing radiation, AMPK, ATM, cell cycle, $p21^{waf/cip}$

Introduction:

Radiotherapy is one of the main therapeutic modality in cancers of lung, prostate and breast origin. Therefore, it is important to elucidate the molecular responses to ionizing radiation (IR) in cells from these tumours. In response to IR-induced DNA damage, the kinase Ataxia Telengiectasia Mutated (ATM) becomes auto-phosphorylated and phosphorylates histones such as H2Ax (γH2Ax), leading to recruitment of DNA repair complexes at Double Strand Break (DSB) sites (1). ATM regulates cell cycle through induction of the tumour suppressor p53 and expression of cyclin-dependent kinase (CDK) inhibitors such as $p21^{waf/cip}$ (2).

The energy sensor adenosine monophosphate (AMP)-activated kinase (AMPK) is a heterotrimeric enzyme composed of one catalytic α subunit and two regulatory subunits, one β and one γ. AMPK is an effector of LKB1, a tumour suppressor mutated in the Peutz-Jeghers syndrome characterized by increased susceptibility to lung, pancreas and breast tumors. AMPK is activated through binding of AMP to its regulatory γ subunit and by α subunit phosphorylation on Thr172 by kinases such as LKB1(3).

AMPK enhances cellular energy levels by stimulation of glucose uptake, glycolysis and fatty acid uptake, and by inhibition of fatty acid and cholesterol synthesis (4). The latter are mediated by inhibition of fatty acid and cholesterol synthesis enzymes, acetyl-CoA carboxylase (ACC) and 3-hydroxy-3-methylglutaryl-coenzyme A (HMG-CoA) reductase,

respectively (4).

Hypoxia and starvation increase AMP levels in cells, regulate the cell cycle, and activate AMPK (5). AMPK regulates p53 through phosphorylation on Ser15. This induces a metabolic check point through an AMPK–p53 axis (6). Biochemical activators of AMPK are being studied. A non-phosphorylated adenosine analogue, 5-aminoimidazole-4-carboxamide-1-β-D-riboside (AICAR), enters cells and becomes converted to a monophosphorylated analogue ZMP. This mimicks AMP and can bind the regulator γ subunit and activate AMPK (7). Furthermore, AMPK is activated by anti-diabetic agents such as thiazolidinediones and the biguanide metformin (7). Metformin is shown to regulate AMPK *in-vitro* and *in-vivo* (7). Retrospective analyses suggest that metformin may improve chemotherapy responses in breast cancer (8). To date, there are no reports combining metformin with radiotherapy to enhance radiation responses. This would be an attractive approach in treating cancers of the lung and prostate, where even high doses of radiotherapy show limited efficacy (9, 10).

Sapkota et al. (2002) (11) showed IR- and ATM-induced LKB1 phosphorylation but AMPK was not investigated in that study. Studies show that p53-null cells fail to arrest in response to AMPK stimulation by AICAR or glucose deprivation (6), indicating an association between AMPK and p53 and the cell cycle.

We hypothesized that, in response to IR, AMPK may link ATM with regulation of the cell cycle and survival. Therefore, we examined the regulation of AMPK by IR, its signalling pathway and cellular effects in human cancer cells. In addition, we began to explore the physiological effects of combining metformin with IR in lung cancer cells.

Materials and Methods:

Cells: Human lung cancer (A549, NCI-H23 and SK-MES-1), prostate cancer (PC3, 22RV1, LNCap) and breast cancer (MCF-7) cells were from American Tissue Culture Collection (Manassas, VA). The H1299 cells were a kind gift from Dr. Simon Powell (Washington University, MO). Cells were maintained at 37^{o}C with RPMI media supplemented with 10% Fetal Bovine Serum (Invitrogen, Burlington, ON). *Antibodies:* Rabbit polyclonals against AMPK, phospho-(Thr^{172})-AMPK, phospho-(Ser^{79})-ACC, phospho-(Ser^{1981})–ATM, LKB-1, phospho-(Ser^{139})-H2Ax (γH2Ax), and mouse monoclonals against p53, p21$^{waf/cip}$, and actin were from Cell Signaling Technology (Mississauga, ON). Alexa Fluor-488 and Alexa Fluor-568 antibodies were from Molecular Probes (Burlington, ON). The anti-α1 and α2 AMPK siRNA transfection kit was obtained from Quiagen (Missisauga, ON). *Agents:* Metformin, compound C (CC) and KU55933 were from Calbiochem (Mississauga, ON).

Treatments: Cells were exposed to 2 to8 Gy ionizing radiation (IR) using a Co^{60} clinical radiation unit. Pre-incubation with drugs was for 1h before IR followed by incubation for 1h unless otherwise indicated. For cell cycle and clonogenic assays agents remained with cells throughout the experiment.

Immunoblotting: Cells were washed, lysed, denatured with Laemmli-SDS-sample buffer, and boiled. Fifteen μg of protein were separated by sodium dodecyl sulfate polyacrylamide gel electrophoresis (SDS-PAGE), transferred to polyvinylidene fluoride (PVDF) membrane and incubated with primary and horseradish peroxidase (HRP)-conjugated secondary antibodies, as described earlier (12).

Densitometry of immunoblots was performed using Image J software (McMaster University Biophotonics Lab, Hamilton, ON). Densitometry values are expressed as percent of control. Mean±SE values of at least 3 independent experiments are shown.

Microscopy: Cells grown on glass cover-slips were radiated, rinsed, fixed using 3% paraformaldehyde, and blocked in 5% fetal bovine in serum/phosphate-buffered saline/0.3%-Triton-X-100. Immunolabeling was performed with anti-γH2Ax-monoclonal followed by anti-mouse-Alexa-568-labelled IgG, and anti-adenosine monophosphate-activated kinase phosphorylation (P-AMPK) polyclonal followed by anti-rabbit-Alexa-488-labelled IgG, as described (13). Cells were stained with Hoechst-33258. Imaging was performed using widefield and confocal microscopy with a Zeiss LSM510 (Toronto, ON) confocal microscope.

*siRNA transfections***:** Cells were incubated with Hyperfect (Qiagen, Mississauga, ON) without or with siRNA against both AMPKα1 and AMPKα2 (anti-AMPK-α-siRNA) and were incubated for 72h, as per manufacturer's protocol.

Cell Cycle Analysis. Twenty four hours after seeding cells were pre-treated with CC (1μM) for 1h followed by IR (8Gy). After 24h, cells were fixed with ethanol and incubated with propidium iodide. Cell cycle analysis was performed using flow cytometry with a FACScan flow cytometer (BD Biosciences, San Jose, CA).

Clonogenic Assays. Five hundred cells were seeded in triplicates for each experiment. After 24h cells were treated with CC (1μM) or Metformin (5μM) followed by IR and an additional 7 day incubation. Then, cells were fixed and stained with mythelene blue and colonies containing >50 cells were counted.

Statistical Analysis. The unpaired T-test was performed to analyze the results using SPSS software (SPSS, Chicago, IL). Results are presented as mean ± SE. Statistical significance was determined at $P<0.05$(*).

Results:

IR activates AMPK in carcinoma cells. We examined first the effects of IR on AMPK phosphorylation and detected a robust IR-induced time- and dose-dependent phosphorylation of the AMPK α subunit at Thr172 without affecting total levels of the protein (Fig. 1A-B). Only the top one of the two bands recognized by the anti-Total-AMPK antibody in Figure 1A (and subsequent figures) is indeed AMPK. This is illustrated in Figure 3D where knock down of both α1 and α2 AMPK subunits eliminates only the top band. Increasing doses of IR 0–8Gy caused enhanced AMPK phosphorylation in both SK-MES and A549 cells (Fig. 1B). AMPK phosphorylation (P-AMPK) reached peak levels at 1h after IR (Fig. 1A) and decreased over time, but remained activated up to 24h later. AMPK phosphorylation was consistent with activation of the enzyme demonstrated by ACC phosphorylation (Fig. 1C). To explore whether IR-activation of AMPK is ubiquitous phenomenon, we examined also other human epithelial cancer lines of lung (A549, SK-MES, H23 and H1299), prostate (PC3, LNCap, 22RV1) and breast (MCF7) origin. We detected similar activation by IR in all cells (Fig. 1D). We focused all subsequent experiments in lung cancer cells.

Subcellular distribution of activated AMPK. With microscopy P-AMPK was examined in combination with DNA staining and phosphorylated histone H2Ax (γH2Ax) in A549 cells. We found that γH2Ax was almost undetectable in the untreated nuclei but IR

caused a robust increase of γH2Ax signal in all cells. Untreated cells had low levels of mainly nuclear P-AMPK (Fig. 2). In parallel with γH2Ax, we detected intense punctuate staining of P-AMPK in the nucleus, within 15 minutes after IR. Only minor enhancement of cytoplasmic staining was detected at that time (see arrows). By 1 h, IR increased significantly the nuclear and particularly the cytoplasmic P-AMPK. In the nucleus P-AMPK did not appear to co-localize with γH2Ax and DNA DSBs. However, we detected consistently a temporal relationship between γH2Ax and P-AMPK levels. The specificity of anti-P AMPK antibody is shown in Fig. E1.

Role of LKB1 in IR-activation of AMPK. We compared the IR-induced phosphorylation of ATM and AMPK amongst LKB1-wild type (SK-MES and H1299) and LKB1-null (A549 and H23) (14) cells. IR activated AMPK and ATM in all cells independent of LKB1 expression (Fig. 3A).

Involvement of ATM in IR-induced AMPK activation. In LKB1-null A549 cells IR activated ATM and AMPK (Fig. 3B) and induced expression of p53 and $p21^{waf/cip}$. To examine whether ATM is involved in AMPK activation by IR we used the specific ATM inhibitor KU-55933 (15). KU-55933 abolished IR-activation of ATM but also of AMPK and induction of p53 and $p21^{waf/cip}$ (Fig. 3B).

AMPK regulates IR-induction of p53 and $p21^{waf/cip}$. To examine the role of AMPK in IR-induction of p53 and $p21^{waf/cip}$, we utilized biochemical and molecular inhibition of AMPK. In A549 cells inhibition of AMPK with compound C (CC) (25μM) abolished IR-activation of AMPK. CC inhibited the activity of AMPK, shown by inhibition of ACC phosphorylation (Fig. 3C), as well as the phosphorylation of the enzyme. Importantly,

AMPK inhibition with CC abolished IR-induction of p53 and $p21^{waf/cip}$. CC and IR effects were similar in A549 and H1299 cells (Fig. 3C). Interestingly, IR induced $p21^{waf/cip}$ not only in p53-wild type A549 cells but also in p53-null H1299 cells. Inhibition of AMPK expression with anti-AMPK-α-siRNA inhibited IR-induction of p53 and $p21^{waf/cip}$, similar to CC (Fig. 3D-E).

AMPK modifies the IR-induced G2/M checkpoint. In H1299 cells IR induced a 2-fold increase (from 14.7% ± 2.1% to 30.7% ± 0.5%) in the cells accumulated at the G2/M phase of the cycle (Fig. 4A). Pre-treatment with CC (1μM) and abolished the IR-mediated G2/M checkpoint in H1299 cells reducing the cell population in G2/M phase back to control levels (of 15.0 $\pm$ 2.8%) (Fig. 4A, non-transfected cells). Similar results were obtained in radiated A549 cells pre-treated with CC and those that were not pretreated (Fig. E2). For all experiments involving long term incubations we used 1μM of CC. Figure 4B shows that 1μM of CC was also able to inhibit IR-induced activation of AMPK and induction of p53 and $p21^{waf/cip}$, in A549, or induction of $p21^{waf/cip}$ alone in H1299 cells, showing once again IR induction of $p21^{waf/cip}$ in the absence of p53.

AMPK knock down with anti-AMPK α subunit siRNA produced results similar to CC in H1299 cells. In vehicle alone treated cells IR increased the proportion of cells in G2/M from 13.6 $\pm$ 2.16% to 28.0 $\pm$ 4.7%, but AMPK knock down reduced this population back to 11.3 $\pm$ 3.2% (Fig 4A, transfected cells).

AMPK activation, clonogenic survival and proliferation. We investigated the effects of IR, CC and metformin on A549 and H1299 cell clonogenic survival. The surviving fraction of cells after 2 Gy (SF2) was 45 $\pm$ 5.0% and 40 $\pm$ 1.2% (in A549 and H1299

cells, respectively) (Fig. 4D). CC alone (1μM) showed a trend to enhance but did not affect significantly basal clonogenic survival, but caused resistance to IR by increasing SF2 to 66 ± 9.8% and 67 ± 2.9% in A549 and H1299 cells, respectively (Fig. 4D). Similar observations were made in PC3 prostate cancer cells (Fig. E3).

Metformin alone (1-5μM) induced a dose-dependent activation of AMPK (Fig. 4C) and at 5μM reduced basal survival to 65 ± 4.53% and 74 ± 1.21% of control (35% and 26% inhibition in A549 and H1299 cells, respectively). However, it also enhanced significantly the IR-activation of AMPK (Fig. 4C) and reduced SF2 further to 28 ± 2.1% and 27 ± 1.15% of control (40% inhibition on SF2 in both cell lines, Fig. 4D), offering at least an additive effect to that of IR. Similar results were obtained in PC3 prostate cancer cells (Fig. E3).

Discussion:

AMPK is recognized as a mediator of tumour suppressor pathways. We, i) explored the regulation of AMPK by IR in human epithelial cancer cells, ii) began analyzing upstream regulators of AMPK activation and downstream effectors and iii) showed evidence of involvement of this enzyme in the IR-induced checkpoint control and clonogenic survival. Furthermore, using the biguanide metformin we have shown that AMPK may be targeted pharmacologically to enhance the IR responses.

IR activation of AMPK.

The regulation of AMPK by therapeutic doses of IR was not examined earlier in cancer cells. Zhang et al. (2008) (16) suggested that UVB inhibits AMPK activity in human keratinocytes, by downregulation of LKB1, while Cao (2009) et al. (17) suggested that

UV-A/-B radiation activates AMPK, in the same cells, through the EGF receptor and LKB1. These results are contradictory and suggest a need for further studies on the regulation of AMPK by UV irradiation.

Our results in lung, prostate and breast cancer cells (Fig. 1 and 3) suggest that activation of AMPK may be a universal effect of IR in human carcinomas. This appears to involve initial nuclear phosphorylation and activation of the enzyme and subsequent translocation into the cytoplasm without a significant alteration of its total cellular levels (Fig. 1). We observed rapid phosphorylation of nuclear AMPK in response to IR, in parallel with induction of the DSB marker γH2Ax (Fig. 2) but no convincing co-localization of the two markers, even at the early times after IR. In addition, we have not observed a modification of the subcellular distribution of total AMPK levels in response to IR (Fig E4). Delayed detection of P-AMPK in the cytoplasm (15min to 1h) suggests that the activated enzyme may translocate from the nucleus into the cytoplasm. Such shuttling of AMPK between nucleus and cytoplasm is suggested to be facilitated by the nuclear exporter Crm1 (18).

Mediators of AMPK activation by IR. IR-activation of AMPK in both LKB1-wild type (H1299) and LKB1-null (A549) cells indicated that LKB1 is not required for activation of AMPK by IR. The concurrent phosphorylation of AMPK and H2Ax after IR suggested a relationship between AMPK activation and ATM. We addressed the role of ATM using the ATM inhibitor KU-55933. The well established specificity of KU-55933 for ATM, which is based on a morpholine moiety on this molecule (15), suggests that ATM may indeed be an upstream regulator of AMPK activity. ATM may interact directly with

AMPK. ATM was shown to phosphorylate purified AMPK α subunit *in-vitro* (19). Consistent with other studies showing ATM-dependent activation of AMPK by Insulin-like Growth Factor-I (IGF-I) (19) or AICAR (20), our results suggest that IR activates AMPK through an LKB1-independent and ATM-dependent pathway. We illustrate this notion in a model in Fig. 5.

Downstream effectors of AMPK. Studies have suggested that AMPK regulates cell cycle and apoptosis through induction of the tumour suppressor of p53 and the CDK inhibitor $p21^{waf/cip}$ (7). We observed that IR rapidly increases the levels p53 and $p21^{waf/cip}$ in lung cancer cells (Fig. 3C). The dependence of p53 and $p21^{waf/cip}$ induction on AMPK was demonstrated by use of both inhibition of AMPK with CC and molecular knockdown with anti-AMPK-α-siRNA (Fig. 3C-E). Inhibition of AMPK phosphorylation by CC has been observed by other investigators (21). CC may inhibit potential upstream AMPK-kinases, because it is known to have activity on other kinases (22). Nevertheless, in our experiments CC produced effects equivalent to AMPK-α-subunit knockdown, suggesting that CC remains a useful tool for analysis of AMPK action. In support of this notion, CC did not inhibit IR-induced ATM and Chk2 phosphorylation in A549 cells (Fig. E5).

Our results suggest that AMPK regulates IR induction of p53 and $p21^{waf/cip}$ (Fig. 3C-E). They are consistent with results of other investigators. Zhou et al. (2009) showed that AMPK inhibition blocks p53 and $p21^{waf/cip}$ expression and cell cycle progression (23) in prostate cancer cells. Future studies should clarify whether the IR induction of p53 and $p21^{waf/cip}$ expression is due to transcriptional regulation or protein stabilization.

p53 transactivates the promoter of *CDKN1A*, the gene encoding $p21^{waf/cip}$. However, this promoter is also regulated by other mediators and transcription factors independent of p53 (24). We observed a p53-independent induction of $p21^{waf/cip}$ by IR as it increased $p21^{waf/cip}$ levels in p53-null H1299 cells (Figs 3C and 4B). We obtained identical results in p53-null PC3 prostate cancer cells (data not shown). This notion has been described earlier (25, 26) and it is depicted in our model (Fig. 5).

Effects on cell cycle.

G2/M inter-phase arrest is a well described IR-induced checkpoint (27). $p21^{waf/cip}$ inhibits the cdc2/Cyclin B complex regulating the G2/M transition (28). We expected that AMPK and $p21^{waf/cip}$ inhibition would abolish IR-induced arrest of cell cycle at G2/M. Indeed, we observed that (Fig. 4A) after either biochemical (CC) or molecular (anti-AMPK-α-siRNA) inhibition of AMPK (Fig. 4A and Fig. E2). Cells show increased radiosensitization at the G2/M phase of the cycle (27), and modification of the G2/M checkpoint by AMPK illustrates its importance in radiation biology. Interestingly, the phosphorylated AMPK α-subunit appears to associate with the mitotic apparatus in dividing cells (29). These findings are congruent with a role of AMPK in G2/M checkpoint suggested by our work.

Effects on clonogenic survival and proliferation.

AMPK and IR regulation of clonogenic survival: A key observation in this study is the involvement of AMPK in IR-induced cytotoxicity. Inhibition of AMPK mediated resistance of lung cancer cells to IR independent of p53 status (Fig. 4D). We made similar observations in p53-null prostate cancer cells (Fig. E3). Jones et al. (2005) (6),

suggested that AMPK mediates p53-dependent G1/S phase arrest and inhibition of proliferation in glucose-deprived mouse embryonic fibroblasts (MEFs). In this report we suggest that in human cancer cells, AMPK facilitates an IR-mediated, p53-independent, G2/M checkpoint and inhibition of survival (as shown by the model in Fig. 5). AMPK may be able to engage different signaling pathways to regulate cell cycle and proliferation in different cells.

Metformin activates AMPK and modifies IR responses: Metformin is an inhibitor of complex I of the mitochondrial respiratory chain that is believed to activate AMPK through an increase in the AMP:ATP ratio (4). We observed that micromolar doses (1-5μM) of metformin alone stimulated AMPK phosphorylation, inhibited clonogenic survival, and enhanced the effects of IR on the two processes (Fig. 4C-D). Our on-going studies show complete reversal of these effects of metformin by CC (not shown) indicating that AMPK may indeed be the mediator of metformin action.

Earlier studies reported requirement of millimolar (mM) doses of metformin to detect an anti-proliferative action of the drug in standard proliferation assays (30). For that, we performed recently standard proliferation experiments in A549 and H1299 cells using increasing doses of metformin. In those experiments we observed a need for higher doses of metformin (2.5-5mM), to obtain significant inhibition on cell proliferation both as a single agent and in combination with IR (Fig. E6). We hypothesize that this discrepancy reflects differences in physiological processes participating in clonogenic survival vs. standard proliferation assays. The presence of a higher number of cells in proliferation assays may have a trophic effect on cancer cells that is adequate to counteract the

inhibition of growth that can be exerted by micromolar doses of metformin. We are examining this further in on-going studies. Metformin may be able to function as an adjunct to radiotherapy in the clinical setting but *in-vivo* studies should first show its efficacy as a radiation sensitizer in *in-vivo* cancer models and clinical studies should establish the maximum tolerated dose of the drug in cancer patients. Overall, our results encourage further investigation of metformin in combination with radiation in carcinoma models.

Conclusions:

In human cancer cells, IR activates AMPK in an LKB1-independent manner to, (1) enhance the cellular levels of p53 and the CDK inhibitor $p21^{waf/cip}$, (2) regulate progression of cells through the G2/M phase of the cell cycle, and (3) inhibit clonogenic survival. Our work suggests that AMPK participates in a signaling axis involving ATM and the CDK inhibitor $p21^{waf/cip}$ (see model in Fig. 5). We also show that the anti-diabetic drug metformin can potentiate the IR activation of AMPK and enhance the cytotoxic effects of IR in cancer cells. AMPK appears to participate in a signaling pathway activated by IR that may be targetable by metformin to further enhance IR responses in human carcinomas.

References:

1. Canman CE, Lim DS. The role of ATM in DNA damage responses and cancer. *Oncogene* 1998;17:3301-3308.
2. Batchelor E, Loewer A, Lahav G. The ups and downs of p53: understanding protein dynamics in single cells. *Nat Rev Cancer* 2009;9:371-377.
3. Hardie DG. AMP-activated/SNF1 protein kinases: conserved guardians of cellular energy. *Nat Rev Mol Cell Biol* 2007;8:774-785.
4. Steinberg GR, Kemp BE. AMPK in Health and Disease. *Physiol Rev* 2009;89:1025-1078.
5. Jones RG, Thompson CB. Tumor suppressors and cell metabolism: a recipe for cancer growth. *Genes Dev* 2009;23:537-548.
6. Jones RG, Plas DR, Kubek S*, et al.* AMP-activated protein kinase induces a p53-dependent metabolic checkpoint. *Mol Cell* 2005;18:283-293.
7. Hardie DG. AMP-activated protein kinase as a drug target. *Annu Rev Pharmacol Toxicol* 2007;47:185-210.
8. Jiralerspong S, Palla SL, Giordano SH*, et al.* Metformin and pathologic complete responses to neoadjuvant chemotherapy in diabetic patients with breast cancer. *J Clin Oncol* 2009;27:3297-3302.
9. Zietman AL, DeSilvio ML, Slater JD*, et al.* Comparison of conventional-dose vs high-dose conformal radiation therapy in clinically localized adenocarcinoma of the prostate: a randomized controlled trial. *Jama* 2005;294:1233-1239.

10. MacRae R, Choy H. Concurrent chemoradiotherapy for inoperable stage III non-small-cell lung cancer. *Curr Oncol Rep* 2003;5:313-317.

11. Sapkota GP, Deak M, Kieloch A*, et al.* Ionizing radiation induces ataxia telangiectasia mutated kinase (ATM)-mediated phosphorylation of LKB1/STK11 at Thr-366. *Biochem J* 2002;368:507-516.

12. Chan N, Koritzinsky M, Zhao H*, et al.* Chronic hypoxia decreases synthesis of homologous recombination proteins to offset chemoresistance and radioresistance. *Cancer Res* 2008;68:605-614.

13. Choudhury A, Zhao H, Jalali F*, et al.* Targeting homologous recombination using imatinib results in enhanced tumor cell chemosensitivity and radiosensitivity. *Mol Cancer Ther* 2009;8:203-213.

14. Matsumoto S, Iwakawa R, Takahashi K*, et al.* Prevalence and specificity of LKB1 genetic alterations in lung cancers. *Oncogene* 2007;26:5911-5918.

15. Hickson I, Zhao Y, Richardson CJ*, et al.* Identification and characterization of a novel and specific inhibitor of the ataxia-telangiectasia mutated kinase ATM. *Cancer Res* 2004;64:9152-9159.

16. Zhang J, Bowden GT. UVB irradiation regulates Cox-2 mRNA stability through AMPK and HuR in human keratinocytes. *Mol Carcinog* 2008;47:974-983.

17. Cao C, Lu S, Kivlin R*, et al.* AMP-activated protein kinase contributes to UV- and H2O2-induced apoptosis in human skin keratinocytes. *J Biol Chem* 2008;283:28897-28908.

18. Kodiha M, Rassi JG, Brown CM*, et al.* Localization of AMP kinase is regulated by stress, cell density, and signaling through the MEK-->ERK1/2 pathway. *Am J Physiol Cell Physiol* 2007;293:C1427-1436.

19. Suzuki A, Kusakai G, Kishimoto A*, et al.* IGF-1 phosphorylates AMPK-alpha subunit in ATM-dependent and LKB1-independent manner. *Biochem Biophys Res Commun* 2004;324:986-992.

20. Sun Y, Connors KE, Yang DQ. AICAR induces phosphorylation of AMPK in an ATM-dependent, LKB1-independent manner. *Mol Cell Biochem* 2007;306:239-245.

21. Mukherjee P, Mulrooney TJ, Marsh J*, et al.* Differential effects of energy stress on AMPK phosphorylation and apoptosis in experimental brain tumor and normal brain. *Mol Cancer* 2008;7:37.

22. Bain J, Plater L, Elliott M*, et al.* The selectivity of protein kinase inhibitors: a further update. *Biochem J* 2007;408:297-315.

23. Zhou J, Huang W, Tao R*, et al.* Inactivation of AMPK alters gene expression and promotes growth of prostate cancer cells. *Oncogene* 2009;28:1993-2002.

24. Abbas T, Dutta A. p21 in cancer: intricate networks and multiple activities. *Nat Rev Cancer* 2009;9:400-414.

25. Macleod KF, Sherry N, Hannon G*, et al.* p53-dependent and independent expression of p21 during cell growth, differentiation, and DNA damage. *Genes Dev* 1995;9:935-944.

26. Huang L, Sowa Y, Sakai T*, et al.* Activation of the p21WAF1/CIP1 promoter independent of p53 by the histone deacetylase inhibitor suberoylanilide hydroxamic acid (SAHA) through the Sp1 sites. *Oncogene* 2000;19:5712-5719.

27. Rudoltz MS, Kao G, Blank KR*, et al.* Molecular Biology of the Cell Cycle: Potential for Therapeutic Applications in Radiation Oncology. *Semin Radiat Oncol* 1996;6:284-294.

28. Woo RA, Poon RY. Cyclin-dependent kinases and S phase control in mammalian cells. *Cell Cycle* 2003;2:316-324.

29. Vazquez-Martin A, Oliveras-Ferraros C, Menendez JA. The active form of the metabolic sensor: AMP-activated protein kinase (AMPK) directly binds the mitotic apparatus and travels from centrosomes to the spindle midzone during mitosis and cytokinesis. *Cell Cycle* 2009;8:2385-2398.

30. Zakikhani M, Dowling R, Fantus IG*, et al.* Metformin is an AMP kinase-dependent growth inhibitor for breast cancer cells. *Cancer Res* 2006;66:10269-10273.

Footnotes:

We appreciate the technical help from Dr. J-P Lu and Mrs. Myrna Espiritus and valuable comments from Dr. Philip Bilan (Sick Children Hospital, Toronto, ON) and Dr. Evangelia Tsiani, (Brock University, St. Catharines, ON) towards the preparation of this manuscript. We appreciate the support from Dr. William K. Evans, (CEO, Juravinski Cancer Center) towards the pursuit of these studies. Financial support was received from the Juravinski Cancer Center and the Hamilton Health Science Foundations.

Abbreviations: IR: ionizing radiation; AMPK: AMP-activated kinase; ATM: ataxia telengiectasia mutated; γH2Ax: phosphorylated histone H2Ax; DSB: double strand break of DNA; CDK: cyclin-dependent kinase; ACC: acetyl-Co enzyme A carboxylase; Compound C: CC; SF2: fraction of cells surviving after 2 Gy or radiation; FBS: Fetal Bovine Serum; (P-): phosphorylated;

Figures:

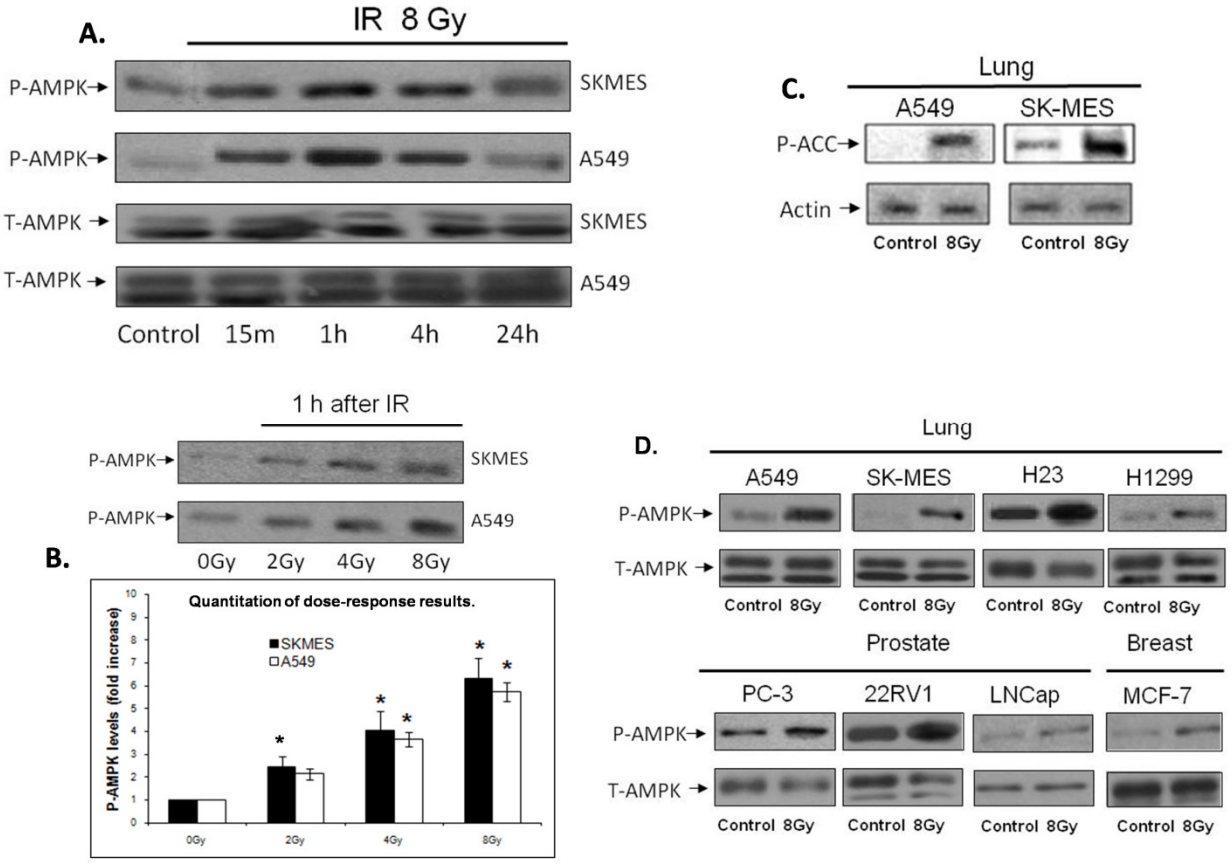

Figure 2.1: IR activates AMPK in human carcinoma cells. Lung, prostate and breast cancer cells were treated with the indicated dose of IR and subjected to lysis and immunoblotting at indicated times. (A) Time-course of AMPK (T-AMPK) phosphorylation (P-AMPK) after 8Gy of IR. (B) Dose-dependence of AMPK phosphorylation by IR. A representative immunoblot is shown. The bar graph shows densitometry results from three independent experiments (*:P<0.05). (C) IR activates AMPK. Untreated or 8 Gy IR-treated cells were subjected to lysis and immunoblotting with an anti-P-ACC antibody (P-ACC). Anti-actin immunoblotting was used as a loading

control. (D) IR activates AMPK in multiple carcinoma cells. Cells were treated with 0 or 8 Gy IR, lysed and subjected to immunoblotting. Representative blots from at least 3 experiments for each condition are shown.

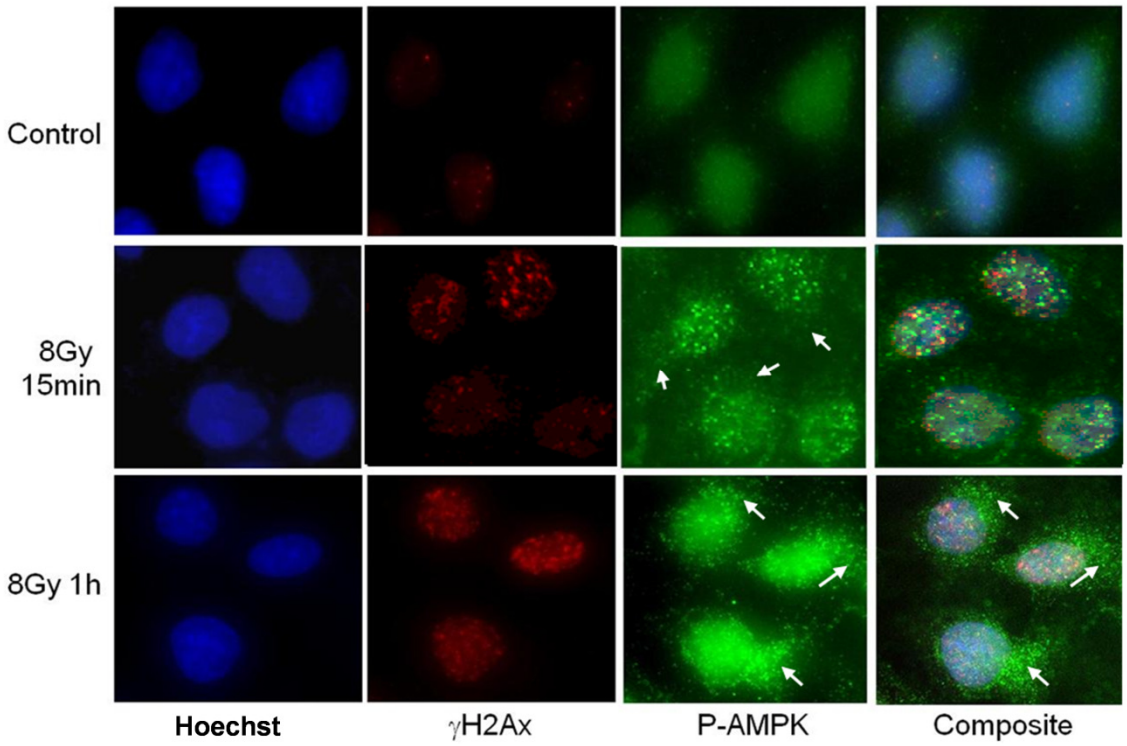

Figure 2.2: Subcellular distribution of phosphorylated AMPKα (P-AMPK). A549 cells were treated with 8 Gy of IR, fixed, and permeabilized after the indicated times (15min or 1h). Cells were labeled with anti-γH2Ax and -P-AMPK antibodies, stained with Hoechst 33258 DNA stain, and examined by microscopy (60x magnification). The arrows indicate extra-nuclear P-AMPK signal. Representative results of 3 experiments are shown.

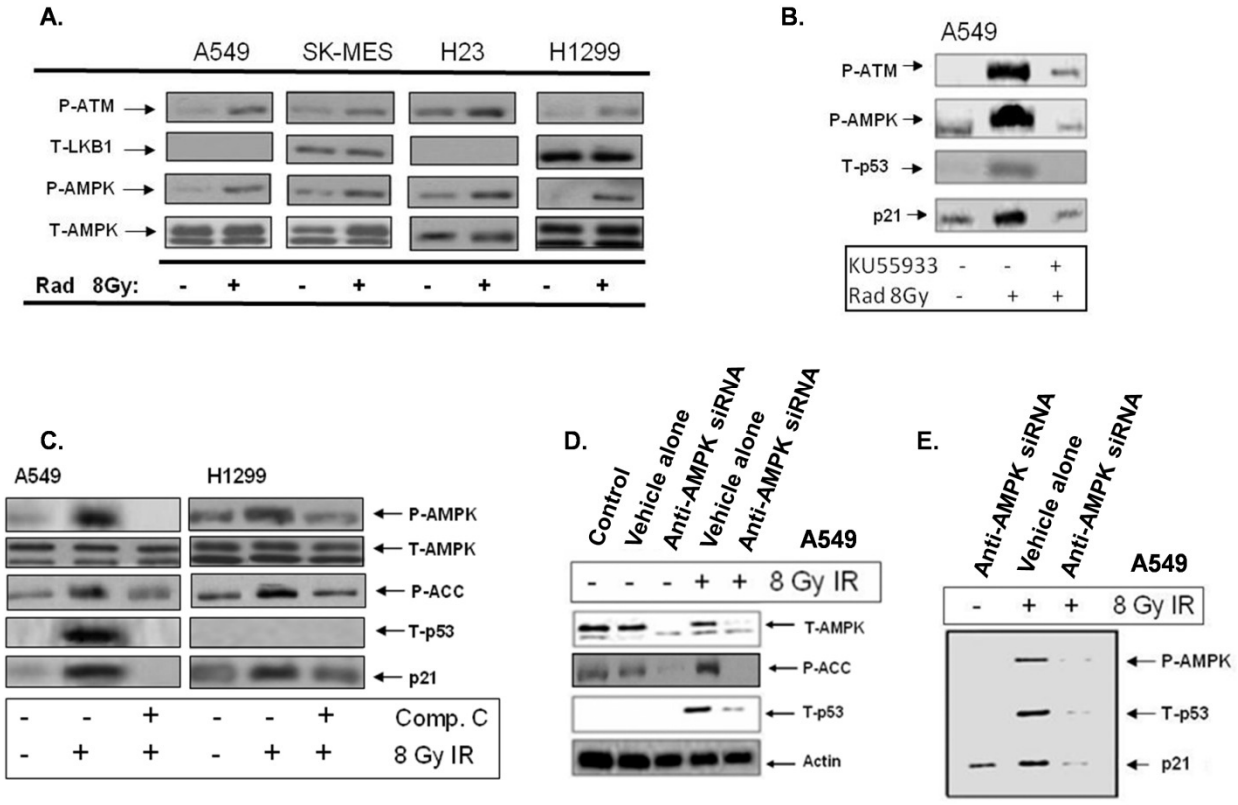

Figure 2.3: Upstream regulators and downstream effectors of AMPK. **(**A) LKB-1-independent activation of AMPK. (B) AMPK activation is dependent on ATM. Lung cancer (A549, SK-MES1, NCI-H23 and NCI-H1299) cells were treated with 0 or 8 Gy of radiation after pre-treatment with or without the ATM inhibitor KU55933 (10μM). Cells were lysed and subjected to immunoblotting with indicated antibodies. Representative immunoblots of 4 experiments are shown. (C) AMPK inhibition by Comp. C (CC) blocks IR-induced phosphorylation of ACC and expression of p53 and $p21^{waf/cip}$ (p21). A549 and H1299 cells were pre-treated with Comp. C (25 μM) before IR, followed by immunoblotting. (D) anti-AMPK-α-siRNA inhibits AMPK expression and activation and

IR-induction of p53. (E) Anti-AMPK-α-siRNA inhibits activation of AMPK and IR-induced expression of p53 and $p21^{waf/cip}$. A549 cells were subjected to molecular knockdown of AMPK and treated with IR (0 or 8 Gy), followed by incubation (1h), lysis, and immunoblotting.

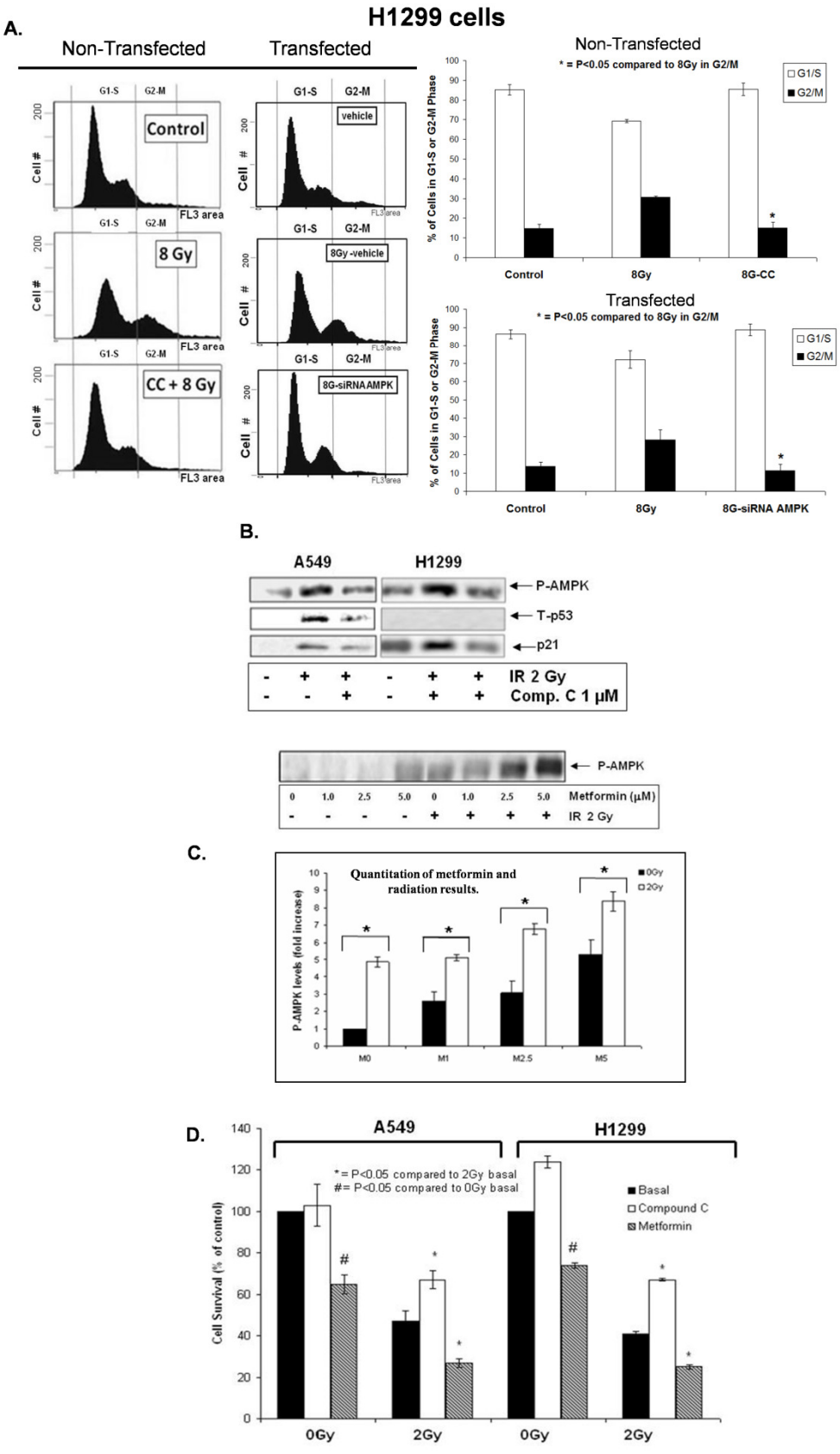
A.
H1299 cells
Non-Transfected
Transfected
Control
vehicle
8 Gy
8Gy -vehicle
CC + 8 Gy
8G-siRNA AMPK
G1-S
G2-M
Cell #
FL3 area
Non-Transfected
* = P<0.05 compared to 8Gy in G2/M
% of Cells in G1-S or G2-M Phase
G1/S
G2/M
Control
8Gy
8G-CC
Transfected
* = P<0.05 compared to 8Gy in G2/M
8G-siRNA AMPK
B.
A549
H1299
P-AMPK
T-p53
p21
IR 2 Gy
Comp. C 1 µM
Metformin (µM)
C.
Quantitation of metformin and radiation results.
P-AMPK levels (fold increase)
0Gy
2Gy
M0
M1
M2.5
M5
D.
A549
H1299
*= P<0.05 compared to 2Gy basal
#= P<0.05 compared to 0Gy basal
Cell Survival (% of control)
Basal
Compound C
Metformin
0Gy
2Gy

Figure 2.4: AMPK participates in IR-regulation of cell cycle and survival. (A) AMPK is involved in IR-regulation of cell cycle. Nontransfected H1299 cells were pre-treated with CC (1μM) for 1h, or not, before treatment with 0 or 8Gy IR (nontransfected). Other cells were transfected with either vehicle alone (vehicle) or anti-AMPK-α-siRNA and were treated with 0 or 8 Gy IR (transfected). Cell cycle phase was analyzed 24h later. Mean results of 3-4 independent experiments are shown in bar graphs. (B) Effects of Compound C (Comp. C) on AMPK phosphorylation (P-AMPK) and induction of p53 and $p21^{waf/cip}$ (p21). A549 or H1299 cells were pre-treated with low doses of Comp. C (1μM) for 1 h before exposure to 2 Gy of IR followed by lysis and immunoblotting. (C) A549 cells were treated with the indicated concentrations of metformin for 1 h before exposure to 2 Gy or IR followed by lysis and immunoblotting. Bar graphs showing densitometry results (Mean$\pm$SE) of three experiments (* $P<0.05$). (D) AMPK inhibition induces radiation resistance, and metformin potentiates IR-induced clonogenic death. Clonogenic assays were pursued with A549 and H1299 cells that were subjected to 0 or 2 Gy of IR without or with pre-incubation with CC (1μM) or metformin (5μM). The results are the Mean$\pm$SE of 3-4 independent experiments.

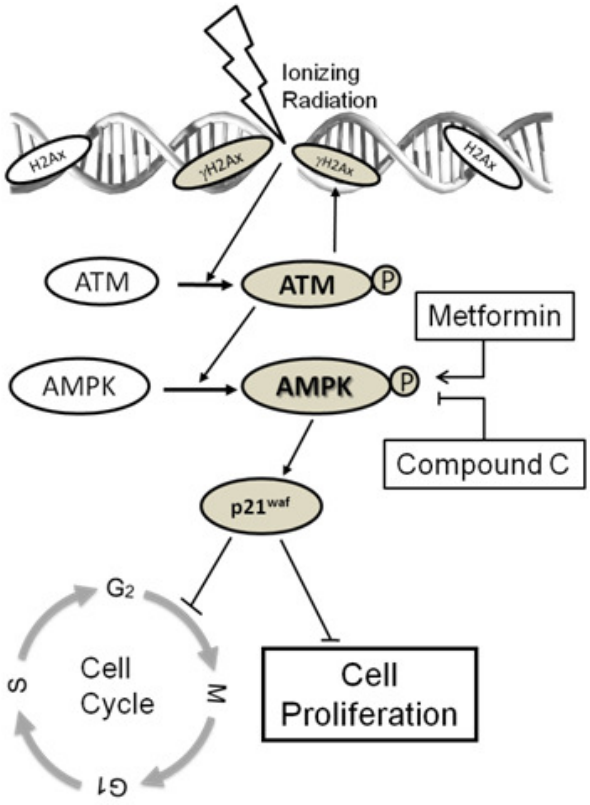

Figure 2.5: Model of molecular pathway of AMPK regulation by IR and its effects on cell cycle and survival. Our results suggest that in cancer cells, IR activates AMPK in an ATM-dependent, LKB1-independent, fashion leading to induction of $p21^{waf/cip}$ expression, regulation of G2/M checkpoint and clonogenic death. AMPK appears to mediate a tumor suppressor pathway that can be targeted by metformin to enhance radiation responses.

Supporting Experiments

Due to space restriction and critical feedback from reviewers, some of the experimental data have not been incorporated in the final version of the paper. However, these experiments were mainly conducted as appropriate controls to validate the specificity of our antibodies, siRNA sequences, and chemical inhibitors (compound C) for AMPK. A list of supporting figures is listed below, as well as a brief explanation of their relevance to the manuscript.

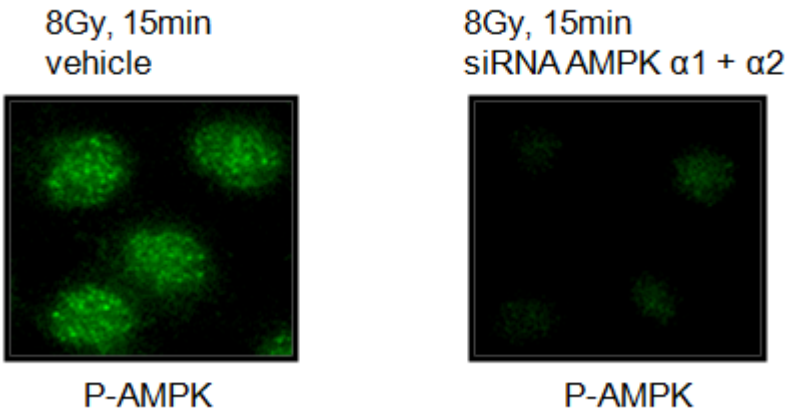

Figure 2.S1: Immunofluorescence microscopy with the anti-Phospho-AMPK antibody in cells transfected with either vehicle alone or siRNA against AMPK α1 + α2. A549 were transfected with either vehicle alone or anti-(α1 + α2 subunit) AMPK siRNA. Cells were incubated for 72 hours and were then subjected to 8 Gy of IR and were fixed and permeabilized 15 min later. Cells were then labelled with anti-phospho-AMPK (α subunit T172, [P-AMPK]) antibody and examined by wide-field fluorescence microscopy.

This experiment was conducted to test the specificity of our phospho-AMPK antibody to be used for immunofluorescence.

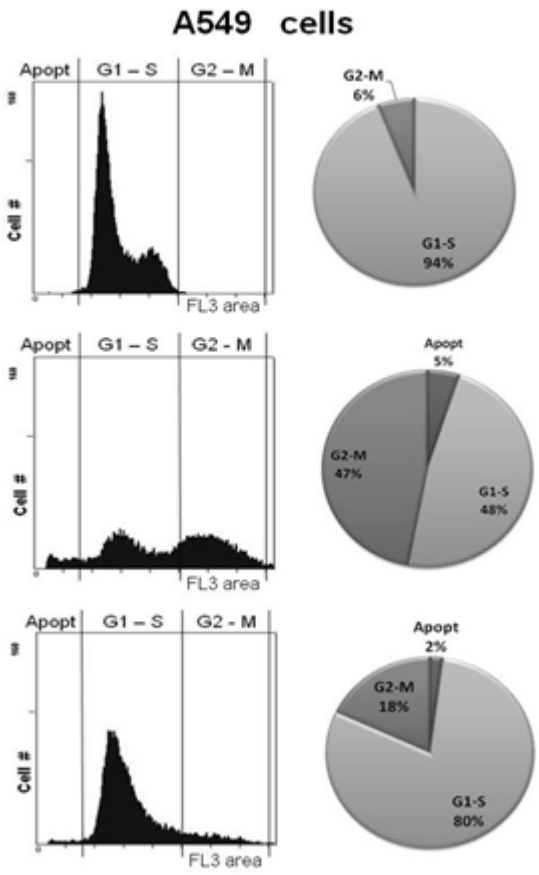

Figure 2.S2: AMPK inhibition with Compound C inhibits the radiation-induced G2-M arrest. A549 cells were pre-treated, or not, with Compound C (1μM) before exposure to 0 or 8 Gy or radiation. Cell cycle analysis was pursued 48 h later.

I initially conducted cell cycle analysis using compound C to block AMPK activity. However, the reviewers were worried about the potential "off-target" effect of this inhibitor. Thus, for the final version of the paper I utilized siRNA against AMPK instead, and kept this figure as supplemental data.

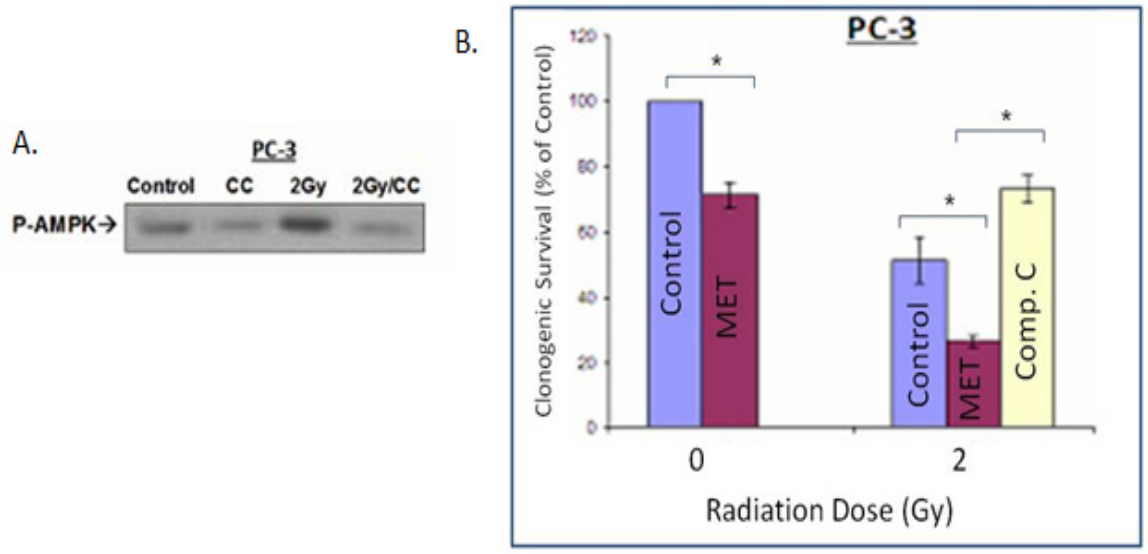

Figure 2.S3: Effects of Compound C and Metformin in PC3 prostate cancer cells. **(**A) PC3 prostate cancer cells were pre-treated with Compound C (CC) (1 μM) before exposure to 2Gy IR followed by incubation for 1 hour, lysis and immunoblotting. (B) Clonogenic survival assays were pursued with PC3 cells that were subjected to 2 Gy of IR without or with pre-incubation with either Compound C (1 μM) or metformin (5 μM), as described in Methods (* $P<0.05$).

This experiment was conducted to demonstrate that modulation of AMPK activity with compound C or metformin could affect radiation sensitivity in prostate cancer cells. This also helped me to put forward the notion that this may be a universal effect in cancer cells, and not just restricted to lung cancer cell lines.

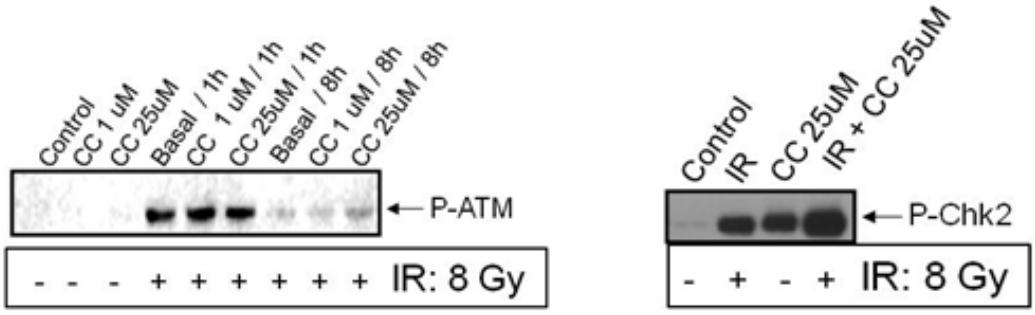

Figure 2.S4: Effects of Compound C on the radiation induced phosphorylation of ATM and Chk2. A549 Lung cancer cells were either left untreated or pretreated with the indicated concentration of compound C (1 or 25 uM) for 1 hour followed by treatment with 8 Gy of IR or not. Cells were then lysed 1 h after radiation (or 8 h after IR only where indicated) and were subjected to electrophoresis and immunoblotting.

This experiment was conducted to demonstrate that compound C does not dramatically affect IR-induced ATM/Chk2 signalling. Conceptually this makes sense since ATM is upstream of AMPK in our model, and compound C should ideally only target AMPK for inhibition.

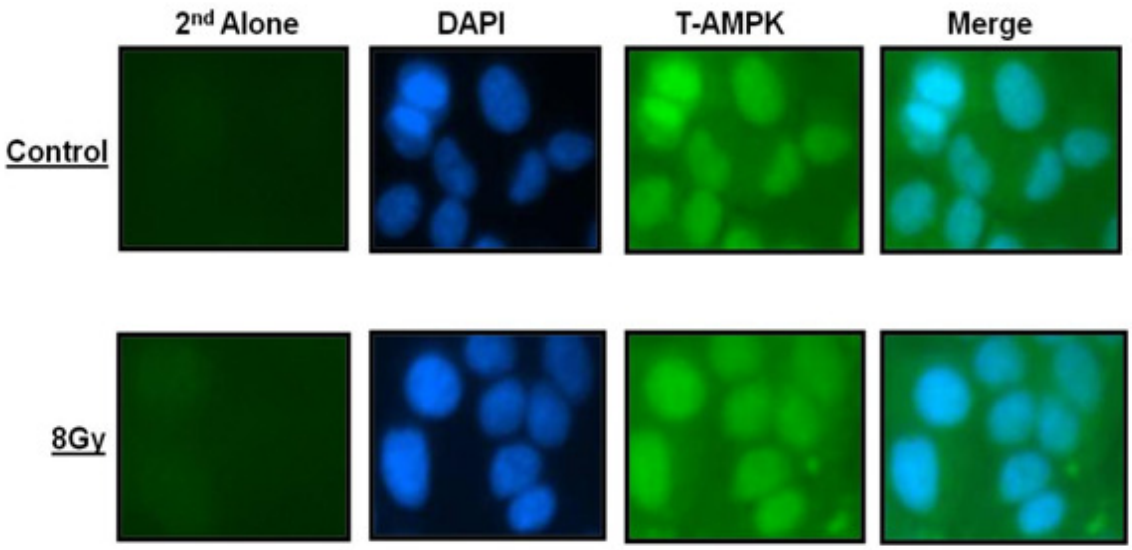

Figure 2.S5: Immunofluorescence microscopy with the anti-Total- AMPK antibody. A549 were treated with 8 Gy of IR or not and fixed and permeabilized after 1 h. Cells were then labelled with anti-total-AMPK antibody, stained with Hoechst 33258 DNA stain and examined by wide-field fluorescence microscopy.

Immunofluorescence was performed with a total-AMPKα antibody to examine if it follows a similar sub-cellular distribution pattern as phosphorylated AMPKα. At 1h, 8Gy IR does not affect the expression or distribution of total AMPKα significantly.

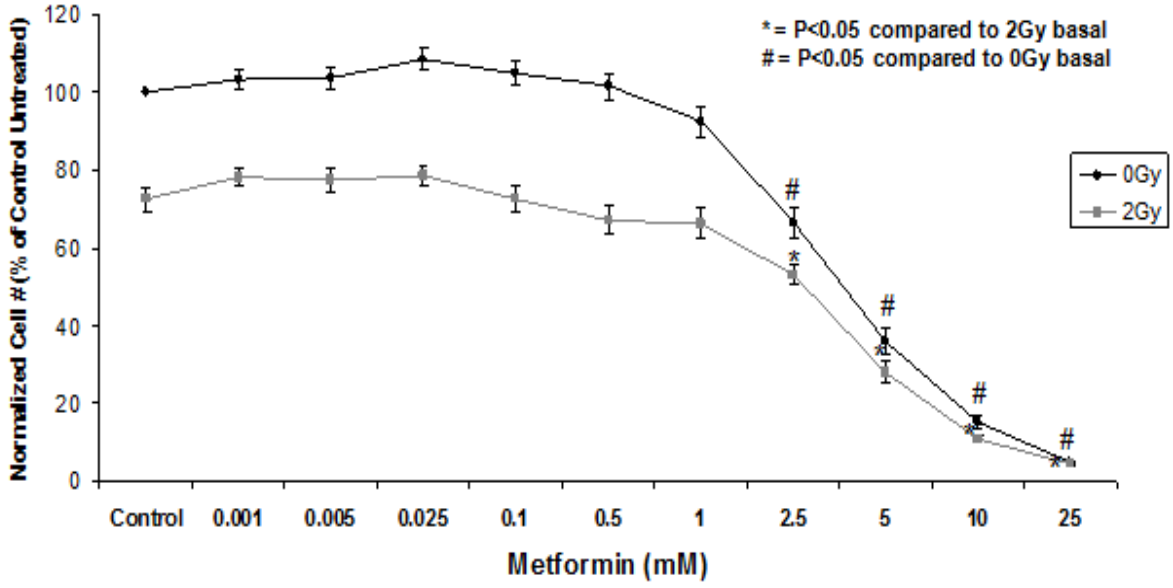

Figure 2.S6: Cell Proliferation Assay with Metformin and ionizing radiation (IR). A549 were treated with the indicated concentrations of metformin 1h prior to exposure to 0-2 Gy of IR and maintained for an additional 96h in an incubator. Cell number was evaluated using the Hoechst stain method (20µg/mL Hoechst 33258 in Tris-NaCl-EDTA (TNE) buffer). The DNA fluorescence was determined using the Cyto-Fluor Multi-well Plate Reader (Applied Biosystems, Toronto) which was then converted to cell number by fitting these values to a standard cell curve. The values were normalized to the untreated control group.

This standard proliferation assay was requested to be used by a review, as it is a commonly utilized tool to measure cancer cell proliferation in response to chemotherapeutic drugs. However, the observed differences in metformin concentration required to have radiosensitizing effects compared to a clonogenic survival assay may be

attributed to how each assay measures cell proliferation. Clonogenic survival assays are considered the "gold standard" for measuring the radiosensitivity of a population of cells. However, a significant disadvantage to this technique is that it is very time-consuming. Conversely, standard proliferation assays (in this case using Hoechst 33258 stain) measures total DNA content to assess cell survival. This method is much faster and allows researchers to screen multiple drugs in one experiment (multi-well plate format), but it does not reliably test true mitotic viability. Thus, many studies have indicated that 1-10mM concentrations of metformin are required to inhibit cancer cell survival (Dowling et al., 2007; Rocha et al., 2011) using standard proliferation assay. However, we have observed in this study that 5μM metformin is sufficient to sensitize A549 cells to IR based on clonogenic survival.

Chapter 3: Lovastatin Sensitizes Lung Cancer Cell to Ionizing Radiation

This chapter contains an author generated version of the paper "Lovastatin sensitizes lung cancer cells to ionizing radiation. Modulation of molecular pathways of radioresistance and tumour suppression", published in the *Journal of Thoracic Oncology* in March 2011. Permission was generously provided by Wolters Kluwer Health (licence # 2761430660841). Please see appendix 3 for an attached copyright licence.

For this paper, I performed A549 cell culture, as well as cultured SK-MES-1 cells which were provided as supplemental data. In addition, I performed western blotting, all immunofluorescence and cell cycle experiments, and generated all of the manuscript figures. Clonogenic survival and cell proliferation assays were carried out by the lab technicians Caiqiong Liu and Sarah Hopmans respectively. I also made significant contributions to the introduction and discussion of the paper, but the outline for the written text of the manuscript was provided by Dr. Theodoros Tsakiridis. Helpful review and suggestions were made by all listed authors for this manuscript.

Context and Background Information

As a continuation of my previous research, I sought to investigate the potential of clinically used drugs to act as radiation sensitizers in cancer cells. Statins are a large family of cholesterol lowering drugs that specifically target and inhibit 3-hydroxy-3-methylglutaryl coenzyme A (HMG-CoA) reductase (Boudreau, Yu, & Johnson, 2010).

Lovastatin is one of the most commonly used statins for cancer research, but its potential as a radiation sensitizer for lung cancer has not been examined. Thus, I initiated

studies to explore the effect of lovastatin alone, and its combined effect with IR on the survival of radiation-resistant A549 lung cancer cells. In addition, I examined the molecular mechanism by which lovastatin inhibits cancer cell survival and its synergistic effects with radiation on signalling pathways involved in radiation resistance and tumour suppression. I was particularly interested to see if lovastatin, like metformin, could activate AMPK and potentiate IR-induced AMPK phosphorylation.

To address the ability of lovastatin to inhibit lung cancer cell survival I initially performed a dose-response in A549 cells (0-50μM range). The clonogenic survival of these cells was significantly inhibited with 10μM lovastatin alone, and was completely abolished with 25-50μM lovastatin. To address its role as a radiation sensitizer, I utilized concentrations of lovastatin between 5-10μM since this was the range where noticeable reductions in clonogenic survival were observed. Indeed, lovastatin significantly enhanced the cytotoxic action of IR, but this effect was reversed in the presence of mevalonate, which is the product of statin inhibition in the cholesterol signalling pathway.

I then began to explore the mechanism of lovastatin action on lung cancer cell signalling. The epidermal growth factor receptor (EGFR) stimulates a number of substrates that supports cell proliferation and radiation resistance, including Ras, Akt, Erk, and mTOR (Zimmermann, Zouhair, Azria, & Ozsahin, 2006). Furthermore, many non-small cell lung cancer (NSCLC) lines, including A549's overexpress EGFR (Xu et al., 2011). To investigate if EGFR-mediated pro-survival signalling was blocked by lovastatin, I treated A549 cells with epidermal growth factor (EGF) alone, or in combination with 5-10μM lovastatin. EGF is a widely used research tool to enhance

growth factor signalling and EGF potently stimulated EGFR, as well as downstream Akt and Erk phosphorylation. However, 24h pre-incubation with lovastatin significantly blocked EGF-induced EGFR and Akt phosphorylation, without dramatically effecting Erk signalling. I observed a similar trend by which lovastatin inhibits Akt signalling in response to IR but did not affect IR-mediated Erk signalling; suggesting that lovastatin preferentially inhibits the EGFR-Akt pathway.

My earlier work (Chapter 2) implicated AMPK as an important mediator of IR-induced cell cycle regulation and target for the radiosensitization of cancer cells. In addition, AMPK also shares the same ability as statins to inhibit the HMG-CoA reductase pathway. Thus, I performed western blotting against phosphorylated AMPK and ACC to see if lovastatin could activate and potentiate IR-induced AMPK activity. Indeed, lovastatin enhanced AMPK and ACC phosphorylation alone and also significantly potentiated the ability of IR (2-8Gy) to activate AMPK in A549 cells.

To see if lovastatin had a functional role in modulating cell cycle progression in response to IR, I performed western blotting and cell cycle analysis in A549 cells treated with lovastatin, IR, or the combination of treatments. IR is established to inhibit cell cycle progression through the induction of p53 and the cyclin dependent kinase inhibitors (CDKI's) p27 and p21 (Wahl, Linke, Paulson, & Huang, 1997). Interestingly, when I examined the protein levels of these markers I observed that lovastatin inhibited the induction of p53, p27, and p21 in response to IR. However, when I conducted cell cycle analysis it became apparent that lovastatin primarily shifts these cells into apoptosis instead of mediating cell cycle arrest.

To confirm these findings I also performed western blotting against the apoptotic marker cleaved caspase 3 (CC3), as well as observed the morphological changes in these cells when they were subjected to lovastatin treatment. Lovastatin alone induced significant expression of CC3, and extended the time-frame of IR-induced CC3 formation. In line with my cell cycle and CC3 results, I also observed that lovastatin caused a time-dependent increase in the formation of apoptotic nuclei in A549 cells. Taken together, I put forward a model of lovastatin action where it can inhibit EGFR-Akt induced radiation resistance and systematically activate AMPK, as well as promote apoptosis in lung cancer cells.

Paper: Lovastatin sensitizes lung cancer cells to ionizing radiation. Modulation of molecular pathways of radioresistance and tumour suppression.

Toran Sanli, M.Sc.[*†], Caiqiong Liu, M.Sc.[*], Ayesha Rashid, M.Sc.[*†], Sarah N. Hopmans, M.Sc.[‡], Evangelia Tsiani, Ph.D.[§], Carrie Schultz, B.Sc.[#], Thomas Farrell, Ph.D.[\\#], Gurmit Singh, Ph.D.[‡], James Wright, M.D.[#†] , and Theodoros Tsakiridis, M.D., Ph.D. [*†#]

[*]Translational Radiation Biology Laboratory, Juravinski Cancer Center and Departments of [†]Oncology, [‡]Pathology and Molecular Medicine and [\\]Medical Physics, McMaster University, [#]Division of Radiation Oncology, Juravinski Cancer Center , Hamilton, and [§]Department of Community Health Science, Brock University, St. Catharines, Ontario, Canada

This work was supported by funds from the Juravinski Cancer Center Foundation.

Address Correspondence to:

Theodoros Tsakiridis, M.D., Ph.D.,

Radiation Oncology,

Juravinski Cancer Center,

699 Concession Street,

Hamilton, Ontario,

Canada L8V 5C2,

Email: theos.tsakiridis@jcc.hhsc.ca

Phone: 905-387-9495 Fax: 905-575-6362

Abstract

Introduction: In this study, we investigated the effect of the 3-hydroxy-3-methylgutaryl-CoA reductase inhibitor lovastatin, as a sensitizer of lung cancer cells to ionizing radiation (IR).

Methods: A549 lung adenocarcinoma cells were treated with 0 to 50 μM lovastatin alone or in combination with 0 to 8 Gy IR and subjected to clonogenic survival and proliferation assays. To assess the mechanism of drug action, we examined the effects of lovastatin and IR on the epidermal growth factor (EGF) receptor and AMP- activated kinase (AMPK) pathways and on apoptotic markers and the cell cycle.

Results: Lovastatin inhibited basal clonogenic survival and proliferation of A549 cells and sensitized them to IR. This was reversed by mevalonate, the product of 3-hydroxy-3-methylgutaryl-CoA reductase. Lovastatin attenuated selectively EGF-induced phosphorylation of EGF receptor and Akt, and IR-induced Akt phosphorylation in a mevalonate-sensitive fashion, without inhibition on extracellular signal-regulated kinase 1/2 phosphorylation by either stimulus. IR phosphorylated and activated the metabolic sensor and tumor suppressor AMPK, but lovastatin enhanced basal and IR- induced AMPK phosphorylation. The drug inhibited IR-induced expression of p53 and the cyclin-dependent kinase inhibitors $p21^{cip1}$ and $p27^{kip1}$, but caused a redistribution of cells from G1-S phase (control and radiated cells) and G2-M phase (radiated cells) of cell cycle into apoptosis. The latter was also evident by induction of nuclear fragmentation and cleavage of caspase 3 by lovastatin in both control and radiated cells.

Conclusions: We suggest that lovastatin inhibits survival and induces

radiosensitization of lung cancer cells through induction of apoptosis, which may be mediated by a simultaneous inhibition of the Akt and activation of the AMPK signaling pathways.

Keywords: Lovastatin, Lung cancer, A549 cells, Radiation sensitizer, Apoptosis, Akt, AMPK, Erk, EGFR, Cell cycle, Cleaved caspase 3.

Introduction:

Radiotherapy is a widely used therapy in all stages of Non-Small Cell Lung Cancer (NSCLC). However, NSCLC demonstrate intrinsic radioresistance that leads to failure of even high dose thorasic radiation[1]. Therefore, there is an urgent need for rational development of effective radiation sensitizers for NSCLC, able to inhibit molecular pathways mediating radiation resistance.

Ionizing radiation (IR) elicits signal transduction leading to cell survival, apoptosis and cell cycle regulation[2]. IR-induced DNA double strand breaks (DSBs) are potentially lethal DNA damages leading to activation of phosphatidylinositol 3-kinase (PI3k)-like family protein kinases such as DNA-PK and Ataxia Telengiectasia Mutated (ATM)[3]. ATM mediates phosphorylation of p53 leading to stabilization of this tumour suppressor and cell cycle arrest at the G1-S or the G2-M check points through induction of the *cip*/*kip* family cyclin-dependent kinase inhibitor (CDKI) $p21^{cip1}$ [4]. $p27^{kip1}$, another *cip/kip* family CDKI, functions independently of the p53-$p21^{cip1}$ pathway, inhibits cyclin E-Cyclin Dependent Kinase (CDK) 2 complex and cycle progression through the G1-S checkpoint[4].

Recently, we reported that the energy sensor AMPK, an established effector of the tumour suppressor LKB1, is activated by IR in a variety of epithelial cancer cells[5]. IR activates AMPK in LKB1-independent but ATM-dependent manner leading to induction of p53 and $p21^{cip1}$, cell cycle arrest at the G2-M check point as well as modulation of the sensitivity of cells to IR. IR is also shown to regulate mediators of the signalling pathway of Epidermal Growth Factor Receptor (EGFR)[6, 7], a well established activator of cancer cell proliferation. IR activates the downstream effector pathways of EGFR such as the phosphatidylinositol 3-kinase (PI3k)–Akt-mammalian target of rapamycin (mTOR), and the Raf–Mitogen Activated Protein kinase (MAPK)-kinase (Mek1)-MAPK p42/44 (also known as extracellular signal regulated kinase [Erk1/2]) pathways. These are known to mediate cell survival and radiation resistance, gene expression and protein synthesis[8, 9].

Small GTP-binding proteins of the Ras family such as Ras, Rac and Rho (A/B) mediate signal transduction downstream of EGFR to activate the PI3k-Akt-mTOR and the Raf-Mek-Erk1/2 pathways. Ras mutations are frequent in lung cancer; they occur in both the H- and K-Ras isoforms and were shown to induce radiation resistance in vitro[10, 11]. For that, extensive work is focused on targeting Ras family members with inhibitors of prenylation, a post-translational modification required for membrane targeting and function of Ras[12].

Members of the statin family of 3-Hydroxy-3-methylgutaryl CoA (HMG-CoA) reductase inhibitors are widely used anti-cholesterol agents which inhibit the conversion of HMG-CoA to mevalonate, a rate-limiting step of the mevalonate–cholesterol biosynthesis pathway[13, 14]. This pathway is also vital for the production of farnesyl and

geranylgeranyl moieties required for the post-translational modification and function of Ras and Rho, respectively[13]. For this reason, statins have been studied extensively as anti-tumour agents.

During the past 20 years a large amount of studies have demonstrated the anti-proliferative and pro-apoptotic effects of statins both in-vitro and in animal models of cancer. Growth inhibition, cell cycle arrest and induction of apoptosis in cancer cells has been demonstrated convincingly[15]. The interest in these drugs was enhanced by epidemiological studies indicating that patients on statins may have lower risk for development of colorectal carcinoma[16] and lung cancer[17]. The Veterans Affairs (VA) Health Care System study showed that use of statins for more than 6 months could offer a 55% risk reduction on the incidence of lung cancer[17], indicating that these agents may have significant chemoprevention action. Further, in prostate cancer statin use is suggested to decrease the risk for advanced and metastatic cancer in epidemiological studies[18], to slow disease progression after radical prostatectomy[19] and, importantly, to reduce disease recurrence in patients treated with curative radiotherapy[20, 21].

Lovastatin is probably the most widely studied statin in cancer. It has been shown to possess anticancer properties *in-vitro* and *in-vivo*[14]. The anti-proliferative action of lovastatin has been demonstrated in lung cancer cells[22] but its role as a potential IR sensitizer or adjunct to radiation has not been examined in lung cancer models. Here, we examined the effects of lovastatin on clonogenic survival of lung cancer cells treated without or with IR and explored the effects of this drug on cell cycle, apoptosis and signalling pathways involved in IR resistance.

Methods:

Materials. Roswell Park Memorial Institue (RPMI) media, fetal bovine serum (FBS), trypsin and antibiotic were purchased from Invitrogen (Burlington, ON). Antibodies against, phospho-EGFR, phospho-Akt, phospho-Erk, p53, phospho-AMPK α-subunit, $p21^{cip1}$, $p27^{kip1}$, cleaved caspase 3, actin, and HRP-conjugated anti-rabbit secondary antibody were purchased from Cell Signalling (Mississauga, ON, Canada). Polyvinylidene difluoride (PVDF) membrane was purchased from Pall Corporation (Port Washington, NY). Lovastatin, mevalonate, and Hoechst 33258 were purchased from Sigma (Toronto, ON). A549 cells were from the American Type Culture Collection (ATCC: Manassa, VA).

Cell Culture and Treatments. A549 cells were grown in RPMI media containing 5mM glucose, 10% (vol/vol) FBS and 1% (vol/vol) antibiotic-antimycotic at 37^{o}C as described previously[23]. Cells were treated with the indicated concentrations of lovastatin 24 hours before radiation.

Clonogenic Assay. A549 cells were subjected to clonogenic assays as described earlier[5]. Briefly, 500 or 1000 cells were seeded into individual wells of a 6-well plate in triplicate and maintained at the indicated doses of lovastatin prior to radiation (2-8Gy). After 7 days, cells were fixed and stained with mythelene blue and viable colonies (>50 cells) were counted. Results are expressed as cell survival fraction compared to untreated control. To evaluate radiation sensitization by lovastatin data were fitted to the linear quadratic equation using Graphpad Prism 5 software (La Jolla, CA) as described previously[24].

Proliferation Assay: Approximately 2500 cells were seeded into a 96 well plate and treated with the indicated concentrations of lovastatin before being exposed to 0Gy, 2Gy or 8Gy IR. Ninety six hours later, the cells were washed with PBS, distilled H_20 was added to each well, and the plates stored at -80^oC until completely frozen. The plates were then thawed and stained with Hoechst working solution (20 µg/mL Hoechst 33258 in a TNE buffer), and fluorescence was determined using the Cyto-Fluor Plate Reader (Applied Biosystems, Toronto, ON).

Immunoblotting. Twenty µg of protein was separated by sodium dodecyl sulfate polyacrylamide gel electrophoresis, transferred to PVDF membrane as described earlier[23]. The primary antibody was detected with HRP-conjugated anti-rabbit secondary antibody and enhanced chemiluminescent detection reagent.

Cell Cycle Analysis. The propidium iodine method was used as previously described[5]. Cells were treated with lovastatin (10µM) before treatment with 0 or 8Gy of IR, were and incubated for the indicated times and were then subjected to flow cytometric cell cycle analysis using a FACScan flow cytometer (Beckton Dickinson, Mississauga, ON).

Immunofluorescence Microscopy. Cells grown on glass coverslips for 24h were treated with lovastatin (10µM) for the indicated times. Then, cells were stained with Hoechst 33258 and images were obtained as previously described[5]. Quantitation of apoptotic cells (showing nuclear fragmentation) was performed by counting the average proportion of apoptotic cells in four high power fields on each slide (100 cells counted in each quadrant of each slide). Values were normalized to the untreated control.

Statistical Analysis. Statistical analyses was performed with unpaired T-test, using SPSS v16.0 software (Somers, NY) and are presented as Mean ± SEM of at least three separate experiments.

Results:

Lovastatin inhibits NSCLC cell survival and enhances the cytotoxicity of IR.

We initiated our studies with clonogenic survival assays. Lovastatin alone caused a dose-dependent inhibition of clonogenic survival in A549 cells (Figure 1*A*). The drug began inhibiting clonogenic survival at a dose of 5 μM (10% reduction in survival), inhibited the majority of clonogenic survival at 25 μM (95% reduction in survival) and completely abolished survival at 50 μM (Figure 1*A*).

Lovastatin sensitized A549 cells to IR (Figure 1*B*). Clonogenic assay values were fitted into a linear quadratic model. Both 5 and 10 μM of the drug showed significant radiosensitization of A549 cells to 2–8 Gy of IR. Almost complete inhibition of clonogenic survival was achieved with 10 μM lovastatin in combination with 8Gy IR. In addition we evaluated proliferation through DNA synthesis analysis using the Hoescht DNA staining method. Five micromolar of lovastatin inhibited basal cell proliferation (by 33%; compared to 0 Gy control) without affecting significantly the proliferation levels after IR (Figure 1*C*). However, at 10 μM, the drug inhibited dramatically cell proliferation in both control cells and those radiated with 2 or 8 Gy (by 63% and 90%, respectively).

Mevalonate prevents lovastatin-induced inhibition of clonogenic survival.

We used mevalonate to examine the specificity of lovastatin for the mevalonate-cholesterol synthesis pathway (Figure 1*D*). Two gray of IR decreased clonogenic survival by 44% compared to control. Lovastatin alone (15 μM) inhibited survival by 75% and by 92% when combined with 2 Gy of IR. In these experiments the higher concentration of 15 μM lovastatin was used to examine whether mevalonate is capable of reversing the effects of even high lovastatin doses. Mevalonate (100 μM) inhibited the lovastatin-induced decrease in cell survival in both non-radiated and radiated cells, suggesting that lovastatin mediates its cytotoxic action solely through inhibition of the mevalonate synthesis pathway.

Lovastatin inhibits EGF-stimulated activation of EGFR and Akt.

To analyze the mechanism of action of lovastatin we examined first its effects on EGF-induced EGFR and downstream effector phosphorylation. EGF induced phosphorylation of EGFR, and the Akt and Erk1/2 kinases (Figure 2). However, lovastatin inhibited EGFR and Akt phosphorylation, in a dose-dependent fashion, without affecting phosphorylation of Erk1/2 (Figure 2).

Modulation of IR-stimulated activation of Akt and AMPK.

Control and lovastatin treated cells were subjected to increasing doses of IR and were analyzed by immunoblotting. IR induced a consistent Akt phosphorylation, even with the lower dose of 2 Gy but Erk phosphorylation was seen only after 4-6 Gy (Figure 3*A*-*C*). Interestingly, lovastatin abolished the IR activation of Akt but did not affect significantly Erk1/2 phosphorylation by IR (Figure 3*A*-*C*). The inhibition of IR-induced Akt phosphorylation by lovastatin was completely reversed by addition of mevalonate

(Figure 3*D*-*E*), consistent with clonogenic survival results (Figure 1*D*). IR also caused a dose-dependent phosphorylation of AMPK that was accompanied by activation of this kinase shown by the enhanced phosphorylation of its established substrate Acetyl CoA carboxylase (P-ACC), as observed earlier[5] (Figure 4*A*-*C*). Interestingly, lovastatin enhanced significantly both basal and radiation-induced AMPK phosphorylation and activity.

Modulation of cell cycle regulators and the cell cycle by lovastatin.

Akt and AMPK pathways regulate cell cycle through modulation of p53 and CDKIs $p27^{kip1}$, and $p21^{cip1}$ [25]. Therefore, we examined whether lovastatin modulates the levels of these cell cycle inhibitors in control and IR-treated cells. We observed a significant increase in the expression of p53, $p27^{kip1}$, and $p21^{cip1}$ in response to IR (Figure 5*A*). However, lovastatin caused an early inhibition of the IR-induced expression of p53, $p27^{kip1}$, and $p21^{cip1}$, within 24 h, and for that we examined the levels of these three cell cycle regulators up to 96 h after initiation of treatments. IR maintained enhanced p53, $p27^{kip1}$, and $p21^{cip1}$ levels up to 96 hours later (Figure 5*A*) but lovastatin inhibited this IR-induced expression, which was almost completely eliminated at 96 h.

Effects on cell cycle phase distribution.

Lovastatin alone did not affect significantly the distribution of cells in the phases of the cell cycle in the first 24 hours (Figure 5*B*). However, lovastatin caused a progressive significant shift of cells into G0/G1 phase, after 24 h, compared to control, and eventually a marked induction of apoptosis by 72 - 96 h (24 h: 2%; 96 h: 89%). IR alone caused a significant arrest of cells in G2/M phase at 48h (Control: 0%; IR: 31%).

However, lovastatin attenuated IR-induced G2/M arrest and shifted cells into G0/G1 phase and apoptosis (IR G2-M: 31%; Lovastatin + IR G2-M: 12%; Figure 5*C*).

Apoptosis events induced by lovastatin.

Finally, we examined the effects of lovastatin and IR on molecular and morphological markers of apoptosis. Cleaved caspase 3 levels, an established marker of apoptosis[26], were analyzed by immunoblotting. Lovastatin alone caused a significant increase in cleaved caspase 3 levels and further potentiated IR-induced expression of this protein at 12 hours (Figure 6*A*). IR-induction of cleaved caspase 3 dissipated after 12 hours, but lovastatin enhanced cleaved caspase 3 levels for up to 48 hours later and decreased thereafter. We analyzed apoptotic events also with morphological analysis of cells treated with lovastatin for 0 to72 h. Consistent with induction of cleaved caspase 3 (Figure 6*A*) and the cell cycle results (Figure 5), lovastatin caused a time-dependent nuclear fragmentation and induction of apoptotic bodies (Figure 6*B*-*C*).

Discussion:

Lovastatin was shown to sensitize human cervix cancer cells to ionizing radiation[27]. Recently, another statin, simvastatin, was shown to inhibit small-cell lung cancer growth in vitro and in vivo[28], and Bellini et al.[29] showed that simvastatin inhibits the proliferation of A549 lung cancer cells. However, the potential benefit of combining statins with therapeutic doses of IR has not been examined in lung cancer models. To our knowledge, this is the first study to demonstrate that lovastatin acts as a radiation sensitizer in NSCLC cells.

Lovastatin regulation of clonogenic survival in control and radiated cells.

We observed that lovastatin sensitized A549 lung cancer cells to therapeutic doses of IR of 2-8 Gy (Figure 1). This was mediated specifically through inhibition of the mevalonate pathway, as exogenous mevalonate completely reversed the decrease in lung cancer cell survival observed by lovastatin (Figure 1*D*). Fritz et al.[27] examined the sensitivity of a number of cancer cell lines to lovastatin but only a few of them showed sensitivity to lovastatin at high doses. HeLa cells required 20-50μM of lovastatin to demonstrate radiosensitization[27]. In this study, lung adenocarcinoma A549 cells showed higher sensitivity to the drug (at 5 and 10 μM), indicating that survival pathways in those cells may be more dependent on protein prenylation events.

Interestingly, in recent experiments investigating the effects of lovastatin in SK-MES lung cancer cells, a cell line of squamous cell carcinoma origin, we have observed an even greater sensitivity to the drug. These results are shown in Figure s1 (Supplemental Digital Content) and indicate a 20 to 50 times greater sensitivity of SK-MES cells to lovastatin compared to adenocarcinoma A549 cells. We are currently investigating in depth the molecular etiology of this higher sensitivity of SK-MES cells and its implications. However, overall, our results demonstrate that lung cancer cells show significant radiosensitization in response to lovastatin that should be explored further in preclinical in-vivo and in clinical studies.

As other statins, beyond lovastatin, have shown anti-proliferative effects in cancer cells[15], one wonders whether lung cancer cell radiosensitization is a phenomenon unique to lovastatin. For that, we began to explore the effects of other statins in A549 cells. In preliminary studies, we observed that simvastatin is also able to inhibit proliferation of

A549 cells (as shown earlier[29]) and to sensitize lung cancer cells to IR. This indicates that radiosensitization is likely a common effect for this class of agents (Figure s2, in Supplemental Digital Content).

Effects on EGFR and effector kinases.

Adenocarcinoma A549 cells have a genetic profile that offers a survival advantage including a K-Ras (Gly12-Ser) mutation[30]. K-Ras activates the PI3k-Akt pathway[31] and that is required for NSCLC tumurogenesis in K-Ras mutant mice[32]. Because it inhibits post-translational modification of Ras GTP-binding proteins, lovastatin is expected to abrogate oncogenic K-Ras and EGFR signalling. In this study, we observed that lovastatin selectively abrogated EGF-stimulated phosphorylation of EGFR and Akt but not Erk1/2. This discrepancy was observed also by Mantha et al.[33] in SCC9 head and neck tumour cells and suggests that, (1) persistent EGFR phosphorylation may not be required for Erk1/2 activation and (2) activation of Erk1/2 alone is not adequate to confer radiation resistance. Our observations suggest that in lung cancer cells, lovastatin is able to inhibit selectively the key pro-survival pathway of Akt. This alone could account for the anti-proliferative and pro-apoptotic effects of the drug.

Lovastatin regulation of IR-activated signals.

Effects on Akt.

Similar to EGF-induced signals, lovastatin attenuated IR-activation of Akt, in a mevalonate-dependent fashion, but did not affect IR-activation of Erk1/2 (Figure 3*A*-*C*). Similarly, Mistafa and Stenius[34] found that statins primarily target the Akt pathway to sensitize pancreatic cancer cells to chemotherapeutic drugs, without effecting Erk. Studies

in K-Ras mutant cells, including A549, have shown that in these cells activation of the EGFR-PI3k-Akt pathway confers radioresistance[35] and that inhibition of this axis by EGFR inhibitors sensitizes cells to IR[36]. Further, Akt is an established mediator of radiation resistance in many cancer cells[37]. The effect of lovastatin to inhibit IR-activation of Akt illustrates a key property of this drug that likely mediates its radio-sensitization action.

Effects on AMPK.

A549 cells also carry a point mutation of the LKB1 gene (codon 37 [Q-Ter]) that generates a truncated LKB1 product[38]. Therefore, these cells lack LKB1-regulated AMPK activation an event that is shown to lead to aberrant activation of the Akt – mTOR pathway activating protein synthesis and survival[39]. In this study, in agreement with earlier studies with statins[40], we observed that lovastatin alone activated AMPK. However, we observed that it also potentiated its activation by IR (Figure 4*C*). Recently, we observed that IR activates AMPK in LKB1 null A549 cells[5]. Our observations in the same cells here suggest that lovastatin also activates AMPK in an LKB1-independent fashion. These observations are significant since AMPK is (1) shown to dephosphorylate and inhibit Akt through increased protein phosphatase 2A (PP2A) activity[41] and (2) inhibit the mTOR pathway by directly phosphorylating either its upstream regulator Tuberous Sclerosis 2 (TSC2) or its binding partner Raptor[39].

Importantly, AMPK activation also mimics statin action since this kinase is known to inhibit HMG-CoA reductase[42]. Therefore, AMPK activation by stimuli such as IR can work synergistically with lovastatin to augment the effects of inhibition of the

mevalonate pathway. Taking these notions together with the discussion earlier, lovastatin seems to be a highly attractive agent with dual potential to enhance the activity of AMPK and inhibit the Akt pathway through a number of potential molecular steps.

Modulation of cell cycle.

Cell cycle regulators.

IR regulates cell cycle through the induction of p53 and CDKIs, $p21^{cip1}$ and $p27^{kip1}$, expression to mediate mainly an arrest at the G2-M checkpoint[43]. We hypothesized that lovastatin's anti-proliferative effects may involve arrest of the cell cycle through enhanced expression of p53 and CDKIs. Although we did observe a potent induction of p53, $p21^{cip1}$, and $p27^{kip1}$ expression by IR alone, lovastatin inhibited IR-induction of p53 and CDKI expression (Figure 5*A*). This may be due to either (1) effects of the drug on global gene transcription and translation or (2) a dependence of p53 and CDKI expression on specific events inhibited by lovastatin. Statins were shown to inhibit mTOR-dependent phosphorylation or deactivation of the translational repressor eukaryotic initiation factor 4E (eIF4E)-binding protein, leading to suppression of initiation of cap-dependent mRNA translation[44]. It should be stressed that we did not detect in our study any significant effects on the levels of any other proteins, including signalling molecules or actin, suggesting that a global effect on gene expression is unluckily. Conversely, Akt activity, which is inhibited by lovastatin, is required for the DNA damage induced stabilization of p53[45] and this mechanism may be active in lovastatin-treated cells. A decrease in $p21^{cip1}$ levels with statin treatment was observed by other investigators in A549 cells[22]. Consistent with observations in HeLa cells[27], our work

suggests that the mechanism of radiosensitization of A549 cells is independent of p53 and the CDKIs $p21^{cip1}$ and $p27^{kip1}$.

Cell cycle.

Lovastatin was shown to inhibit cell cycle progression at G0/G1 phase and promote apoptosis in thyroid cancer[46], breast cancer[47], glioblastoma[48], cervical cancer cells[27] and squamous cell carcinomas[49]. In this study, we observed that lovastatin treatment shifted cells into G0/G1 phase with a markedly increased proportion of cells moving into apoptosis after 48 h of treatment (Figure 5*B*). Prolonged treatment with lovastatin (96h) induced marked induction of apoptosis in non-radiated cells and caused a reversal of the G2-M checkpoint arrest induced by IR and a G0/G1 and apoptotic distribution (Figure 5*B*-*C*). It is possible that inhibition of the IR-induced G2-M arrest by lovastatin induced radio-sensitization through prevention of DNA repair and induction of genomic instability.

Induction of apoptosis.

Consistent with the cell cycle analysis results, we observed that lovastatin alone induced cleaved caspase 3, a significant contributor to protein degradation. Although IR caused a reversible induction of this marker that was not detectable after 24h, lovastatin enhanced and prolonged the IR-induced cleaved caspase 3 formation for up to 72h (Figure 6*A*). Furthermore, morphological analysis verified a progressive formation of apoptotic bodies with continued incubation with lovastatin (Figure 6*B*-*C*). Overall, our results are consistent with other studies[22,50], suggesting apoptosis as major mechanism of

the cytotoxic action of lovastatin and suggests that this is also a predominant mode of action of the drug when combined with radiation in lung cancer cells.

Potential for clinical development in Lung Cancer in combination with radiotherapy.

A number of clinical studies explored the potential of lovastatin to achieve tumoricidal doses in human patients. Typical doses of lovastatin aiming to control cholesterol levels in humans are approximately 1mg/kg/day and are shown to yield serum lovastatin concentrations in the range of 0.15 – 0.3 μM[51]. Early phase dose-escalation studies have explored a number of regiments, and in a study of 7 consecutive days treatment, in 4 week cycles, doses up to 25mg/kg/day were tolerated without severe myopathy[51]. Ubiquinone is utilized to address myopathy. Under these conditions, maximum tolerated doses (MTD) were not reached, and systemic drug concentrations reached 0.1- 3.92 μM [51]. In a study with end-stage head and neck and cervix cancers patients[52], a regiment of 7.5mg/kg/day for 21 consecutive days in 4 week cycles was defined as MTD in patients with good renal function. Although no objective responses were seen in this study, where lovastatin was used as a single agent, the authors still reported a 23% rate of stable disease at 3 months[52], which is indeed encouraging in patients with end-stage disease.

The aforementioned studies suggest that it is possible to achieve safely tumouricidal and radiosensitizing doses of lovastatin in cancer patients. Our work indicates that some lung cancer tumours may exhibit sensitivity to lovastatin even in the high nanomolar range (Figure s1 in Supplemental Digital Content and discussion earlier) making it even more plausible that lovastatin will sensitize tumours to IR in human

patients. Overall, these data indicate that this drug deserves further investigation with in-vivo preclinical and clinical studies. Although, other statins may also be able to radio-sensitize lung tumour cells (Figure s2 in Supplemental Digital Content and discussion above), lovastatin remains the best studied agent in this class, in both the pre-clinical and the clinical setting and, therefore, is the most favourable candidate for further development.

Conclusions:

Figure 7 illustrates our model of the action of lovastatin in lung cancer cells. Our work suggests that lovastatin is a promising agent with significant anti-tumour properties as a single agent as well as a radiation sensitizer. Lovastatin seems to function mainly through induction of apoptosis. This effect may be mediated by a unique simultaneous inhibition of the pro-survival Akt and activation of the tumour suppressor AMPK pathways. This work presents compelling evidence which support further investigation of lovastatin as a radiation sensitizer in-vivo. Work in animal models of lung cancer will expedite the development of this drug to the clinical setting in early phase studies in combination with radiotherapy.

Acknowledgments:

Supported by funds from the Juravinski Cancer Center Foundation. We appreciate the support by Dr. William K. Evans (CEO, Juravinski Cancer Center), in the pursuit of this study.

List of Supplemental Digital Content

Figure s1: Lovastatin inhibits SK-MES cell clonogenic survival and sensitizes these cells to ionizing radiation.

Figure s2: Simvastatin inhibits A549 cell clonogenic survival and sensitizes these cells to ionizing radiation.

References:

1. Schuurbiers OC, Kaanders JH, van der Heijden HF*, et al.* The PI3-K/AKT-pathway and radiation resistance mechanisms in non-small cell lung cancer. *J Thorac Oncol* 2009;4:761-767.
2. Bernhard EJ, Maity A, Muschel RJ*, et al.* Effects of ionizing radiation on cell cycle progression. A review. *Radiat Environ Biophys* 1995;34:79-83.
3. Hartlerode AJ, Scully R. Mechanisms of double-strand break repair in somatic mammalian cells. *Biochem J* 2009;423:157-168.
4. Vidal A, Koff A. Cell-cycle inhibitors: three families united by a common cause. *Gene* 2000;247:1-15.
5. Sanli T, Rashid A, Liu C*, et al.* Ionizing Radiation Activates AMP-activated Kinase (AMPK). A target for radiosensitization of human cancer cells. *International Journal of Radiation OncologyBiologyPhysics,* 2010;In Press.
6. Park CM, Park MJ, Kwak HJ*, et al.* Ionizing radiation enhances matrix metalloproteinase-2 secretion and invasion of glioma cells through Src/epidermal growth factor receptor-mediated p38/Akt and phosphatidylinositol 3-kinase/Akt signaling pathways. *Cancer Res* 2006;66:8511-8519.
7. Zimmermann M, Zouhair A, Azria D*, et al.* The epidermal growth factor receptor (EGFR) in head and neck cancer: its role and treatment implications. *Radiat Oncol* 2006;1:11.

8. Nakamura JL, Karlsson A, Arvold ND*, et al.* PKB/Akt mediates radiosensitization by the signaling inhibitor LY294002 in human malignant gliomas. *J Neurooncol* 2005;71:215-222.

9. Le Tourneau C, Siu LL. Molecular-targeted therapies in the treatment of squamous cell carcinomas of the head and neck. *Curr Opin Oncol* 2008;20:256-263.

10. Fritz G, Kaina B. Rho GTPases: promising cellular targets for novel anticancer drugs. *Curr Cancer Drug Targets* 2006;6:1-14.

11. Bernhard EJ, Stanbridge EJ, Gupta S*, et al.* Direct evidence for the contribution of activated N-ras and K-ras oncogenes to increased intrinsic radiation resistance in human tumor cell lines. *Cancer Res* 2000;60:6597-6600.

12. Lerner EC, Zhang TT, Knowles DB*, et al.* Inhibition of the prenylation of K-Ras, but not H- or N-Ras, is highly resistant to CAAX peptidomimetics and requires both a farnesyltransferase and a geranylgeranyltransferase I inhibitor in human tumor cell lines. *Oncogene* 1997;15:1283-1288.

13. Goldstein JL, Brown MS. Regulation of the mevalonate pathway. *Nature* 1990;343:425-430.

14. Chan KK, Oza AM, Siu LL. The statins as anticancer agents. *Clin Cancer Res* 2003;9:10-19.

15. Sassano A, Platanias LC. Statins in tumor suppression. *Cancer Lett* 2008;260:11-19.

16. Poynter JN, Gruber SB, Higgins PD*, et al.* Statins and the risk of colorectal cancer. *N Engl J Med* 2005;352:2184-2192.

17. Khurana V, Bejjanki HR, Caldito G*, et al.* Statins reduce the risk of lung cancer in humans: a large case-control study of US veterans. *Chest* 2007;131:1282-1288.

18. Platz EA, Leitzmann MF, Visvanathan K*, et al.* Statin drugs and risk of advanced prostate cancer. *J Natl Cancer Inst* 2006;98:1819-1825.

19. Hamilton RJ, Banez LL, Aronson WJ*, et al.* Statin medication use and the risk of biochemical recurrence after radical prostatectomy: results from the Shared Equal Access Regional Cancer Hospital (SEARCH) Database. *Cancer* 2010;116:3389-3398.

20. Kollmeier MA, Katz MS, Mak K*, et al.* Improved Biochemical Outcomes with Statin Use in Patients with High-Risk Localized Prostate Cancer Treated with Radiotherapy. *Int J Radiat Oncol Biol Phys* 2010.

21. Gutt R, Tonlaar N, Kunnavakkam R*, et al.* Statin use and risk of prostate cancer recurrence in men treated with radiation therapy. *J Clin Oncol* 2010;28:2653-2659.

22. Maksimova E, Yie TA, Rom WN. In vitro mechanisms of lovastatin on lung cancer cell lines as a potential chemopreventive agent. *Lung* 2008;186:45-54.

23. Tsakiridis T, Vranic M, Klip A. Disassembly of the actin network inhibits insulin-dependent stimulation of glucose transport and prevents recruitment of glucose transporters to the plasma membrane. *J Biol Chem* 1994;269:29934-29942.

24. Liu SK, Coackley C, Krause M*, et al.* A novel poly(ADP-ribose) polymerase inhibitor, ABT-888, radiosensitizes malignant human cell lines under hypoxia. *Radiother Oncol* 2008;88:258-268.

25. Motoshima H, Goldstein BJ, Igata M*, et al.* AMPK and cell proliferation--AMPK as a therapeutic target for atherosclerosis and cancer. *J Physiol* 2006;574:63-71.

26. Janicke RU, Sprengart ML, Wati MR*, et al.* Caspase-3 is required for DNA fragmentation and morphological changes associated with apoptosis. *J Biol Chem* 1998;273:9357-9360.

27. Fritz G, Brachetti C, Kaina B. Lovastatin causes sensitization of HeLa cells to ionizing radiation-induced apoptosis by the abrogation of G2 blockage. *Int J Radiat Biol* 2003;79:601-610.

28. Khanzada UK, Pardo OE, Meier C*, et al.* Potent inhibition of small-cell lung cancer cell growth by simvastatin reveals selective functions of Ras isoforms in growth factor signalling. *Oncogene* 2006;25:877-887.

29. Bellini MJ, Polo MP, de Alaniz MJ*, et al.* Effect of simvastatin on the uptake and metabolic conversion of palmitic, dihomo-gamma-linoleic and alpha-linolenic acids in A549 cells. *Prostaglandins Leukot Essent Fatty Acids* 2003;69:351-357.

30. Valenzuela DM, Groffen J. Four human carcinoma cell lines with novel mutations in position 12 of c-K-ras oncogene. *Nucleic Acids Res* 1986;14:843-852.

31. Shaw RJ, Cantley LC. Ras, PI(3)K and mTOR signalling controls tumour cell growth. *Nature* 2006;441:424-430.

32. Gupta S, Ramjaun AR, Haiko P*, et al.* Binding of ras to phosphoinositide 3-kinase p110alpha is required for ras-driven tumorigenesis in mice. *Cell* 2007;129:957-968.

33. Mantha AJ, Hanson JE, Goss G*, et al.* Targeting the mevalonate pathway inhibits the function of the epidermal growth factor receptor. *Clin Cancer Res* 2005;11:2398-2407.

34. Mistafa O, Stenius U. Statins inhibit Akt/PKB signaling via P2X7 receptor in pancreatic cancer cells. *Biochem Pharmacol* 2009;78:1115-1126.

35. Toulany M, Dittmann K, Kruger M*, et al.* Radioresistance of K-Ras mutated human tumor cells is mediated through EGFR-dependent activation of PI3K-AKT pathway. *Radiother Oncol* 2005;76:143-150.

36. Toulany M, Kasten-Pisula U, Brammer I*, et al.* Blockage of epidermal growth factor receptor-phosphatidylinositol 3-kinase-AKT signaling increases radiosensitivity of K-RAS mutated human tumor cells in vitro by affecting DNA repair. *Clin Cancer Res* 2006;12:4119-4126.

37. Gupta AK, McKenna WG, Weber CN*, et al.* Local recurrence in head and neck cancer: relationship to radiation resistance and signal transduction. *Clin Cancer Res* 2002;8:885-892.

38. Sanchez-Cespedes M, Parrella P, Esteller M*, et al.* Inactivation of LKB1/STK11 is a common event in adenocarcinomas of the lung. *Cancer Res* 2002;62:3659-3662.

39. Steinberg GR, Kemp BE. AMPK in Health and Disease. *Physiol Rev* 2009;89:1025-1078.

40. Sun W, Lee TS, Zhu M*, et al.* Statins activate AMP-activated protein kinase in vitro and in vivo. *Circulation* 2006;114:2655-2662.

41. Kim KY, Baek A, Hwang JE*, et al.* Adiponectin-activated AMPK stimulates dephosphorylation of AKT through protein phosphatase 2A activation. *Cancer Res* 2009;69:4018-4026.

42. Shackelford DB, Shaw RJ. The LKB1-AMPK pathway: metabolism and growth control in tumour suppression. *Nat Rev Cancer* 2009;9:563-575.

43. Niculescu AB, 3rd, Chen X, Smeets M*, et al.* Effects of p21(Cip1/Waf1) at both the G1/S and the G2/M cell cycle transitions: pRb is a critical determinant in blocking DNA replication and in preventing endoreduplication. *Mol Cell Biol* 1998;18:629-643.

44. Woodard J, Sassano A, Hay N*, et al.* Statin-dependent suppression of the Akt/mammalian target of rapamycin signaling cascade and programmed cell death 4 up-regulation in renal cell carcinoma. *Clin Cancer Res* 2008;14:4640-4649.

45. Boehme KA, Kulikov R, Blattner C. p53 stabilization in response to DNA damage requires Akt/PKB and DNA-PK. *Proc Natl Acad Sci U S A* 2008;105:7785-7790.

46. Laezza C, Fiorentino L, Pisanti S*, et al.* Lovastatin induces apoptosis of k-ras-transformed thyroid cells via inhibition of ras farnesylation and by modulating redox state. *J Mol Med* 2008;86:1341-1351.

47. Keyomarsi K, Sandoval L, Band V*, et al.* Synchronization of tumor and normal cells from G1 to multiple cell cycles by lovastatin. *Cancer Res* 1991;51:3602-3609.

48. Bouterfa HL, Sattelmeyer V, Czub S*, et al.* Inhibition of Ras farnesylation by lovastatin leads to downregulation of proliferation and migration in primary cultured human glioblastoma cells. *Anticancer Res* 2000;20:2761-2771.

49. Dimitroulakos J, Ye LY, Benzaquen M*, et al.* Differential sensitivity of various pediatric cancers and squamous cell carcinomas to lovastatin-induced apoptosis: therapeutic implications. *Clin Cancer Res* 2001;7:158-167.

50. Wu J, Wong WW, Khosravi F*, et al.* Blocking the Raf/MEK/ERK pathway sensitizes acute myelogenous leukemia cells to lovastatin-induced apoptosis. *Cancer Res* 2004;64:6461-6468.

51. Sleijfer S, van der Gaast A, Planting AS*, et al.* The potential of statins as part of anti-cancer treatment. *Eur J Cancer* 2005;41:516-522.

52. Knox JJ, Siu LL, Chen E*, et al.* A Phase I trial of prolonged administration of lovastatin in patients with recurrent or metastatic squamous cell carcinoma of the head and neck or of the cervix. *Eur J Cancer* 2005;41:523-530.

Figures:

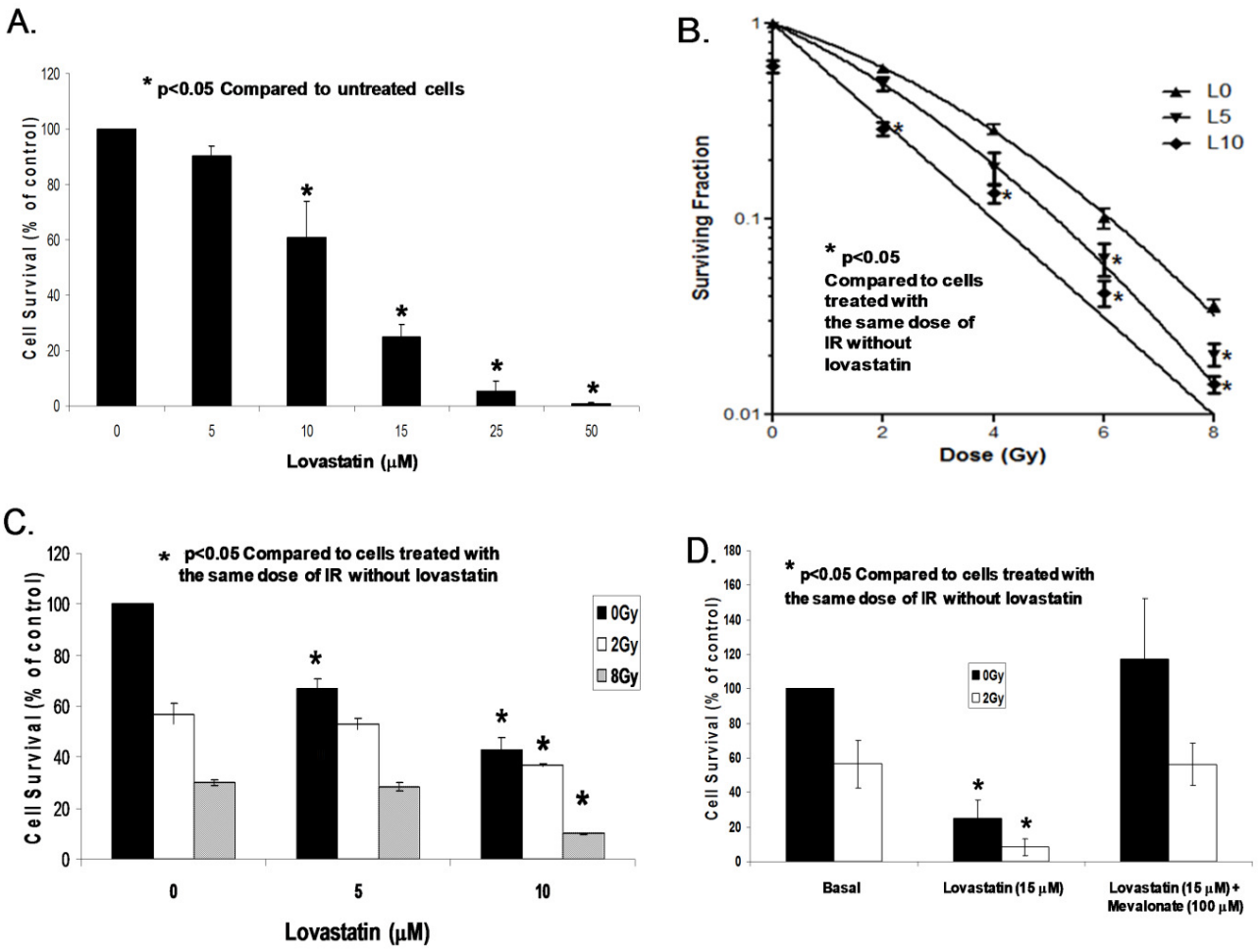

Figure 3.1: Lovastatin inhibits non-small cell lung cancer cell clonogenic survival and sensitizes cells to ionizing radiation. *A*, A549 cells were subjected to clonogenic assays as described in the Methods section. Results from five to eight independent experiments were normalized to the controls and are shown as the mean ± standard error (SE). *B*, Cells were subjected to increasing doses of ionizing radiation (IR) after incubation without (L0) or with 5 μM (L5) or 10 μM lovastatin (L10) and subjected to clonogenic assays. Results from five to six independent experiments were normalized to the controls and are shown

as the mean ± SE. *C*, Cell proliferation was evaluated after treatment with indicated concentrations of lovastatin for 24 hours before treatment with indicated doses of IR. Proliferation was evaluated 96h later as described in Methods section. Results from three independent experiments were normalized to the controls and are shown as the mean ± SE. *D*, Cells were subjected to 2 Gy of IR without or with pre-incubation with either lovastatin alone (15 μM), or mevalonate (100 μM) and lovastatin before treatment with 2Gy IR followed by clonogenic assays. Results are the mean ± SEM of three independent experiments.

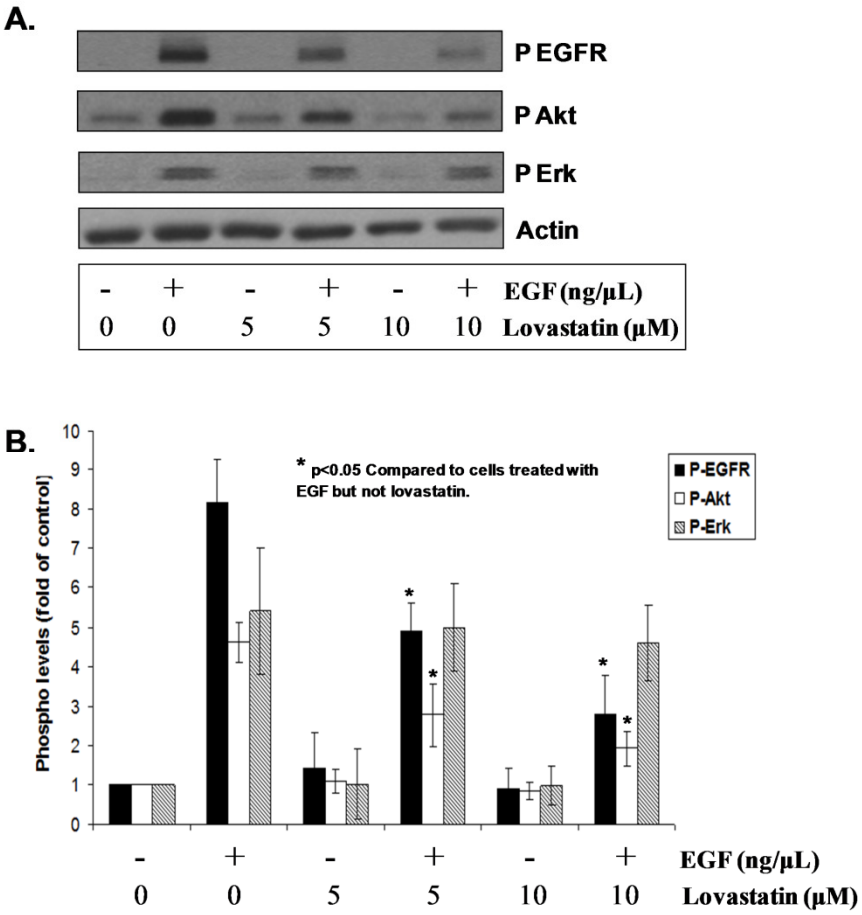

Figure 3.2: Lovastatin modulates epidermal growth factor (EGF)-stimulated Akt phosphorylation. *A*, Cells were pre-incubated with or without the indicated concentrations of lovastatin for 24 hours before exposure to EGF (1 ng/µL). Cells were then lysed 30min after exposure to EGF, followed by immunoblotting with antibodies against phoshorylated EGFR, Akt, Erk, or total actin. Representative immunoblots are shown. *B*, Densitometry values (mean±SEM) from three to four independent immunobloting experiments are displayed in the graph.

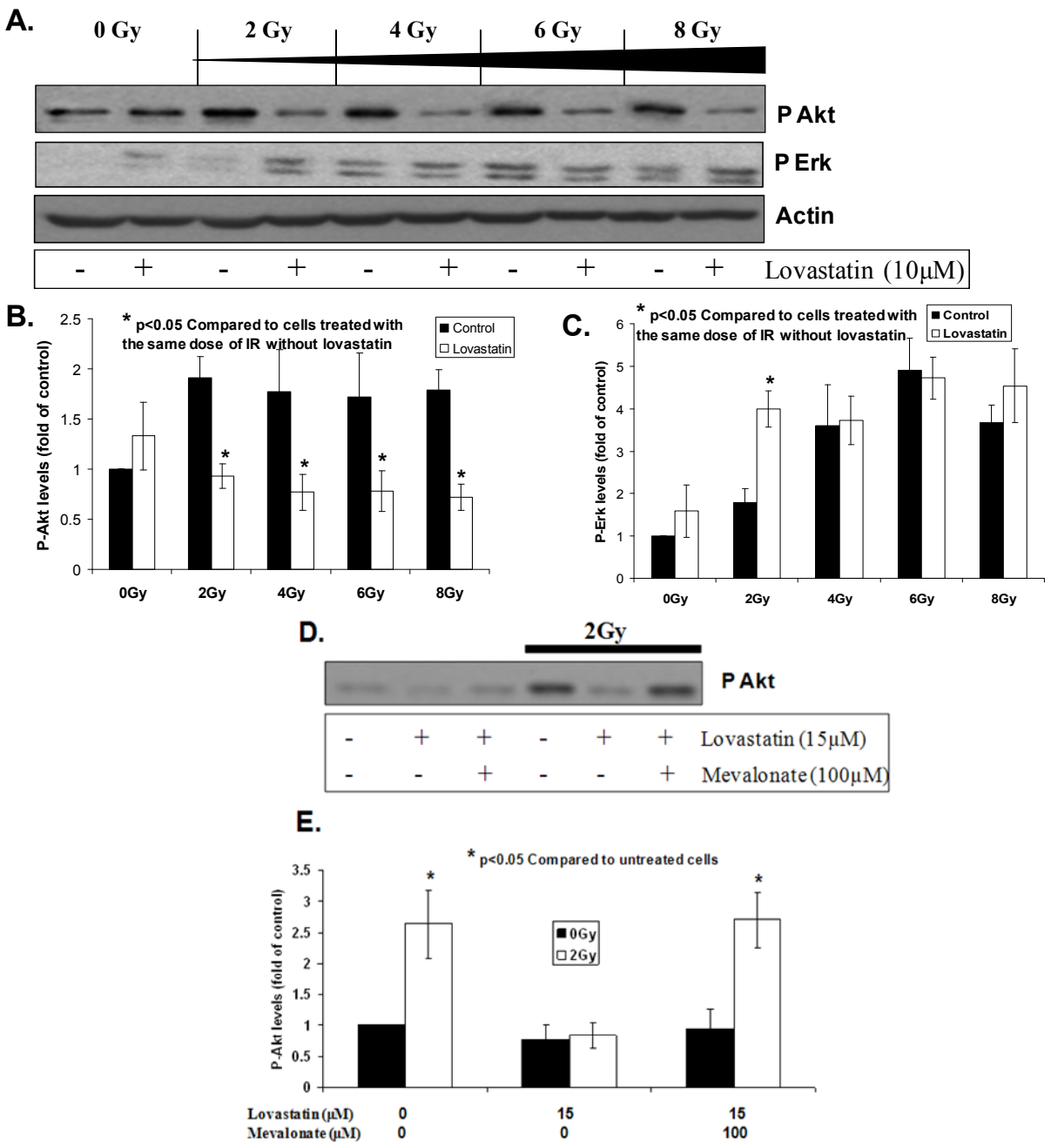

Figure 3.3: Lovastatin modulates ionizing radiation (IR)-induced Akt but not Erk phosphorylation. Cells were pre-incubated with or without lovastatin (10μM) for 24 hours before exposure to the indicated dose of IR. *A*, Cells were then lysed 1 hour after the

indicated doses of IR, followed by immunoblotting with indicated antibodies. *B-C*, Densitometry values of immunoblots (mean±SEM) from three independent immunobloting experiments are shown. *D*, Cells were treated with or without 15μM lovastatin or mevalonate (100μM) for 24 hours before exposure to 2Gy IR. Cell lysates were subjected to immunobloting. A representative immunblot is shown. *E*, Densitometry values (mean±SEM) from three independent immunobloting experiments are displayed.

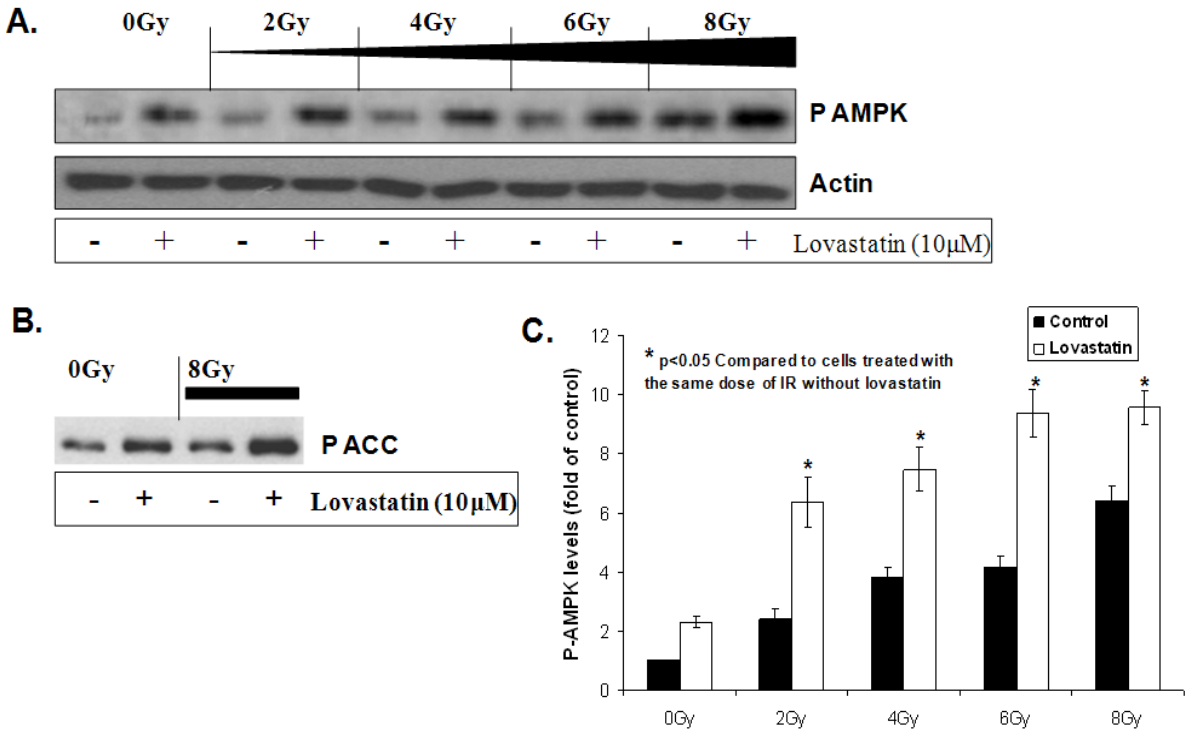

Figure 3.4: Lovastatin modulates ionizing radiation (IR)-induced AMPK phosphorylation. *A*, Cells were pre-incubated with 10µM lovastatin 24 hours before treatment with the indicated dose of IR, lysed and subjected to immunoblotting with the indicated antibodies. A representative immunoblot from at least three independent experiments is shown. *B*, Cells were pre-incubated with 10µM lovastatin 24 hours before treatment with 0Gy or 8Gy IR. Immunoblotting was performed with an antibody against phoshorylated ACC. *C*, Mean±SEM of densitometry values from three to four experiments performed in experiment *A*, are shown.

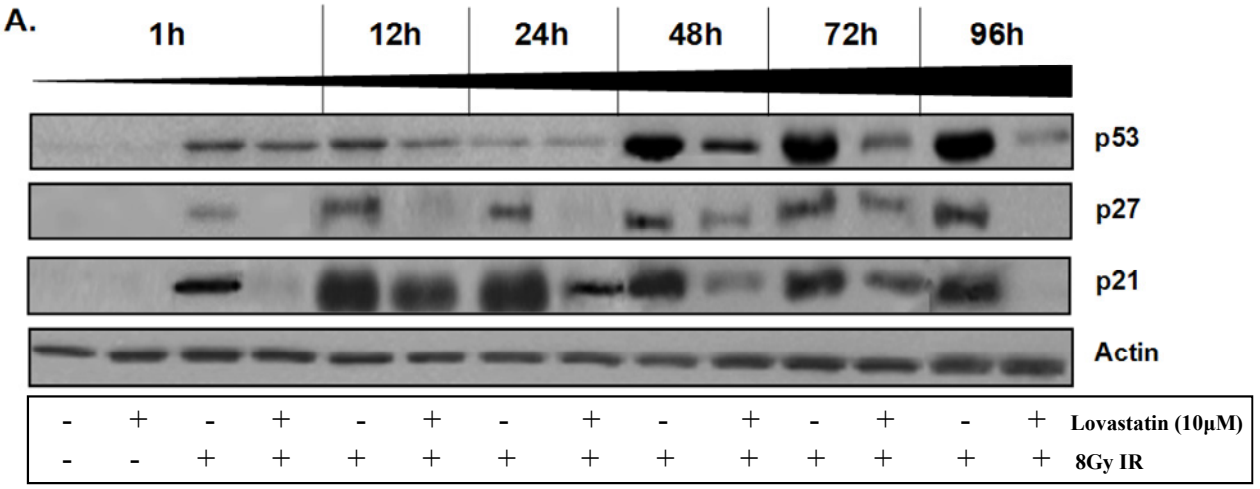
A.
1h
12h
24h
48h
72h
96h
p53
p27
p21
Actin
- + - + - + - + - + - + - + Lovastatin (10μM)
- - + + + + + + + + + + + + 8Gy IR

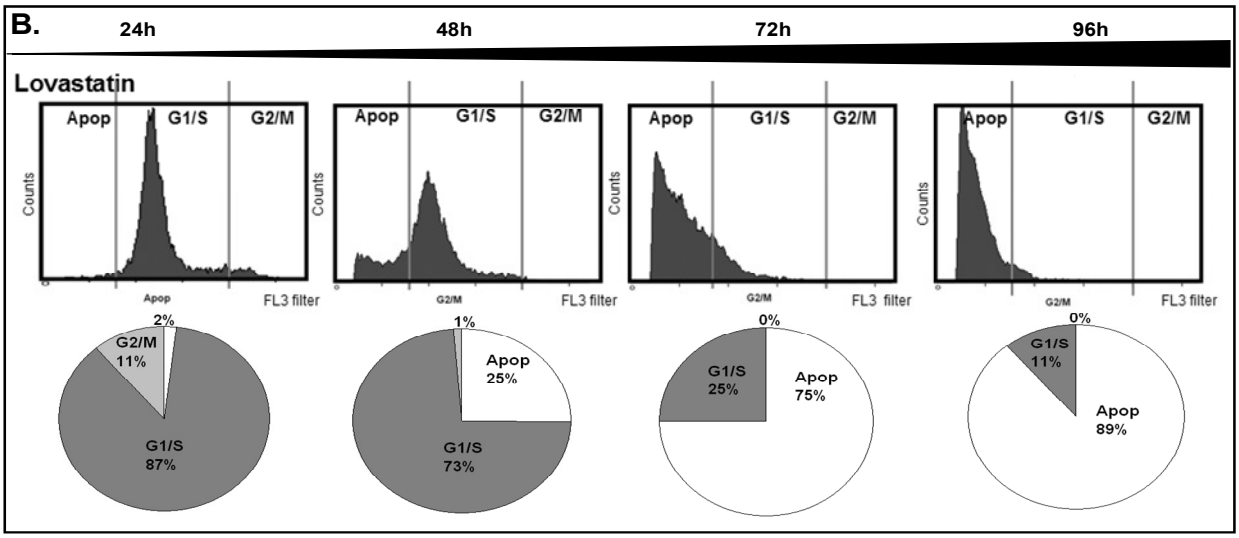
B.
24h
48h
72h
96h
Lovastatin
Apop
G1/S
G2/M
Counts
FL3 filter
2%
G2/M 11%
G1/S 87%
1%
Apop 25%
G1/S 73%
0%
G1/S 25%
Apop 75%
0%
G1/S 11%
Apop 89%

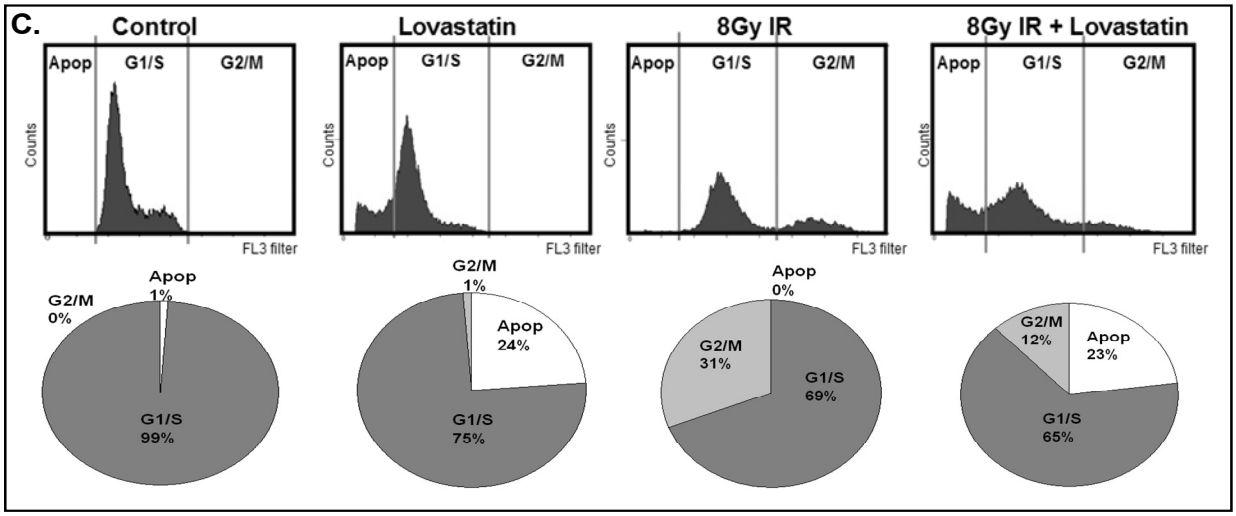
C.
Control
Lovastatin
8Gy IR
8Gy IR + Lovastatin
Apop
G1/S
G2/M
Counts
FL3 filter
Apop 1%
G2/M 0%
G1/S 99%
G2/M 1%
Apop 24%
G1/S 75%
Apop 0%
G2/M 31%
G1/S 69%
G2/M 12%
Apop 23%
G1/S 65%

Figure 3.5: Lovastatin modulates ionizing radiation (IR)-induced expression cell cycle inhibitors and the cell cycle. *A*, Cells were treated with 10μM lovastatin with or without a single dose of 8Gy IR. Cells were then lysed at the indicated times (1-96 hours), followed by immunoblotting with antibodies that recognize p53, $p27^{kip1}$, and $p21^{Waf/cip}$. A representative immunoblot from at least three independent experiments is shown. *B*, Cells were treated with 10 μM lovastatin for the indicated times, followed by cell cycle analysis. The results were quantified as % distribution in apoptosis (Apop), G1/S phase, and G2/M phases. *C*, Cells were treated without or with lovastatin were exposed to 0 or 8Gy IR. Cell cycle analysis was performed 48h later.

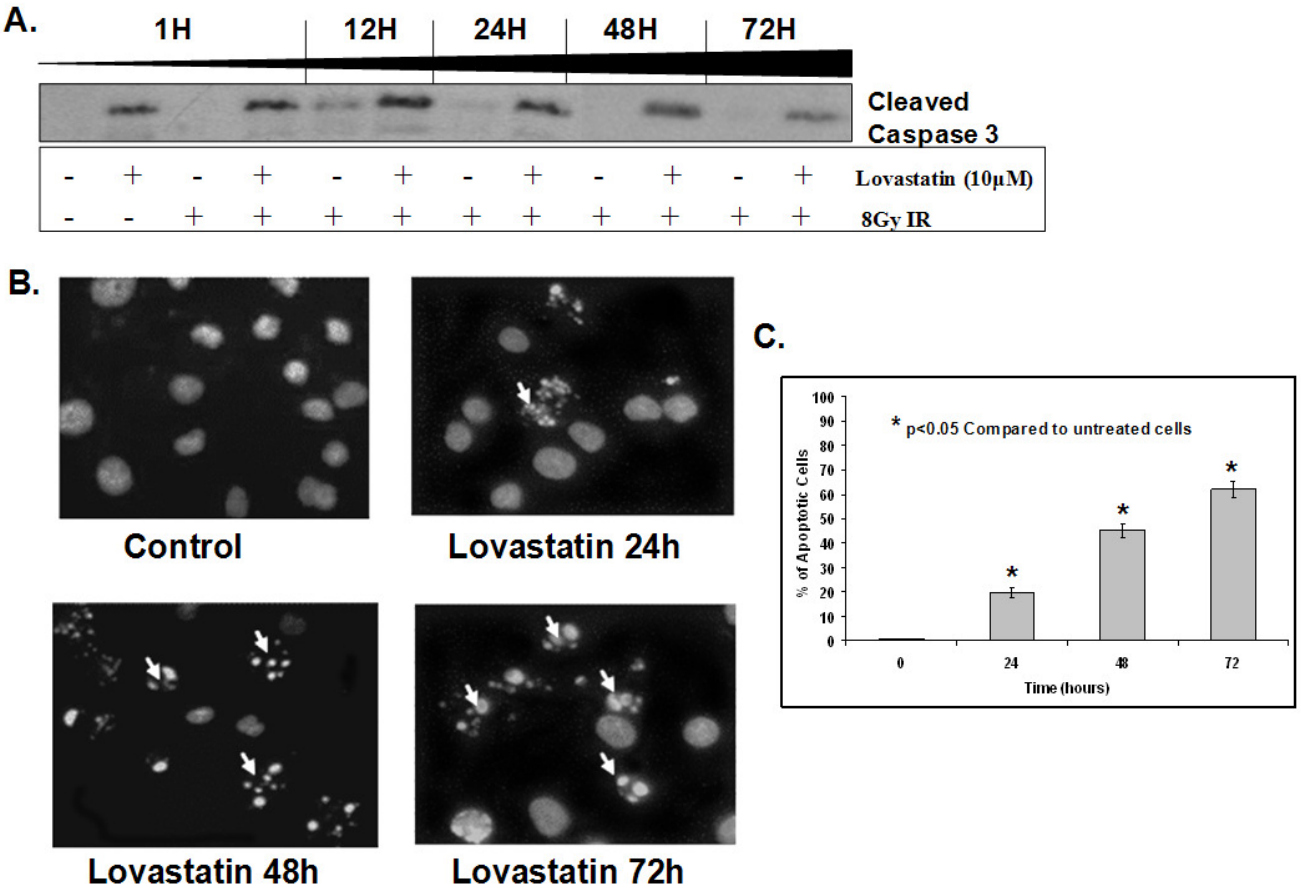

Figure 3.6: Lovastatin induces cancer cell apoptosis. *A*, Cells were pre-treated with or without lovastatin prior to exposure to 8Gy ionizing radiation (IR) and were lysed at the indicated times after radiation (24 – 72 hours). Cleaved caspase 3 induction was analyzed by immnoblotting. *B*, After treatment with lovastatin (10μM) for the indicated times, cells were fixed and stained with Hoechst, and the nuclear morphology was analyzed with fluorescence microscopy. A representative, from three independent experiments is shown. *C*, Nuclear fragmentation was quantitated in three independent experiments as described in the Methods sections. Results are normalized to control untreated cells (0 time with lovastatin).

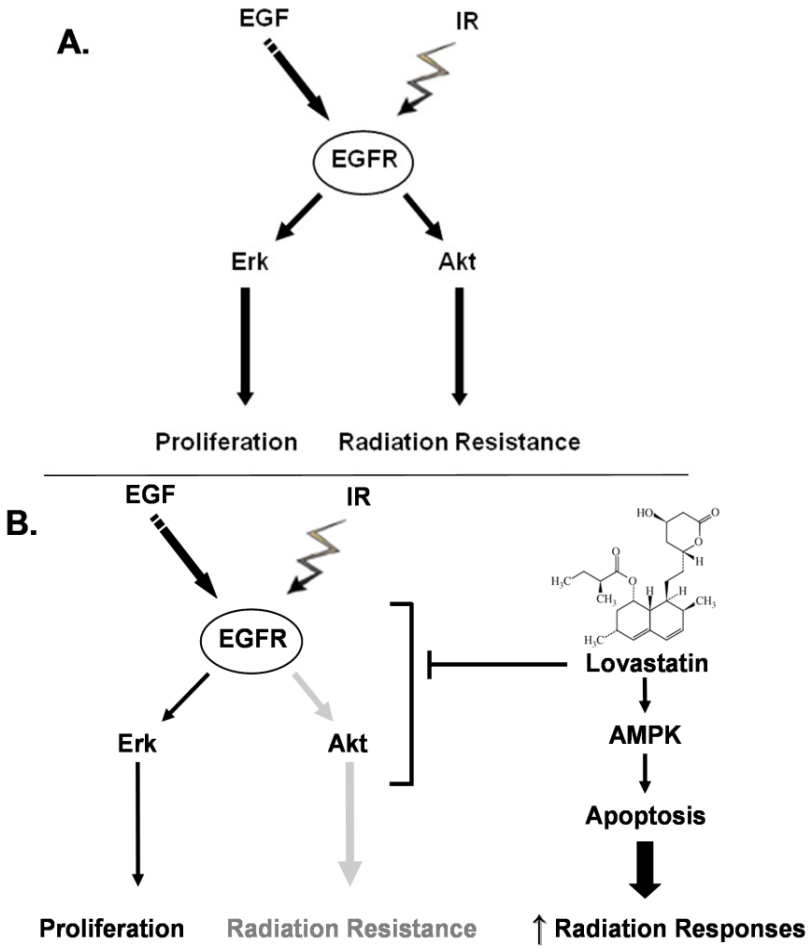

Figure 3.7: Model of lovastatin-induced sensitization of lung cancer cells to radiation. *A*, Stimulation of epidermal growth factor receptor (EGFR) signalling and activation of Erk and Akt stimulate proliferation and induce radiation resistance in lung cancer cells. *B*, Lovastatin inhibits Akt and stimulates activation of AMPK leading to apoptosis and radiation sensitization. IR = ionizing radiation.

Supporting Experiments

Initially, I examined the effect of lovastatin on the cell survival of both A549 and SK-MES-1 lung cancer cells. However, due to space limitation I focused the efforts of this paper on the more radiation-resistant A549 cells. The affect of lovastatin on SK-MES-1 cell survival alone and in combination with radiation are shown in Figure 3.S1.

In addition, a reviewer requested that our lab examine the action of different statins on the clonogenic survival of A549 cells treated with the drug alone on in combination with radiation. Figure 3.S2 demonstrates that simvastatin has a similar, if not more potent effect, to block A549 cell proliferation when compared to lovastatin.

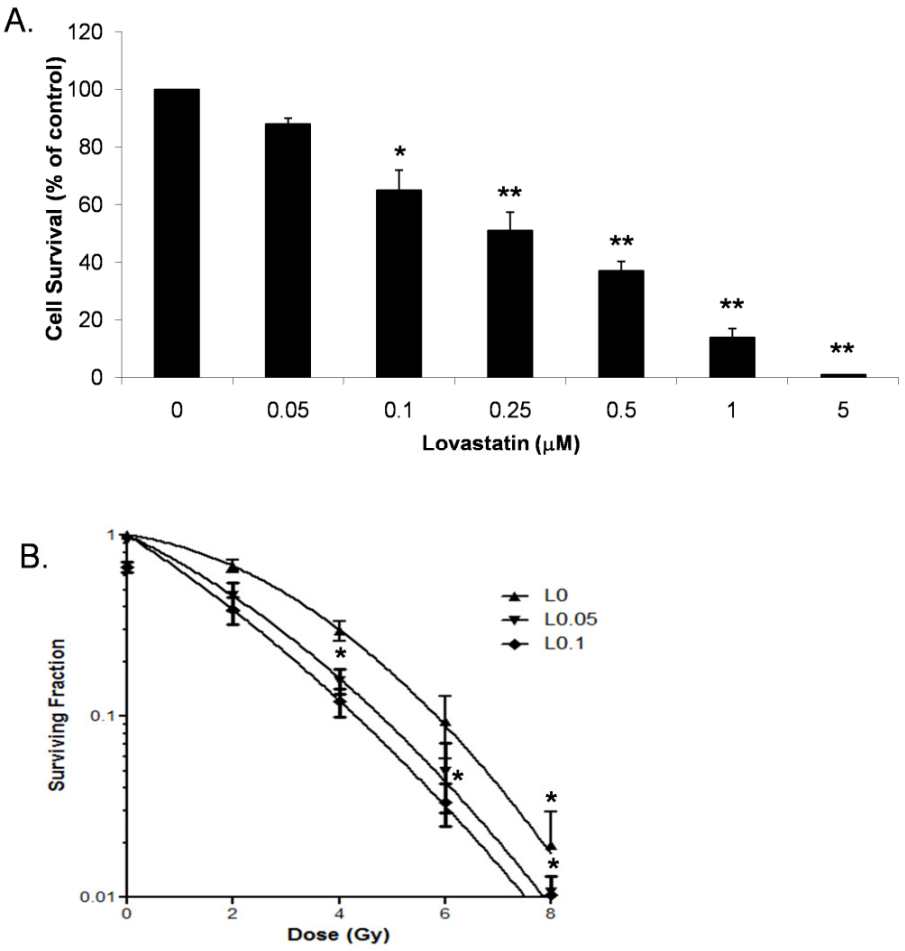

Figure 3.S1: Lovastatin inhibits SK-MES cell clonogenic survival and sensitizes these cells to ionizing radiation. *A*, SK-MES cells were treated with the indicated concentrations of lovastatin and subjected to clonogenic assays. Results from 4-6 independent experiments were normalized to the controls and are shown as the mean ± SE. * = P<0.05 compared to untreated cells, ** = P<0.01 compared to untreated cells *B*, Cells were subjected to increasing doses of IR after incubation without (0) or with lovastatin and subjected to clonogenic assays. The results were normalized to the controls and fitted to the linear quadratic equation using Graphpad Prism 5 software. Values are

expressed as the mean ± SE from 5 independent experiments. * = P<0.05 compared to radiation treatment alone.

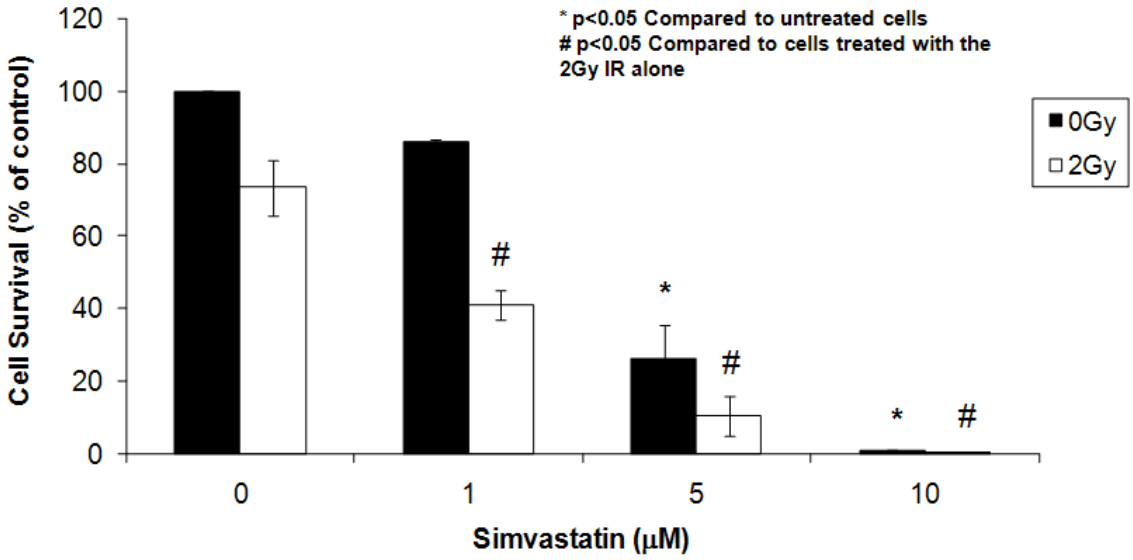

Figure 3.S2: Simvastatin inhibits A549 cell clonogenic survival and sensitizes these cells to ionizing radiation. A549 cells were pre-incubated with the indicated concentrations of simvastatin for 24 hours before exposure to 0-2Gy IR. Results from 2-3 independent experiments were normalized to the controls and are shown as the mean ± SE.

Chapter 4: Ionizing Radiation Regulates AMPK Expression in Cancer Cells

This chapter contains an author generated version of the paper "Ionizing radiation regulates the expression of AMP-activated protein kinase (AMPK) in epithelial cancer cells. *Modulation of cellular signals regulating cell cycle and survival*." This manuscript has been accepted into *Radiotherapy and Oncology* in December 2011.

For this paper, I performed all the cell culture and western blotting for the various normal and cancer lung, prostate, and breast cancer cell lines. In addition, I carried out the immunoflourescence, cell cycle analysis, and survival experiments in the wildtype mouse embryo fibroblast (WT MEFs) and AMPKα1/α2 knockout MEFs (AMPKα$^{-/-}$-MEFs). The western blotting (including quantitation of the blots) and statistical analysis for the MEF experiments were conducted by Yaryna Storozhuk, and the real-time PCR experiments were carried out by Dr. Katja Linher-Melville. The writing of this manuscript was done collaboratively between myself and Dr. Theodoros Tsakiridis. However, helpful comments and suggestions were also provided by all listed authors for this paper.

Context and Background Information

To expand upon or initial observations that IR regulates AMPK activity (Chapter 2), in this paper I addressed if IR is also capable of modulating the long-term subunit expression of this enzyme. Specifically, I investigated which subunits of AMPK are expressed in normal and cancer cells of lung, prostate, and breast origin, and which subunits are affected by IR exposure (24-48h post 8Gy IR). In addition, I employed the use of mouse embryonic fibroblast (MEFs) derived from knockout mice that lack

AMPKα1/2 (generated from Dr. Benoit Viollet's lab) to examine the impact of AMPK signalling on pathways that regulate cell cycle and survival in response to IR.

I initiated this study by probing an array of lung (A549, H1299, SKMES, and H23), prostate (PC3 and 22RV1), and breast (MDA-MB-231 and MCF7) cancer cell lines, as well as their respective normal tissues (MRC5-lung, PNT1A-prostate, and 184B5-breast) for the protein expression of each AMPK subunit. It should be noted that the expression of various AMPK subunit isoforms may be tissue specific. For example, AMPKγ3 is restricted to skeletal muscle (Steinberg & Kemp, 2009), and was not examined in this study. All of these cell lines showed detectable levels of each AMPK subunit (α1, α2, β1, β2, γ1, γ2) with the exception of AMPKα2 in breast cancer cells. I then examined if IR could modulate the mRNA and protein levels of AMPK in A549 lung cancer cells. Indeed, 24-48h following a single fraction of 8Gy IR the phosphorylation of AMPK, as well as the protein and mRNA expression of AMPK was enhanced (with the exception of the AMPKγ2 subunit).

I then utilized AMPKα1/2 (AMPK-/-) MEFs as a model that lacks functional AMPK to address its role on molecular pathways that are triggered by IR, and are involved in cell cycle and survival. To confirm that these cells are truly deficient in AMPK, I first measured AMPK phosphorylation and AMPKα expression in wildtype (Wt) and AMPK-/- MEFs. Compared to Wt MEFs, the AMPK-/- cells completely lacked protein expression of AMPK, as well as phosphorylation of its downstream target Acetyl CoA Carboxylase (ACC). This set of experiments confirmed that these AMPK-/- MEFs obtained from Dr. Viollet's lab were indeed devoid of AMPKα1/2 expression.

Since our lab has previously implicated AMPK as part of an ATM-p53 signalling axis that response to IR, I then examined in AMPK-/- MEFs the ATM pathway at the basal level and in response to 8Gy IR. Interestingly, compared to Wt MEFs, the AMPK-/- cells showed significant increases in total ATM protein levels, as well as enhanced phosphorylation (P-) of its downstream substrates Chk2 and γH2Ax. In addition, Wt MEFs showed an expected increase in their levels of ATM, P-Chk2, and γH2Ax in response to 8Gy IR, but the AMPK-/- MEFs showed the opposite, having a reduced response by IR. A similar trend was observed when I performed immunofluorescent microscopy on MEF cells labeled with an antibody against γH2Ax, where Wt MEFs exhibited increased γH2Ax foci in response to IR and AMPK-/- MEFs had decreased γH2Ax foci upon IR treatment.

As mentioned in the last paper (Chapter 3) the Akt-mTOR pathway can contribute to radiation resistance and proliferation in cancer cells. Using the AMPK-/- MEFs, I investigated how this pathway is affected at the basal level and in response to IR without functional AMPK. As expected, the activity of Akt and mTOR was enhanced in the absence of AMPK (measured by Akt and 4EBP1 protein phosphorylation). In addition, compared to Wt MEFs, IR did not further potentiate the activation of the Akt-mTOR pathway in MEFs that lack AMPK. These results coupled with the observation made on the ATM pathway in AMPK-/- MEFs suggest that AMPK may mediate an oppressive role on these pathways, or that loss of AMPK triggers DNA damage and survival responses (such as increased ROS) that upregulated the ATM-mTOR axis. In addition, AMPK also appears to be required for the normal response of these molecules to IR.

The role of AMPK in modulating signals that regulate cell cycle and survival was also evaluated using the MEF model. Our lab, as well as others (Jones et al., 2005) have suggested that AMPK can regulate p53 to induce a stress-activated checkpoint. Interestingly, when I probed for p53 and p21 levels in AMPK-/- MEFs, I observed that the protein levels of p53 and p21 were elevated compared to Wt MEFs. Furthermore, in response to IR the levels of p53 and p21 displayed the opposite effect, having lower levels in AMPK-/- MEFs compared to untreated cells. These results were further validated when I performed cell cycle analysis on Wt and AMPK-/- MEFs and found that MEFs lacking AMPK fail to arrest in the G2/M phase of cell cycle compared to Wt MEFs. Moreover, the proliferation rates of AMPK-/- MEFs showed a trend to be slightly elevated at the basal state, and in response to IR compared to Wt MEFs.

Overall, this study has indicated that AMPK is widely expressed in normal and cancer cells of lung, prostate, and breast origin, and that IR can enhance its activity and expression. Furthermore, using MEFs that lack functional AMPK has helped evaluate its role in regulating pathways that modulate cell cycle, survival, and genomic stability at the basal state and in response to IR.

Paper: Ionizing radiation regulates the expression of AMP-activated protein kinase (AMPK) in epithelial cancer cells. Modulation of cellular signals regulating cell cycle and survival.

Toran Sanli[1,3], Yaryna Storozhuk[1,2], Katja Linher-Melville[3], Robert G. Bristow[4], Keith Laderout[5], Benoit Viollet[6], James Wright[2], Gurmit Singh[3], and Theodoros Tsakiridis[1,2]

[1]Translational Radiation Biology Laboratory, Juravinski Cancer Center, Dept. of [2]Oncology and [3]Physiology and Pharmacology, McMaster University, Hamilton and [4]Dept. Radiation Oncology, University of Toronto, Toronto, Ontario, Canada, [5]SRI International, Menlo Park, California USA, and [6]INSERM U567, CNRS UMR 8104, Université Paris Descartes, Paris, France

Key Words: AMPK, ionizing radiation, cell cycle, ATM

Address Correspondence to:

Theodoros Tsakiridis, M.D., Ph.D.,

Department of Oncology,

Juravinski Cancer Center and McMaster University,

699 Concession Street,

Hamilton, Ontario,

Canada L8V 5C2;

Tel.: 905-387-9495x64704, Fax: (905) 575-6362,

Email: theos.tsakiridis@jcc.hhsc.ca

Abstract

Purpose: To analyze the i) expression of AMPK in a variety of epithelial cancer cells, ii) regulation of AMPK subunit expression by ionizing radiation (IR) and iii) impact of AMPK on signaling pathways regulating cell cycle and survival.

Methods and Materials: Human lung, prostate, and breast normal and cancer cells were treated with 0 or 8Gy IR and mRNA and protein levels of AMPK were evaluated by RT-PCR and immunoblotting 24 or 48h later. Untreated and radiated Wild Type (WT) and AMPK$\alpha^{-/-}$ mouse embryonic fibroblasts (MEFs) were analyzed by immunoblotting using total- and phosphorylation-specific antibodies. Histone H2Ax was examined by fluorescence microscopy. The cell cycle and survival of WT and AMPK-/- MEFs was also evaluated following 8Gy IR.

Results: AMPK subunits were found widely expressed in normal and cancer epithelial cells. IR increased subunit protein levels and stimulated gene transcription in cancer cells. AMPK$\alpha^{-/-}$-MEFs showed enhanced basal total levels of ATM and phosphorylation of its substrates histone H2Ax, but inhibited response of these markers and of checkpoint kinase Chk2 phosphorylation to IR. AMPK$\alpha^{-/-}$-MEFs showed increased basal levels of p53 and cyclin-dependent kinase inhibitors $p21^{cip1}$, but lack of response of both genes to IR. They had increased basal levels and activation of the Akt-mTOR-$p70^{S6K}$/4-EBP1 signalling pathway. IR increased Akt, $p70^{S6K}$ and 4-EBP1 phosphorylation in WT-MEFs, but this was reduced in AMPK$\alpha^{-/-}$-MEFs. AMPK$\alpha^{-/-}$-MEFs failed to arrest at the G2-M checkpoint after IR and showed a trend for radio-resistance in proliferation assays.

Conclusions: AMPK is widely expressed in human normal and cancer epithelial cells and its gene transcription, protein levels, and enzymatic activity is stimulated by IR. Work with AMPKα knockout cells suggests that AMPK i) may mediate a suppressive regulation on basal expression and activity of ATM and its downstream effector pathways Chk2/ p53-$p21^{cip1}$ and Akt-mTOR, ii) facilitates the normal response of these pathways to IR and, iii) mediates the IR-induced G2-M checkpoint.

Introduction

Radiotherapy (RT) is a common therapeutic modality for the treatment of epithelial tumors of lung, prostate, and breast origin. However, cancer cells of these tumors often demonstrate resistance to ionizing radiation (IR), fail to arrest cell cycle to repair DNA damage, and continue to proliferate under genotoxic stress [1, 2]. In normal cells, IR-induced double strand DNA breaks (DSB)s lead to activation of the kinase Ataxia Telengiectasia Mutated (ATM), which responds through auto-phosphorylation and activation of DNA repair pathways, including phosphorylation of the histone H2Ax (γH2Ax) [3], a signal for recruitment of molecular DNA repair complexes. However, ATM regulates multiple other nuclear and cytoplasmic events leading to cell cycle arrest, gene expression, cell growth and resistance to cytotoxic agents. ATM stimulates IR-induced cycle arrest through activation of checkpoint kinases (Chks), p53, and cyclin-dependent kinase inhibitors (CDKI)s such as $p21^{cip1}$ [2]. In addition, ATM regulates the pro-survival and radio-resistance pathway of Akt–mammalian target of rapamycin (mTOR), which controls gene transcription and translation and cell survival in response to tyrosine kinase receptors stimulation [4]. Akt is regulated by upstream

phosphoinositide-dependent kinases (PDKs) such as PDK1 that phosphorylates Akt on T308 leading to activation of the enzyme [5]. A second, yet unidentified, PDK2 phosphorylates Akt on S473, and studies suggested that ATM may function as PDK2 [4]. Akt mediates activation of mTOR through i) phosphorylation and inhibition of Tuberous Sclerosis Complex 2 (TSC2), which inactivates the GTPase activity of the GTP-binding protein Rheb leading to mTOR activation [6] and ii) through phosphorylation of PRAS40, a member of the functional mTOR complex mTORC1 [7]. mTORC1 stimulates gene translation and survival through phosphorylation-mediated activation of the ribosomal $p70^{S6K}$ and phosphorylation-mediated inhibition of the translation initiation inhibitor 4-EBP1 [5].

The serine/threonine kinase AMPK is a key regulator of cellular energy homeostasis and carbohydrate and lipid metabolism at times of metabolic stress [8, 9]. AMPK functions as a heterotrimeric complex composed of a catalytic α-subunit and regulatory β and γ-subunits [9]. Two α(1/2), two β(1/2) and three γ(1/2/3)-subunits have been identified in mammalian cells [8]. AMPK subunit genes are localized in separate chromosomes and are identified as PRKA A1-2, B1-2, or G1-3 [8].

AMPK functions downstream of the tumour suppressor liver kinase-B 1 (LKB1), that is defective in Peutz-Jegerhs syndrome, which is associated with epithelial cancers such as lung and breast [10]. LKB1 phosphorylates AMPK on α-Thr172, an event required for its activation [9]. During energy stress AMPK inhibits energy consuming anabolic processes such as protein synthesis, cell cycle and proliferation and stimulate

substrate uptake and energy generation through processes such as stimulation of glucose uptake [8].

AMPK mediates a metabolic checkpoint on cell cycle through induction of p53 [11]. Further, this enzyme inhibits mTORC1-stimulated translation through, i) Ser1387 phosphorylation-mediated activation of TSC2 and ii) phosphorylation of Raptor an essential component of mTORC1 [12]. Recently, we suggested that AMPK is activated rapidly by IR, in an LKB1-independ manner, and it may be a novel target for radio-sensitization in human cancers [13]. We observed that AMPK participates in an ATM-AMPK-p53/p21^{cip1} signalling pathway that facilitates the IR-induced G2-M checkpoint. Additionally, we showed that AMPK can be modulated by widely used drugs such as the anti-diabetic agent metformin and the anti-cholesterol drug lovastatin, which have radio-sensitizing properties in lung cancer cells [13, 14].

Here we, i) analyzed the expression of AMPK subunits in various epithelial cancer cells, ii) examined whether IR alters their expression, and iii) investigated further the role of AMPK in signaling pathways involved in DNA repair, cell cycle and survival using the model of AMPK$\alpha^{-/-}$ MEFs.

Materials and Methods

Cells: MRC5 (lung), PNT1A (prostate), and 184B5 (breast) epithelial cells, as well as human lung cancer (A549, H23 and SK-MES-1), prostate cancer (PC3 and 22RV1) and breast cancer (MCF-7 and MDA-MB-231) cells were from American Tissue Culture Collection. The H1299 cells were a kind gift from Dr. Simon Powell (Washington University, MO). Wild type (WT) and AMPKα1/α2 knockout mouse embryo fibroblast

(AMPKα$^{-/-}$-MEFs), were generated by Dr. Benoit Viollet as previously described [15]. Cells were maintained at 37^{o}C as previously described [13].

Antibodies: Rabbit polyclonals against all AMPK subunits, phospho-(Thr^{172})-AMPK, phospho-(Ser^{79})-ACC, ATM, phospho-(Ser^{139})-H2Ax (γH2Ax), phospho-(Thr^{68})-Chk2, Akt, phospho-(Ser^{473})-Akt, phospho-(Thr^{308})-Akt, mTOR, phospho-(Thr^{389})-p70-S6K, phospho-(Thr$^{37/46}$)-4EBP1, and mouse monoclonals against p53, p21^{cip1}, and actin were from Cell Signaling Technology (Mississauga, ON). Alexa Fluor-488 antibody was from Molecular Probes (Burlington, ON).

Treatments: Cells were exposed to 0 or 8Gy ionizing radiation (IR) using a clinical Linear Accelerator radiotherapy unit.

Immunoblotting: Following treatments cells were washed in PBS, lysed. Twenty μg of protein from each sample was subjected to immunoblotting as previously described [13].

Microscopy: Cells were fixed, immune-labeled with anti-γH2Ax antibody and imaged using a 40x wide-field microscope as previously described [13].

Real Time PCR. Total RNA was extracted from cells, cDNA was prepared, and real time PCR was carried out as described previously [16]. The following primer pairs were based on PrimerBank (Harvard Medical School) IDs: AMPKα1 (15214987a1), AMPKα2 (157909838b2), AMPKβ2 (4885561a3), and AMPKγ2 (33186925a3). Primers for AMPKβ1 correspond to FOR: 5'-GCATGGTGGCCATAAGACG-3' and REV: 5'-GCGGGAGCTTTATCATTCAC-3' and for AMPKγ1 to FOR: 5'-CATCCTCAAGAGACCCCAGA-3' and REV: 5'-CACCGTTAGTCACCAAAGCA-3'. Primers used to amplify the RPII housekeeping gene were reported previously [16].

Cell Cycle Analysis: Twenty four hours after seeding cells were treated with or without IR (8Gy). After 48h, cells were fixed with ethanol and incubated with propidium iodide. Cell cycle analysis was conducted as previously described [13].

Cell Proliferation Assay: Five thousand cells were plated onto a 6-well plated and treated with IR 24h later. The plates were allowed to proliferate for an additional 72h before being fixed with 10% formalin and stained with crystal violet solution (0.1% crystal violet in 25% methanol). The cells were then washed and solubilized with 0.05M NaH2PO4 (in 50% ethanol) before being analyzed on a BioTech multiplate reader (Winooski, VT).

Statistical Analysis. Unpaired T-test was performed to analyze the results using SPSS software. Results are presented as mean ± SE. Statistical significance was determined at $P<0.05$(*).

Results

AMPK subunit expression in normal and cancer cell lines.

We analyzed first the protein expression of each AMPK isoform in lung (A549, H1299 and H23: adenocarcinoma, SKMES: squamous cell carcinoma), prostate (PC3: hormone-insensitive and 22Rv1:hormone-sensitive), and breast (MB231: ER-negative and MCF7: ER-positive) cancer cells, as well as in normal lung (MRC5), prostate (PNT1A), and breast (184B5) epithelial cells (Fig. 1). The AMPKγ3 isoform is restricted to skeletal muscle cells [8], and was not investigated in this study.

All cell lines showed detectable levels of AMPK subunits (Fig. 1). Compared to normal epithelial (MRC5), lung cancer cells showed similar protein levels of α1 subunit

but A549, H1299 and SK-MES cells had increased levels of the α2 catalytic subunit. Prostate cancer cells showed higher levels of both α1/2 subunits compared to normal prostate epithelial line (PNT1A). Conversely, breast normal and cancer cell lines appeared to express α1 but lack the α2 subunit (Fig. 1). The regulatory β1/2 subunits of AMPK were not highly expressed in lung cancer cells compared to normal epithelial, except in H1299 cells, but were found elevated in prostate and breast cancer lines compared to their normal counterparts (Fig. 1). Finally, we detected similar expression of the regulatory γ-subunits (γ1/2) of AMPK in both normal and cancer cell lines with the exception that γ2 was not detected in 184B5 normal breast epithelial cells (Fig. 1).

IR enhances AMPK subunit expression:

We examined the effects of IR on AMPK subunit expression in A549 cells (Fig. 2). Twenty four hours following a single fraction of 8Gy IR we observed increased protein levels of each AMPK subunit and they were significantly higher at 48h (Fig. 2a). These findings correlated with increased subunit mRNA expression that was most significant at 48h (Fig. 2b). All AMPK subunits showed a statistically significant response to IR with increased mRNA levels except γ2.

Role of AMPK in propagation of IR signaling events.

We utilized AMPKα$^{-/-}$-MEFs as a model lacking AMPK to examine the impact of this enzyme on molecular pathways involved in cell cycle control and survival (Fig. 3). Compared to WT-MEFs, AMPKα$^{-/-}$-MEFs showed complete lack of phosphorylation of Acetyl CoA Carboxylase (P-ACC) at basal levels, indicating lack of AMPK activity consistent with the absence of total- and P-AMPK (Fig. 3a). WT-MEFs responded rapidly

to IR (8Gy) with increased phosphorylation of AMPK and ACC and a small increase in total AMPK levels, within 1h after IR, but this was effectively abolished in AMPKα$^{-/-}$-MEFs that lack AMPKα (Fig. 3a).

AMPK involvement in ATM signal transduction.

We showed earlier that IR activation of AMPK takes place downstream of ATM [13] and recent reports suggest involvement of AMPK in mitosis and genomic stability [17]. For that, we examined in AMPKα$^{-/-}$-MEFs ATM signaling pathway, including ATM and its downstream targets Chk2 and histone H2Ax (γH2Ax), representing ATM activity. Surprisingly, AMPKα$^{-/-}$-MEFs showed significantly increased total ATM protein levels as well as γH2AX compared to WT-MEFs (Fig. 3a). Furthermore, IR alone enhanced acutely the levels of ATM, phosphorylated Chk2, and γH2AX in WT-MEFs but, importantly, all those events were inhibited in AMPKα$^{-/-}$-MEFs (Fig. 3a). Results from 3 independent experiments were quantitated and are summarized in Figure 3b. The γH2AX immunoblotting results were verified with immunofluorescence microscopy, which also showed enhanced γH2AX foci in untreated AMPKα$^{-/-}$-MEFs, increased foci in WT-MEFs after IR but a reduced response in AMPKα$^{-/-}$-MEFs (Fig. 3c).

Survival signals: AMPKα$^{-/-}$-MEFs showed increased total protein levels of Akt and mTOR. In addition, lack of AMPK resulted in increased phosphorylation of Ser473 on Akt but not T308 (Fig. 4a). Increased mTOR levels in AMPKα$^{-/-}$-MEFs were associated with significantly elevated phosphorylation of p70^{S6k} and 4-EBP1, indicating a generalized stimulation of this pathway leading to protein synthesis and survival when AMPK is absent (Fig. 4a). Furthermore, 8Gy IR increased significantly the

phosphorylation levels of Akt (T308), $p70^{S6k}$ and 4-EBP1 in WT MEFs but, apart from Akt (T308), IR did not enhance significantly further the already enhanced activation of this pathway in AMPK$\alpha^{-/-}$-MEFs (Fig. 4a). Figure 4c shows quantitated immunoblotting results from 3-4 independent experiments.

Signals regulating cell cycle: We and others have suggested that p53 functions downstream of AMPK [11, 13]. Surprisingly, we observed that lack of AMPK catalytic activity in AMPK$\alpha^{-/-}$-MEFs was associated with increased total p53 and $p21^{cip1}$ levels compared to WT-MEFs (Fig. 4b). WT-MEFs exhibited an increase of their levels of p53 and $p21^{cip1}$ in response to 8Gy IR (Fig. 4b). However, AMPK$\alpha^{-/-}$-MEFs failed to respond to IR and showed if anything a trend for reduced levels of p53 and $p21^{cip1}$ after IR (Fig. 4b). The results of three independent experiments were quantitated in Fig. 4c.

AMPK involvement in cell cycle regulation and survival.

We have previously implicated AMPK in the IR-induced G2-M checkpoint in lung cancer cells using AMPK knockdown with specific anti-AMPKα1/2 subunit siRNAs [13]. To verify these results in cells lacking AMPK, we analyzed cell cycle distribution in WT and AMPK$\alpha^{-/-}$-MEFs before or 48 h after IR of 8Gy (Fig. 5a-b). WT-MEFs demonstrated a shift in cells from G1/S to G2/M in response to IR (G1/S: 82% and G2/M: 18% for untreated vs G1/S: 62% and G2/M: 38% for 8Gy treated cells) (Fig. 5a-b). Conversely, AMPK$\alpha^{-/-}$-MEFs cells did not exhibit a detectable change in cell cycle distribution in response to IR (G1/S: 77% and G2/M: 23% for untreated, vs. G1/S: 78% and G2/M: 22% for 8Gy, Fig. 5a-b). These findings are consistent with our earlier work

[13] and the results of Figures 3a-b and 4b-c, indicating lack of induction of p53 and $p21^{cip1}$ in AMPK$\alpha^{-/-}$-MEFs after IR.

Our earlier findings [13] and those of Figures 3 and 4, suggested that AMPK can suppress survival and that its absence may mediate radiation resistance. We compared the proliferation rates of WT and AMPK$\alpha^{-/-}$-MEFs at their basal state and after IR (Fig. 5c). AMPK$\alpha^{-/-}$-MEFs showed i) a tendency to proliferate at a slightly increased rate compared to WT-MEFs (100% WT vs. 105% AMPK$\alpha^{-/-}$) and ii) a partial resistance to IR (2 and 8Gy), which, however, did not reach statistical significance in these experiments (15% increased over the control after 2Gy IR and 8% after 8Gy) (Fig. 5c).

Discussion

Our earlier work with lung cancer cells suggested that AMPK may be a sensor of not only metabolic but also genomic stress [13]. This indicated the importance of AMPK and highlighted the need to understand better its expression patterns and its role in signal transduction in radiated cells.

AMPK gene expression in tumour cells.

AMPK is ubiquitously expressed in mammalian cells, but the expression of each subunit isoform (α1/2, β1/2, and γ1-3) is tissue-specific [8, 9]. In this study we analyzed eight different human epithelial tumour and three non-tumour cell lines of lung, prostate and breast origin. With the exception of AMPKα2 in breast cancer cells and AMPKγ3 (not examined here), we observed detectable protein levels of all subunits in both normal and cancer cell lines (Fig. 1). The expression of β1/2 subunits differed between normal epithelial and cancer cell lines representing each tissue, but the trend was reversed in lung

vs. breast and prostate cell lines, having lower vs. higher levels in cancer cell lines compared to normal cells, respectively. Currently, the significance of these differences remains unclear and warrants further investigation.

Regulation of AMPK gene expression by IR.

Regulation of AMPK subunit expression has been investigated in animal tissues [8] but studies in human tissues, particularly in human tumour cells, are limited. In this study we observed that 24-48h following a single dose of 8Gy, IR elevated AMPK subunit protein levels in lung cancer cells (Fig. 2a). In addition, we have also observed that IR is capable of increasing the AMPK subunit protein levels of breast cancer cells (supplemental Fig. s1), indicating that this phenomenon may be a universal response to IR. Furthermore, PCR analysis demonstrated an induction of AMPK mRNA expression within 24-48h following IR (Fig. 2b), suggesting that in cancer cells, AMPK gene expression is regulated not only at the translational but also at the transcriptional level.

The specific molecular mechanisms that regulate AMPK gene expression have not been elucidated. Feng et al (2007) [18] suggested that IR stimulates AMPKβ1/2 gene expression in HCT116 and H1299 cells in a p53-dependent manner. They related this effect of IR to the presence of putative p53 consensus binding sites on the AMPKβ1 and β2 promoters. In contrast to our findings, they did not detect enhancement of AMPKα or AMPKγ subunit transcription [18]. This discrepancy may be related to the different cancer cell lines used and the time points investigated (24h vs 48h in our study). In our study induction of α1/2 and γ1 gene expression by IR became more obvious 48h after IR delivery (Fig. 2). It has been shown that the p53-dependent cellular stress sensors

sestrin1/2 interacts directly with AMPK and regulates its activity under genotoxic challenges [19]. Furthermore, IR was shown to stimulate Sestrin2 expression [20]. Early results from our laboratory suggest that IR increases significantly the sestrin2 protein levels in lung and breast cancer cell lines (supplemental Fig. s2). In ongoing studies we are investigating the role of sestrin2 in IR-induced AMPK expression and activity.

Role of AMPK in signal transduction.

Lack of AMPK deregulates ATM signal transduction.

It was intriguing to observe in AMPK$\alpha^{-/-}$-MEFs a significant enhancement of basal ATM protein levels that was associated with stimulation of its activity seen as increased γH2Ax, detected by both immunoblotting and fluorescence microscopy (Fig. 3). These findings suggest that AMPK may not be a mere effector of ATM-induced signal transduction, but also regulator of basal ATM expression and activity. Lack of AMPK may either deregulate basal ATM activity leading to phosphorylation of H2Ax in the absence of DNA damage, or alternatively induce a state of genomic instability leading to DNA breaks in untreated cells. This latter scenario would implicate AMPK in carcinogenesis and it should be investigated carefully in the near future. Furthermore, the mechanism of regulation of ATM expression and activity by AMPK needs to be explored in future studies.

In response to 8Gy IR, WT-MEFs showed the well-established stimulation in the ATM/γH2Ax/Chk2 cascade (Fig. 3). However, AMPK$\alpha^{-/-}$-MEFs showed decreased activity of this pathway upon IR treatment, decreased induction of γH2Ax and inhibited Chk2 phosphorylation (Fig. 3). This compromised response of ATM to IR appears to

have implications in signal transduction to downstream effectors of ATM such as p53 and Akt-mTOR, discussed below. Our observation suggests that AMPK may exert control over basal ATM activity and support normal propagation of ATM signaling after IR.

Lack of AMPK leads to activation of Akt – mTOR pathway.

Similar to other studies [21], we observed enhanced phosphorylation levels of mTOR and 4-EBP1 in AMPKα$^{-/-}$-MEFs (Fig. 4a), which is attributed to the absence of inhibitory effects of AMPK on mTOR in those cells [21, 22]. Here, we have detected significantly higher levels of total Akt and mTOR and enhanced S473-Akt phosphorylation in AMPKα$^{-/-}$-MEFs indicating an overall stimulation of Akt-mTOR signaling pathway in cells lacking AMPK. These observations are novel. However, the concept of reciprocal regulation of the AMPK and the Akt pathways in cells has been described earlier in neuronal tissues in response to AMPK activating agents [23]. Enhancement of ATM signaling (Fig. 3) may provide a mechanism for the increased activity of the Akt/mTOR pathway seen in AMPKα$^{-/-}$-MEFs. Consistent with the proposed function of ATM as PDK2 [4], we observed that enhanced ATM activity in untreated AMPKα$^{-/-}$-MEFs was associated with enhanced S473-Akt phosphorylation but not Akt-T308. Enhanced ATM activity in AMPKα$^{-/-}$-MEFs may indeed regulate Akt through S473 phosphorylation.

The responses of the two key targets of mTOR and regulators of gene translation 4-EBP1 and p70^{S6k}, were consistent with the overall behavior of the Akt-mTOR pathway and levels of Akt-S473 phosphorylation. Phosphorylation of 4-EBP1 and p70^{S6k} was significantly increased in untreated AMPKα$^{-/-}$-MEFs which, unlike wild type MEFs,

showed only a small, non-significant, response to IR, reflecting the poor overall responsiveness of this pathway to IR in absence of AMPK activity.

Regulation of the p53-p21^{cip1} pathway, cell cycle and survival.

Since we previously observed that AMPK induces the expression of p53 and p21^{cip1} [13], we hypothesized that AMPKα$^{-/-}$-MEFs cells would show defective levels of these molecules. However, the expression of p53 and p21^{cip1} were increased compared to WT-MEFs, although the latter was not statistically significant (Fig. 4b). Since AMPK and p53 positively regulate each other under metabolic stress [11, 19], it is possible that loss of AMPK in the MEF model initiates feedback loops of expression and activation of p53 as a means to control cycle progression. The induction of p53 expression may be the result of enhanced ATM expression and activity that may regulate p53 in an AMPK-independent manner. Furthermore, studies [24] suggested a role of Akt (which we found upregulated in AMPKα$^{-/-}$-MEFs) in stabilization of p53.

Importantly, we did not observed enhanced p53 and p21^{cip1} levels after IR in AMPKα$^{-/-}$-MEFs (Fig. 4b). This is consistent with our observations in cancer cells that AMPK acts as transducer of IR signals to regulate expression of p53 and p21^{cip1}. Furthermore, the results of figure 5a-b consolidate our earlier observations in cancer cells that AMPK participates in the mediation of IR-induced G2-M checkpoint [13].

Unlike our observations in cancer cells [13], we could not show strong evidence of a role of AMPK in radiation sensitivity in the AMPKα$^{-/-}$-MEF model. We observed only a trend but not a statistically significant resistance to IR in AMPKα$^{-/-}$-MEFs grown in standard growth media (Fig. 5c and supplemental Fig. s3). AMPK is known to

stimulate autophagy in cells under energy stress and autophagy has been proposed to support cell survival and resistance to IR [25, 26]. We have observed detectable levels of the autophagy marker LC3 in untreated wild type MEFs, low levels in AMPK$\alpha^{-/-}$-MEFs and general lack of response of this marker to IR in both cell types (see supplemental Fig. s4). Very recently, Zannella et al [27] suggested that under conditions of no- or low-glucose (0 or 1 mM) AMPK$\alpha^{-/-}$-MEFs are more sensitive to IR but they detected no such effect on clonogenic survival in AMPK$\alpha^{-/-}$-MEFs grown in standard growth media. Overall, we believe that, although AMPK may influence cell survival through autophagy in cells under energy stress, the main effect of this enzyme in cancer cells is likely different, promoting an anti-proliferative action. Although MEFs are useful models to study signal transduction, we think that they are inappropriate models to draw conclusions for the response of cancer cells to cytotoxic therapies.

Conclusions

The present study showed that AMPK subunits are widely expressed in human epithelial cancer cells. IR stimulates expression of AMPK subunit genes and enhances its protein levels. AMPK appears to participate in signaling events that regulate basal ATM activity and response to IR. Loss of AMPK leads to deregulation of ATM activity, abnormal stimulation of the Akt-mTOR-p70^{S6k}/4-EBP1, and p53-p21^{cip1} pathways, lack of normal response of these key enzymes to IR and the loss of the IR-induced G2-M checkpoint. Overall, this work supports further in-depth investigation of AMPK as a target for radio-sensitization of cancer cells and potential involvement of this molecule in genomic stability.

Acknowledgments

Funding was kindly provided by the Canadian Institute of Health Research and Hamilton Health Sciences

References

[1] Galanty Y, Belotserkovskaya R, Coates J, et al. Mammalian SUMO E3-ligases PIAS1 and PIAS4 promote responses to DNA double-strand breaks. Nature 2009; 462:935-9.

[2] Lavin MF. Ataxia-telangiectasia: from a rare disorder to a paradigm for cell signalling and cancer. Nat Rev Mol Cell Biol 2008; 9:759-69.

[3] Derheimer FA and Kastan MB. Multiple roles of ATM in monitoring and maintaining DNA integrity. FEBS Lett 2010; 584:3675-81.

[4] Viniegra JG, Martinez N, Modirassari P, et al. Full activation of PKB/Akt in response to insulin or ionizing radiation is mediated through ATM. J Biol Chem 2005; 280:4029-36.

[5] Wullschleger S, Loewith R and Hall MN. TOR signaling in growth and metabolism. Cell 2006; 124:471-84.

[6] Furic L, Livingstone M, Dowling RJ and Sonenberg N. Targeting mTOR-dependent tumours with specific inhibitors: a model for personalized medicine based on molecular diagnoses. Curr Oncol 2009; 16:59-61.

[7] Wang X, Hawk N, Yue P, et al. Overcoming mTOR inhibition-induced paradoxical activation of survival signaling pathways enhances mTOR inhibitors' anticancer efficacy. Cancer Biol Ther 2008; 7:1952-8.

[8] Steinberg GR and Kemp BE. AMPK in Health and Disease. Physiol Rev 2009; 89:1025-78.

[9] Viollet B, Horman S, Leclerc J, et al. AMPK inhibition in health and disease. Crit Rev Biochem Mol Biol 2010; 45:276-95.

[10] Fogarty S and Hardie DG. Development of protein kinase activators: AMPK as a target in metabolic disorders and cancer. Biochim Biophys Acta 2009; 1804:581-91.

[11] Jones RG, Plas DR, Kubek S, et al. AMP-activated protein kinase induces a p53-dependent metabolic checkpoint. Mol Cell 2005; 18:283-93.

[12] Hardie DG. AMPK and Raptor: matching cell growth to energy supply. Mol Cell 2008; 30:263-5.

[13] Sanli T, Rashid A, Liu C, et al. Ionizing Radiation Activates AMP-Activated Kinase (AMPK): A Target for Radiosensitization of Human Cancer Cells. Int J Radiat Oncol Biol Phys 2010; 78:221-9.

[14] Sanli T, Liu C, Rashid A, et al. Lovastatin sensitizes lung cancer cells to ionizing radiation: modulation of molecular pathways of radioresistance and tumor suppression. J Thorac Oncol 2011; 6:439-50.

[15] Laderoute KR, Amin K, Calaoagan JM, et al. 5'-AMP-activated protein kinase (AMPK) is induced by low-oxygen and glucose deprivation conditions found in solid-tumor microenvironments. Mol Cell Biol 2006; 26:5336-47.

[16] Linher-Melville K, Zantinge S, Sanli T, et al. Establishing a relationship between prolactin and altered fatty acid beta-oxidation via carnitine palmitoyl transferase 1 in breast cancer cells. BMC Cancer 2011; 11:56.

[17] Vazquez-Martin A, Oliveras-Ferraros C, Lopez-Bonet E and Menendez JA. AMPK: Evidence for an energy-sensing cytokinetic tumor suppressor. Cell Cycle 2009; 8:3679-83.

[18] Feng Z, Hu W, de Stanchina E, et al. The regulation of AMPK beta1, TSC2, and PTEN expression by p53: stress, cell and tissue specificity, and the role of these gene products in modulating the IGF-1-AKT-mTOR pathways. Cancer Res 2007; 67:3043-53.

[19] Budanov AV and Karin M. p53 target genes sestrin1 and sestrin2 connect genotoxic stress and mTOR signaling. Cell 2008; 134:451-60.

[20] Budanov AV, Shoshani T, Faerman A, et al. Identification of a novel stress-responsive gene Hi95 involved in regulation of cell viability. Oncogene 2002; 21:6017-31.

[21] Gwinn DM, Shackelford DB, Egan DF, et al. AMPK phosphorylation of raptor mediates a metabolic checkpoint. Mol Cell 2008; 30:214-26.

[22] Sabatini DM. mTOR and cancer: insights into a complex relationship. Nat Rev Cancer 2006; 6:729-34.

[23] King TD, Song L and Jope RS. AMP-activated protein kinase (AMPK) activating agents cause dephosphorylation of Akt and glycogen synthase kinase-3. Biochem Pharmacol 2006; 71:1637-47.

[24] Boehme KA, Kulikov R and Blattner C. p53 stabilization in response to DNA damage requires Akt/PKB and DNA-PK. Proc Natl Acad Sci U S A 2008; 105:7785-90.

[25] Wu WK, Coffelt SB, Cho CH, et al. The autophagic paradox in cancer therapy. Oncogene 2011;

[26] Chaachouay H, Ohneseit P, Toulany M, et al. Autophagy contributes to resistance of tumor cells to ionizing radiation. Radiother Oncol 2011; 99:287-92.

[27] Zannella VE, Cojocari D, Hilgendorf S, et al. AMPK regulates metabolism and survival in response to ionizing radiation. Radiother Oncol 2011;

Figures:

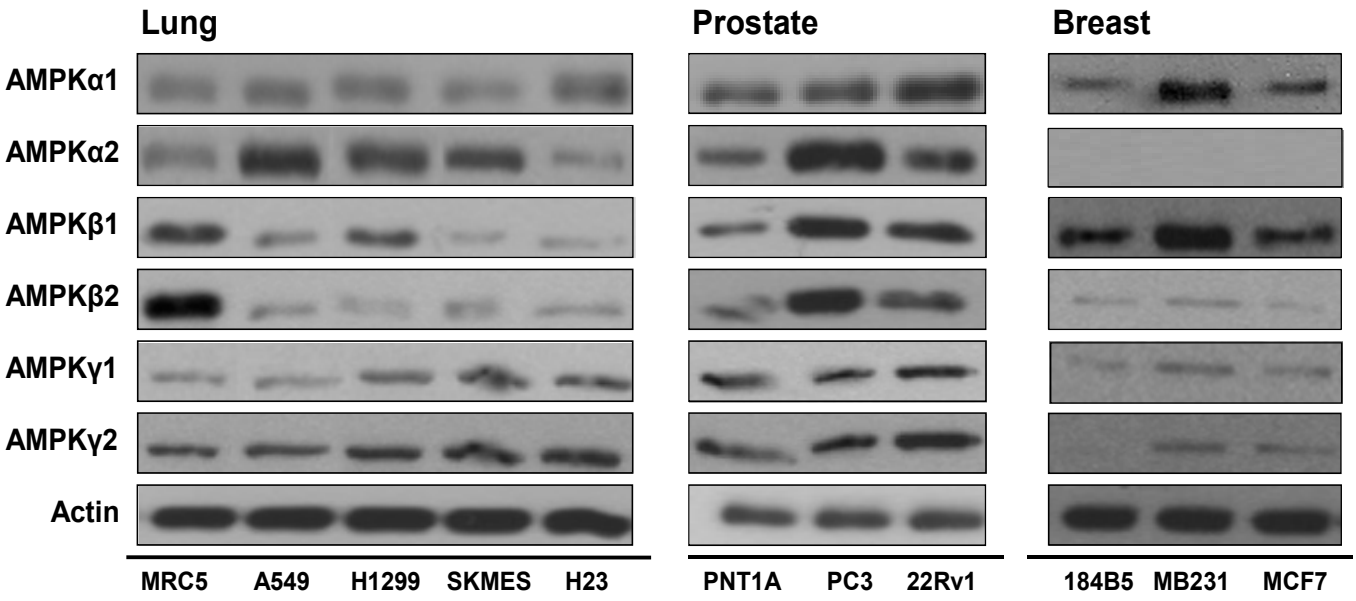

Figure 4.1: AMPK subunit expression in human lung, prostate and breast normal and cancer cell lines. The indicated cell lines were lysed and subject to immunoblotting with the indicated AMPK subunit or actin antibodies. A representative immunoblot from 3 independent experiments is shown.

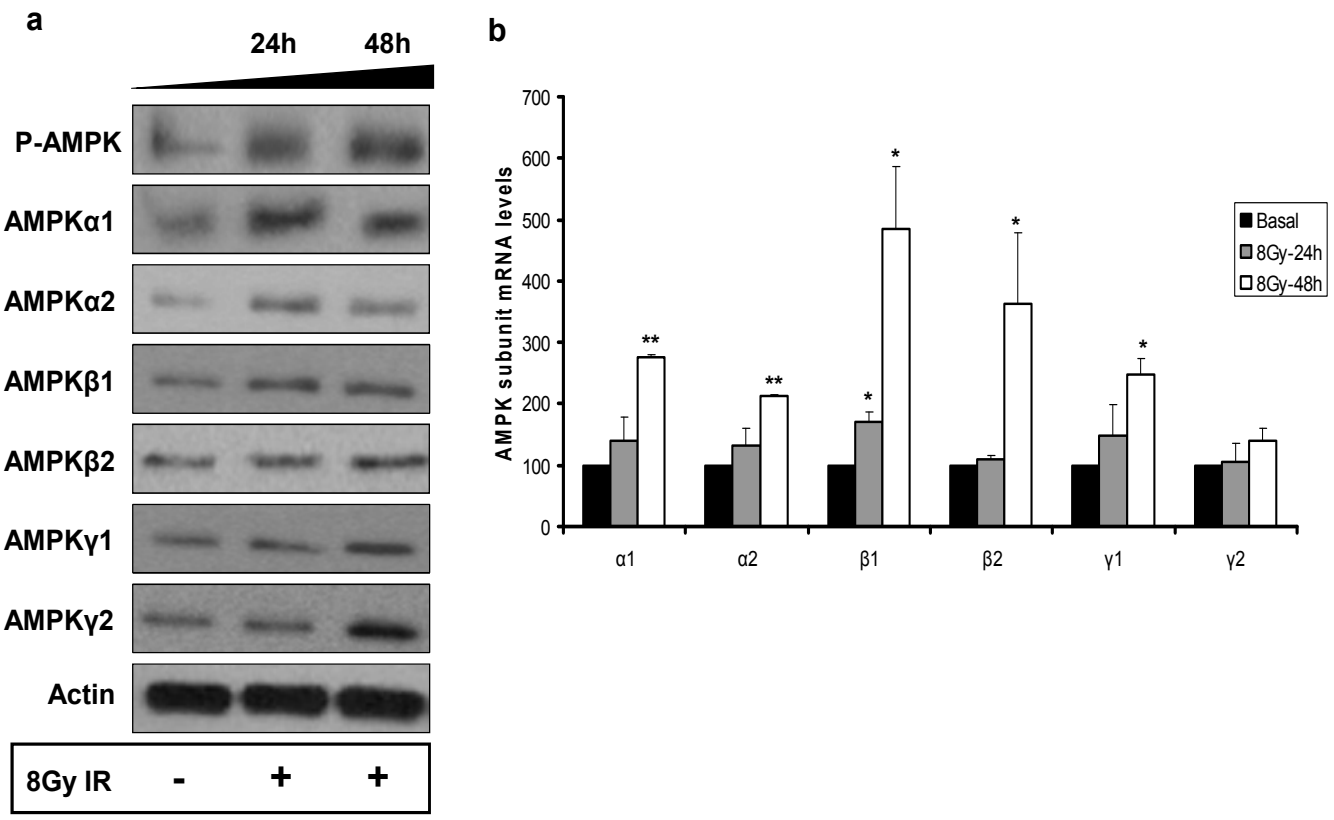

Figure 4.2: IR increases AMPK subunit expression in lung cancer cells. A549 lung cancer cells were treated with or without a single dose of 8Gy IR and lysed after the indicated times. (a) Immunoblotting was performed with the indicated phospho and total AMPK antibodies. A representative immunoblot from 3 independent experiments is shown. (b) Real time PCR was performed with the indicated AMPK subunit primers. The results are presented as the mean ± SE of 2-3 independent experiments (* = $P<0.05$, ** = $P<0.01$).

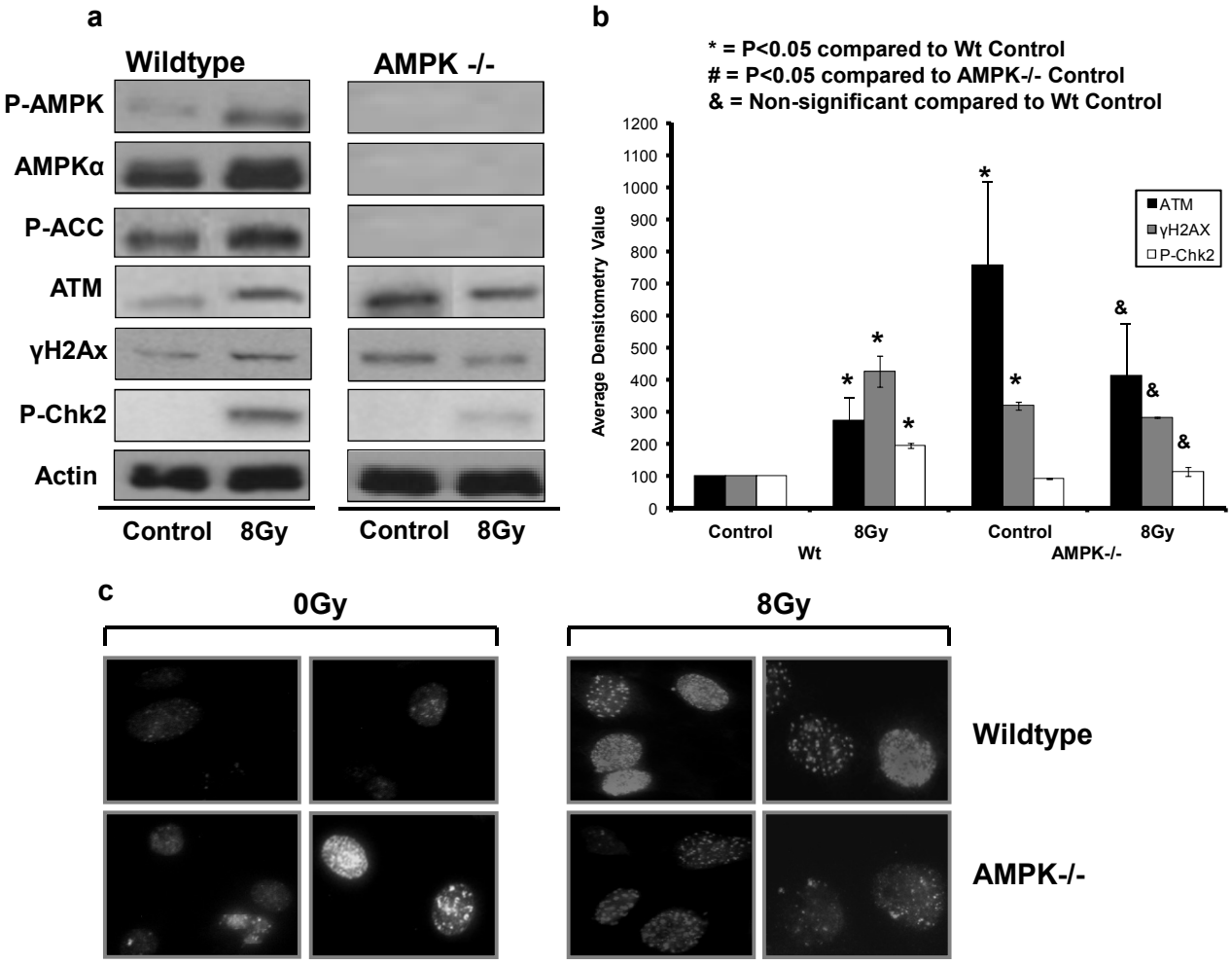

Figure 4.3: Involvement of AMPK in the pathway of DNA repair. (a) Wildtype (*Wt.*) or AMPKα$^{-/-}$-MEFs (AMPK-/-) were lysed in lysis buffer and subjected to western blotting with antibodies against the AMPK and ATM pathway. (b) The densitometry of untreated or IR-treated MEF cells in (a) were quantitated and presented as the mean ± SE of 3 independent experiments. (c) MEF cells were immunostained with γH2AX and images were obtained from a widefield fluorescent microscope. A representative section from each sample is shown.

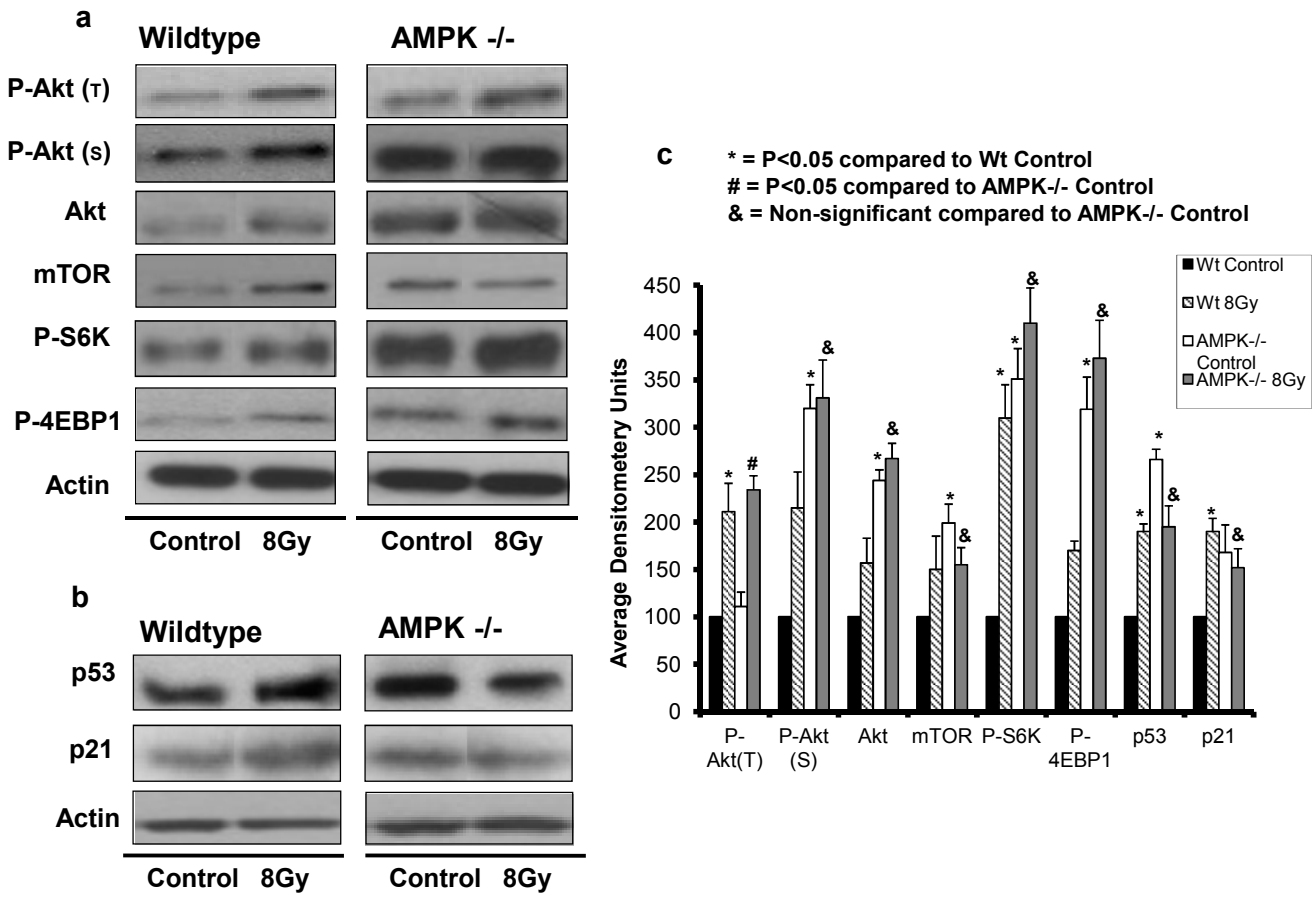

Figure 4.4: Downstream targets of AMPK. Wildtype (*Wt.*) or AMPKα$^{-/-}$-MEFs (AMPK-/-) were lysed in lysis buffer and subjected to western blotting with the indicated antibodies against the (a) Akt/mTOR pathway, as well as the (b) p53/p21^{cip1} pathway. A representative immunoblot from 3 independent experiments is shown. (c) The densitometry of the MEF cells in (a, b) and were quantitated and presented as the mean ± SE of 3 independent experiments.

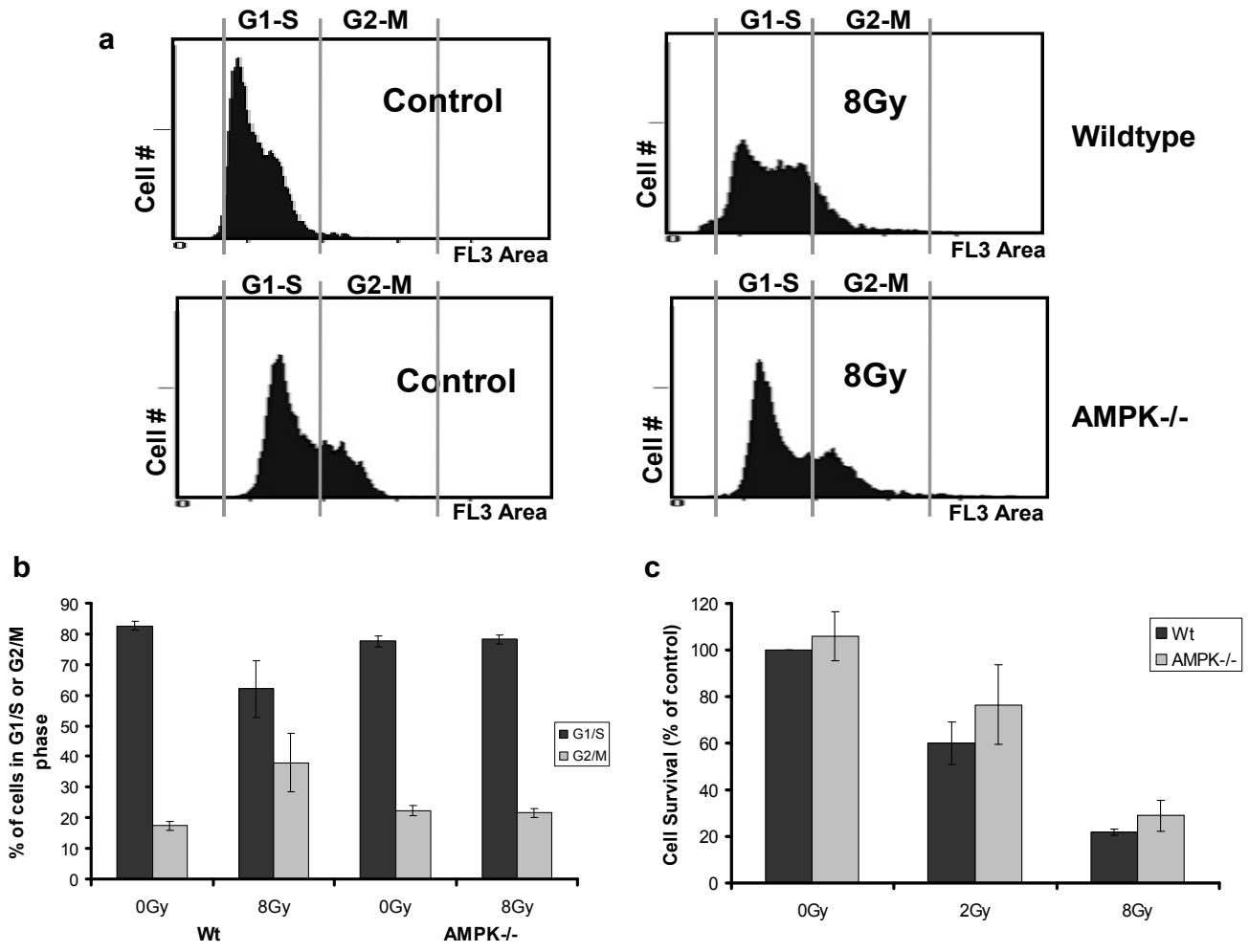

Figure 4.5: Cell cycle regulation and survival in the absence of AMPK. (a) Wildtype (Wt) or AMPK$\alpha^{-/-}$-MEFs (AMPK-/-) were treated with or without a dose of 8Gy IR and fixed in ethanol 48h later. These cells were then stained with propidium iodide and subjected to cell cycle analysis. (b) The results from the experiments in (a) were quantitated and presented as mean ± SE from 3 independent experiments. (c) Wildtype or AMPK$\alpha^{-/-}$-MEFs were treated with the indicated dose of IR and allowed to proliferate for 72h. The cells were then fixed and stained with crystal violet and presented as mean ± SE from 3 independent experiments.

Supporting Experiments

Due to space restriction, some of the experimental data has not been incorporated into to final version of the paper. Though, additional experiments for this manuscript were conducted and incorporated as supplemental data (Figures 4.S1-4.S4). These experiments were carried out to help expand the notion that IR can enhance AMPK subunit expression in multiple cancer cell lines, as well as to elucidate the mechanism by which IR facilitates this effect. In addition, subsequent MEF experiments were conducted to further address the ability of AMPKα-/- MEFs to exhibit radiation resistance.

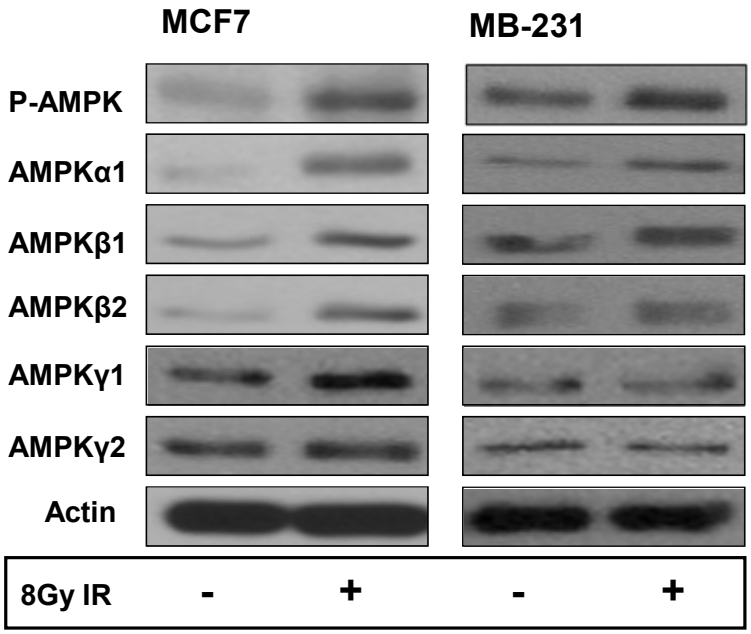

Figure 4.S1: IR enhances AMPK expression in breast cancer cells. MCF7 or MDA-MB-321 cells were treated with or without 8Gy IR and subjected to western blotting with the indicated antibodies. A representative immunoblot from 3 independent experiments is shown.

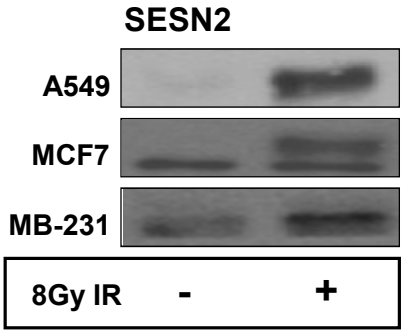

Figure 4.S2: SESN2 is enhanced by IR in lung and breast cancer cells. The indicated cell lines were treated with or without 8Gy IR and subjected to western blotting with an antibody against sestrin2 (SESN2). A representative immunoblot from 3 independent experiments is shown.

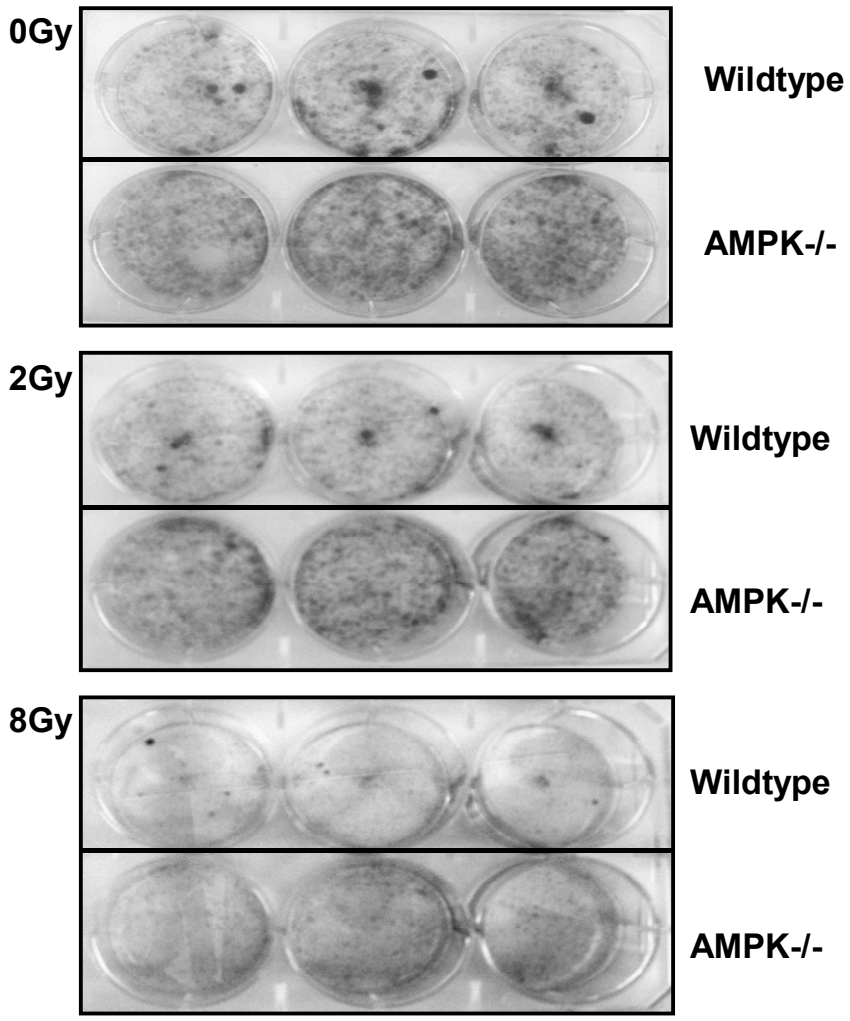

Figure 4.S3: AMPK expression modulates IR-mediate cell survival. Wildtype or AMPK$\alpha^{-/-}$-MEFs (AMPK-/-) were treated with the indicated dose of IR and allowed to proliferate for 72h. The cells were then fixed and stained with crystal violet. A representative image from 3 independent experiments is shown.

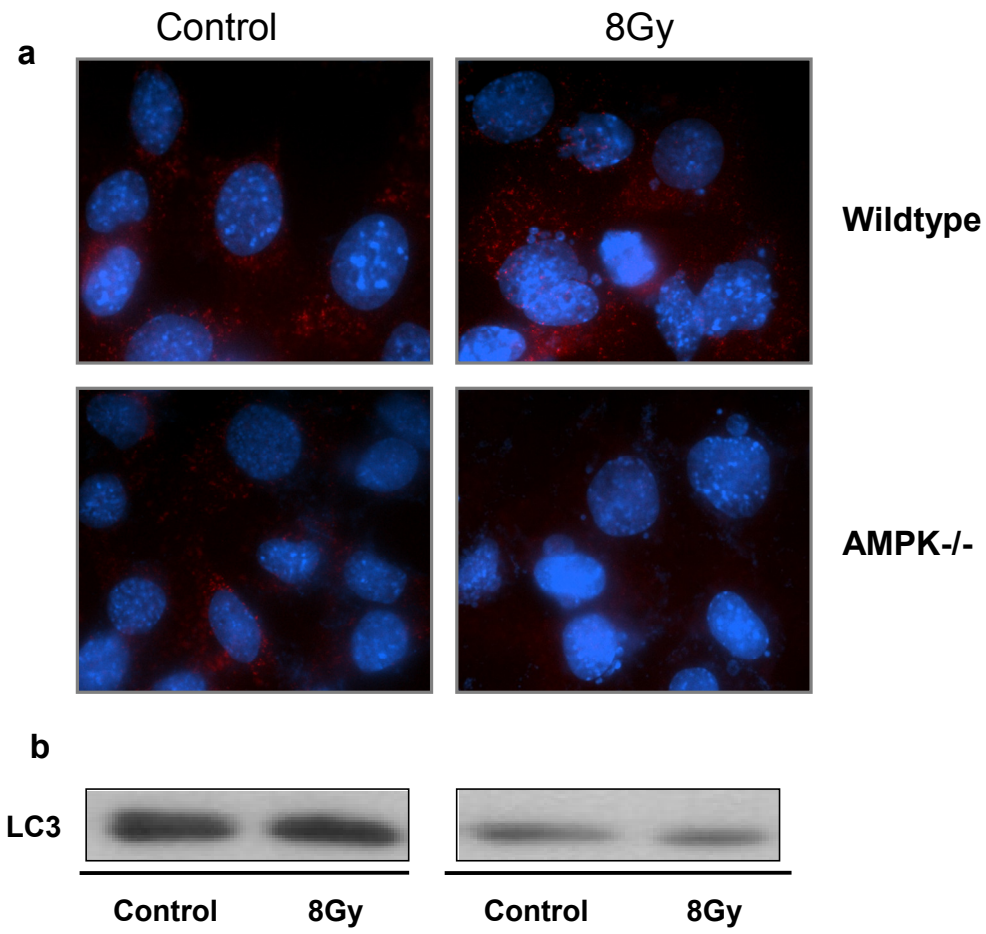

Figure 4.S4: Role of AMPK in Autophagy. MEFs were treated with or without 8Gy IR and fixed 24h later. (a) The cells were then labeled with LC3 antibody (red) or DAPI (blue) and imaged at 40x. (b) MEF cells were treated with or without 8Gy IR and lysed 24h later. These samples were then subjected to western blotting with an antibody against LC3. A representative immunoblot from 3 independent experiments is shown.

Chapter 5: Sestrin2 Modulates AMPK Activity and Expression

This chapter contains an author created version of the manuscript "Sestrin2 modulates AMPK subunit expression and its response to ionizing radiation in breast cancer cells." This manuscript has been accepted into *PLoS ONE* in January 2012.

For this paper I conducted all of the experiments, generated the figures, and wrote the manuscript. Dr. Katja Linher-Melville generated the Sestrin2 Flag-tagged overexpression vector (Sesn2F), and aided in transfecting the MCF7 breast cancer cells with this construct. Supportive suggestions for writing the paper were provided by Dr. Katja Linher-Melville, Dr. Theodoros Tsakiridis, and Dr. Gurmit Singh.

Context and Background Information

Recently, the family of stress-activated proteins, known as sestrins (SESN1-3), was shown to regulate many important aspects of cell signalling and survival in response to genotoxic agents (Budanov et al., 2010). Lately, my interest in these proteins was piqued when two of the SESN2 members (SESN1/2) were reported to be enhanced by IR, as well as regulate AMPK activity. Based on these observations I initially hypothesized that these SESN family members may also regulate AMPK subunit expression in response to IR. Thus, I conducted experiments to address the ability of SESN1/2 to regulate AMPK expression and activity alone and in response to IR in breast cancer cells. However, it should be noted that the focus of this paper was on SESN2, since it was the most widely studied of the SESNs and has also been implicated as a tumour suppressor (Budanov et al., 2010). For supporting data on the ability of SESN1 to regulate AMPK expression and activity, please see appendix 2.

To adequately address the ability of SESN2 to interact with and regulate AMPK subunit expression, I first needed to identify the composition of the predominant AMPK heterotrimeric complex (consisting of one α, one β, and one γ subunit each) in my selected cancer model. MCF7 cells were selected for this study because they are commonly used breast cancer cells that are easily transfected with overexpression vectors or siRNA silencing constructs. In addition, I also obtained a stably-integrated tetracycline-inducible SESN2 system in MCF7 cells (Tet-OFF SESN2 cells) from Dr. Michael Karin's laboratory at the University of California for this study.

To elucidate the most prominent AMPK heterotrimeric complex in MCF7 cells, I performed serial immunoprecipitations (IPs) with antibodies against each AMPK subunit (α1, α2, β1, β2, γ1, γ2, γ3). These antibodies were purchased as part of an AMPK subunit antibody sampler kit from Cell Signalling Technology. However, not all of these antibodies were recommended for IP (the α1, or γ-subunit antibodies), and it was very difficult to find commercial AMPK antibodies against each subunit for this procedure. Nevertheless, these antibodies were good for Western blotting, and based on our results I speculated that the major AMPK active complex in MCF7 cells is the α1β1γ1 heterotrimer.

I then overexpressed SESN2 into these cells using a SESN2-Flag tagged expression vector (Sesn2F), and subsequently immunoprecipitated out total SESN2 protein using a Flag-specific antibody. Interestingly, I found that when I ran Western blots on these IP samples that not only was SESN2 present, but also the AMPKα1β1γ1 trimer, as well as LKB1. In addition, I also measured AMPK phosphorylation on α-

Thr172 and β1-Ser108 (a marker of AMPK activity), as well as α1-Ser485 (marker of AMPK inhibition) following SESN2 overexpression and observed that enhanced SESN2 led to an overall upregulation of AMPK activity.

To identify the sub-cellular localization and interaction between activated AMPK and SESN2, I performed immunofluorescence using antibodies against phosphorylated (Thr172) AMPK and total SESN2 in MCF7 cells that were transiently transfected with Sesn2F. Based on my observations, phosphorylated AMPKα (Thr172) was shown to be in close proximity with SESN2 predominantly in the cytoplasm of MCF7 cells.

I then investigated the ability of SESN2 to modulate the total protein levels of LKB1 and AMPK by performing a Sesn2F dose-response in MCF7 cells. Even at very low levels of SESN2 overexpression (0.05μg Sesn2F); the total levels of LKB1 and AMPK (α1β1γ1) were significantly enhanced. To further confirm these results, I also utilized MCF7 Tet-OFF SESN2 cells that have conditional SESN2 overexpression via removal of doxycycline (Dox) from their growth medium. Dox removal in the cells for 24h showed the same trend as Sesn2F overexpression with regards to enhancing LKB1 and AMPK expression. Moreover, I measured the mRNA levels of LKB1 and AMPKα1β1γ1 in this system and found that they were also elevated, suggesting that enhanced SESN2 can positively regulate the transcription and protein expression of the LKB1-AMPK signalling axis.

Since my previous work (Chapters 2 and 4) has indicated that AMPK activity and expression is enhanced by IR, I sought to examine if SESN2 mediates this effect. To achieve this, I utilized siRNA against SESN2 and silenced the expression of SESN2 prior

to treating MCF7 cells with a single dose of 8Gy IR. Indeed, pretreatment of MCF7 with SESN2 siRNA attenuated the ability of IR to enhance AMPK phosphorylation and expression, indicating that SESN2 is required for radiation-induced AMPK modulation.

Since IR is also known to stimulate pathways of pro-survival (including Akt and mTOR), I then addressed if SESN2 overexpression could block the IR-induced increase in Akt-mTOR signalling, as well as act as a radiation sensitizer in MCF7 cells. Enhanced SESN2 had a tendency to inhibit Akt and mTOR activity alone, as well as to attenuate any effect of 8Gy IR to increase their activity. In addition, chronic overexpression of SESN2 using the Tet-OFF SESN2 system has anti-proliferative effects on MCF7 cells alone, as well as having significantly sensitized these cells to radiation. Interestingly, the anti-proliferative and radio-sensitizing effects of SESN2 were completely reversed when the cells were treated with the AMPK inhibitor compound C, demonstrating that SESN2 works through the AMPK pathway to modulate cell survival in cancer cells. Taken together, it seems likely that SESN2 works synergistically with the AMPK, providing sustained activation and expression of this pathway under times of genotoxic stress to provide tumour suppression and regulate cell viability.

SESTRIN2 MODULATES AMPK SUBUNIT EXPRESSION

Paper: Sestrin2 modulates AMPK subunit expression and its response to ionizing radiation in breast cancer cells.

Toran Sanli[1], Katja Linher-Melville[1], Theodoros Tsakiridis[2], and Gurmit Singh[1*]

Research Department, Juravinski Cancer Center and Departments of [1]Pathology and Molecular Medicine and [2]Oncology, McMaster University, Hamilton, Ontario, Canada

[*]Correspondence and reprint requests to: Dr. Gurmit Singh
Department of Pathology and Molecular Medicine
McMaster University
Hamilton, Ontario, Canada
Tel: 905-387-9711 ext. 67500
Fax: 905-575-6368
E-mail: gurmit.singh@jcc.hhsc.ca

E-mails: Toran Sanli; sanlit@mcmaster.ca, Katja Linher-Melville; linherk@mcmaster.ca, Theodoros Tsakiridis; theos.tsakiridis@jcc.hhsc.ca, Gurmit Singh; gurmit.singh@jcc.hhsc.ca

Abstract

Background: The sestrin family of stress-responsive genes (SESN1-3) are suggested to be involved in regulation of metabolism and aging through modulation of the AMPK-mTOR pathway. AMP-activated protein kinase (AMPK) is an effector of the tumour suppressor LKB1, which regulates energy homeostasis, cell polarity, and the cell cycle. SESN1/2 can interact directly with AMPK in response to stress to maintain genomic integrity and suppress tumorigenesis. Ionizing radiation (IR), a widely used cancer therapy, is known to increase sestrin expression, and acutely activate AMPK. However, the regulation of AMPK expression by sestrins in response to IR has not been studied in depth.

Methods and Findings: Through immunoprecipitation we observed that SESN2 directly interacted with the AMPKα1β1γ1 trimer and its upstream regulator LKB1 in MCF7 breast cancer cells. SESN2 overexpression was achieved using a Flag-tagged SESN2 expression vector or a stably-integrated tetracycline-inducible system, which also increased AMPKα1 and AMPKβ1 subunit phosphorylation, and co-localized with phosphorylated AMPKα-Thr127 in the cytoplasm. Furthermore, enhanced SESN2 expression increased protein levels of LKB1 and AMPKα1β1γ1, as well as mRNA levels of LKB1, AMPKα1, and AMPKβ1. Treatment of MCF7 cells with IR elevated AMPK expression and activity, but this effect was attenuated in the presence of SESN2 siRNA. In addition, elevated SESN2 inhibited IR-induced mTOR signalling and sensitized MCF7 cells to IR through an AMPK-dependent mechanism.

Conclusions: Our results suggest that in breast cancer cells SESN2 is associated with AMPK, it is involved in regulation of basal and IR-induced expression and activation of this enzyme, and it mediates sensitization of cancer cells to IR.

Keywords: *Sestrin2, AMPK, ionizing radiation, LKB1, metabolism*

Introduction

In various malignancies including breast cancer, mitogen activated signals can become constitutively activated leading to increased metabolism and genotoxic stress [1]. There are various cellular compensatory mechanisms that respond genomic stress, including the tumour suppressor p53, which suppresses cell growth and propagation through the induction of numerous target genes [2]. Some products of p53 activation that are important in mediating stress-signalling include AMP-activated protein kinase (AMPK), Tuberous sclerosis 2 (TSC2), and sestrin1/2 (SESN1/2) [3, 4]

Sestrins (SESN) are a small family of stress-sensitive genes that are conserved across several species including *Caenorhabditis elegans, Drosophila melanogaster*, and mammals [5, 6]. Mammals express 3 different SESN family members characterized as SESN1-3. SESN1 and SESN2 were classified as members of the growth arrest and DNA damage (GADD) genes family that could regulate cell growth and viability under different cellular pressures [7, 8]. SESN3 was identified shortly after SESN2 through *in silico* analysis and was found to be a target of the forkhead transcription factors (FoxO) family [9, 10]. SESN also exhibit antioxidant properties and can inhibit intracellular ROS through restoration of overoxidized peroxiredoxins, the enzymes involved in sequestering H_20_2 [5]. More recently, SESN have been shown to modulate important physiological

signalling events that are independent of their redox function [11]. The *Drosophila* ortholog of sestrin (dSESN) is a negative feedback regulator of TOR through AMPK regulation, and dSESN deletion from flies leads to the accumulation of age-associated pathologies [6]. Conversely, mammalian SESN1/2 was shown to act as a scaffolding protein and form an active complex with AMPK and TSC2 to block mTOR signalling in response to genotoxic stress [4]. Furthermore, SESN2 also plays a role in the regulation of autophagy and exhibits tumour suppressive proprieties [12, 13].

AMPK is a heterotrimeric enzyme that is comprised of a catalytic α-subunit, as well as β and γ regulator subunits [14]. There are multiple isoforms of each AMPK subunit (α1, α2, β1, β2, γ1, γ2, and γ3) that allow for up to 12 different heterotrimeric AMPK combinations, each containing one of the α, β, and γ subunits [15]. However, the expression of these various AMPK subunits are tissue specific [15, 16]. For example, the catalytic AMPKα1 subunit is primarily found in endothelial cells, nerves, and smooth muscle [17]. Conversely, the other catalytic AMPKα2 subunit is mainly restricted to skeletal muscle and myocardial tissue [17]. AMPK acts as a fuel gauge by maintaining the ratio of cellular AMP/ATP. Metabolic stressors such as hypoxia, heat shock, and glucose deprivation can also activate AMPK [18, 19], as well as upstream kinases such as liver kinase B1 (LKB1). LKB1 is a tumour suppressor that is mutated in Peutz-Jeghers syndrome and can regulates AMPK by directly phosphorylating it on its Thr172 residue of the catalytic α subunit to increase AMPK activity [15, 20].

Radiation therapy is a common cancer treatment, and recently our laboratory has described that ionizing radiation (IR) can activate AMPK in various cancer cell lines [21].

Exposure to IR causes DNA damage, which in turn activates the kinase ataxia-telangiectasia mutated (ATM) to facilitate cell cycle arrest through stabilization of p53 [22]. IR has also been reported to enhanced expression of SESN1/2 [8] and modulate protein synthesis [23], all in an attempt to repair DNA damage if possible, or induce apoptosis. Here we present evidence that SESN2 not only activates AMPK, but also regulates the expression of AMPK subunits. In addition, we show that SESN2 mediates IR-induced AMPK expression and facilitates radiosensitization of breast cancer cells.

Results:

SESN2 associates with AMPKα1β1γ1 and increases its phosphorylation in MCF7 cells:

To examine the effect of SESN2 modulation on AMPK expression and activity, we first identified the most prominent AMPK heterotrimeric complex in MCF7 breast cancer cells by performing serial immunoprecipitations with antibodies against each AMPK subunit (α1-2, β1-2, β2, and γ1-3), followed by immunoblotting (Figure 1A). AMPKα1, shown to be the major α-subunit in MCF7 cells [4] was highly associated with both AMPKβ1 and AMPKγ1 subunits. Conversely, the α2-subunit of AMPK was not detected by western blotting in these cells (Figure 1A). AMPKβ1 and AMPKβ2 are both expressed in this cell line, and the β1-subunit shares a stronger affinity with α1 and γ1 AMPK subunits (Figure 1A). Of the three γ-AMPK subunits, only the γ1 isoform of AMPK was detected in MCF7 cells and contributes to the active AMPK heterotrimeric complex (Figure 1A). Thus, the main AMPK active complex in MCF7 cells is the α1β1γ1 heterotrimer.

To assess the potential interaction of SESN2 with the AMPKα1β1γ1 complex, we immunoprecipitated SESN2 from MCF7 cells that were transiently transfected with 1μg of a SESN2-Flag tagged expression vector (Sesn2F, Figure 1B). In agreement with previous studies, we found that SESN2 associates with AMPKα1 [4], as well as AMPKβ1 and AMPKγ1 subunits (Figure 1B). Since LKB1 is the major upstream kinase for AMPK, we examined whether LKB1 associates in a complex with SESN2 and AMPK. Indeed, LKB1 was present in immunoprecipitated Sesn2F treated MCF7 lysates (Figure 1B).

The activation state of AMPK was then evaluated with antibodies that detect phosphorylation of AMPK on α-Thr172, α1-Ser485, and β1-Ser108 residues, which are markers of AMPK activity (α-Thr172 and β1-Ser108) and inhibition (α1-Ser485) [24]. Transfection of MCF7 cells with 1μg of Sesn2F led to a significant increase in AMPKα Thr172 and AMPKβ1 Ser108 phosphorylation levels and reduced AMPKα1 Ser485 phosphorylation, indicating an overall upregulation in the state of AMPK activation (Figure 1C-D).

Subcellular distribution of SESN2 and activated AMPK:

Although SESN2 has been described to interact with AMPK, the cellular localization of this interaction has not been identified. To address this we utilized immunoflourescence microscopy with antibodies against total SESN2 and phosphorylated Thr172-AMPKα (P-AMPK) in MCF7 cells (Figure 2A-B). Cells were transfected with either empty-Flag vehicle (control), or 1μg Sesn2F for 48h before fixation and labeling with the indicated antibodies. In control cells, SESN2 was detected mainly in the cytoplasm. On the other hand, phosphorylated AMPKα (P-AMPK) levels were low,

showing very faint distributed in both nuclear and cytoplasmic cellular compartments (Figure 2A). However, in cells treated with Sesn2F both SESN2 and phosphorylated AMPK (P-AMPK) levels were enhanced, with SESN2 remaining largely in the cytoplasm. In addition, SESN2 overexpression led to a redistribution of active AMPK that shared close proximity with SESN2 in the cytoplasm (Figure 2B).

SESN2 enhances AMPK subunit expression

To explore the effects of SESN2 on AMPK and LKB1 expression, we performed a SESN2 dose-response (0.05-1μg Sesn2F) transfection experiment in MCF7 cells to identify the optimal SESN2 levels required to modulate AMPK (Figure s1). A dose-dependent increase in SESN2 expression was achieved by increasing concentrations of Sesn2F cDNA (Figure s1A). However, the increase in AMPK subunit and LKB1 expression did not follow the same pattern, with noticeable effects on protein expression achieved at a dose as low as 0.05μg Sesn2F. However, phosphorylation of AMPK and its downstream AMPK substrate, Acetyl CoA Carboxylase (P-ACC), a marker of AMPK activity, exhibited a dose-response enhancement with increasing concentrations of Sesn2F cDNA treatment that was parallel to that of SESN2 expression (Figure s1B).

To further validate these findings we utilized MCF7 Tet-OFF SESN2 cells that have conditional SESN2 overexpression via removal of doxycyclin (Dox) from their growth medium (Figure s1C-D). With the exception of AMPKγ1, we observed significant increases in SESN2, LKB1, AMPKα1, AMPKβ1, P-AMPKα (Thr172), and P-ACC levels following 24h of Dox removal from the MCF7 Tet-OFF SESN2 media (Figure s1C-D). In contrast, SESN2 expression was associated with only a trend for increased AMPKγ1

levels that was not statistically significant (Figure s1C-D). In addition, we measured the mRNA levels of SESN2, LKB1, and AMPKα1β1γ1 following 24h Dox withdrawal and observed a very significant increase in AMPKα1 levels (785 ± 47% fold compared to control, $P<0.01$, Figure s1E). In addition, the mRNA levels of SESN2, LKB1, and AMPKβ1 were significantly enhanced (191 ± 23%, 221 ± 35%, and 171 ± 22% fold compared to control respectively, $P<0.05$, Figure s1E).

SESN2 plays a role in IR-induced AMPK activity/expression:

We hypothesized that radiation-induced AMPK activity/expression is dependent on SESN2. To examine this, we used siRNA against SESN2 in MCF7 cells that were treated with 8Gy of IR (Figure 3). SESN2 siRNA was added 48h prior to a single dose of 8Gy IR. Twenty four hours after IR, the cells were lysed and the protein expression and phosphorylation of AMPK was evaluated (Figure 3A-B). SESN2 siRNA alone did not significantly affect basal protein levels of AMPK subunits. MCF7 cells exhibited a significant increase in SESN2 and AMPK subunit expression 24h after IR (8Gy), as well as enhanced AMPKα and ACC phosphorylation (Figure 3A-B). However, the IR-induced increase in expression of all main AMPK subunits in MCF7 α1, β1 and γ1 and AMPKα-T172 phosphorylation was attenuated in cells that were pre-treated with siRNA against SESN2 (Figure 3A-B), indicating that SESN2 plays a role in mediating IR-induced AMPK regulation.

Enhanced SESN2 inhibits pro-survival pathways and sensitizes MCF7 cells to IR through AMPK:

We also examined the effect of SESN2 overexpression, IR, or the combined treatment on the activity of the Akt/mTOR survival pathway (Figure 4A-B). MCF7 tet-OFF SESN2 cells showed increased SENS2 levels after removal of doxycyclin and showed a trend for reduced phosphorylation of Akt, mTOR, and the mTOR substrate, p70-S6K (Figure 4A-B). Conversely, IR (8Gy) treatment led to a general stimulation of the Akt/mTOR pathway, but SESN2 overexpression 24h prior to IR treatment significantly inhibited IR-induced activation of the Akt/mTOR signalling (Figure 4A-B).

To examine whether the effects of SESN2 overexpression and IR treatment, leading to inhibition of the Akt signaling pathway, influence cancer cell survival after IR, a clonogenic survival assay using radiation doses (0-8Gy) was conducted (Figure 4C). As expected, MCF7 cells that were treated with IR alone demonstrated a dose-dependent decrease in clonogenic survival. In addition, SESN2 overexpression had significant radiosensitizing effects particularly when combined with 4-8Gy IR (Figure 4C). Furthermore, to evaluate the role of AMPK in mediating SESN2-induced radiosensitization, we treated MCF7 cells with the AMPK chemical inhibitor compound C (CC) prior to SESN2 overexpression and exposure to 2Gy IR (Figure 4D). Enhanced SESN2 levels and 2Gy IR significantly inhibited MCF7 cell survival alone, and had an additive effect when both treatments were combined. On the other hand, CC did not significantly affect the survival of MCF7 cells alone, but showed a trend to reduce the ability of 2Gy IR to decrease breast cancer cell survival. Interestingly, CC significantly attenuated the ability of SESN2 overexpression to reduce cell survival alone and in response to IR.

Discussion

SESN are a family of highly conserved, stress-inducible genes that can defend the cell against oxidative damage and oncogenic signalling [4, 25]. Recently, two members of this family, SESN1/2, have been found to play an important role in suppressing mTOR in response to genotoxic challenge through the regulation of AMPK signalling [4]. In addition, SESN2 has been implicated as a tumour suppressor that can inhibit angiogenesis and promote autophagy [2], underscoring the importance of elucidating the molecular mechanism by which SESN2 regulates pathways of metabolism and suvival. In this study, we have focused our efforts on investigating the relationship between SESN2 and its interaction with AMPK at the basal level, and in response to IR in breast cancer cells.

This study has identified that the primary active AMPK heterotrimeric complex in MCF7 cells is AMPKα1β1γ1. SESN2 was shown to form a protein complex with AMPKα1β1γ1 and LKB1 in MCF7 cells. In addition, we observed that SESN2 overexpression significantly enhanced the phosphorylation of AMPK on both α-Thr172 and β-Ser108 residues. SESN2 and LKB1 have been established to enhance α-Thr172 phosphorylation of AMPK [4, 26]. Conversely, β-Ser108 phosphorylation of AMPK is primarily achieved through auto-phosphorylation, and the ability of upstream kinases to directly target this site remains elusive [27]. Furthermore, SESN2 overexpression opposed AMPKα1-Ser485 phosphorylation, which has been identified as an inhibitory residue that blocks subsequent α-Thr172 phosphorylation by LKB1 [24]. Therefore, SESN2 may facilitate AMPK phosphorylation through a combination of recruitment of LKB1 and increased enzyme auto-phosphorylation.

Although the sub-cellular distribution of SESN2 may fluctuate between cytoplasmic and nuclear compartments, we observed that SESN2 is mainly localized in the cytoplasm of MCF7 cells. On the other hand, the localization of AMPK subunits varies dependent on the specific isoform, as well as their response to different stress stimuli [28, 29]. As we have observed in the past [21] and currently, there was a faint distribution of phosphorylated AMPK in both the nuclear and cytoplasmic compartments in unstimulated cells. However, SESN2 overexpression enhanced AMPK phosphorylation that was mainly prominent in the cytoplasm. Based on these observations it is likely that the majority of SESN2-AMPK interaction occurs within the cytoplasm of MCF7 cells.

Importantly, we also explored the effect of SESN2 overexpression on the total levels of LKB1, AMPK, P-AMPKα, and P-ACC. We observed for the first time that enhanced SESN2 expression alone can increase the mRNA and protein expression of the AMPK pathway (Figure s1). In particular, SESN2, P-AMPKα, and P-ACC exhibited a dose-dependent increase in expression following 0.05-1μg Sesn2F treatment. However, the increase in LKB1 and AMPKα1β1γ1 expression in response to Sesn2F did not depict a classic dose-response pattern. These results suggest that LKB1/AMPK expression is very sensitive to changes in SESN2 levels (0-0.05μg), while the activity of AMPK can be enhanced beyond a low concentration of Sesn2F (0.05-1μg) (please refer to Figure s1A-B).

Moreover, utilization of MCF7 Tet-OFF SESN2 cells experienced similar increases in SESN2 as a low dose of Sesn2F, which also translated into enhanced LKB1/AMPK expression levels (Figure s1C-D). These cells also demonstrated significant

increases in the mRNA levels of LKB1, AMPKα1, and AMPKβ1 suggesting that SESN2 may not only stabilize the association of these kinases, but also enhance their transcription as well (Figure s1E). The ability of SESN2 to alter gene transcription has not been investigated, but it has been speculated that SENS1/2 are part of a positive feedback loop that regulates p53 and AMPK expression and activity under times of genotoxic stress [4, 30]. For example, p53 is known to regulate SESN2 and AMPKβ1 gene expression [3, 8], while AMPKα is able to phosphorylate as well as transcriptionally regulate p53 in response to stress [31]. The most significant increase in mRNA levels with SENS2 overexpression in the AMPK pathway was AMPKα1, which supports the notion of AMPKα-mediated phosphorylation and stabilization of p53. In support of this notion, we have observed that Sesn2F treatment in MCF7 cells is also capable of increasing the phosphorylation and expression levels of p53 (Figure s2). Overall, there is a great deal of communication between the SESN2, p53, and the AMPK signalling pathway in response to stress stimuli that still requires investigation.

We have previously showed that 8Gy IR can acutely activate AMPK in multiple cancer cell lines [21]. However, the long-term effects of radiation or the influence of SESN on AMPK expression was not examined. In this study, we utilized IR as an agent to enhance SESN2 and found that not only was SESN2 levels increased 24h-post 8Gy IR, but the expression and activity of the AMPK active complex (AMPKα1β1γ1) was elevated as well. Conversely, the IR-induced increase in AMPK and P-ACC expression was attenuated in MCF7 when they were pre-treated with siRNA against SESN2. We also observed the same trend in radiated A549 lung cancer cells, where IR-induced AMPK

activity and expression was prevented with SESN2 siRNA (Figure s3). Taken together, these results suggest that IR induces a prolonged increase in SESN2 levels, which may be required for the sustained expression of the AMPK complex (α1β1γ1) in response to stress-stimuli.

Finally, we examined the effect of enhanced SESN2 on pathways of pro-survival and cell cycle regulation that are affected by IR. Increased SESN2 expression inhibited Akt phosphorylation on both Ser473 and Thr308 residues in MCF7 Tet-OFF SESN2 cells, which are required for full Akt activation [32]. In addition, the phosphorylation of mTOR and its downstream substrate p70-S6K was also decreased with enhanced SESN2, validating the role of SESN2 as a negative regulator of mTOR signalling. IR (8Gy) treatment alone increased the expression of Akt/mTOR in MCF7 Tet-OFF SESN2 cells. However, this effect was attenuated when IR was combined with SESN2 overexpression, which translated into significant enhancement of IR-induced cell cytotoxicity when clonogenic survival was measured. In addition, we observed that the capability of SESN2 to augment cell death alone and in response to IR was dependent of AMPK activity, as compound C attenuated the SESN2-mediated reduction in MCF7 cell survival.

This model of SESN2 overexpression has been previously reported to modulate cell viability depending on the type of stress condition [8]. Enhanced SESN2 via the MCF7 Tet-OFF system sensitizes cell to DNA damaging treatments like UV radiation, and as we have shown, IR. However, overexpression of SESN2 was also established to protect cells from apoptosis induced by glucose deprivation [8]. Interestingly, AMPK is also required for prolonged cell survival upon glucose withdrawal [18] and irradiation

during starvation [33], reinforcing the relationship between SESN2 and AMPK to modulate cell survival under different cellular pressures.

Taken together, our model supports the notion that SESN2 is stress-activated gene that regulates AMPK activity by orchestrating recruitment of LKB1, as well as increasing LKB1/AMPKαβγ expression (Figure 5). In addition, we show for the first time that SESN2 blocks IR-induced Akt-mTOR signalling and acts as a radiation sensitizer in breast cancer cells (Figure 5). Future studies should elucidate the specific mechanism by which SESN2 phosphorylates AMPK, and examine its potential to act as a transcription factor that regulates metabolic gene expression.

Materials and Methods

Materials. DMEM media (5mM glucose), RPMI media, fetal bovine serum (FBS), trypsin and antibiotic were purchased from Invitrogen (Burlington, ON, Canada). Antibodies against LKB1, phospho-AMPK α-subunit-(Thr172), phospho-AMPK α1-subunit-(Ser485), phospho-AMPK β-subunit-(Ser108), phospho-Acetly-CoA-Carboxylase (P-ACC), AMPKα1-2, AMPKβ1-2, AMPKγ1-3, phosphor-mTOR, phospho-p70-S6K, actin, and HRP-conjugated anti-rabbit secondary antibody were purchased from Cell Signalling (Mississauga, ON, Canada). Sestrin2 (SESN2) antibody was obtained from ProteinTech Group (Chicago, IL, USA). Polyvinylidene difluoride (PVDF) membrane was purchased from Pall Corporation (Port Washington, NY, USA). The FLAG-tag vector and antibodies were from Sigma (Toronto, ON, Canada). MCF7 cells were from the American Type Culture Collection (ATCC: Manassa, VA). The sestrin2

MCF7 tetracycline-OFF (Tet-OFF) cells was a kind gift from Dr. Michael Karin's laboratory (University of California, San Diego).

Cell Culture and Treatments. MCF7 cells were grown in DMEM media that was supplemented with 10% (v/v) FBS and 1% (v/v) antibiotic-antimycotic. These cells were grown at 37^{o}C as previously described [21]. Cells were treated with 2 to 8Gy IR using a clinical Linear Accelerator radiotherapy unit. The Tet-OFF MCF7 cells were maintained in standard DMEM growth medium supplemented with 0.5μg/mL of doxycycline, and for SESN2 overexpression this medium was replaced with normal DMEM for 24h [4]. Lipofectamin-2000 was used as a transfection reagent, and the cells were treated with plasmid vectors as previously described [4]. For siRNA transfection, cells were incubated with HiPerFect with or without siRNA against SESN2 for the indicated times, as per manufacturer's protocol [21].

Clonogenic Assay. MCF7 Tet-OFF cells were subjected to clonogenic assays as described earlier [21]. In brief, 1000 cells were seeded into individual wells of a 6-well plate in triplicate 24h before doxycycline withdrawal. Following 24h of doxycyline removal, the cells were treated with a single dose of radiation (0-8Gy). After 7 days cells were fixed with mythelene blue and viable colonies (>50 cells) were counted. To assess radiation sensitization by SESN2, data was fitted to the linear quadratic equation using Graphpad Prism 5 software as previously described [34].

Immunoprecipitation Assay. Following treatments, MCF7 cells were lysed in lysis buffer [20mM Tris (pH 7.5), 150mM NaCl, 1mM EDTA, 1mM EGTA, 1% Triton X-100, 2.5mM $Na_4P_20_7$, 1mM β-glycerolphosphate, 1mM Na_3VO_4] containing one complete

mini protease inhibitor cocktail tablet (Roche, Quebec Canada). 200μL of lysate were then incubated with antibodies against the AMPK subunits or an anti-Flag antibody overnight, followed by the addition of 20μL of protein A agarose beads (Sigma, Toronto, ON) for an additional 2h. The samples were then repeatedly centrifuged and washed with lysis buffer prior to the addition of SDS-sample buffer and boiling.

Immunoblotting. Twenty μg of protein was separated by SDS-PAGE and transferred to PVDF membranes as described earlier [21]. The primary antibody was detected with HRP-conjugated anti-rabbit or anti-mouse secondary antibody and ECL detection reagent.

Real Time PCR. Total RNA was extracted from MCF7 cells, cDNA was prepared, and real time PCR was carried out as previously described [35]. The *AMPKα1* primer pairs were based on the PrimerBank (Harvard Medical School) ID 15214987a1. Primers for *SESN2* correspond to FOR: 5'-GCGAGATCAACAAGTTGCTGG-3' and REV: 5'-ACAGCCAAACACGAAGGAGG-3', and for *LKB1* FOR: 5'-GAGCTGATGTCGGTGGGTATG-3', and REV: 5'-CACCTTGCCGTAAGAGCCT-3', and for *AMPKβ1* FOR: 5'-GCATGGTGGCCATAAGACG-3' and REV: 5'-GCGGGAGCTTTATCATTCAC-3', and for *AMPKγ1* FOR: 5'-CATCCTCAAGAGACCCCAGA-3' and REV: 5'-CACCGTTAGTCACCAAAGCA-3'. Primers used to amplify the *RPII* housekeeping gene were reported previously [35].

Densitometry. The densitometry of immunoblots was performed using Image J software. Densitometry values are expressed as a percent change over the control value and are shown as mean ± SE of at least 3 independent experiments.

Immunofluorescence Microscopy. Following treatments, cells were washed in PBS and fixed using 3% paraformaldehyde. The cells were labeled with the indicated primary antibodies and anti-mouse Alexa488 and anti-rabbit Alexa568 secondary antibodies were added the following day. The cells were then stained with DAPI and images were obtained as described previously [21].

Statistical Analysis. Statistical analyses were performed using a student's T-test, or when appropriate, a one-way ANOVA with SPSS v16.0 software (Somers, NY). The results are presented as Mean ± SE of at least 3 separate experiments.

Acknowledgements

The authors would like to thank Dr. Andrei Budanov for providing the SESN2 construct and MCF7 Tet-OFF cells.

References

1. Benz CC and Yau C (2008) Ageing, oxidative stress and cancer: paradigms in parallax. Nat Rev Cancer 8: 875-879.

2. Budanov AV, Lee JH and Karin M (2010) Stressin' Sestrins take an aging fight. EMBO Mol Med 2: 388-400.

3. Feng Z, Hu W, de Stanchina E, Teresky AK, Jin S, et al. (2007) The regulation of AMPK beta1, TSC2, and PTEN expression by p53: stress, cell and tissue specificity, and the role of these gene products in modulating the IGF-1-AKT-mTOR pathways. Cancer Res 67: 3043-3053.

4. Budanov AV and Karin M (2008) p53 target genes sestrin1 and sestrin2 connect genotoxic stress and mTOR signaling. Cell 134: 451-460.

5. Budanov AV, Sablina AA, Feinstein E, Koonin EV and Chumakov PM (2004) Regeneration of peroxiredoxins by p53-regulated sestrins, homologs of bacterial AhpD. Science 304: 596-600.

6. Lee JH, Budanov AV, Park EJ, Birse R, Kim TE, et al. (2010) Sestrin as a feedback inhibitor of TOR that prevents age-related pathologies. Science 327: 1223-1228.

7. Velasco-Miguel S, Buckbinder L, Jean P, Gelbert L, Talbott R, et al. (1999) PA26, a novel target of the p53 tumor suppressor and member of the GADD family of DNA damage and growth arrest inducible genes. Oncogene 18: 127-137.

8. Budanov AV, Shoshani T, Faerman A, Zelin E, Kamer I, et al. (2002) Identification of a novel stress-responsive gene Hi95 involved in regulation of cell viability. Oncogene 21: 6017-6031.

9. Chen CC, Jeon SM, Bhaskar PT, Nogueira V, Sundararajan D, et al. (2010) FoxOs inhibit mTORC1 and activate Akt by inducing the expression of Sestrin3 and Rictor. Dev Cell 18: 592-604.

10. Peeters H, Debeer P, Bairoch A, Wilquet V, Huysmans C, et al. (2003) PA26 is a candidate gene for heterotaxia in humans: identification of a novel PA26-related gene family in human and mouse. Hum Genet 112: 573-580.

11. Budanov AV (2010) Stress-responsive Sestrins link p53 with redox regulation and mTOR signaling. Antioxid Redox Signal

12. Maiuri MC, Malik SA, Morselli E, Kepp O, Criollo A, et al. (2009) Stimulation of autophagy by the p53 target gene Sestrin2. Cell Cycle 8: 1571-1576.

13. Sablina AA, Budanov AV, Ilyinskaya GV, Agapova LS, Kravchenko JE, et al. (2005) The antioxidant function of the p53 tumor suppressor. Nat Med 11: 1306-1313.

14. Steinberg GR and Kemp BE (2009) AMPK in Health and Disease. Physiol Rev 89: 1025-1078.

15. Fogarty S and Hardie DG (2009) Development of protein kinase activators: AMPK as a target in metabolic disorders and cancer. Biochim Biophys Acta 1804: 581-591.

16. Iseli TJ, Oakhill JS, Bailey MF, Wee S, Walter M, et al. (2008) AMP-activated protein kinase subunit interactions: beta1:gamma1 association requires beta1 Thr-263 and Tyr-267. J Biol Chem 283: 4799-4807.

17. Viollet B, Athea Y, Mounier R, Guigas B, Zarrinpashneh E, et al. (2009) AMPK: Lessons from transgenic and knockout animals. Front Biosci 14: 19-44.

18. Jones RG, Plas DR, Kubek S, Buzzai M, Mu J, et al. (2005) AMP-activated protein kinase induces a p53-dependent metabolic checkpoint. Mol Cell 18: 283-293.

19. Hardie DG (2008) AMPK: a key regulator of energy balance in the single cell and the whole organism. Int J Obes (Lond) 32 Suppl 4: S7-12.

20. Hemminki A, Markie D, Tomlinson I, Avizienyte E, Roth S, et al. (1998) A serine/threonine kinase gene defective in Peutz-Jeghers syndrome. Nature 391: 184-187.

21. Sanli T, Rashid A, Liu C, Harding S, Bristow RG, et al. (2010) Ionizing Radiation Activates AMP-Activated Kinase (AMPK): A Target for Radiosensitization of Human Cancer Cells. Int J Radiat Oncol Biol Phys 78: 221-229.

22. Bristow RG and Hill RP (2008) Hypoxia and metabolism. Hypoxia, DNA repair and genetic instability. Nat Rev Cancer 8: 180-192.

23. Braunstein S, Badura ML, Xi Q, Formenti SC and Schneider RJ (2009) Regulation of protein synthesis by ionizing radiation. Mol Cell Biol 29: 5645-5656.

24. Horman S, Vertommen D, Heath R, Neumann D, Mouton V, et al. (2006) Insulin antagonizes ischemia-induced Thr172 phosphorylation of AMP-activated protein kinase alpha-subunits in heart via hierarchical phosphorylation of Ser485/491. J Biol Chem 281: 5335-5340.

25. Nogueira V, Park Y, Chen CC, Xu PZ, Chen ML, et al. (2008) Akt determines replicative senescence and oxidative or oncogenic premature senescence and sensitizes cells to oxidative apoptosis. Cancer Cell 14: 458-470.

26. Shaw RJ, Kosmatka M, Bardeesy N, Hurley RL, Witters LA, et al. (2004) The tumor suppressor LKB1 kinase directly activates AMP-activated kinase and regulates apoptosis in response to energy stress. Proc Natl Acad Sci U S A 101: 3329-3335.

27. Woods A, Vertommen D, Neumann D, Turk R, Bayliss J, et al. (2003) Identification of phosphorylation sites in AMP-activated protein kinase (AMPK) for upstream AMPK kinases and study of their roles by site-directed mutagenesis. J Biol Chem 278: 28434-28442.

28. Kodiha M, Rassi JG, Brown CM and Stochaj U (2007) Localization of AMP kinase is regulated by stress, cell density, and signaling through the MEK-->ERK1/2 pathway. Am J Physiol Cell Physiol 293: C1427-1436.

29. Salt I, Celler JW, Hawley SA, Prescott A, Woods A, et al. (1998) AMP-activated protein kinase: greater AMP dependence, and preferential nuclear localization, of complexes containing the alpha2 isoform. Biochem J 334 (Pt 1): 177-187.

30. Hay N (2008) p53 strikes mTORC1 by employing sestrins. Cell Metab 8: 184-185.

31. Okoshi R, Ozaki T, Yamamoto H, Ando K, Koida N, et al. (2008) Activation of AMP-activated protein kinase induces p53-dependent apoptotic cell death in response to energetic stress. J Biol Chem 283: 3979-3987.

32. Wullschleger S, Loewith R and Hall MN (2006) TOR signaling in growth and metabolism. Cell 124: 471-484.

33. Zannella VE, Cojocari D, Hilgendorf S, Vellanki RN, Chung S, et al. (2011) AMPK regulates metabolism and survival in response to ionizing radiation. Radiother Oncol

34. Sanli T, Liu C, Rashid A, Hopmans SN, Tsiani E, et al. (2011) Lovastatin sensitizes lung cancer cells to ionizing radiation: modulation of molecular pathways of radioresistance and tumor suppression. J Thorac Oncol 6: 439-450.

35. Linher-Melville K, Zantinge S, Sanli T, Gerstein H, Tsakiridis T, et al. (2011) Establishing a relationship between prolactin and altered fatty acid beta-oxidation via carnitine palmitoyl transferase 1 in breast cancer cells. BMC Cancer 11: 56.

Figures:

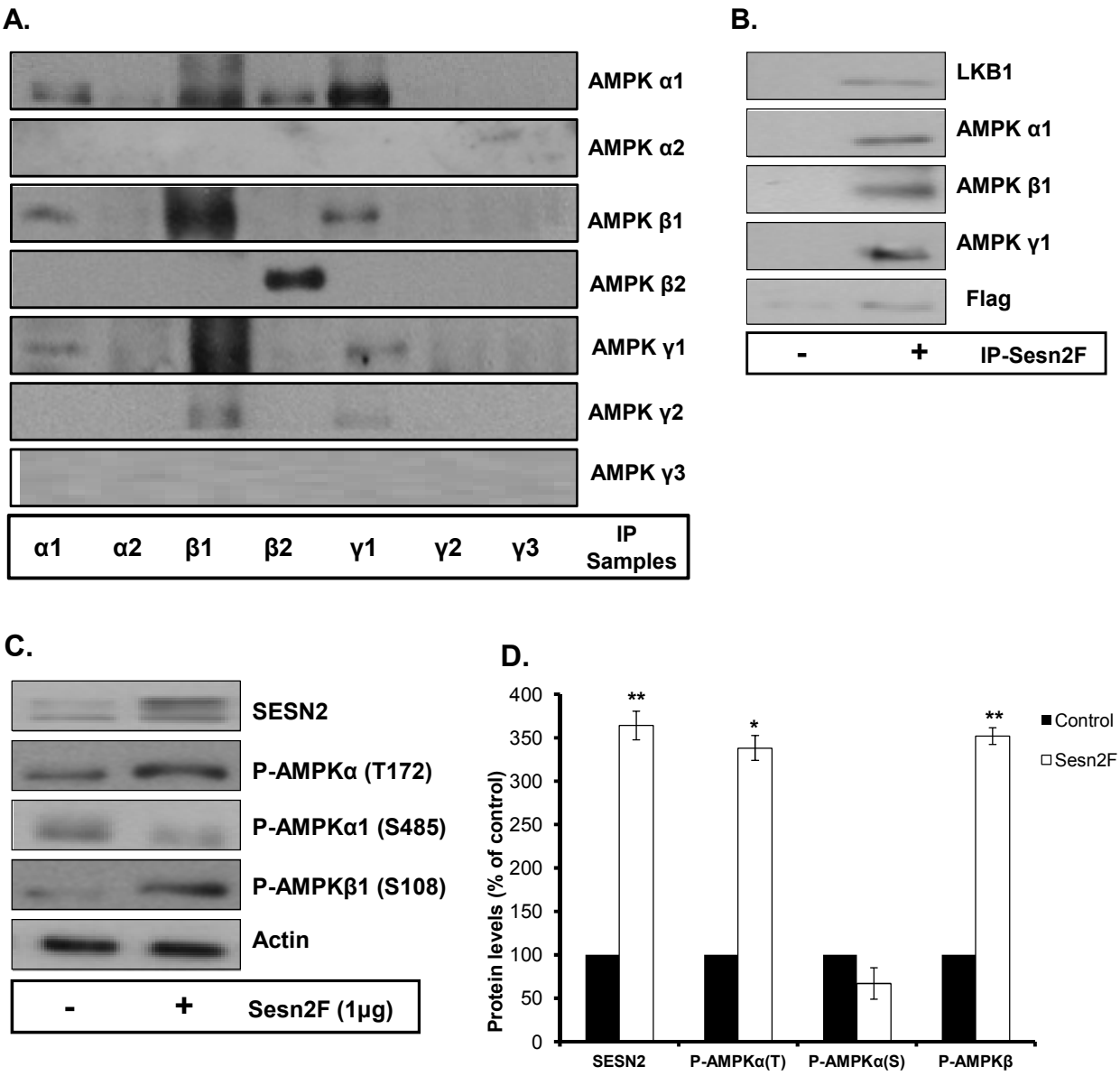

Figure 5.1: SESN2 interacts and regulates AMPKα1β1γ1 activity in MCF7 cells. (**A**) MCF7 cells were plated into a 10cm dish and grown until fully confluent. The cells were then lysed with lysis buffer and immunoprecipitation was performed with the indicated AMPK subunit antibodies. These samples were then subjected to western blotting with

AMPK subunit antibodies. A representative immunoblot from 3 independent experiments is shown. (**B**) Cells were transfected with 1μg empty Flag vector (-) or 1μg Sesn2F (+). Forty eight hours later the cells were lysed and immunoprecipitation was performed with an anti-Flag antibody. The samples were then subjected to western blotting with the indicated antibodies. (**C**) MCF7 cells were treated with 1μg empty Flag vector (-) or 1μg Sesn2F (+). Forty eight hours later the cells were lysed and subjected to western blotting with the indicated phosphorylated AMPK antibodies. (**D**) The results from (**C**) were quantitated and expressed as the mean and SE from 3 independent experiments (* = $P<0.05$ and ** = $P<0.01$ compared to control).

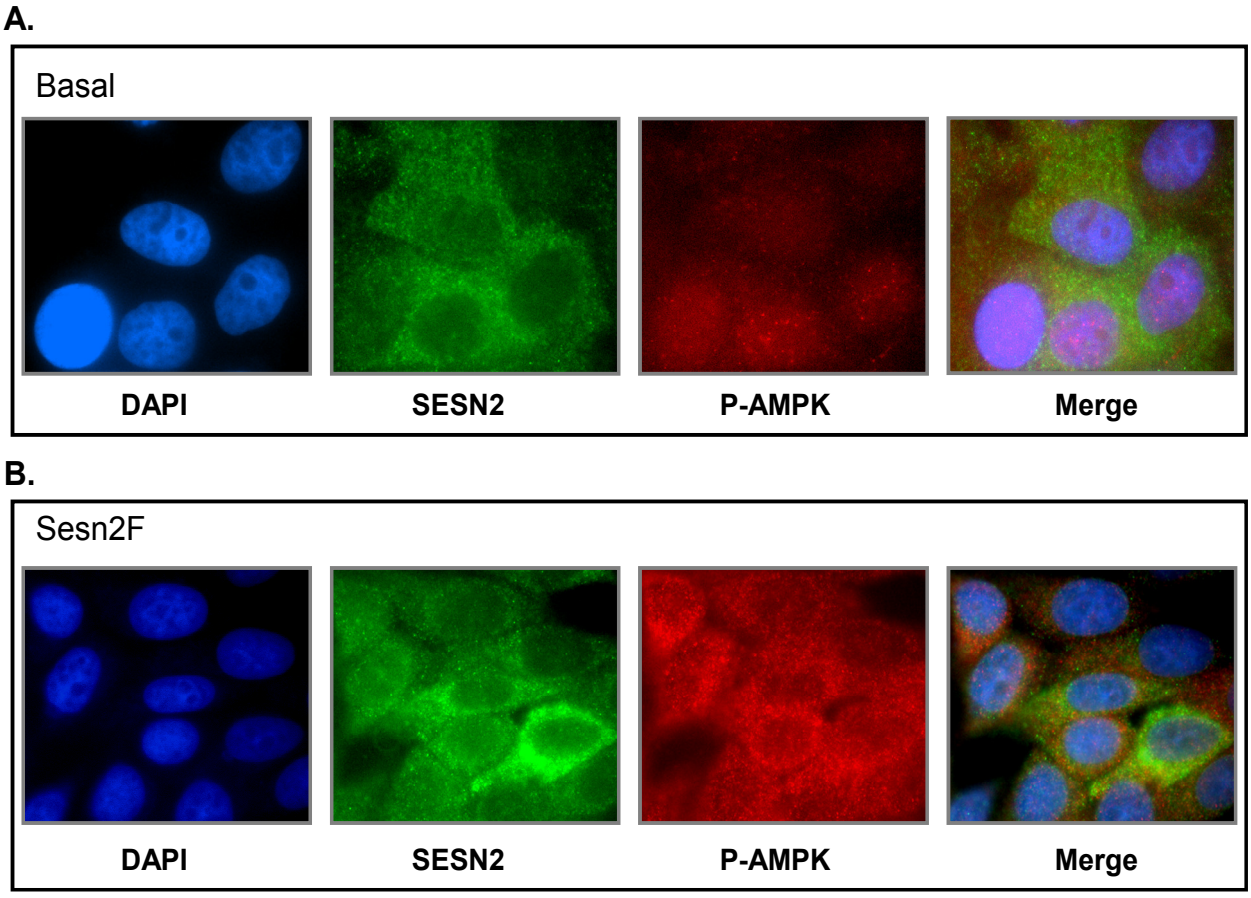

Figure 5.2: SESN2 is found in close proximity with active AMPK in the cytoplasm of MCF7 cells. (**A**) Untreated MCF7 cells were fixed and stained with DAPI (blue), SESN2 (green), or P-AMPKα (red). (**B**) MCF7 cells were transfected with 1μg Sesn2F vector (Sesn2F) for 24h, followed by fixation and staining with DAPI (blue), SESN2 (green), or P-AMPK (red). The cells were then imaged at 40x and merged images are displayed on the right. Representative images from 3 independent experiments are shown.

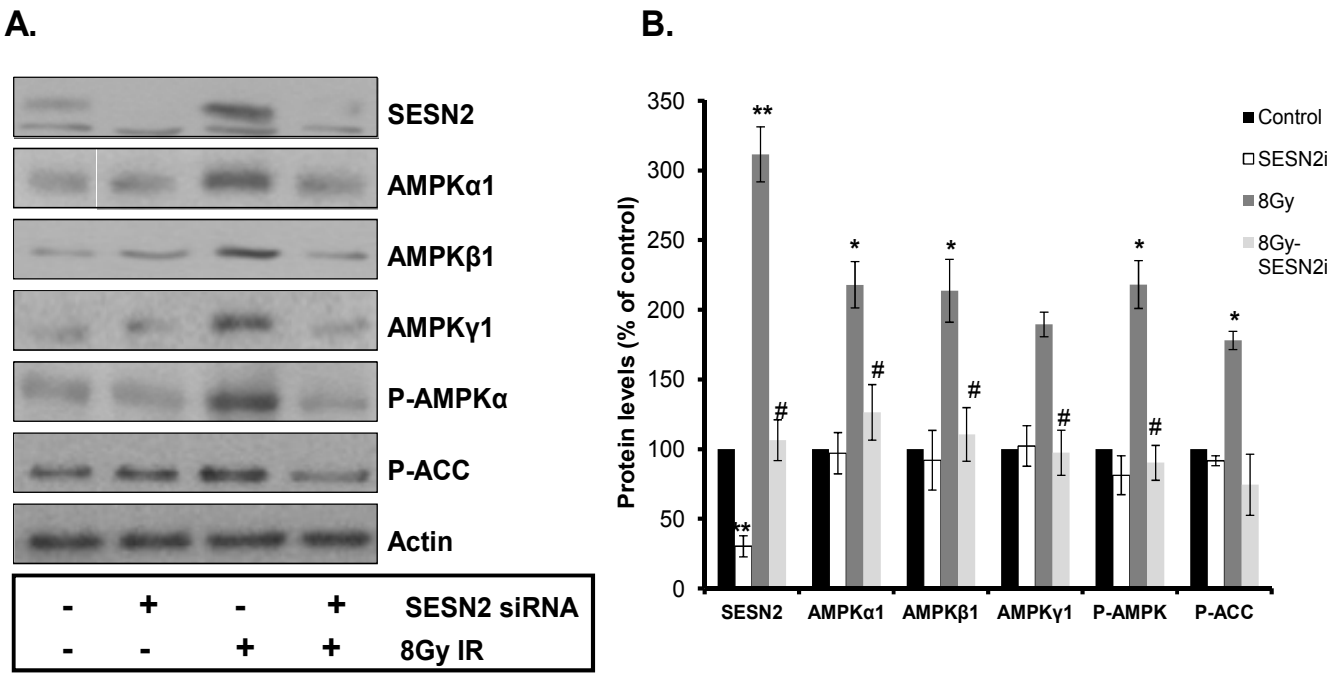

Figure 5.3: IR-induced expression and activity of AMPK is dependent on SESN2. (**A**) MCF7 cells were treated with SESN2 siRNA for 48h prior to being exposed to a single dose of 8Gy IR. The cells were lysed 24h after IR and western blotting was performed with the indicated antibodies. A representative immunoblot from 3-4 independent experiments is shown. (**B**) The results from (**A**) were quantitated and expressed as the mean and SE from 4 independent experiments (* = $P<0.05$ compared to control, ** = $P<0.01$ compared to control, # = $P<0.05$ compared to 8Gy IR).

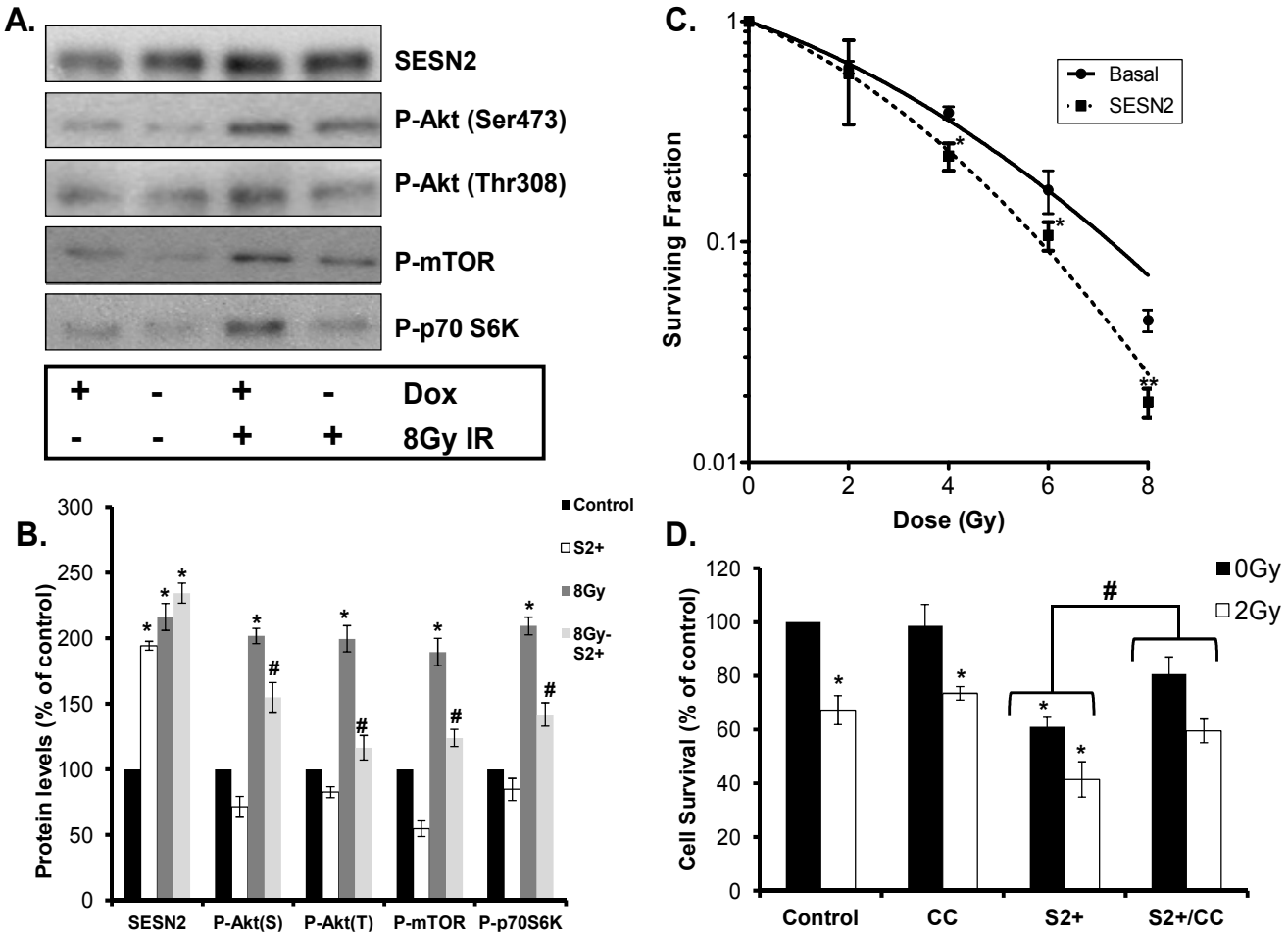

Figure 5.4: SESN2 in combination with IR modulates pathways of pro-survival and inhibits cell proliferation. (**A**) MCF7 Tet-OFF SESN2 cells were incubated in the presence (+) or absence (-) of Dox-containing medium for 24h before exposure to 8Gy IR. Twenty four hours later the cells were lysed and subjected to western blotting with the indicated antibodies. A representative immunoblot from 3 independent experiments is shown. (**B**) The results from (**A**) were quantitated and expressed as the mean and SE from 3 independent experiments (* = P<0.05 compared to control and # = P<0.05 compared to 8Gy IR). (**C**) MCF7 Tet-OFF SESN2 cells were incubated in the presence (basal) or

absence (SESN2) of Dox-containing medium for 24h before exposure to the indicated doses of IR. Seven days later the cells were fixed and stained with mythelene blue and the clonogenic survival was calculated. Results from 3 independent experiments were averaged and presented as the mean and SE (* = P<0.05 and ** = P<0.01 compared to the corresponding IR treatment alone) and plotted on a logarithmic scale using the linear quadratic equation. The results were normalized so that both the untreated (basal) and SESN2 overexpressing cells (SESN2) start at the same point (**D**) MCF7 Tet-OFF SESN2 cells were incubated in the presence (control) or absence (S2+) of Dox-containing medium and treated with or without 1μM compound C (CC) for 24h before exposure to 2Gy IR. Seven days later the cells were fixed and stained with mythelene blue and the clonogenic survival was calculated. Results from 3 independent experiments were averaged and presented as the mean and SE (* = P<0.05 compared to control and # = P<0.05 compared to S2+ alone).

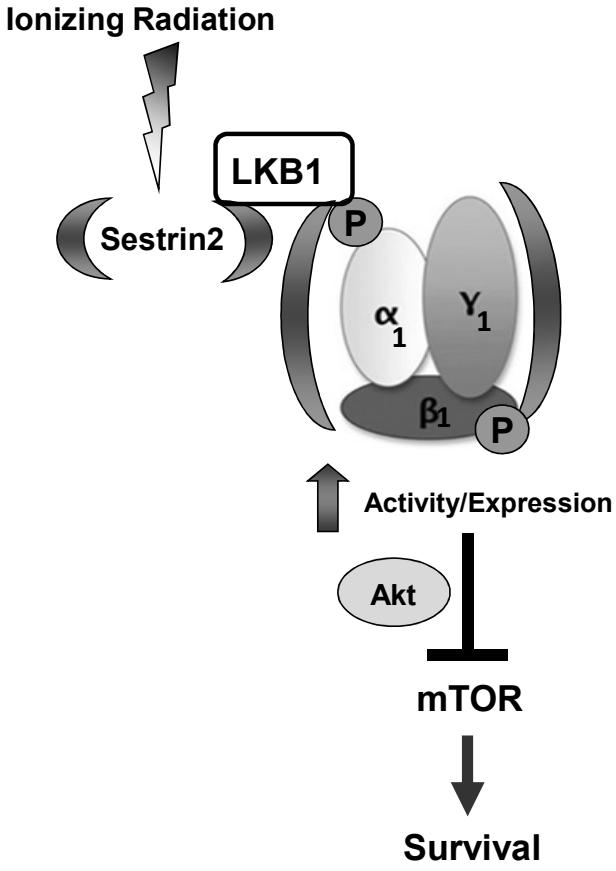

Figure 5.5: A proposed model of SESN2-mediated AMPK regulation in response to IR in MCF7 cells. In response to genotoxic stress (IR), SESN2 is enhanced and leads to the formation of an active LKB1/AMPKα1β1γ1 complex. SESN2 may stabilize the AMPK complex, or transcriptionally regulate AMPK and enhance its expression. Both SESN2 and AMPK may then coordinate mTOR suppression, which translates into enhanced IR-induced cancer cell killing.

Supporting Experiments

Due to space restriction and suggestions by the reviewers of this paper, some of the experimental data has not been incorporated into the final version of the manuscript. However, additional experiments for this manuscript were conducted and incorporated as supplemental data (Figures 5.S1-5.S3). These experiments were done to demonstrate the SESN2 is capable of enhancing the expression, as well as the activity of the AMPK/p53 signalling pathway. Additionally, data from A549 cells also demonstrated that, similar to MCF7 breast cancer cells, loss of SESN2 (via SESN2 siRNA) attenuates the effect of IR-induced AMPK signalling.

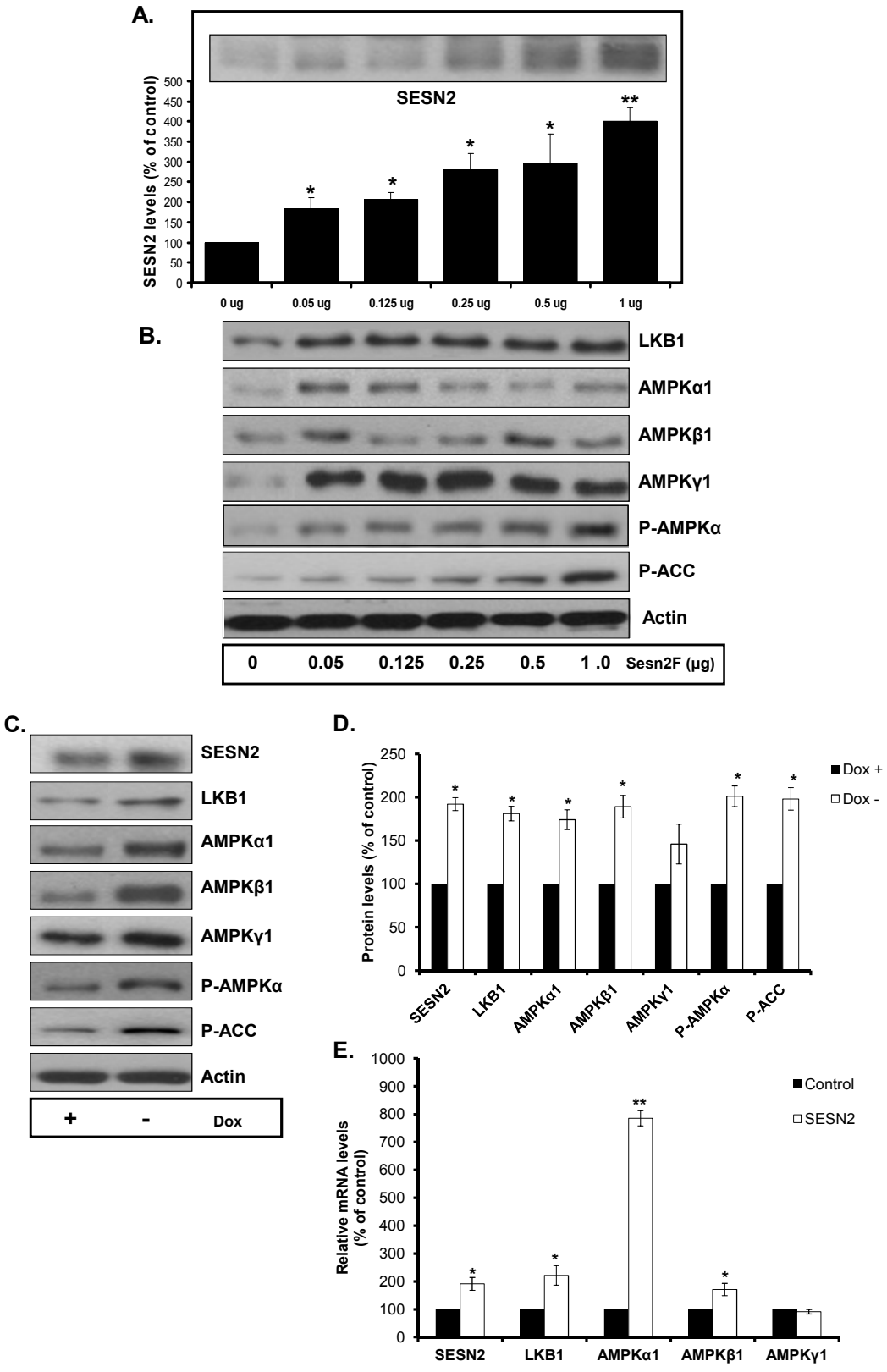
A.
SESN2
SESN2 levels (% of control)
0 ug
0.05 ug
0.125 ug
0.25 ug
0.5 ug
1 ug
B.
LKB1
AMPKα1
AMPKβ1
AMPKγ1
P-AMPKα
P-ACC
Actin
0 0.05 0.125 0.25 0.5 1 .0 Sesn2F (µg)
C.
SESN2
LKB1
AMPKα1
AMPKβ1
AMPKγ1
P-AMPKα
P-ACC
Actin
+ - Dox
D.
Protein levels (% of control)
Dox +
Dox -
SESN2
LKB1
AMPKα1
AMPKβ1
AMPKγ1
P-AMPKα
P-ACC
E.
Relative mRNA levels (% of control)
Control
SESN2
SESN2
LKB1
AMPKα1
AMPKβ1
AMPKγ1

Figure 5.S1: SESN2 overexpression enhances AMPK and LKB1 levels. (**A**) MCF7 cells were transiently transfected with 0.05-1 μg Sesn2F vector for 24h, followed by cell lysis and western blotting with a SESN2 antibody (0μg is defined as cells transfected with an empty-Flag vector). The results from western blotting were quantitated and expressed as the mean and SE from 3 independent experiments (* = $P<0.05$ and ** = $P<0.01$ compared to control). (**B**) MCF7 cells were transfected with 0.05-1 μg Sesn2F vector for 24h, followed by cell lysis and western blotting with the indicated antibodies. (**C**) MCF7-tet-off cells were incubated in the presence (+) or absence (-) of Dox-containing medium for 24h and subjected to western blotting with the indicated antibodies. (**D**) The results from (**C**) were quantitated and expressed as the mean and SE from 4 independent experiments (* = $P<0.05$ compared to control). (**E**) The SESN2, LKB1, and AMPK mRNA levels from MCF7-tet-off cells that were incubated in the presence (Dox +) or absence (Dox -) of Dox-containing medium for 24h were measured. The results are presented as the mean and SE from 4 experiments (* = $P<0.05$ and ** = $P<0.01$ compared to control).

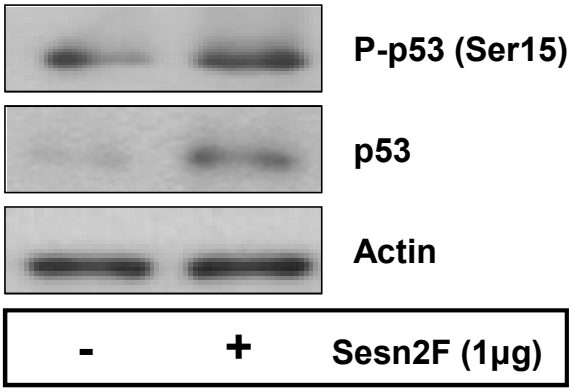

Figure 5.S2: SESN2 increases p53 phosphorylation and expression in MCF7 cells. MCF7cells were treated with 1µg Sesn2F for 48h before lysis and western blotting with the indicated antibodies against p53. Actin was used as a loading control. A representative immunoblot from 3 independent experiments is shown.

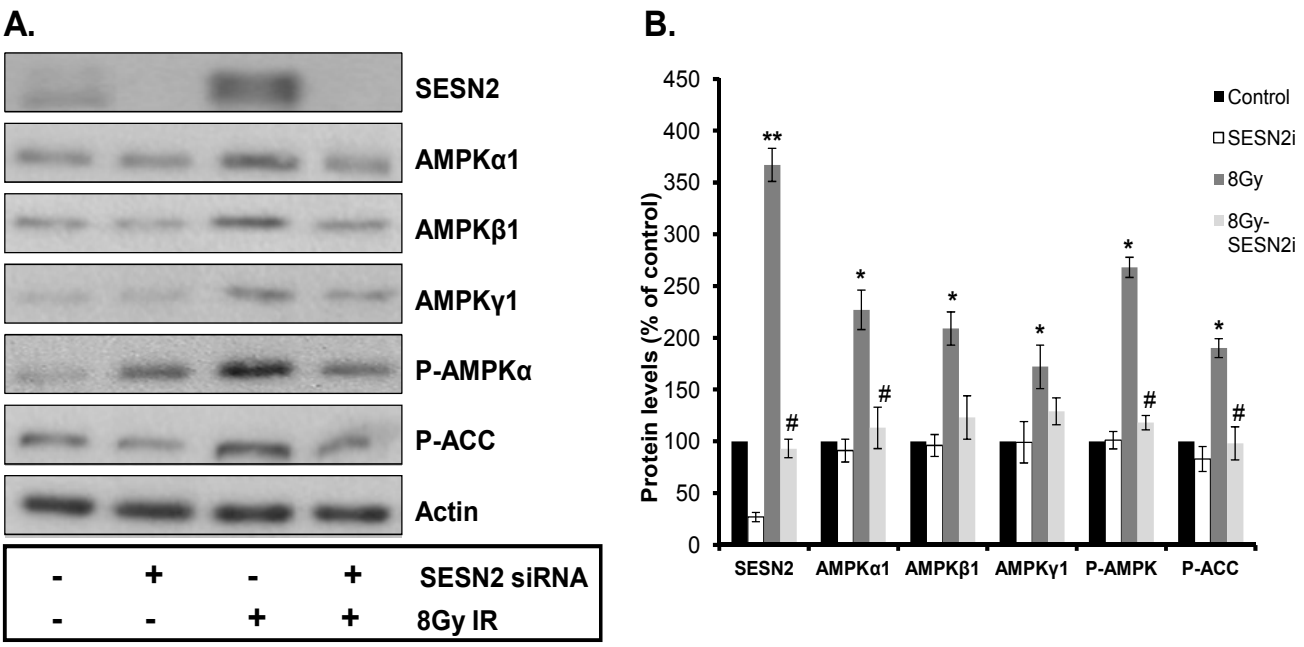

Figure 5.S3: SESN2 is required for IR-induced AMPK activity and expression in A549 cells. (**A**) A549 cells were treated with SESN2 siRNA for 48h before exposure to 8Gy IR. 24h later the cells were lysed and subjected to western blotting with the indicated antibodies. (**B**) The protein levels from (**A**) were quantitated and expressed as the mean and SE of 3 independent experiments. ** = P<0.01 compared to control, * = P<0.05 compared to control, # = P<0.05 compared to 8Gy IR.

Chapter 6: Conclusions

The hypothesis tested in this thesis was:

"*AMP-activated protein kinase (AMPK) is a signalling molecule that regulates radiation responses in cancer cells. Ionizing radiation (IR) enhances AMPK activity and expression to modulate cell cycle and survival. In addition, agents that potentiate AMPK activity are synergistic with IR to decrease cancer cell survival.*"

Stemming from this hypothesis, several testable objectives were obtained and became the main body of experimental work presented in this dissertation. Each of these objectives will be addressed individually in this discussion, and the major findings from each objective will be summarized and conclusions will be drawn as to whether or not they support the hypothesis.

Objective 1: *To investigate the role of AMPK responses to ionizing radiation in cancer cells.*

The null hypothesis to this statement would be that IR does not impact AMPK signalling in cancer cells. However, IR is an established cell stress agent that is known to stimulate other signalling pathways that facilitate DNA repair, cell cycle arrest, and protein synthesis (Braunstein, Badura, Xi, Formenti, & Schneider, 2009). Furthermore, the response of these pathways to IR can occur transiently, with an early-response phase that involves the rapid phosphorylation of substrates, or long-term changes that involve the post-translational modification of proteins and alterations in gene expression.

Chapter 2 of this thesis clearly demonstrates that AMPK is rapidly phosphorylated in response to IR in multiple epithelial cancer cell lines. Moreover, this event occurred in

the absence of LKB1, but was shown to be dependent on the DNA-damage sensor ATM in A549 lung cancer cells. Furthermore, the experiments conducted in this chapter implicate AMPK as a central regulator of IR-induced G2/M cell cycle arrest through regulation of $p21^{cip1}$. Inhibition of AMPK through molecular (siRNA) or chemical (compound C) means also prevented IR-mediated G2/M arrest and led to radiation resistance in lung cancer cells, supporting the notion that AMPK responds to IR by becoming rapidly activated, and subsequently facilitates radiation-induced cell cycle arrest.

In addition, the experimental work carried out in later chapters shed light on the long-term modulation of AMPK expression in response to IR. Indeed, chapter 4 demonstrated that not only is the activity of AMPK increased in response to radiation, but also following 24-48h after IR, the subunit expression levels of AMPK increase as well. The mRNA and protein levels of each AMPK subunit (with the exception of γ2 mRNA) were significantly enhanced 48h-post treatment with 8Gy IR. In terms of the mechanism by which IR regulates AMPK levels, chapter 5 identified that SESN2 was required for sustained AMPK activity and expression following exposure to IR. Taken together, there is ample evidence to reject the null hypothesis and support the alternative, which is that AMPK does respond to IR in cancer cells by activation through ATM and sustained expression via SESN2 signalling (as illustrated in Figure 6.1).

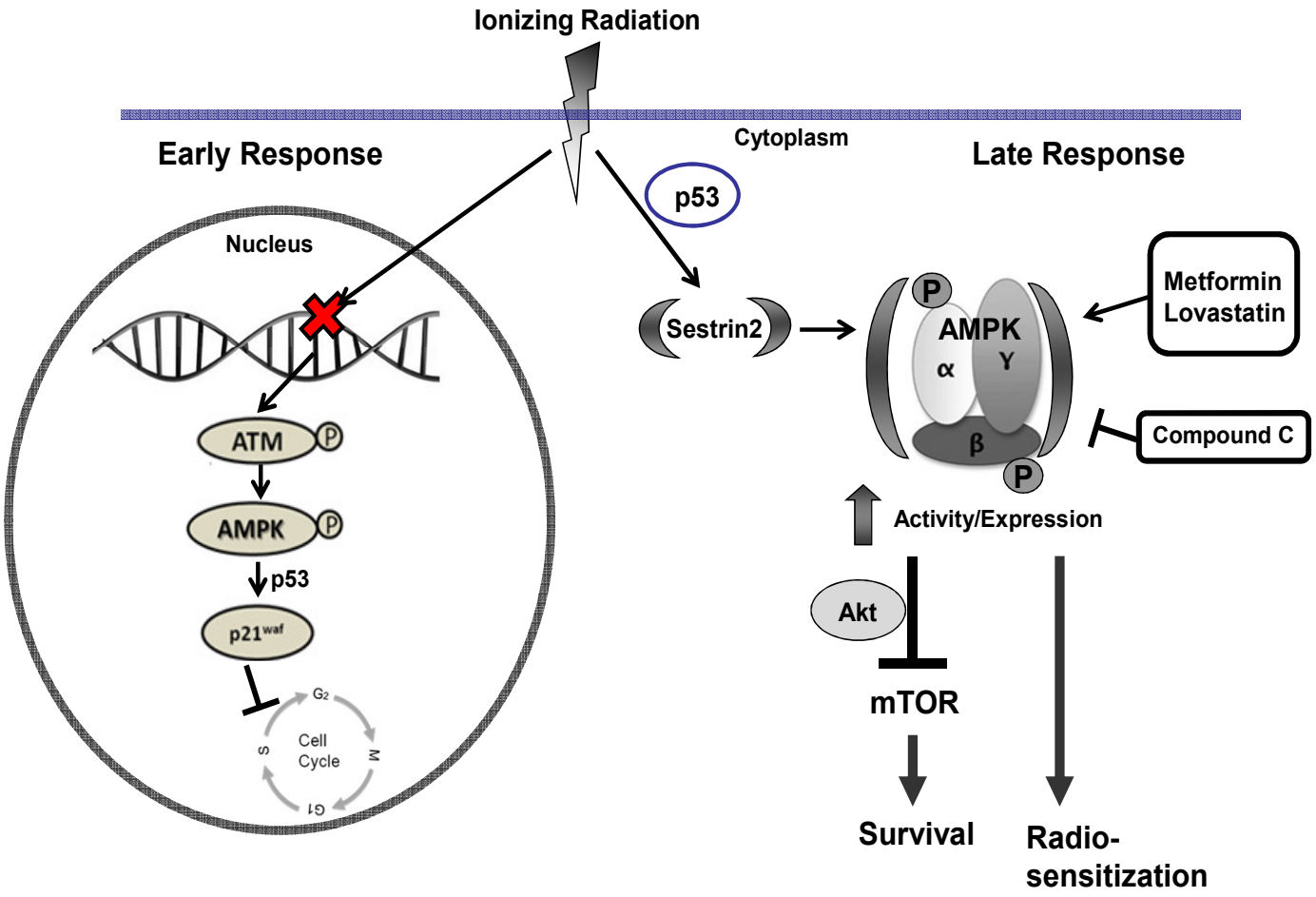

Figure 6.1: Theoretical model of AMPK's response to IR in cancer cells. The red "X" indicates DNA damage induced by IR.

Objective 2: *To evaluate the ability of drugs that activate AMPK as radiation sensitizers in cancer cells.*

In this case, the default statement for this objective would be that agents that increase AMPK activity would have no therapeutic benefit as a radiation sensitizer for cancer. However, experimental evidence from this thesis contradicts this statement, indicating that both chemical and molecular activation of AMPK can potentiate IR-induced cell death in cancer cells. Early work from chapter 2 showed that low doses of

metformin had a synergistic effect with IR to inhibit the clonogenic survival of lung cancer cells. In addition, chapter 3 demonstrated that lovastatin could work as an adjuvant for radiotherapy that allowed for the radiosensitization of lung cancer cells through induction of apoptosis. Overall, the default statement for this objective cannot be supported based on the evidence favouring the opposite notion that agents that activate AMPK can work as radiation sensitizers in cancer cells.

Objective 3: *To examine the impact of AMPK on cell signalling pathways that regulate (a) DNA repair, and (b) survival in response to IR.*

The null hypothesis for this prediction would be that AMPK is not involved in pathways that regulate DNA repair or survival alone or in response to IR. To evaluate this objective I primarily utilized mouse embryo fibroblasts (MEFs) that are deficient in AMPKα1/2 (AMPK-/-), and examine the basal and IR-stimulated state of the ATM/p53 and Akt/mTOR pathways (chapter 4). Interestingly, at the basal level the ATM/p53 DNA-damage sensing pathway was upregulated in AMPK-/- MEFs compared to their corresponding wildtype (Wt) MEF counterparts. This observation suggests that AMPK may be involved in a suppression of this pathway, or perhaps that lack of AMPK may enhance genomic instability in the cell that results in the chronic accumulation of ATM and p53. Furthermore, AMPK-/- MEFs do not display the characteristic increase in these signalling molecules when treated with IR, implying that AMPK plays a role in the signal transduction pathway that regulates DNA-damage responses triggered by radiation.

On the other hand, the Akt-mTOR pro-survival pathway is enhanced in untreated AMPK-/- MEFs compared to Wt MEFs. However, this observation is not totally

unexpected, since AMPK has been implicated as a suppressor of the Akt/mTOR pathway. Additionally, Akt and mTOR failed to respond to IR treatment in AMPK-/- MEFs, showing a reduction in their overall activation, much like the radiation response of the ATM pathway. Taken together, AMPK clearly has a role in the regulation of pathways that affect DNA-damage and cell survival, and therefore the null hypothesis should be rejected.

To this end, it is tempting to speculate that AMPK may play a role in guarding the genome by suppressing unregulated proliferation, malignant transformation, as well as orchestrating appropriate DNA-damage checkpoints in response to stress. In support of this notion, AMPK-/- MEFs were recently characterized in assuming a Warburg phenotype similar to cancer cells, having elevated rates of glycolysis and an increase in ROS levels (presented data from Dr. Russell Jones laboratory, *McGill University*).

Objective 4: *To identify the role of SESN2 in (a) modulating AMPK expression and activity, as well as (b) regulate pathways that are stimulated by IR.*

The corresponding null hypothesis to this objective is that SESN2 does not play a role in regulating AMPK expression or activity, and that it is not involved in IR-mediated cell signalling. The experiments from chapter 5 address this question by examining the effect of SESN2 overexpression on AMPK regulation, as well as its ability to modulate radiation responses in breast cancer cells. SESN2 was found to directly interact with the primary AMPK heterotrimer (AMPKα1β1γ1), as well as its upstream regulator LKB1 in MCF7 breast cancer cells. In addition, enhanced SESN2 increased AMPK activity and increased the expression of LKB1 and AMPK subunits at both the mRNA and protein

level. Interestingly, SESN2 was also found to enhance AMPK subunit expression in LKB1-deficient A549 lung cancer cells (Figure A3, Appendix 2), implying that SESN2 may modulate AMPK independent of LKB1, or that this is a tissue-specific effect for SESN2 in cancers of lung origin.

With respect to radiation-induced cell signalling, inhibition of SESN2 attenuated the ability of IR to promote AMPK activation and expression. Conversely though, overexpression of SESN2 blocked the characteristic IR-stimulated activation of the Akt/mTOR pathway and acted as a radiation sensitizer in MCF7 cells. Thus, these observations provide evidence for the involvement of SESN2 in positively regulating AMPK, suppressing IR-induced pro-survival signalling, and working as a sensitizing agent for MCF7 cells targeted with radiation. As such, the null hypothesis for this objective should be rejected.

Future Directions

All of the objectives have implicated AMPK as a sensor and mediator of IR-induced cell signalling in cancer cells and support the principal hypothesis. However, while the *in vitro* model provides a strong basis for understanding the molecular mechanisms involved in IR-mediated AMPK responses in cancer cells (please refer to Figure 6.1), it is not an ideal system to understand the pathological implications of modulating AMPK in tumours treated with radiotherapy. The next rational step would be to examine the effect of IR treatment on AMPK activity and expression on *in vivo* models of cancer. For example, nude mice could be subcutaneously injected with a human cancer cell line, and the subsequent tumour that develops could be treated with IR and the AMPK levels examined. In addition, the bioavailability and benefit of AMPK activators (discussed earlier in this thesis) as adjuvants for radiation therapy could be better evaluated in a living organism, as well as provide a clinical basis for the rational development of specific and potent activators of AMPK as anti-cancer therapies. It is worth noting that other researchers in our laboratory are currently investigating the ability of metformin to act as a radiation sensitizer in nude mice with lung cancer xenografts.

To a similar extent, from a clinical standpoint, it would be interesting to generate a tumour-bank from biopsies taken from primary human tumour cells of patients with cancer that have undergone radiotherapy. These tumours can then be subjected to immunohistochemistry analysis with antibodies that measure AMPK expression and activity to see if enhanced AMPK expression is correlated with better IR-treatment responses. In reference to this point, a recent study has performed this type of analysis on

primary breast cancer tumours and found that decreased AMPK phosphorylation (Thr172) correlated with enhanced axillary node metastasis (Hadad et al., 2009). Although, it should be noted that these samples were obtained from a cohort of patients that did not undergo radiotherapy.

Moreover, the impact of AMPK on pathways that regulate genomic integrity, as well as uncontrolled proliferation at the basal level and in response to IR should be better evaluated in human tumours *in vivo*. This could be achieved by stably knocking down the AMPKα1 subunit in MCF7 cells (they only express the α1-catalytic subunit of AMPK) using a small-hairpin RNA (shRNA) construct that targets and silences AMPKα1 gene expression via RNA interference. Once this stable cell line is generated, it could then be subcutaneously injected into nude mice and their tumour growth-kinetics measured once they have been classified into untreated or IR-treated groups. Furthermore, at endpoint these tumours could be excised and subjected to molecular analysis (PCR, western blotting, or immunohistochemistry) to determine the activity and expression of pathways that govern DNA damage/repair, cell cycle regulation, and proliferation. Specifically, the ATM/p53 pathway should be closely monitored, as we observed that AMPK-/- MEFs has elevated basal levels of these molecular markers and they have an abnormal response to IR (Figure 6.2).

In addition, AMPK has recently been implicated in phosphorylating multiple substrates required for mitosis, as well as being a passenger of the mitotic apparatus in non-transformed and cancer cell lines (Banko et al., 2011; Vazquez-Martin, Oliveras-Ferraros, & Menendez, 2009).

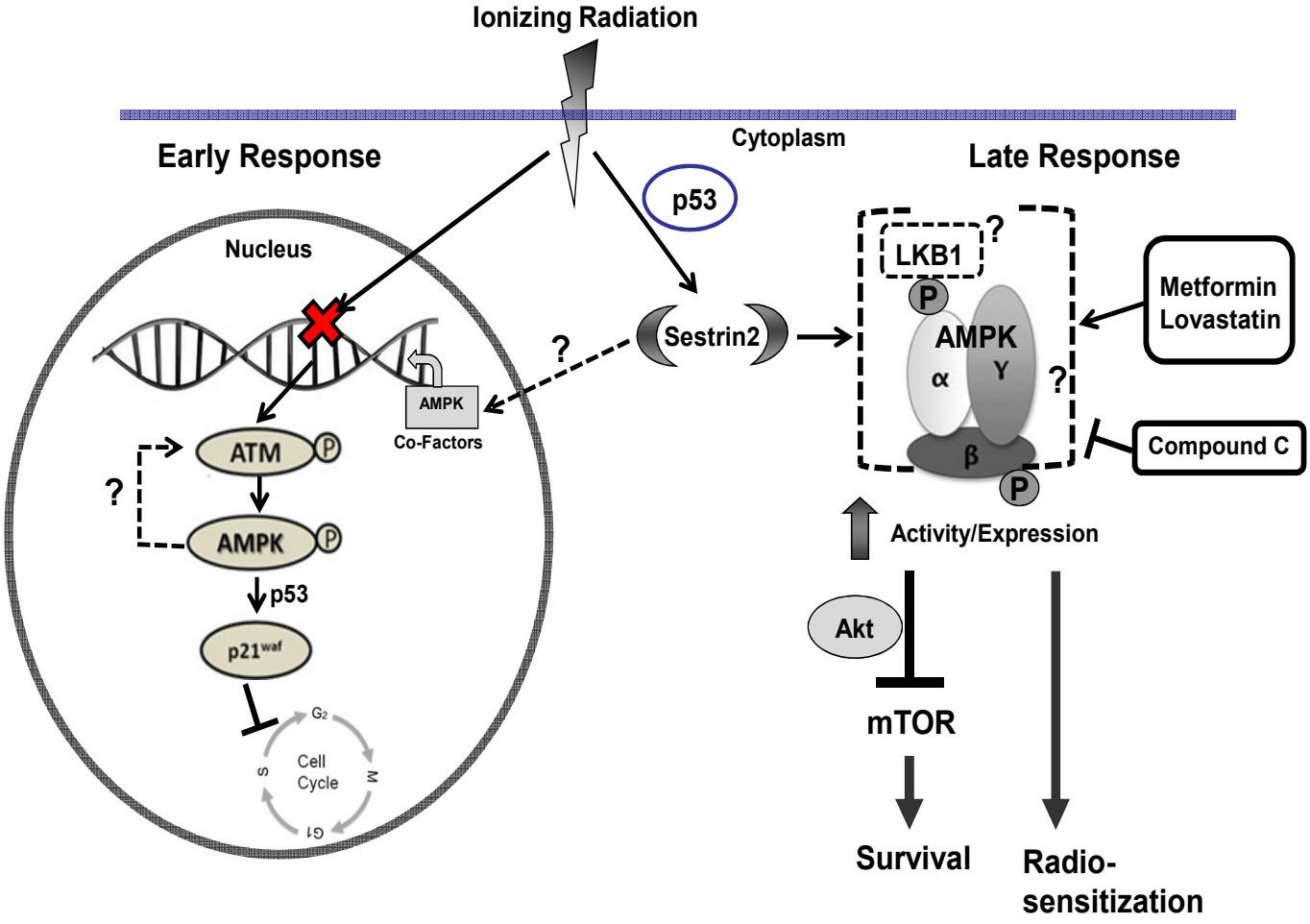

Figure 6.2: Diagrammatic model of future directions. The red "X" indicates DNA damage induced by IR. The question marks associated with the dashed black lines indicate molecular mechanisms that still need to be elucidated in future experiments.

Given the role of AMPK as a metabolic and genotoxic stress-sensor, it would be interesting to observe the localization and activation of AMPK in various stages of mitosis in untreated or IR-treated cancer cells. The effects of modulating AMPK activity using inhibitors or activators on the mitotic apparatus (chromosomes, spindle fibres, and DNA content) could also be analyzed in cancer cells. This could readily be addressed by

arresting cancer cells in different stages of mitosis following IR or AMPK-altering treatments and immunostaining them with specific antibodies that measure AMPK activity (phosphorylation) and expression, as well as identify mitotic structures. Interestingly, ATM has also been recently implicated as a mitotic passenger that regulates spindle checkpoints (C. Yang et al., 2011), reinforcing the dynamic relationship between AMPK and ATM cross-talk to maintain the integrity of the genome.

Furthermore, the finding that SESN2 is involved in regulating AMPK activity and expression in response to IR is very novel. However, as seen in my graphic model (Figure 6.2), the specific mechanism by which SESN2 phosphorylates AMPK and enhances its expression is still not fully understood. As shown in chapter 5, SESN2 co-localizes with the upstream AMPK-kinase LKB1, as well as the active AMPK heterotrimer in MCF7 cells. I initially suggested that SESN2 may recruit LKB1 to phosphorylate AMPK as the major mechanism for SESN2-mediated AMPK activation. However, our laboratory and others (Budanov et al., 2010) have observed that SESN2 potentiates AMPK activity in LKB1-negative A549 cells (Figure A3). In addition, siRNA against SESN2 was shown to block IR-induced AMPK phosphorylation (Figure A4) in these cells. On the other hand, it is possible that a yet to be identified kinase for AMPK may also be recruited by SESN2 to facilitate AMPK activation.

Thus, further investigation into understanding the mechanism of SESN2-induced AMPK activation is necessary. A more detailed analysis and mapping of the structure of SESN2 would aid in predicting if this protein itself can act as a potential AMPK-kinase. Alternatively, it is generally accepted that SESN2-mediated AMPK binding promotes a

conformational change within the structure of AMPK that enhances this enzymes kinase activity (Budanov & Karin, 2008).

Another important future step in this study would be to characterize the specific mechanism by which SESN2 regulates AMPK expression levels. Chapter 5 demonstrated that the mRNA expression of AMPK was enhanced by SESN2 overexpression. In addition, I also observed the reciprocal interaction, whereby blocking SESN2 expression via RNA interference (siRNA against SESN2) had a trend to reduce the mRNA expression levels of AMPK (especially for the AMPK α1-subunit, Figure A5). Based on these findings it is possible that SESN2 can act as a transcription factor alone, or as a potential co-factor for increased AMPK transcription (Figure 6.2). An appropriate method to determine this would be to perform a chromatin immunoprecipitation (ChIP) assay against SESN2 in cells that overexpress this protein or in irradiated cells. By using an antibody against SESN2 the ChIP assay can reveal any direct interaction between the SESN2 protein and target AMPK DNA sequences, which if were present, would implicate SESN2 as a transcription factor for AMPK.

Chapter 5 also revealed that enhanced SESN2 increases the protein levels of AMPK. This observation may be explained if SESN2 were indeed a transcription factor for AMPK. However, an alternative explanation may be that the scaffolding properties of SESN2 prevents AMPK protein degradation, and thereby promotes sustained AMPK expression in response to stress (in this case, induced by IR). If this were the case, where SESN2 stabilizes the AMPK heterotrimer, then identifying how SESN2 anchors to AMPK is an important issue to address in the future. One approach to address this would

be to examine if SESN2 binds to individual AMPK subunits (i.e. α1 subunit only) by knocking down the expression of the remaining subunits that would normally form an active AMPK heterotrimer. It is also possible that SESN2 may act as an adenine nucleotide mimetic (similar to AICAR), that binds to one of the CBS domains of the AMPKγ subunit to stabilize and activate AMPK.

Summary

The central theory that this dissertation has attempted to establish is that AMPK plays a vital role in coordinating appropriate stress-signalling responses in lieu of cellular IR exposure. As such, molecular or chemical modulation of AMPK has been shown in this thesis to alter radiation responses in cancer cells, which may have future clinical implication as a biomarker for radiotherapy.

Following some background information on AMPK signalling and radiobiology, data in the form of separate manuscripts were presented to address the mechanism by which IR activates AMPK in various epithelial cancer cell lines. My first manuscript (chapter 2) demonstrated that AMPK is rapidly phosphorylated *in vitro* and that it is required to facilitate IR-induced G2/M cell cycle arrest, as well as act as a central target for radiation sensitization. A subsequent paper identified that lovastatin activates AMPK and sensitizes lung cancer cells to IR by blocking EGFR-Akt-mTOR signalling and increasing programmed cell death (chapter 3). In addition, a later paper provided novel observation about the involvement of AMPK signalling in regulating pathways that control DNA damage and cell proliferation, as well as the effect of IR on AMPK expression (chapter 4). Furthermore, a final paper (chapter 5) addressed the role of the sestrin family member, SESN2, in controlling AMPK activity and expression alone and in response to IR. In addition, potential future studies where presented following the papers to identify areas of AMPK signalling that require further investigation.

Overall, it has become evident that AMPK is not only involved in regulating energy metabolism, but also in modulating signalling pathways in response to a variety of

cellular stresses, which if left unchecked promote a malignant environment. This is perhaps the reason why researchers and clinicians have adopted drugs that target other metabolic diseases, such as metformin for type 2 diabetes (an AMPK activator), and geared it for potential clinical use in cancer patients. This may be of great future benefit as many conventionally used chemotherapeutic drugs currently target specific genes that may be mutated in cancer, whereas targeting pathways in metabolism is a universal physiological process. Thus, by understanding better the basic science of AMPK signalling and its response to metabolic and genotoxic stress, we may also discover novel therapeutic approaches to treat cancer, as well as other diseases of metabolism.

Reference List

Agarwal, B., Rao, C. V., Bhendwal, S., Ramey, W. R., Shirin, H., Reddy, B. S., et al. (1999). Lovastatin augments sulindac-induced apoptosis in colon cancer cells and potentiates chemopreventive effects of sulindac. *Gastroenterology, 117*(4), 838-847.

Aggarwal, B. B., Bhardwaj, A., Aggarwal, R. S., Seeram, N. P., Shishodia, S., & Takada, Y. (2004). Role of resveratrol in prevention and therapy of cancer: preclinical and clinical studies. *Anticancer Res, 24*(5A), 2783-2840.

Alexander, A., & Walker, C. L. (2010). Differential localization of ATM is correlated with activation of distinct downstream signaling pathways. *Cell Cycle, 9*(18), 3685-3686.

Anisimov, V. N., Berstein, L. M., Egormin, P. A., Piskunova, T. S., Popovich, I. G., Zabezhinski, M. A., et al. (2005). Effect of metformin on life span and on the development of spontaneous mammary tumors in HER-2/neu transgenic mice. *Exp Gerontol, 40*(8-9), 685-693.

Antonoff, M. B., & D'Cunha, J. (2010). Teaching an old drug new tricks: metformin as a targeted therapy for lung cancer. *Semin Thorac Cardiovasc Surg, 22*(3), 195-196.

Bain, J., Plater, L., Elliott, M., Shpiro, N., Hastie, C. J., McLauchlan, H., et al. (2007). The selectivity of protein kinase inhibitors: a further update. *Biochem.J., 408*(3), 297-315.

Banko, M. R., Allen, J. J., Schaffer, B. E., Wilker, E. W., Tsou, P., White, J. L., et al. (2011). Chemical Genetic Screen for AMPKalpha2 Substrates Uncovers a Network of Proteins Involved in Mitosis. *Mol Cell, 44*(6), 878-892.

Barnes, K., Ingram, J. C., Porras, O. H., Barros, L. F., Hudson, E. R., Fryer, L. G., et al. (2002). Activation of GLUT1 by metabolic and osmotic stress: potential involvement of AMP-activated protein kinase (AMPK). *J Cell Sci, 115*(Pt 11), 2433-2442.

Bartrons, R., & Caro, J. (2007). Hypoxia, glucose metabolism and the Warburg's effect. *J Bioenerg Biomembr, 39*(3), 223-229.

Bateman, A. (1997). The structure of a domain common to archaebacteria and the homocystinuria disease protein. *Trends Biochem Sci, 22*(1), 12-13.

Baur, J. A., & Sinclair, D. A. (2006). Therapeutic potential of resveratrol: the in vivo evidence. *Nat Rev Drug Discov, 5*(6), 493-506.

Ben Sahra, I., Laurent, K., Loubat, A., Giorgetti-Peraldi, S., Colosetti, P., Auberger, P., et al. (2008). The antidiabetic drug metformin exerts an antitumoral effect in vitro and in vivo through a decrease of cyclin D1 level. *Oncogene, 27*(25), 3576-3586.

Bensimon, A., Aebersold, R., & Shiloh, Y. (2011). Beyond ATM: the protein kinase landscape of the DNA damage response *FEBS Lett., 585*(11), 1625-1639.

Bhagwat, S. V., & Crew, A. P. (2010). Novel inhibitors of mTORC1 and mTORC2. *Curr Opin Investig Drugs, 11*(6), 638-645.

Bodmer, M., Becker, C., Meier, C., Jick, S. S., & Meier, C. R. (2011). Use of metformin and the risk of ovarian cancer: a case-control analysis. *Gynecol Oncol, 123*(2), 200-204.

Boudreau, D. M., Yu, O., & Johnson, J. (2010). Statin use and cancer risk: a comprehensive review. *Expert.Opin.Drug Saf, 9*(4), 603-621.

Bowker, S. L., Majumdar, S. R., Veugelers, P., & Johnson, J. A. (2006). Increased cancer-related mortality for patients with type 2 diabetes who use sulfonylureas or insulin. *Diabetes Care, 29*(2), 254-258.

Braunstein, S., Badura, M. L., Xi, Q., Formenti, S. C., & Schneider, R. J. (2009). Regulation of protein synthesis by ionizing radiation. *Mol Cell Biol, 29*(21), 5645-5656.

Bristow, R. G., & Hill, R. (1998). Molecular and Cellular Basis of Radiotherapy *The Basic Science of Oncology* (Vol. 3, pp. 295-321). Toronto: McGraw-Hill.

Browne, G. J., Finn, S. G., & Proud, C. G. (2004). Stimulation of the AMP-activated protein kinase leads to activation of eukaryotic elongation factor 2 kinase and to its phosphorylation at a novel site, serine 398. *J Biol Chem, 279*(13), 12220-12231.

Budanov, A. V., & Karin, M. (2008). p53 target genes sestrin1 and sestrin2 connect genotoxic stress and mTOR signaling. *Cell, 134*(3), 451-460.

Budanov, A. V., Lee, J. H., & Karin, M. (2010). Stressin' Sestrins take an aging fight. *EMBO Mol.Med., 2*(10), 388-400.

Budanov, A. V., Sablina, A. A., Feinstein, E., Koonin, E. V., & Chumakov, P. M. (2004). Regeneration of peroxiredoxins by p53-regulated sestrins, homologs of bacterial AhpD. *Science, 304*(5670), 596-600.

Budanov, A. V., Shoshani, T., Faerman, A., Zelin, E., Kamer, I., Kalinski, H., et al. (2002). Identification of a novel stress-responsive gene Hi95 involved in regulation of cell viability. *Oncogene, 21*(39), 6017-6031.

Bungard, D., Fuerth, B. J., Zeng, P. Y., Faubert, B., Maas, N. L., Viollet, B., et al. (2010). Signaling kinase AMPK activates stress-promoted transcription via histone H2B phosphorylation. *Science, 329*(5996), 1201-1205.

Buzzai, M., Jones, R. G., Amaravadi, R. K., Lum, J. J., DeBerardinis, R. J., Zhao, F., et al. (2007). Systemic treatment with the antidiabetic drug metformin selectively impairs p53-deficient tumor cell growth. *Cancer Res., 67*(14), 6745-6752.

Campbell, M., & Farrell, S. (2011). Glycolysis *Biochemistry* (7th ed., pp. 481-505). Belmont CA: Brooks Cole.

Carling, D., Zammit, V. A., & Hardie, D. G. (1987). A common bicyclic protein kinase cascade inactivates the regulatory enzymes of fatty acid and cholesterol biosynthesis. *FEBS Lett, 223*(2), 217-222.

Carlson, C. A., & Kim, K. H. (1973). Regulation of hepatic acetyl coenzyme A carboxylase by phosphorylation and dephosphorylation. *J Biol Chem, 248*(1), 378-380.

Carmichael, J., Degraff, W. G., Gamson, J., Russo, D., Gazdar, A. F., Levitt, M. L., et al. (1989). Radiation sensitivity of human lung cancer cell lines. *Eur.J.Cancer Clin.Oncol., 25*(3), 527-534.

Chaachouay, H., Ohneseit, P., Toulany, M., Kehlbach, R., Multhoff, G., & Rodemann, H. P. (2011). Autophagy contributes to resistance of tumor cells to ionizing radiation. *Radiother Oncol, 99*(3), 287-292.

Chen, C. C., Jeon, S. M., Bhaskar, P. T., Nogueira, V., Sundararajan, D., Tonic, I., et al. (2010). FoxOs inhibit mTORC1 and activate Akt by inducing the expression of Sestrin3 and Rictor. *Dev Cell, 18*(4), 592-604.

Cool, B., Zinker, B., Chiou, W., Kifle, L., Cao, N., Perham, M., et al. (2006). Identification and characterization of a small molecule AMPK activator that treats key components of type 2 diabetes and the metabolic syndrome. *Cell Metab, 3*(6), 403-416.

Corton, J. M., Gillespie, J. G., Hawley, S. A., & Hardie, D. G. (1995). 5-aminoimidazole-4-carboxamide ribonucleoside. A specific method for activating AMP-activated protein kinase in intact cells? *Eur J Biochem, 229*(2), 558-565.

Davies, S. P., Sim, A. T., & Hardie, D. G. (1990). Location and function of three sites phosphorylated on rat acetyl-CoA carboxylase by the AMP-activated protein kinase. *Eur J Biochem, 187*(1), 183-190.

Ditch, S., & Paull, T. T. (2011). The ATM protein kinase and cellular redox signaling: beyond the DNA damage response. *Trends Biochem Sci*.

Dowling, R. J., Goodwin, P. J., & Stambolic, V. (2011). Understanding the benefit of metformin use in cancer treatment. *BMC Med, 9*, 33.

Dowling, R. J., Zakikhani, M., Fantus, I. G., Pollak, M., & Sonenberg, N. (2007). Metformin inhibits mammalian target of rapamycin-dependent translation initiation in breast cancer cells. *Cancer Res., 67*(22), 10804-10812.

Evans, J. M., Donnelly, L. A., Emslie-Smith, A. M., Alessi, D. R., & Morris, A. D. (2005). Metformin and reduced risk of cancer in diabetic patients. *BMJ, 330*(7503), 1304-1305.

Fantin, V. R., St-Pierre, J., & Leder, P. (2006). Attenuation of LDH-A expression uncovers a link between glycolysis, mitochondrial physiology, and tumor maintenance. *Cancer Cell, 9*(6), 425-434.

Fernandez-Capetillo, O., Lee, A., Nussenzweig, M., & Nussenzweig, A. (2004). H2AX: the histone guardian of the genome. *DNA Repair (Amst), 3*(8-9), 959-967.

Fogarty, S., & Hardie, D. G. (2010). Development of protein kinase activators: AMPK as a target in metabolic disorders and cancer. *Biochim.Biophys.Acta, 1804*(3), 581-591.

Foretz, M., Hebrard, S., Leclerc, J., Zarrinpashneh, E., Soty, M., Mithieux, G., et al. (2010). Metformin inhibits hepatic gluconeogenesis in mice independently of the LKB1/AMPK pathway via a decrease in hepatic energy state. *J Clin Invest, 120*(7), 2355-2369.

Fritz, G., Brachetti, C., & Kaina, B. (2003). Lovastatin causes sensitization of HeLa cells to ionizing radiation-induced apoptosis by the abrogation of G2 blockage. *Int J Radiat Biol, 79*(8), 601-610.

Gatenby, R. A., & Gillies, R. J. (2004). Why do cancers have high aerobic glycolysis? *Nat Rev Cancer, 4*(11), 891-899.

Gledhill, J. R., Montgomery, M. G., Leslie, A. G., & Walker, J. E. (2007). Mechanism of inhibition of bovine F1-ATPase by resveratrol and related polyphenols. *Proc Natl Acad Sci U S A, 104*(34), 13632-13637.

Goldstein, L. B. (2007). Statins for stroke prevention. *Curr Atheroscler Rep, 9*(4), 305-311.

Graaf, M. R., Richel, D. J., van Noorden, C. J., & Guchelaar, H. J. (2004). Effects of statins and farnesyltransferase inhibitors on the development and progression of cancer. *Cancer Treat Rev, 30*(7), 609-641.

Gwinn, D. M., Shackelford, D. B., Egan, D. F., Mihaylova, M. M., Mery, A., Vasquez, D. S., et al. (2008). AMPK phosphorylation of raptor mediates a metabolic checkpoint. *Mol Cell, 30*(2), 214-226.

Hadad, S. M., Baker, L., Quinlan, P. R., Robertson, K. E., Bray, S. E., Thomson, G., et al. (2009). Histological evaluation of AMPK signalling in primary breast cancer. *BMC Cancer, 9*, 307.

Hall, E. J., Astor, M., Bedford, J., Borek, C., Curtis, S. B., Fry, M., et al. (1988). Basic radiobiology. *Am.J.Clin.Oncol., 11*(3), 220-252.

Hardie, D. G. (2005). New roles for the LKB1-->AMPK pathway. *Curr Opin Cell Biol, 17*(2), 167-173.

Hardie, D. G. (2008). AMPK: a key regulator of energy balance in the single cell and the whole organism. *Int.J.Obes.(Lond), 32 Suppl 4*, S7-12.

Hardie, D. G. (2011). AMP-activated protein kinase--an energy sensor that regulates all aspects of cell function. *Genes Dev., 25*(18), 1895-1908.

Hardie, D. G., Carling, D., & Gamblin, S. J. (2011). AMP-activated protein kinase: also regulated by ADP? *Trends Biochem.Sci., 36*(9), 470-477.

Hardie, D. G., & Hawley, S. A. (2001). AMP-activated protein kinase: the energy charge hypothesis revisited. *Bioessays, 23*(12), 1112-1119.

Hatzivassiliou, G., Zhao, F., Bauer, D. E., Andreadis, C., Shaw, A. N., Dhanak, D., et al. (2005). ATP citrate lyase inhibition can suppress tumor cell growth. *Cancer Cell, 8*(4), 311-321.

Hawley, S. A., Pan, D. A., Mustard, K. J., Ross, L., Bain, J., Edelman, A. M., et al. (2005). Calmodulin-dependent protein kinase kinase-beta is an alternative upstream kinase for AMP-activated protein kinase. *Cell Metab, 2*(1), 9-19.

Hindler, K., Cleeland, C. S., Rivera, E., & Collard, C. D. (2006). The role of statins in cancer therapy. *Oncologist, 11*(3), 306-315.

Hong, S. P., Leiper, F. C., Woods, A., Carling, D., & Carlson, M. (2003). Activation of yeast Snf1 and mammalian AMP-activated protein kinase by upstream kinases. *Proc Natl Acad Sci U S A, 100*(15), 8839-8843.

Howard, A., & Pelc, S. (1953). Synthesis of deoxyribonucleic acid in normal and irradiated cells and its relation to chromosome breakage. *Heredity, 6*(6), 261-273.

Hsieh, T. C., & Wu, J. M. (2010). Resveratrol: Biological and pharmaceutical properties as anticancer molecule. *Biofactors, 36*(5), 360-369.

Imamura, K., Ogura, T., Kishimoto, A., Kaminishi, M., & Esumi, H. (2001). Cell cycle regulation via p53 phosphorylation by a 5'-AMP activated protein kinase activator, 5-aminoimidazole- 4-carboxamide-1-beta-D-ribofuranoside, in a human hepatocellular carcinoma cell line. *Biochem Biophys Res Commun, 287*(2), 562-567.

Isakovic, A., Harhaji, L., Stevanovic, D., Markovic, Z., Sumarac-Dumanovic, M., Starcevic, V., et al. (2007). Dual antiglioma action of metformin: cell cycle arrest and mitochondria-dependent apoptosis. *Cell Mol Life Sci, 64*(10), 1290-1302.

Isebaert, S. F., Swinnen, J. V., McBride, W. H., Begg, A. C., & Haustermans, K. M. (2011). 5-Aminoimidazole-4-Carboxamide Riboside Enhances Effect of Ionizing Radiation in PC3 Prostate Cancer Cells. *Int J Radiat Oncol Biol Phys*.

Jones, R. G., Plas, D. R., Kubek, S., Buzzai, M., Mu, J., Xu, Y., et al. (2005). AMP-activated protein kinase induces a p53-dependent metabolic checkpoint. *Mol.Cell, 18*(3), 283-293.

Jorgensen, S. B., Nielsen, J. N., Birk, J. B., Olsen, G. S., Viollet, B., Andreelli, F., et al. (2004). The alpha2-5'AMP-activated protein kinase is a site 2 glycogen synthase kinase in skeletal muscle and is responsive to glucose loading. *Diabetes, 53*(12), 3074-3081.

Kim, J. J., & Tannock, I. F. (2005). Repopulation of cancer cells during therapy: an important cause of treatment failure. *Nat Rev Cancer, 5*(7), 516-525.

Kopnin, P. B., Agapova, L. S., Kopnin, B. P., & Chumakov, P. M. (2007). Repression of sestrin family genes contributes to oncogenic Ras-induced reactive oxygen species up-regulation and genetic instability. *Cancer Res, 67*(10), 4671-4678.

Kourelis, T. V., & Siegel, R. D. (2011). Metformin and cancer: new applications for an old drug. *Med Oncol*.

Lavin, M. F., & Kozlov, S. (2007). ATM activation and DNA damage response *Cell Cycle, 6*(8), 931-942.

Lee, J. H., Budanov, A. V., Park, E. J., Birse, R., Kim, T. E., Perkins, G. A., et al. (2010). Sestrin as a feedback inhibitor of TOR that prevents age-related pathologies. *Science, 327*(5970), 1223-1228.

Livak, K. J., & Schmittgen, T. D. (2001). Analysis of relative gene expression data using real-time quantitative PCR and the 2(-Delta Delta C(T)) Method. *Methods, 25*(4), 402-408.

Lizcano, J. M., Goransson, O., Toth, R., Deak, M., Morrice, N. A., Boudeau, J., et al. (2004). LKB1 is a master kinase that activates 13 kinases of the AMPK subfamily, including MARK/PAR-1. *EMBO J, 23*(4), 833-843.

Lunt, S. Y., & Vander Heiden, M. G. (2011). Aerobic glycolysis: meeting the metabolic requirements of cell proliferation. *Annu Rev Cell Dev Biol, 27*, 441-464.

Machrouhi, F., Ouhamou, N., Laderoute, K., Calaoagan, J., Bukhtiyarova, M., Ehrlich, P. J., et al. (2010). The rational design of a novel potent analogue of the 5'-AMP-

activated protein kinase inhibitor compound C with improved selectivity and cellular activity. *Bioorg.Med.Chem.Lett., 20*(22), 6394-6399.

Masciullo, V., Khalili, K., & Giordano, A. (2000). The Rb family of cell cycle regulatory factors: clinical implications. *Int.J.Oncol., 17*(5), 897-902.

Mihaylova, M. M., & Shaw, R. J. (2011). The AMPK signalling pathway coordinates cell growth, autophagy and metabolism. *Nat Cell Biol, 13*(9), 1016-1023.

Mizushima, N. (2010). The role of the Atg1/ULK1 complex in autophagy regulation. *Curr Opin Cell Biol, 22*(2), 132-139.

Mladenov, E., & Iliakis, G. (2011). Induction and repair of DNA double strand breaks: the increasing spectrum of non-homologous end joining pathways. *Mutat.Res., 711*(1-2), 61-72.

Momcilovic, M., Hong, S. P., & Carlson, M. (2006). Mammalian TAK1 activates Snf1 protein kinase in yeast and phosphorylates AMP-activated protein kinase in vitro. *J Biol Chem, 281*(35), 25336-25343.

Moreno-Sanchez, R., Rodriguez-Enriquez, S., Marin-Hernandez, A., & Saavedra, E. (2007). Energy metabolism in tumor cells. *FEBS J, 274*(6), 1393-1418.

Nagata, Y., Takahashi, A., Ohnishi, K., Ota, I., Ohnishi, T., Tojo, T., et al. (2010). Effect of rapamycin, an mTOR inhibitor, on radiation sensitivity of lung cancer cells having different p53 gene status. *Int J Oncol, 37*(4), 1001-1010.

Nath, N., McCartney, R. R., & Schmidt, M. C. (2003). Yeast Pak1 kinase associates with and activates Snf1. *Mol Cell Biol, 23*(11), 3909-3917.

Oakhill, J. S., Chen, Z. P., Scott, J. W., Steel, R., Castelli, L. A., Ling, N., et al. (2010). beta-Subunit myristoylation is the gatekeeper for initiating metabolic stress sensing by AMP-activated protein kinase (AMPK). *Proc Natl Acad Sci U S A, 107*(45), 19237-19241.

Oakhill, J. S., Scott, J. W., & Kemp, B. E. (2009). Structure and function of AMP-activated protein kinase. *Acta Physiol (Oxf), 196*(1), 3-14.

Ostrau, C., Hulsenbeck, J., Herzog, M., Schad, A., Torzewski, M., Lackner, K. J., et al. (2009). Lovastatin attenuates ionizing radiation-induced normal tissue damage in vivo. *Radiother Oncol, 92*(3), 492-499.

Owen, M. R., Doran, E., & Halestrap, A. P. (2000). Evidence that metformin exerts its anti-diabetic effects through inhibition of complex 1 of the mitochondrial respiratory chain. *Biochem J, 348 Pt 3*, 607-614.

Pang, T., Zhang, Z. S., Gu, M., Qiu, B. Y., Yu, L. F., Cao, P. R., et al. (2008). Small molecule antagonizes autoinhibition and activates AMP-activated protein kinase in cells. *J Biol Chem, 283*(23), 16051-16060.

Pawlik, T. M., & Keyomarsi, K. (2004). Role of cell cycle in mediating sensitivity to radiotherapy. *Int.J.Radiat.Oncol.Biol.Phys., 59*(4), 928-942.

Peeters, H., Debeer, P., Bairoch, A., Wilquet, V., Huysmans, C., Parthoens, E., et al. (2003). PA26 is a candidate gene for heterotaxia in humans: identification of a novel PA26-related gene family in human and mouse. *Hum Genet, 112*(5-6), 573-580.

Podgorsak, E. (2005). *Radiation Biology: A Handbook for Teachers and Students* (Vol. 42). Vienna: International Atom Energy Agency.

Powell, S. N., & Kachnic, L. A. (2003). Roles of BRCA1 and BRCA2 in homologous recombination, DNA replication fidelity and the cellular response to ionizing radiation. *Oncogene, 22*(37), 5784-5791.

Rashid, A., Liu, C., Sanli, T., Tsiani, E., Singh, G., Bristow, R. G., et al. (2011). Resveratrol Enhances Prostate Cancer Cell response to Ionizing Radiation. Modulation of the AMPK, Akt and mTOR Pathways. *Radiat Oncol, 6*(1), 144.

Reed, S. I., Bailly, E., Dulic, V., Hengst, L., Resnitzky, D., & Slingerland, J. (1994). G1 control in mammalian cells. *J.Cell Sci.Suppl, 18*, 69-73.

Rocha, G. Z., Dias, M. M., Ropelle, E. R., Osorio-Costa, F., Rossato, F. A., Vercesi, A. E., et al. (2011). Metformin amplifies chemotherapy-induced AMPK activation and antitumoral growth. *Clin.Cancer Res., 17*(12), 3993-4005.

Rodier, F., Campisi, J., & Bhaumik, D. (2007). Two faces of p53: aging and tumor suppression. *Nucleic Acids Res., 35*(22), 7475-7484.

Rossoni, L. V., Wareing, M., Wenceslau, C. F., Al-Abri, M., Cobb, C., & Austin, C. (2011). Acute simvastatin increases endothelial nitric oxide synthase phosphorylation via AMP-activated protein kinase and reduces contractility of isolated rat mesenteric resistance arteries. *Clin Sci (Lond), 121*(10), 449-458.

Rudner, J., Ruiner, C. E., Handrick, R., Eibl, H. J., Belka, C., & Jendrossek, V. (2010). The Akt-inhibitor Erufosine induces apoptotic cell death in prostate cancer cells and increases the short term effects of ionizing radiation. *Radiat Oncol, 5*, 108.

Rudoltz, M. S., Kao, G., Blank, K. R., Muschel, R. J., & McKenna, W. G. (1996). Molecular Biology of the Cell Cycle: Potential for Therapeutic Applications in Radiation Oncology. *Semin.Radiat.Oncol., 6*(4), 284-294.

Sakamoto, K., Goransson, O., Hardie, D. G., & Alessi, D. R. (2004). Activity of LKB1 and AMPK-related kinases in skeletal muscle: effects of contraction, phenformin, and AICAR. *Am J Physiol Endocrinol Metab, 287*(2), E310-317.

Sancar, A., Lindsey-Boltz, L. A., Unsal-Kacmaz, K., & Linn, S. (2004). Molecular mechanisms of mammalian DNA repair and the DNA damage checkpoints. *Annu.Rev.Biochem., 73*, 39-85.

Sanli, T., Rashid, A., Liu, C., Harding, S., Bristow, R. G., Cutz, J. C., et al. (2010). Ionizing radiation activates AMP-activated kinase (AMPK): a target for radiosensitization of human cancer cells. *Int J Radiat Oncol Biol Phys, 78*(1), 221-229.

Sarbassov, D. D., Guertin, D. A., Ali, S. M., & Sabatini, D. M. (2005). Phosphorylation and regulation of Akt/PKB by the rictor-mTOR complex. *Science, 307*(5712), 1098-1101.

Scott, S. L., Gumerlock, P. H., Beckett, L., Li, Y., & Goldberg, Z. (2004). Survival and cell cycle kinetics of human prostate cancer cell lines after single- and multifraction exposures to ionizing radiation. *Int J Radiat Oncol Biol Phys, 59*(1), 219-227.

Sharma, P., Farrell, T., Patterson, M. S., Singh, G., Wright, J. R., Sur, R., et al. (2009). In vitro survival of nonsmall cell lung cancer cells following combined treatment

with ionizing radiation and photofrin-mediated photodynamic therapy. *Photochem Photobiol, 85*(1), 99-106.

Shaw, R. J. (2006). Glucose metabolism and cancer. *Curr Opin Cell Biol, 18*(6), 598-608.

Skvortsova, I., Skvortsov, S., Stasyk, T., Raju, U., Popper, B. A., Schiestl, B., et al. (2008). Intracellular signaling pathways regulating radioresistance of human prostate carcinoma cells. *Proteomics, 8*(21), 4521-4533.

Steel, G. (2002). *Basic Clinical Radiobiology* (Vol. 3). London: Hodder Arnold.

Steel, G. G., McMillan, T. J., & Peacock, J. H. (1989). The 5Rs of radiobiology. *Int J Radiat Biol, 56*(6), 1045-1048.

Steinberg, G. R., & Kemp, B. E. (2009). AMPK in Health and Disease. *Physiol Rev., 89*(3), 1025-1078.

Stracker, T. H., & Petrini, J. H. (2011). The MRE11 complex: starting from the ends. *Nat Rev Mol Cell Biol, 12*(2), 90-103.

Sullivan, J. E., Brocklehurst, K. J., Marley, A. E., Carey, F., Carling, D., & Beri, R. K. (1994). Inhibition of lipolysis and lipogenesis in isolated rat adipocytes with AICAR, a cell-permeable activator of AMP-activated protein kinase. *FEBS Lett, 353*(1), 33-36.

Suntharaling, N., Podgorsak, E., & Hendry, J. (2009). Basic Radiobiology *Radiation Physics for Medical Physicists* (Vol. 2, pp. 485-504). Philadelphia: Springer.

Sutherland, C. M., Hawley, S. A., McCartney, R. R., Leech, A., Stark, M. J., Schmidt, M. C., et al. (2003). Elm1p is one of three upstream kinases for the Saccharomyces cerevisiae SNF1 complex. *Curr Biol, 13*(15), 1299-1305.

Tannock, I., & Hill, R. (1998). *The Basic Science of Oncology* (Vol. 3). Toronto: McGraw-Hill Professional.

Thomas, C. B., Meade, J. C., & Holmes, E. W. (1981). Aminoimidazole carboxamide ribonucleoside toxicity: a model for study of pyrimidine starvation. *J Cell Physiol, 107*(3), 335-344.

Toulany, M., Schickfluss, T. A., Eicheler, W., Kehlbach, R., Schittek, B., & Rodemann, H. P. (2011). Impact of oncogenic K-RAS on YB-1 phosphorylation induced by ionizing radiation. *Breast Cancer Res., 13*(2), R28.

Tyson, J. J., Csikasz-Nagy, A., & Novak, B. (2002). The dynamics of cell cycle regulation 30. *Bioessays, 24*(12), 1095-1109.

van Veelen, W., Korsse, S. E., van de Laar, L., & Peppelenbosch, M. P. (2011). The long and winding road to rational treatment of cancer associated with LKB1/AMPK/TSC/mTORC1 signaling. *Oncogene, 30*(20), 2289-2303.

Vazquez-Martin, A., Oliveras-Ferraros, C., & Menendez, J. A. (2009). The active form of the metabolic sensor: AMP-activated protein kinase (AMPK) directly binds the mitotic apparatus and travels from centrosomes to the spindle midzone during mitosis and cytokinesis. *Cell Cycle, 8*(15), 2385-2398.

Velasco-Miguel, S., Buckbinder, L., Jean, P., Gelbert, L., Talbott, R., Laidlaw, J., et al. (1999). PA26, a novel target of the p53 tumor suppressor and member of the GADD family of DNA damage and growth arrest inducible genes. *Oncogene, 18*(1), 127-137.

Wahl, G. M., Linke, S. P., Paulson, T. G., & Huang, L. C. (1997). Maintaining genetic stability through TP53 mediated checkpoint control. *Cancer Surv., 29*, 183-219.

Walworth, N. C. (2000). Cell-cycle checkpoint kinases: checking in on the cell cycle 7. *Curr.Opin.Cell Biol., 12*(6), 697-704.

Warburg, O., Wind, F., & Negelein, E. (1927). The Metabolism of Tumors in the Body. *J Gen Physiol, 8*(6), 519-530.

Weinberg, F., & Chandel, N. S. (2009). Mitochondrial metabolism and cancer. *Ann N Y Acad Sci, 1177*, 66-73.

Wong, W. W., Tan, M. M., Xia, Z., Dimitroulakos, J., Minden, M. D., & Penn, L. Z. (2001). Cerivastatin triggers tumor-specific apoptosis with higher efficacy than lovastatin. *Clin Cancer Res, 7*(7), 2067-2075.

Woo, R. A., & Poon, R. Y. (2003). Cyclin-dependent kinases and S phase control in mammalian cells. *Cell Cycle, 2*(4), 316-324.

Woods, A., Dickerson, K., Heath, R., Hong, S. P., Momcilovic, M., Johnstone, S. R., et al. (2005). Ca2+/calmodulin-dependent protein kinase kinase-beta acts upstream of AMP-activated protein kinase in mammalian cells. *Cell Metab, 2*(1), 21-33.

Xiao, B., Sanders, M. J., Underwood, E., Heath, R., Mayer, F. V., Carmena, D., et al. (2011). Structure of mammalian AMPK and its regulation by ADP. *Nature, 472*(7342), 230-233.

Xu, F., Tian, Y., Huang, Y., Zhang, L. L., Guo, Z. Z., Huang, J. J., et al. (2011). EGFR inhibitors sensitize non-small cell lung cancer cells to TRAIL-induced apoptosis. *Chin J.Cancer, 30*(10), 701-711.

Yang, C., Tang, X., Guo, X., Niikura, Y., Kitagawa, K., Cui, K., et al. (2011). Aurora-B mediated ATM serine 1403 phosphorylation is required for mitotic ATM activation and the spindle checkpoint. *Mol Cell, 44*(4), 597-608.

Yang, P. M., Liu, Y. L., Lin, Y. C., Shun, C. T., Wu, M. S., & Chen, C. C. (2010). Inhibition of autophagy enhances anticancer effects of atorvastatin in digestive malignancies. *Cancer Res, 70*(19), 7699-7709.

Zakikhani, M., Dowling, R., Fantus, I. G., Sonenberg, N., & Pollak, M. (2006). Metformin is an AMP kinase-dependent growth inhibitor for breast cancer cells. *Cancer Res., 66*(21), 10269-10273.

Zang, M., Zuccollo, A., Hou, X., Nagata, D., Walsh, K., Herscovitz, H., et al. (2004). AMP-activated protein kinase is required for the lipid-lowering effect of metformin in insulin-resistant human HepG2 cells. *J Biol Chem, 279*(46), 47898-47905.

Zhou, G., Myers, R., Li, Y., Chen, Y., Shen, X., Fenyk-Melody, J., et al. (2001). Role of AMP-activated protein kinase in mechanism of metformin action. *J Clin Invest, 108*(8), 1167-1174.

Zimmermann, M., Zouhair, A., Azria, D., & Ozsahin, M. (2006). The epidermal growth factor receptor (EGFR) in head and neck cancer: its role and treatment implications. *Radiat.Oncol., 1*, 11.

Appendix 1: General Methodology

This section describes the methods that were commonly used in more detail than was possible in the sandwiched manuscripts.

Cell Culture Technique

Lung, breast, and prostate cancer cell, as well as MRC5 (lung), PNT1A (prostate), and 184B5 (breast) epithelial cells were grown and maintained in T-flasks with their recommended base medium according to the American Tissue Culture Collection (ATCC) recommendations. The media was supplemented with 10% (v/v) fetal bovine serum (FBS) and 1% (v/v) antibiotic-antimycotic solution (100 U/mL penicillin, 100 µg/mL streptomycin and 250 ng/mL amphotericin B), and the cells were grown in an atmosphere of 5% CO_2 at 37°C. Cells were regularly trypsinized once they became confluent by washing with 2mL of 1XPBS followed by trypsinization with approximately 1mL of 2x 0.1% EDTA-trypsin. Once trypsin was added, the cells were placed back into the incubator (5% CO_2 at 37°C) for 3-5 minutes to allow cells to disconnect from the flask. Fresh media was then added to the flask to de-activate the trypsin. Excess cells were then removed, leaving a small number in the flask to which new media was added.

The sestrin2 MCF7 tetracycline-OFF (Tet-OFF) cells was a kind gift from Dr. Michael Karin's laboratory (University of California, San Diego). These cells were maintained in standard DMEM growth medium (10% FBS and 1% A/A) supplemented with 0.5µg/mL of doxycycline, and for SESN2 overexpression this medium was replaced with normal DMEM (10% FBS and 1% A/A) for 24h.

IR and Cell Treatments

Cells were exposed to 2–8Gy of IR using a clinical Linear Accelerator radiotherapy unit (Juravinski Cancer Centre, Hamilton, ON, Canada). All experiments were conducted using cells that were grown in BD falcon plastic-ware (6-well plates or 10 cm petri dishes). Appropriate dosimetry was carried out by Dr. Thomas Farrell (a medical physicist) to make certain that accurate delivery of the indicated dose of radiation was achieved under these cell culture conditions. For IR treatments, the cells were removed from the incubator and put into a plastic container with a sterile draping placed over top of the container for transportation to the radiotherapy unit. Radiation delivery was performed by a trained radiation therapist. Following the treatment with IR, cells were placed back into the incubator until the end of the experiment.

All drug treatments (including AMPK activators and inhibitors) were dissolved in DMSO or water according to the manufacturer's recommendations. Working stock solutions of these drugs were then created by dissolving them in the base medium in which the corresponding cells were being grown. Drugs were added 1-24h prior to IR treatments unless otherwise indicated.

Measuring Cell Proliferation and Survival

Clonogenic Survival Assays

Five hundred to one thousand cells (depending on the specific cell line's proliferation rate) were seeded into individual wells of 6-well plates and maintained in 2 mL 10% FBS serum medium. Each treatment condition was performed in triplicate. 24h later, the cells were treated with or without the indicated drugs for 1-24h prior to exposure

to the indicated dose of IR. After ~7-14 days (depending on the doubling rate of the specific cell line) the cells were fixed and stained with 0.05% methylene blue for 5min. Colonies containing >50 cells were then manually counted as viable colonies under a microscope. Averages were taken of the triplicate wells for each treatment. Treatment values were normalized to control values and plotted in graph format (bar graph or line graph) using Microsoft Office Excel. For radiation dose-response curves (0-8Gy), the values were plotted on a logarithmic scale and fitted to the linear quadratic equation using the formula $\mathbf{S(D) = e^{-\alpha D-\beta D2}}$ and GraphPad Prism 5 software.

Crystal Violet Assay *(this protocol was adapted from Dr. Eric Seidlitz)*

The crystal violet stain procedure can be used to determine cell proliferation or cell number in fixed adherent cell cultures without using a fluorescence marker. The procedure itself is based on the ability of crystal violet to bind to DNA. After all unbound stain is washed away, the stain is completely solubilized and the resulting supernatant is analyzed using a plate reader to measure absorbance at a wavelength appropriate for the stain. Cell proliferation can be interpolated by normalizing all treatment groups to the untreated control absorbance value.

Stain 0.5% (w/v) crystal violet stain in 25% (v/v) methanol
Solubilizer 0.05 M NaH_2PO_4 in 50% Ethanol (FW 138.0 g/mole)

Procedure:

1. Remove media and fix cells with 25% (v/v) methanol for 10 minutes (using the same volume as media).
2. Remove methanol and stain for 10 minutes at room temperature.
    a. For a 96 well plate, add 50 μL of crystal violet stain to each well.
3. Remove stain and rinse with fresh tap water until stain can no longer be removed.
    a. For 96 wells, simply dump out the stain then rinse with tap water in a large container. Replace water at least 3 times to ensure adequate removal of unbound stain.

4. Allow plate to dry plate overnight for later reading or proceed to next step directly.
5. Add solubilizer to return adhered stain to solution..
    a. For a 96 well plate, add 100 µL of 0.05 M NaH_2PO_4 in 50% Ethanol to each well.
    b. Shake gently for at least 30 minutes.
6. Read Absorbance on the plate reader at 570 nm, after 1 sec. of low agitation.

Hoechst 33258 Assay *(this protocol was adapted from Dr. Helga Duivenvoorden)*

This assay, using Hoechst 33258 / Bisbenzimide H33258 Fluorochrome, trichloride (Calbiochem #382061) is used to measure cell proliferation based on the adherence of the fluorescent Hoechst dye to DNA. Cell number can also be estimated based on interpolation from a standard curve generated with differential seeding of the same cell lines used in the experiments. Similar to crystal violet staining, cell proliferation can be determined by normalizing all treatment groups to the untreated control absorbance value.

Solutions:

TNE buffer:	10 mM Tris pH=7.4, 2 M NaCl, and 1 mM EDTA
Hoechst stock solution:	10 mg/mL Hoechst in H_2O (light sensitive, wrapped in aluminium foil, store at 4°C; Hoechst 33258 / Bisbenzimide H33258 Fluorochrome trichloride, Calbiochem, Cat#382061)
Hoechst working solution:	20 µg/mL Hoechst in TNE (protect from light)

Procedure:

- At the time point of interest, wash cell monolayers in 96 well plates twice with PBS.
- Add 100 µL Milli-Q water to disrupt the cells
- Wrap in plastic wrap to prevent evaporation (while keeping it level) and freeze at -80°C (at least until completely frozen, but can be frozen for weeks). This freezing step ensures that cells are fully disrupted in preparation for stain to access the nuclei.
- Take the plate from the freezer, put at room temperature until completely thawed (~1 hr).
- Add 100 µL Hoechst working solution/well (with the previously added water, this makes a total of 200 µL in each well)

- Measure fluorescence using excitation λ=360 nm, emission λ=460 nm with the Cytofluor plate reader (template = Hchst_96.mft; gain typically ~65 to yield raw values above 2000).

Western blotting

Western blotting can be utilized to assess the presence of a particular protein of interest in samples of cultured cells or tissue, using cell lysis and an antibody against the target protein. Cells are grown and treated as desired, and then washed with PBS prior to rapid protein extraction. Using a cell lysate buffer solution, cells are lysed and the resulting rudimentary proteins harvested and collected in centrifuge tubes. Following centrifugation, the total protein concentration is measured using a protein assay prior to subsequent analysis. The basis of Western blotting is to separate proteins of equal concentration by molecular weight and charge using electrophoresis on a polyacrylamide gel. These proteins are then transferred to a membrane (nitrocellulose or polyvinylchloride) using another electrostatic gradient. The proteins that have been transferred to the membrane can then be visualized using antibodies to a specific protein of interest. A common procedure for identifying the location of an antibody is to link it to an enzyme (such as horse radish peroxidase) and visualize it using a light-emitting reaction (for example, using an ECL kit that utilizes luminol as a substrate to sense peroxidase activity via production of light emission). The end-product of western blotting is an image on film showing the distribution of proteins in separate lanes with a molecular weight marker lane as a reference point.

Material Preparation:
1.5M Tris-HCl, pH 8.8 -Store at 4˚C.
27.23g Tris base (18.15g/100ml)
80ml deionized water

Adjust to pH 8.8 with 6N HCl. Bring to total volume 150ml with deionized water.

0.5M Tris-HCl, pH 6.8 –Store at 4˚C.
6g Tris base
60ml deionized water
Adjust to pH 6.8 with 6N HCl and bring total volume to 100ml with deionized water.

10x TBS (Tris- buffered saline) (1L) Store at room temperature.
24.2g Tris base
80g NaCl
Adjust pH to 7.6 with HCl. Use at 1x TBS.

Blocking Buffer (150ml) Store at room temperature (fresh daily).
15ml 10x TBS
135ml water
7.5g 5% w/v nonfat dry milk and then
0.15ml Tween- 20 (100%)

0.15ml Tween- 20 (100%) Primary Antibody Dilution Buffer (20ml). Store at 4˚C.
2ml 10x TBS
18ml water
1.0g BSA and then
20ul Tween- 20 (100%)

Wash Buffer TBS/T
1x TBS
0.1% Tween- 20

10x Electrode Running Buffer (store at 4°C)
15.15g Tris base
72g Glycine
5.0g SDS
Dissolve and bring volume to 500ml with DD water. Do not adjust pH with acid or base.
Dilute 50ml of 10x stock with 450ml water before use.

Transfer Buffer (1L) (store at 4°C to improve heat dissipation, make fresh)

25mM Tris base	3.03g
0.2M glycine	15.01g
20% methanol	200ml/ 800ml DD water

Solutions for Protein Preparation: *(adapted from Dr. Evangelia Tsiani)*
1. **SDS Sample Buffer** (*store at room temperature)*:
3.55ml deionized water

1.25ml 0.5M Tris-HCl, pH 6.8
2.50ml glycerol
2.00ml 10% (w/v) SDS *(10g in 90ml water and bring to 100ml)*
0.20ml 0.5% (w/v) bromophenol blue (*0.05g/ 9.95ml water)*
Add 50µl β-mercaptoethanol to 950µl SDS Sample Buffer before use.

2. **Cell Lysis Buffer** *(prevent dephosphorylation by phosphatases)*
20mM Tris (pH 7.5) *(1.21g in 500ml water and adjust pH with HCl)*
150mM NaCl *(4.38g)*
1mM EDTA *(0.14g)*
1mM EGTA *(0.19g)*
1% Triton X-100 *(5mL)*
2.5mM sodium pyrophosphate *(0.56g)* **(phosphatase inhibitor)**
1mM β-glycerolphosphate *(0.11g)* **(phosphatase inhibitor)**
1mM Na3VO4 *(0.09g)* **(tyrosine phosphatase inhibitor)**
1µg/ml leupeptin *(0.5mg)* **(serine/thiol protease inhibitor)**
Add 1mM PMSF **(serine protease inhibitor)** before use and chill on ice. *(0.174g/ml = 0.087g/500µl methanol for 1M stock- therefore add 1µl/ml to buffer)*
Store at 4°C for 1- 2 weeks or at -20°C for longer time periods.

Cell Lysis:

1. Treat cells as described in Glucose Transport Assay.
2. After treatment, pour off medium and wash cells twice with HBS and aspirate.
3. Lyse cells with 50µl of 0.05N NaOH and pipette into 1.5mL eppendorf tube.
4. Remove 50µl for Protein Assay.
5. Add equal amount of SDS Sample Buffer and immediately boil for 5 minutes and freeze at -20°C.

Protein Assay

Protein assay dye (BioRad) was prepared and filtered for protein concentration determination. BSA protein standards (0, 0.1, 0.2, 0.4, 0.6, 0.8, 0.9, 1.0mg/ml) were used to create a standard protein curve. 10µl of each protein standard and lysed samples were pipetted into separate wells of a 96-well plate in triplicate. 250µL of protein assay dye (1:4 ratio in water) was then added into each well. The absorbance was measured using a BioTek PowerWave XL plate reader at 570nm, and the final concentration of the protein samples were calculated in Microsoft Excel. The final protein concentration was ascertained using the equation $y=mx+b$, where x is the average absorbance of the triplicate sample and both m and b are derived from the linear equation generated by Excel from the standard curve.

Gel Preparation:

Resolving Gel Buffer (10%) bottom (30 minutes minimum)

12.3ml DD water

9.9ml 30% Acrylamide/ Bis Solution
7.5ml 1.5M Tris- Hcl, pH 8.8
0.3ml 10% w/v SDS

Right before pouring the gel, add 150µl 10% APS (0.01g/ 100µl) made fresh daily and 15µl TEMED and swirl.

Add 100% ethanol to smoothen gel layer and wash with water after gel is set.

Stacking Gel Buffer (4%) top (1 hour minimum)

18.3ml DD water
3.9ml 30% Acrylamide/ Bis Solution
7.5ml 0.5M Tris-HCl, pH 6.8
0.3ml 10% w/v SDS

Right before pouring the gel, add 150µl 10% APS (0.01g/ 100µl) made fresh daily and 30µl TEMED and swirl.

Electrophoresis:

1. Place gels in electrode assembly and add **diluted running buffer** in reservoir and allow to overflow into tank (500ml).
2. Thaw samples and vortex for 15 seconds.
3. Boil for 5 minutes.
4. Microcentrifuge for 5 minutes.
5. Use micropipette to load wells with sample (25µl optimum). Remember to load molecular weight standard (5µl). *(20- 30µg protein/ well)*
6. Run at 150V for ~1 hour depending on thickness of resolving gel. (stop when dye runs out of the bottom)
7. When complete, use a razor to remove the stacking gel only and place the remaining gel in transfer buffer with agitation.

PVDF Membrane Transfer:

1. Prepare transfer buffer ahead of time and chill at 4°C.
2. Assemble transfer apparatus and get ice packs.
3. PVDF membranes must be equilibrated in 100% methanol before placed in transfer buffer (always wear gloves when handling membranes).
4. Soak membranes, filter papers, and fiber pads in transfer buffer for 15 minutes to equilibrate and then assemble sandwich immersed in transfer buffer to avoid bubbles.

Black side- fiber pad- filter paper- gel- membrane- filter paper- fiber pad- clear side

5. Place cassette in module and stir bar. Fill tank completely with transfer buffer and pack with ice.
6. Transfer for 1 hour at 100V.

Membrane Blocking and Antibody Detection:

1. Wash PVDF membrane for 5 minutes at room temperature with 10ml 1x TBS.
2. Incubate in blocking buffer for 1 hour at room temperature in agitator.
3. Rinse with 50µl Tween20, 45ml DD water, and 5ml 1x TBS.

4. Incubate with primary antibody (usually 1:1000 or 10µl/ 10ml) diluted in primary antibody dilution buffer overnight at 4°C (cold room) with gentle agitation. Cover with saran wrap to avoid evaporation.

Recover antibody and add sodium azide for conservation. Use 0.02% final concentration.

5. Wash 3 times for 5 minutes with 15ml TBS/T.
6. Incubate with HRP- conjugated secondary antibody (usually 1:2000 or 5µl/ 10 ml) to detect biotinylated protein markers, in blocking buffer with agitation at room temperature.
7. Repeat washing with TBS/T 3 times for 5 minutes each.

Protein Detection in Dark Room:

1. Incubate membrane for 1 minute in 2ml GE Healthcare ECL Reagent (1:1 ratio of buffer A and buffer B) with gentle agitation at room temperature. (It is light sensitive!)
2. Place in clear wrap into film cassette.
3. Expose to autoradiography film and insert into film developer (10 second exposure should indicate proper exposure time).

Immunoprecipitation

Immunoprecipitation (IP) is a process that allows for the precipitation of protein of interest (that may exist in a complex of other proteins) out of a solution by using a specific antibody against it. This antibody-protein complex can then be bound to solid-phase substrates, such as agarose beads, before the sample is centrifuged. The "heavier" protein of interest (bound by the antibody and beads), along with any other proteins that associate with it, will form the precipitate at the bottom of the centrifuge tube. The remaining supernatant left in the sample can then be discarded.

Procedure:

1) Allocate 200µL of whole cell lysate that was lysed in lysis buffer for the IP procedure.
2) Select an antibody against your protein of interest and incubated it (at a 1:50 volume ratio) directly in the lysate overnight a 4°C. If the protein of interest is tagged with a Flag-vector, then use a Flag-tagged primary antibody.
3) The following morning add 20µL of protein A agarose beads (Sigma, St. Louis, MO) to the sample and agitate for 1-3 hours at 4°C.
4) The cell lysate can then be microcentrifuged at max speed for 30sec at 4°C, the supernatant removed, and washed with 500µL cell lysis buffer.

5) Repeat step 4 at least 4-5x before proceeding to the final step.
6) The pellet can then be re-suspended in 20µL of 3x SDS sample buffer and boiled at 100 ^{o}C for 5min. 15µL of protein sample can then be loaded onto SDS-PAGE gel to be analyzed by western blotting.

Real Time Polymerase Chain Reaction (RT-PCR)

The basic application of PCR can be utilized to amplify a very small template of RNA or DNA into large quantities within a short period of time. The process is now automated using a PCR machine to copy a short region of DNA multiple times in a test tube by using DNA polymerase. The PCR machine carries out a cycle of processes in which the following sequence of events are repeated over and over again to amplify the specified DNA sequence:

1. Double-stranded DNA is denatured by heat into single-stranded DNA.
2. Short primer pairs to a specific gene of interest are incorporated into the reaction.
3. DNA polymerase catalyzes the production of the complementary new strand of DNA.

Specifically, this reaction requires a few vital components to produce the multiple copies of the DNA sequence. As already stated, the procedure requires short primers on either side of the DNA stand (forward and reverse) to your gene of interest. In addition, Taq polymerase (from the bacteria *Thermus aquaticus*) is required to amply the DNA because it can withstand the high temperatures (95^{0}C) that are required to denature the double-stranded DNA without itself being degraded. Finally, free nucleotides (dNTPs for DNA, and NTPs for RNA) in supplied in a buffer are necessary as building-blocks for the reaction.

Fairly recently, a new method to quantitate the amount of DNA has been developed. This process is called "real time" PCR (RT-PCR), because it allows for the researcher to view (in real time) the increase in DNA being generated through each cycle as it is being amplified. Two available methods for the detection of DNA in RT-PCR includes the use of non-specific fluorescent dyes that interact with double-stranded DNA, and sequence-specific DNA probes consisting of oligonucleotides that are tagged with a fluorescent reporter (e.x. SYBR green) which allows for quantitation following the hybridization of the probe with its complementary DNA target.

Procedure:

Isolation of RNA from Cells in Culture *(Adapted from Qiagen RNeasy Mini Handbook)*

1. Following treatments, harvest cells directly by adding 350µL RLT buffer and collecting lysates in 1.5mL eppendorf tube. These samples can then be homogenized immediately or stored at -80^{0}C for later use.
2. Homogenize the lysate by passing them through a 20-gauge needle at least 10x. Then add one voluem (350µL) of 70% ethanol to the lysate and mix by pipetting (do not centrifuge).
3. Transfer the sample to an RNeasy spin column placed in a 2mL collection tube (supplied). Close the lid gently and centrifuge for 15s at >10,000 rpm (max speed on lab centrifuge). Discard the flow-through.
4. Add 700µL Beffer RW1 to the RNeasy spin column. Close the lid and centrifuge for 15s at >10,000 rpm to wash the spin column membrane. Discard the flow-through.
5. Add 500µL Buffer RPE to the RNeasy spin column. Close the lid and centrifuge for 15s at >10,000 rpm to wash the spin column membrane. Discard the flow-through.
6. Add 500µL Buffer RPE to the RNeasy spin column. Close the lid and centrifuge for 2min at >10,000 rpm to wash the spin column membrane.
7. Place the RNeasy spin column in a new 2mL collection tube (supplied), and discard the old collection tube with the flow-through. Close the lid and centrifuge at max speed for 1min.
8. Place the RNeasy spin column in a new 1.5mL collection tube (supplied). Add 30-50µL RNase-free water (depending on how much RNA yield you believe there will be). Close the lid and centrifuge for 1min at >10,000 rpm to elute the RNA.
9. Proceed to DNase treatment protocol.

DNase Treatment Protocol *(adapted from Dr. Katja Linher-Melville)*

Materials:

DNA-free-AMBION Kit

1. Place DNase enzyme on ice and thaw DNase Inactivation Reagent.
2. Add 10% volume of 10x DNase 1 buffer to RNA sample (if 50 µl of RNase-free water was added to spin column add 5 µl 10x DNase 1 buffer).
3. Add 1 µl of DNase 1 enzyme to mixture.
4. Incubate at 37ºC for 30 mins (Using heat block, monitor temperature using thermometer because enzyme works optimally at 37ºC).
5. Resuspend DNase inactivation reagent by flicking and vortexing. Add 10% volume of slury to sample. Flick to get into solution. Incubate at room temperature for 2 mins (Add DMCA if too thick).
6. Vortex lightly, centrifuge at max for 1 min to pellet the reagent. Put supernatant into new 1.5 mL tubes and discard the pellet. Put tubes on ice (can freeze at -80ºC until ready).

Spectrometry of Samples

1. Turn on UV on spec station 5 minutes before usage (UV-VIS→ when light bulb stops flashing it is warm)
2. Prepare samples: 1 tube RNase-free water (72 µl) and sample tubes (2 µl RNA + 70 µl water) *Mix samples by pipetting
   Final volume/Sample volume= Dilution Factor (i.e. 72/2= Dilution factor of 36)
3. Select mode: Nucleic Acid, 260/280 Ratio then enter
4. Spec box is in cabinet under Beckman spectrometer, take up all of the volume of sample and pipette into crack (wipe sides to get rid of dust).
5. Place box in spectrometer with the dot facing you, hit Blank 0-0 Reading.
6. After reading shake out box in biohazardous waste, wipe and load next sample. Hit read
7. Record OD 260 and OD 260/280 for each sample
8. For RNA want OD 260/280 Ratio in the range of 1.8-1.9, anything over 2.0 suggests protein carryover and should be repeated
   [(OD 260 x 40) x Dilution Factor]/ 1000 = µg/µl of RNA

cDNA Synthesis using SuperScript III (Invitrogen)

This procedure is intented to convert 1pg to 5µg of total RNA or 1pg to 500ng of poly(A) RNA into first-strand cDNA:

1. Mix and briefly centrifuge each component before using.
2. Combine the following components into a 0.2 or 0.5mL tube:
   i) Up to 5µg total RNA
   ii) 1µL of each primer pair to your gene of interest (FOR and REV)
   iii) 1µL of 50µM oligo(dT)
   iv) 1µL of 10mM dNTP mix
   v) Top up to 10µL using DEPC-treated water
3. Incubate at 65^0C for 5min, then place on ice for at least 1min.

4. Prepare the following cDNA synthesis mix, adding each component in the indicated order (for 1x reaction mixture):
   i) 2µL 10x RT buffer
   ii) 4µL 25mM MgCl2
   iii) 2µL 0.1M DTT
   iv) 1µL RNaseOUT (40U/µL0
   v) 1µL SuperScript III RT (200U/µL)
5. Add 10µL of cDNA synthesis mix to each RNA/primer mixture, mix gently, and collect by brief centrifugation. Incubate as follows.
   i) Oligo(dT) for 50min at 50^0C
   ii) Random hexamer primed for 10min at 25^0C followed by 50min at 50^0C
6. Terminate the reactions at 85^0C for 5min. Chill on ice
7. Collect the reactions by brief centrifugation. Add 1µL of RNase H to each tube and incubate for 20min at 37^0C
8. cDNA synthesis reactions can be stored at -20^0C or used for PCR immediately

RT-PCR Machine Protocol

1. Before beginning prepare a Master Mix for each primer pair you will be using

Master Mix	
10 pmol/µl primer FOR	0.5 µl x (Number of reactions +1)
10 pmol/µl primer REV	0.5 µl x (Number of reactions +1)
2.75 µl dH_20	2.75 µl x (Number of reactions +1)
6.25 µl SYBR Green Premix	6.25 µl x (Number of reactions +1)

2. To each tube add 10 µl Master Mix + 2.5 µl cDNA= 12.5 µl final reaction volume
3. Turn on RT machine and open software Bio-Rad CFX Manager
4. Create a New Experiment
5. Select existing→ Katja folder→ Katja RT protocol
6. Next on bottom right
7. Select existing plate→ Katja plate setup→ Edit selected
8. Highlight→ Sample type→ Unknown→ Load SYBR
9. Save and next
10. Edit sample volume to 13 µl
11. Start run and save in new folder

Cycling conditions were as follows: 95°C for 1 min, 40 total cycles of 95°C for 10 sec, 60°C for 25 sec, and melt peak determination (95°C for 15 sec, increasing from 65°C to 95°C with 0.5°C increments for 5 sec each). Parallel reactions were carried out for the *RPII* housekeeping gene to calculate relative mRNA levels by real time PCR using the $2^{-[\Delta][\Delta]Ct}$ method (Livak & Schmittgen, 2001).

Forward (FOR) and reverse (REV) primers used to amplify the human target genes of interest were designed based on modifications to existing PCR primer pairs for gene expression detection and quantification listed in PrimerBank with annealing temperatures of 60°C (http://pga.mgh.harvard.edu/primerbank/index.html). The amplification efficiencies were tested for each primer pair, the specificity of the melt curves was assessed, and the integrity of each product was verified by gel electrophoresis.

Table 2: List of PCR Primer Pairs Used.

Gene Name	*Sequence (5' → 3')*
AMPKα1 FOR	AGAAGCAGAAACACGACGGG
AMPKα1 REV	GCGGATTTTTCCTACCACATCA
AMPKα2 FOR	CTGTAAGCATGGACGGGTTGA
AMPKα2 REV	AAATCGGCTATCTTGGCATTCA
AMPKβ1 FOR	GCATGGTGGCCATAAGACG
AMPKβ1 REV	GCGGGAGCTTTATCATTCAC
AMPKβ2 FOR	CAGTCAGCTTGGCACAATTAAC
AMPKβ2 REV	TCCTCAGATCGAAACGCATACA
AMPKγ1 FOR	CATCCTCAAGAGACCCCAGA
AMPKγ1 REV	CACCGTTAGTCACCAAAGCA
AMPKγ2 FOR	GAGCCTGAACGGTTAGAGAATC
AMPKγ2 REV	GCTTCGTCCTCGAACTCCAG
LKB1 FOR	GAGCTGATGTCGGTGGGTATG
LKB1 REV	CACCTTGCCGTAAGAGCCT
SESN2 FOR	GCGAGATCAACAAGTTGCTGG
SESN2 REV	ACAGCCAAACACGAAGGAGG
RPII-I FOR	GGGTGCTGAGTGAGAAGGAC
RPII-I REV	AGCCATCAAAGGAGATGACG

SESN2 Overexpression using a Flag-tagged Vector

The creation of the pCMV-FLAG-MAT-Tag-1 SESN2 expression vector (Sesn2F) was carried out by Dr. Katja Linher-Melville. Sub-cloning of SESN2 cDNA

was obtained through PCR amplification of the human SESN2 primers (obtained from Dr. Micheal Karin's lab) containing corresponding endonuclease reinstruction sites and Flag-tagged sequences; FOR: 5'-AAAAGCTTGCCACCATGGATTACAAGGACGAC-GACGATAAGATGATCGTGGCGGA-3'; REV: 5'-AAGCGGCCGCTCAGGTCAT-GTAGCGGGA-3'.

Transfecting this vector into human cancer cells lines was conducted as follows:

1) In one tube, combine 1μg of SESN2 plasmid DNA (Sesn2F) in 250μL of serum-free media without antibiotics.
2) In a second tube, combine 10μL of lipofectamine 2000 transfection reagent (Invitrogen) in 250μL of serum-free media and incubate at room temperature for 5min.
3) Mix the two tubes containing the Sesn2F and lipofectamine together and incubate at room temperature for 30min.
4) Change the media in your cells that will receive the vector (in a 6-well plate), replacing them with 1.5mL of complete culture media per well.
5) Add the 0.5mL of combined transfection mix (Sesn2F + lipofectamine) drop-wise down the side of each appropriate well, swirl gently to mix, and incubate the cells at 37^0C for 48h before terminating the transfection.

siRNA-Mediated Gene Silencing

To investigate the role of AMPK and SESN2 in molecular signalling pathways regulated by IR, we knocked down their activity by silencing the expression AMPKα1/2 and SESN2. RNAi is a process whereby the addition of double-stranded RNA (dsRNA) into a cell leads to targeted posttranscriptional gene silencing (QIAGEN protocol manual). In mammalian cells, it was found that short interfering RNA (siRNA) oligos of 23 nucleotides could effectively shut down the expression of a specific target gene that correspond to the siRNA sequence. To this end, pre-designed siRNA sequences (we used 2 siRNA sequence per gene) against AMPKα1 (*sequence 1: Hs_PRKAA1_5* and *sequence2: Hs_PRKAA1_6*), AMPKα2 (*sequence1: Hs_PRKAA2_6* and *sequence2:*

Hs_PRKAA2_7), and SESN2 (*sequence1: Hs_SESN2_2* and *sequence2: Hs_SESN2_7*) were obtained through the QIAGEN RNAi database (GeneGlobe).

Procedure:

1) Approximately 50,000 - 80,000 cells were seeded into 6-well plates in 2mL of media, and allowed to adhere for approximately 4-5 hours.
2) For generation of the vehicle-siRNA complex, a 100 µL preparation was prepared in a 1 mL eppendorf tube for each transfection (1x reaction) as follows:
   i) Add 65.5µL of serum and antibiotic free media to the tube
   ii) Add 15µL of one siRNA sequence (final concentration is 25nM) to the media in the tube. **Ex.** For AMPKα1 siRNA, add the Hs_PRKAA1_5 sequence first
   iii) Add 15µL of the other siRNA sequence (final concentration is 25nM) to the media in the tube. **Ex.** For AMPKα1 siRNA, then add the Hs_PRKAA1_6 sequence
   iv) Add 4.5 µL of HiPerFect transfection reagent to this mixture in the tube.
   v) Vortex the tube gently, and allow the reaction to incubate for 10min at room temperature
3) Remove the existing media from the 6-well plates by aspiration and replace with 0.5mL of fresh complete growth media.
4) Add the 100µL transfection reaction (siRNA + the HiPerFect) drop-wise to the desired wells of the 6-well plate and incubate overnight at 37^0C. The final volume of media in the plate should now be 0.6mL per well. In addition, insure that you keep one well available as a vehicle control that contains only HiPerFect
5) The following morning remove the media containing the transfection reaction and replace with 2mL of fresh complete growth media.
6) Continue with any additional treatments or allow the cell to grow for an additional 72h before lysis

Immunofluorescence Protocol

The following protocol provides the general steps used in most conventional fluorescent microscopes to allow for the detection of specific protein of interest (labeled with fluorescent antibodies or dyes).

1) Add sterile cover slips (you can flame waft them) to 6-well plates before the addition of cells.
2) Grow cells and treat with radiation or drugs for desired time.
3) Wash cells gently with cold PBS (2x).
4) Treat the cells with 2-4% formaldehyde in PBS for 20min at RT.
5) Wash the cells with PBS 3x at 5min each.

6) Block cells with 5% normal-serum diluted in PBS with 0.3% Triton-X-100 for 1h at RT. This will also permeabilize the cells.
7) During this time you can dilute the primary antibody to 1:100 in PBS with 1% BSA and 0.3% Trition-X-100. There is no need to rinse between blocking and primary incubation. Allow the primary antibody to incubate overnight at 4^{o}C.
8) Repeat washing with PBS 3x at 5min each.
9) The next day dilute your secondary antibody in the same dilution as before, and incubate in the dark for 1h RT.
10) Repeat washing with PBS 3x at 5min each.
11) Remove the cover slip from the 6-well dish and place it cell-side down onto a glass slide dotted with a single drop of Vectashield (antifade).
12) Seal the edges of the cover slip to the glass slide by using fast dry nail polish.

Using the Microscope:

1) Turn on the following equipment in the correct order and wait for 30min for the scope to warm up: **i)** the mercury lamp, **ii)** the filter wheel box, **iii)** the microscope bright field, **iv)** the digital camera, **v)** the Mac computer.
2) Open the OpenLab v5.0 software program on the computer (it is on the bottom screen scroll menu).
3) Adjust the microscope filters appropriately to visualize your cells. To start locate your cells using the 40x lens and the bright field view only (BF button, aka #3 on the button panel to the right of the microscope). The focus is the left knob.
4) Once you have located your cells turn off the bright field and turn on the fluorescence. To do this make sure that the fluorescence filter is on (#1,2 on the button panel to the right of the microscope). Also make sure that the rod at the base of the microscope is pulled out so the fluorescent light can pass through. Turn off the lights, so it is dark!
5) Final, make sure that you set the button panel on the right of the microscope to the correct filter (#2 is DAPI, #3 is FITC, and #4 is TX-RED) and that it is aligned with the correct filter wheel position (as indicated on the front of the microscope). The filter wheel is located directly under the microscope lenses (#1 is DAPI, #2 is FITC, etc).
6) Once you have a good image you can take a picture of it using the OpenLab software. Click on the video camera icon located on the left panel of the screen. You can adjust the exposure time, gain, and background using the icons on the right side of the screen. To take a picture you need to pull out the rod at the base of the eyepiece until you can no longer see your cells through the microscope. However, the cells will now appear on the computer screen.
7) Pictures are black-and-white unless you add the colour via the software scheme. There is a colour grid icon on the left hand side of the screen. Click it and select the colour you would like to see (usually the same colour as your dye).
8) To save a picture to the Mac and transport it to the lab PC, click the Grab icon on the bottom screen scroll menu. Then select the capture mode from the drop-down menu and hit selection. Then drag a box over the picture you want to save and

"save as" to the HD drive of the Mac. If you open the picture in the HD drive you can convert it to JPEG for easy transfer later.

9) When you are done turn off everything in the same order it was turned on. Leave the microscope off for 30min before you put the protective plastic overtop of the microscope. If you don't wait the heat from the microscope will burn holes in the plastic!

Cell Cycle Analysis

Cell cycle analysis is performed with a flow cytometer, which is a machine that can rapid evaluate the DNA content of a large population of homogenous cells. This is achieved by running a suspension of labelled cells [using the DNA stain propidum iodide (PI)] through the flow cytometer which in turn, passes them through an internal electronic detector that analyses the DNA content of each cell individually. Once an entire sample of cells is examined, the flow cytometer can generate graphically the distribution of all the cells through each phase of the cell cycle.

Procedure:

1) Grow cells in 10cm culture dishes for 24h prior to treatments
2) Once treatments are finished, remove the medium, wash with PBS, and trypsinize the cells.
3) Collect the trypsinized cells in normal growth media and spin them down at 1200 RPM for 5min.
4) Re-suspend the cells in 1mL PBS and count them using a haemocytometer (to determine the amount of PI stain to be added).
5) Fix the cells with 3mL of 70% ethanol and stored overnight at -20°C.
6) To prepare for analysis, the cells were centrifuged at 1300 RPM for 5min to remove the ethanol, washed with 1X PBS and stained with PI solution containing 100 µL Triton X-100 and 100µL of PI (1mg/mL) in 10mL of 1X PBS.
7) The cells were then subjected to flow cytometric cell cycle analysis using a Beckman Coulter Epics XL flow cytometer.

Statistical Analyses

Parametric statistical tests were utilized in this thesis as the data were normally distributed and maintained homoscedasticity. The majority of the experiments presented

the data as the mean and standard error (SE) of at least 3 independent trials that were normalized to their respective untreated control. An unpaired students T test was used to detect significant difference between two specific groups (i.e control vs. radiation). When more than two groups were being compared, a one-way analysis of variance (ANOVA) was utilized to determine main effects between each treatment (i.e. control vs. radiation, vs. drug). Differences between groups were considered significant at a P value of <0.05. Statistical Package for the Social Sciences (SPSS) version 16.0 software was used to calculate these values.

Appendix 2: Supporting Experiments

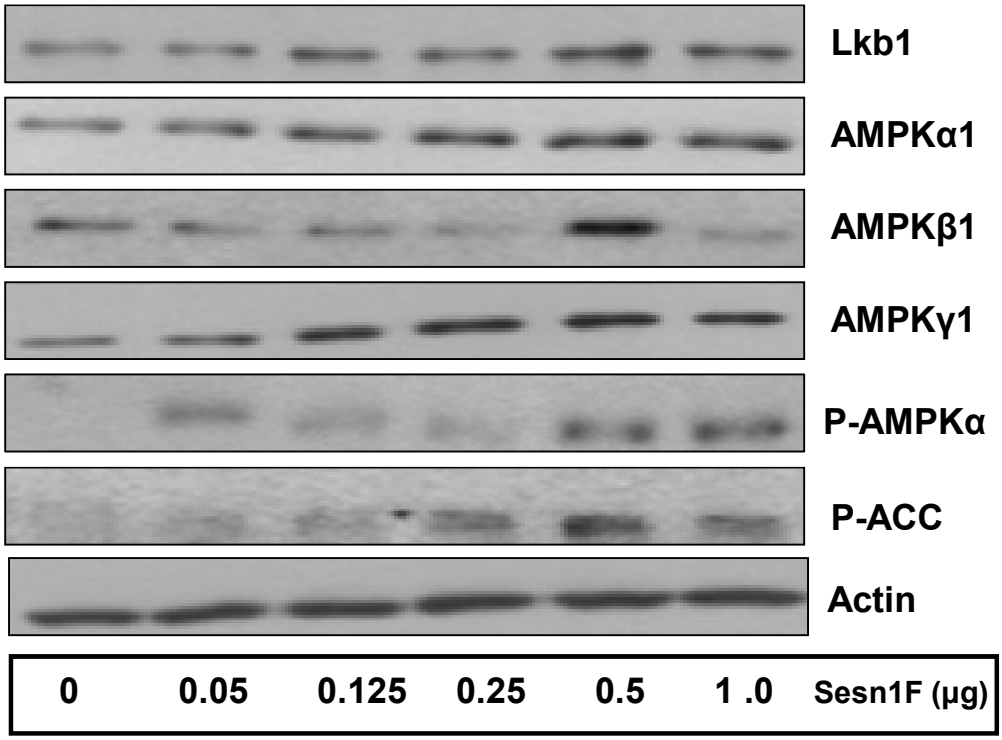

Figure A1: SESN1overexpression enhances LKB1 and AMPK levels in MCF7 cells. The cells were transiently transfected with 0.05-1 μg Sesn1F vector for 24h, followed by cell lysis and western blotting with the indicated antibodies. A representative immunoblot from 3 independent experiments is shown.

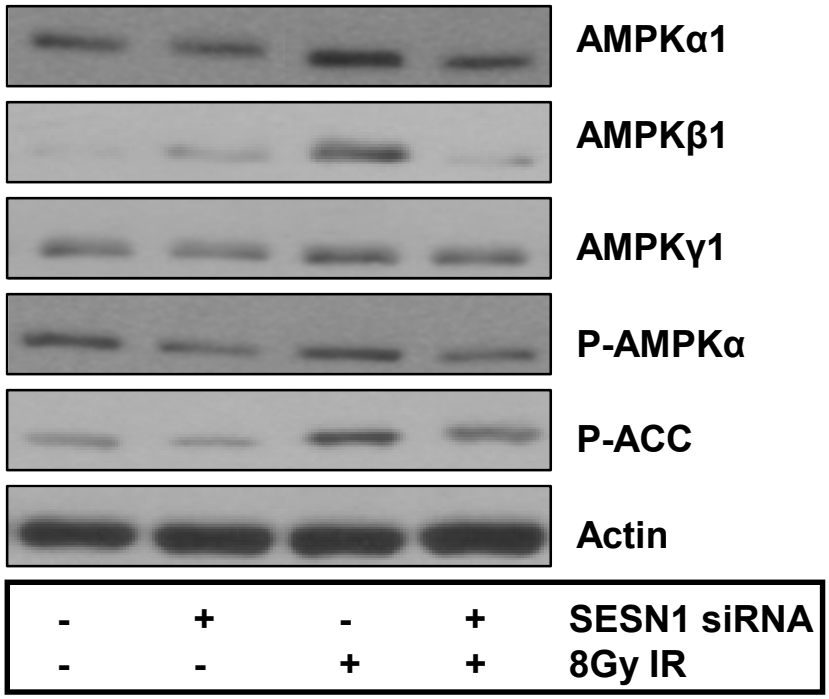

Figure A2: IR-induced expression and activity of AMPK requires SESN1. MCF7 cells were treated with SESN1 siRNA for 48h prior to being exposed to a single dose of 8Gy IR. The cells were lysed 24h after IR and western blotting was performed with the indicated antibodies. A representative immunoblot from 3-4 independent experiments is shown.

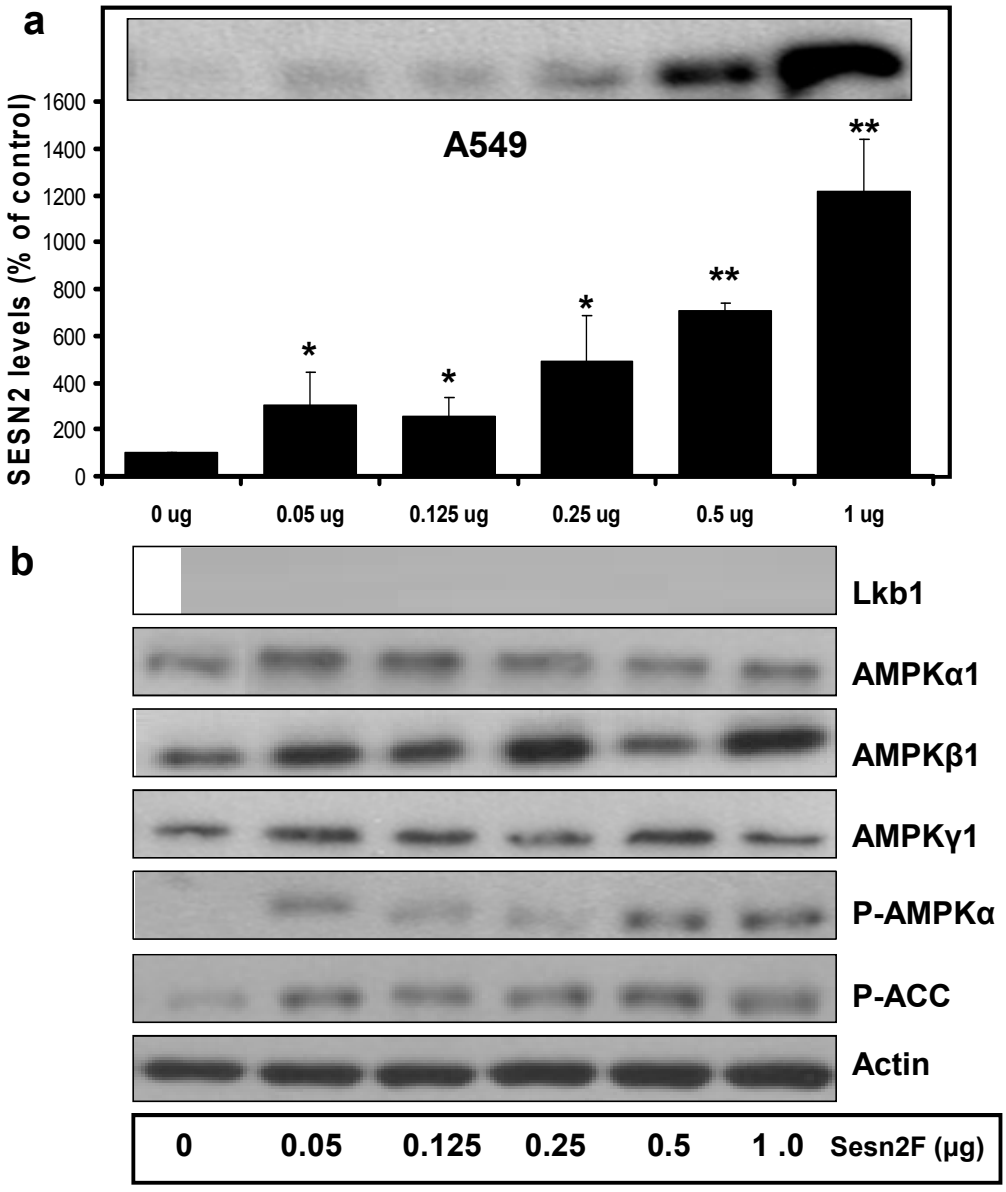

Figure A3: SESN2 overexpression modulates AMPK levels in lung cancer cells. A549 cells were treated with the indicated concentration of Sesn2F for 48h before cell lysis and western blotting with the indicated antibodies. A representative immunoblot from 4 independent experiments is shown. * = $P<0.05$ compared to control, ** = $P<0.01$ compared to control.

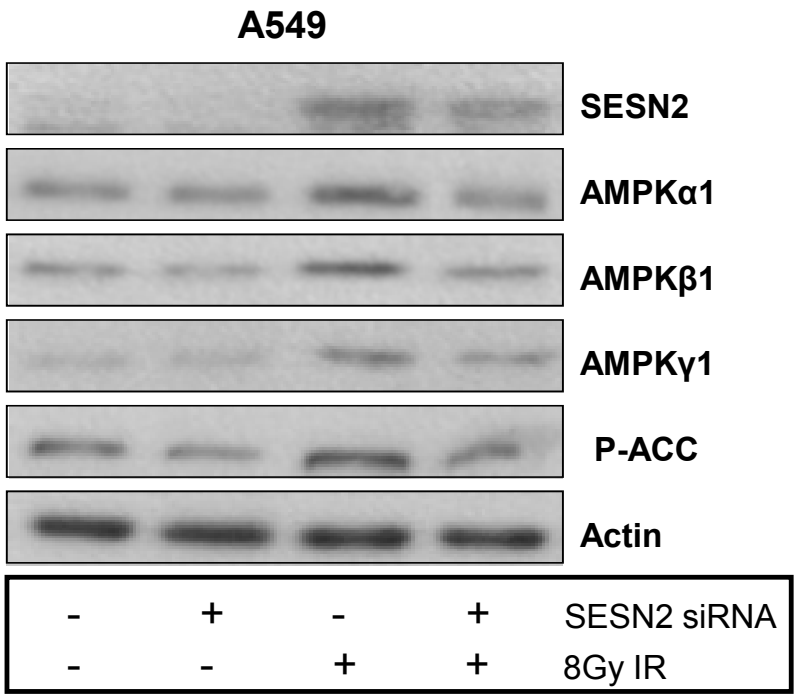

Figure A4: IR-induced AMPK modulation requires SESN2 in lung cancer cells. A549 cells were treated with SESN2 siRNA for 48h prior to being exposed to a single dose of 8Gy IR. The cells were lysed 24h after IR and western blotting was performed with the indicated antibodies. A representative immunoblot from 3 independent experiments is shown.

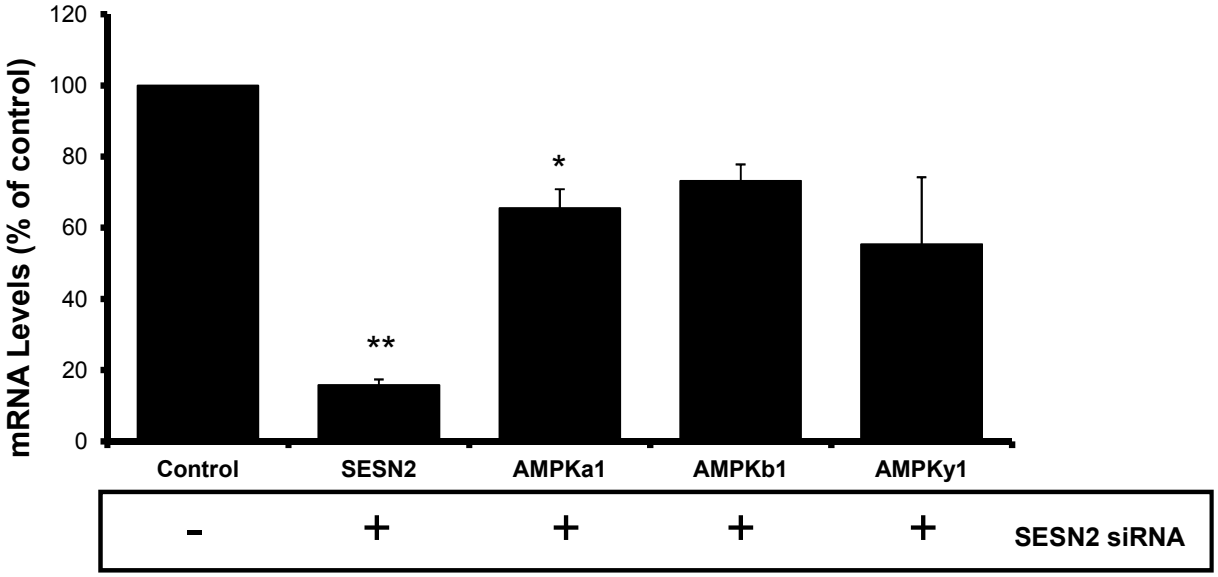

Figure A5: SESN2 siRNA decreases AMPK mRNA expression levels. MCF7 cells were treated with SESN2 siRNA 72h prior to cell lysis. RT-PCR was then conducted using the indicated primers. * = $P<0.05$ compared to control, ** = $P<0.01$ compared to control.

Appendix 3: Copyright Licence Agreements for Papers

This is a License Agreement between Toran Sanli ("You") and Elsevier ("Elsevier") provided by Copyright Clearance Center ("CCC"). The license consists of your order details, the terms and conditions provided by Elsevier, and the payment terms and conditions.

All payments must be made in full to CCC. For payment instructions, please see information listed at the bottom of this form.

Supplier	Elsevier Limited The Boulevard,Langford Lane Kidlington,Oxford,OX5 1GB,UK
Registered Company Number	1982084
Customer name	Toran Sanli
Customer address	699 Concession St. Hamilton, Ontario L8V 5C2
License number	2753680830643
License date	Sep 21, 2011
Licensed content publisher	Elsevier
Licensed content publication	International Journal of Radiation Oncology*Biology*Physics
Licensed content title	**Ionizing Radiation Activates AMP-Activated Kinase (AMPK): A Target for Radiosensitization of Human Cancer Cells**
Licensed content author	Toran Sanli,Ayesha Rashid,Caiqiong Liu,Shane Harding,Robert G. Bristow,Jean-Claude Cutz,Gurmit Singh,James Wright,Theodoros Tsakiridis
Licensed content date	1 September 2010
Licensed content volume number	78
Licensed content issue number	1
Number of pages	9
Start Page	221
End Page	229
Type of Use	reuse in a thesis/dissertation
Portion	full article
Format	both print and electronic
Are you the author of this Elsevier article?	Yes
Will you be translating?	No
Order reference number	
Title of your thesis/dissertation	THE ROLE OF AMP-ACTIVATED PROTIEN KINASE (AMPK) IN MEDIATING RADIATION REPONSES IN CANCER CELLS
Expected completion date	Jun 2012
Estimated size (number of pages)	250
Elsevier VAT number	GB 494 6272 12
Permissions price	0.00 USD
VAT/Local Sales Tax	0.0 USD / 0.0 GBP
Total	0.00 USD

Terms and Conditions

INTRODUCTION

1. The publisher for this copyrighted material is Elsevier. By clicking "accept" in connection with completing this

licensing transaction, you agree that the following terms and conditions apply to this transaction (along with the Billing and Payment terms and conditions established by Copyright Clearance Center, Inc. ("CCC"), at the time that you opened your Rightslink account and that are available at any time at http://myaccount.copyright.com).

GENERAL TERMS

2. Elsevier hereby grants you permission to reproduce the aforementioned material subject to the terms and conditions indicated.

3. Acknowledgement: If any part of the material to be used (for example, figures) has appeared in our publication with credit or acknowledgement to another source, permission must also be sought from that source. If such permission is not obtained then that material may not be included in your publication/copies. Suitable acknowledgement to the source must be made, either as a footnote or in a reference list at the end of your publication, as follows:

"Reprinted from Publication title, Vol /edition number, Author(s), Title of article / title of chapter, Pages No., Copyright (Year), with permission from Elsevier [OR APPLICABLE SOCIETY COPYRIGHT OWNER]." Also Lancet special credit - "Reprinted from The Lancet, Vol. number, Author(s), Title of article, Pages No., Copyright (Year), with permission from Elsevier."

4. Reproduction of this material is confined to the purpose and/or media for which permission is hereby given.

5. Altering/Modifying Material: Not Permitted. However figures and illustrations may be altered/adapted minimally to serve your work. Any other abbreviations, additions, deletions and/or any other alterations shall be made only with prior written authorization of Elsevier Ltd. (Please contact Elsevier at permissions@elsevier.com)

6. If the permission fee for the requested use of our material is waived in this instance, please be advised that your future requests for Elsevier materials may attract a fee.

7. Reservation of Rights: Publisher reserves all rights not specifically granted in the combination of (i) the license details provided by you and accepted in the course of this licensing transaction, (ii) these terms and conditions and (iii) CCC's Billing and Payment terms and conditions.

8. License Contingent Upon Payment: While you may exercise the rights licensed immediately upon issuance of the license at the end of the licensing process for the transaction, provided that you have disclosed complete and accurate details of your proposed use, no license is finally effective unless and until full payment is received from you (either by publisher or by CCC) as provided in CCC's Billing and Payment terms and conditions. If full payment is not received on a timely basis, then any license preliminarily granted shall be deemed automatically revoked and shall be void as if never granted. Further, in the event that you breach any of these terms and conditions or any of CCC's Billing and Payment terms and conditions, the license is automatically revoked and shall be void as if never granted. Use of materials as described in a revoked license, as well as any use of the materials beyond the scope of an unrevoked license, may constitute copyright infringement and publisher reserves the right to take any and all action to protect its copyright in the materials.

9. Warranties: Publisher makes no representations or warranties with respect to the licensed material.

10. Indemnity: You hereby indemnify and agree to hold harmless publisher and CCC, and their respective officers, directors, employees and agents, from and against any and all claims arising out of your use of the licensed material other than as specifically authorized pursuant to this license.

11. No Transfer of License: This license is personal to you and may not be sublicensed, assigned, or transferred by you to any other person without publisher's written permission.

12. No Amendment Except in Writing: This license may not be amended except in a writing signed by both parties

(or, in the case of publisher, by CCC on publisher's behalf).

13. Objection to Contrary Terms: Publisher hereby objects to any terms contained in any purchase order, acknowledgment, check endorsement or other writing prepared by you, which terms are inconsistent with these terms and conditions or CCC's Billing and Payment terms and conditions. These terms and conditions, together with CCC's Billing and Payment terms and conditions (which are incorporated herein), comprise the entire agreement between you and publisher (and CCC) concerning this licensing transaction. In the event of any conflict between your obligations established by these terms and conditions and those established by CCC's Billing and Payment terms and conditions, these terms and conditions shall control.

14. Revocation: Elsevier or Copyright Clearance Center may deny the permissions described in this License at their sole discretion, for any reason or no reason, with a full refund payable to you. Notice of such denial will be made using the contact information provided by you. Failure to receive such notice will not alter or invalidate the denial. In no event will Elsevier or Copyright Clearance Center be responsible or liable for any costs, expenses or damage incurred by you as a result of a denial of your permission request, other than a refund of the amount(s) paid by you to Elsevier and/or Copyright Clearance Center for denied permissions.

LIMITED LICENSE

The following terms and conditions apply only to specific license types:

15. **Translation**: This permission is granted for non-exclusive world **English** rights only unless your license was granted for translation rights. If you licensed translation rights you may only translate this content into the languages you requested. A professional translator must perform all translations and reproduce the content word for word preserving the integrity of the article. If this license is to re-use 1 or 2 figures then permission is granted for non-exclusive world rights in all languages.

16. **Website**: The following terms and conditions apply to electronic reserve and author websites:
Electronic reserve: If licensed material is to be posted to website, the web site is to be password-protected and made available only to bona fide students registered on a relevant course if:
This license was made in connection with a course,
This permission is granted for 1 year only. You may obtain a license for future website posting,
All content posted to the web site must maintain the copyright information line on the bottom of each image,
A hyper-text must be included to the Homepage of the journal from which you are licensing at http://www.sciencedirect.com/science/journal/xxxxx or the Elsevier homepage for books at http://www.elsevier.com , and
Central Storage: This license does not include permission for a scanned version of the material to be stored in a central repository such as that provided by Heron/XanEdu.

17. **Author website** for journals with the following additional clauses:

All content posted to the web site must maintain the copyright information line on the bottom of each image, and he permission granted is limited to the personal version of your paper. You are not allowed to download and post the published electronic version of your article (whether PDF or HTML, proof or final version), nor may you scan the printed edition to create an electronic version,
A hyper-text must be included to the Homepage of the journal from which you are licensing at http://www.sciencedirect.com/science/journal/xxxxx , As part of our normal production process, you will receive an e-mail notice when your article appears on Elsevier's online service ScienceDirect (www.sciencedirect.com). That e-mail will include the article's Digital Object Identifier (DOI). This number provides the electronic link to the published article and should be included in the posting of your personal version. We ask that you wait until you receive this e-mail and have the DOI to do any posting.
Central Storage: This license does not include permission for a scanned version of the material to be stored in a central repository such as that provided by Heron/XanEdu.

18. **Author website** for books with the following additional clauses:

Authors are permitted to place a brief summary of their work online only.
A hyper-text must be included to the Elsevier homepage at http://www.elsevier.com

All content posted to the web site must maintain the copyright information line on the bottom of each image
You are not allowed to download and post the published electronic version of your chapter, nor may you scan the printed edition to create an electronic version.
Central Storage: This license does not include permission for a scanned version of the material to be stored in a central repository such as that provided by Heron/XanEdu.

19. **Website** (regular and for author): A hyper-text must be included to the Homepage of the journal from which you are licensing at http://www.sciencedirect.com/science/journal/xxxxx. or for books to the Elsevier homepage at http://www.elsevier.com

20. **Thesis/Dissertation**: If your license is for use in a thesis/dissertation your thesis may be submitted to your institution in either print or electronic form. Should your thesis be published commercially, please reapply for permission. These requirements include permission for the Library and Archives of Canada to supply single copies, on demand, of the complete thesis and include permission for UMI to supply single copies, on demand, of the complete thesis. Should your thesis be published commercially, please reapply for permission.

21. **Other Conditions**:

v1.6

If you would like to pay for this license now, please remit this license along with your payment made payable to "COPYRIGHT CLEARANCE CENTER" otherwise you will be invoiced within 48 hours of the license date. Payment should be in the form of a check or money order referencing your account number and this invoice number RLNK.
Once you receive your invoice for this order, you may pay your invoice by credit card. Please follow instructions provided at that time.

Make	**Payment**	**To:**
Copyright	**Clearance**	**Center**
Dept		**001**
P.O.	**Box**	**843006**
Boston,	**MA**	**02284-3006**

For suggestions or comments regarding this order, contact RightsLink Customer Support: customercare@copyright.com or +1-877-622-5543 (toll free in the US) or +1-978-646-2777.

Gratis licenses (referencing $0 in the Total field) are free. Please retain this printable license for your reference. No payment is required.

This is a License Agreement between Toran Sanli ("You") and Wolters Kluwer Health ("Wolters Kluwer Health") provided by Copyright Clearance Center ("CCC"). The license consists of your order details, the terms and conditions provided by Wolters Kluwer Health, and the payment terms and conditions.

All payments must be made in full to CCC. For payment instructions, please see information listed at the bottom of this form.

License Number	2761430660841
License date	Oct 03, 2011
Licensed content publisher	Wolters Kluwer Health
Licensed content publication	Journal of Thoracic Oncology
Licensed content title	**Lovastatin Sensitizes Lung Cancer Cells to Ionizing Radiation: Modulation of Molecular Pathways of Radioresistance and Tumor Suppression**
Licensed content author	Toran Sanli, Caiqiong Liu, Ayesha Rashid, et al
Licensed content date	Jan 1, 2011
Volume Number	6
Issue Number	3
Type of Use	Dissertation/Thesis
Requestor type	Individual
Title of your thesis / dissertation	THE ROLE OF AMP-ACTIVATED PROTIEN KINASE (AMPK) IN MEDIATING RADIATION REPONSES IN CANCER CELLS
Expected completion date	Jun 2012
Estimated size(pages)	250
Billing Type	Invoice
Billing address	699 Concession St. Hamilton, Ontario L8V 5C2 Canada
Customer reference info	
Total	0.00 USD
Terms and Conditions	

Terms and Conditions

1. A credit line will be prominently placed and include: for books - the author(s), title of book, editor, copyright holder, year of publication; For journals - the author(s), title of article, title of journal, volume number, issue number and inclusive pages.
2. The requestor warrants that the material shall not be used in any manner which may be considered derogatory to the title, content, or authors of the material, or to Wolters Kluwer.
3. Permission is granted for one time use only as specified in your correspondence. Rights herein do not apply to future reproductions, editions, revisions, or other derivative works. Once term has expired, permission to renew must be made in writing.
4. Permission granted is non-exclusive, and is valid throughout the world in the English language and the

languages specified in your original request.

5. Wolters Kluwer cannot supply the requestor with the original artwork or a "clean copy."
6. The requestor agrees to secure written permission from the author (for book material only).
7. Permission is valid if the borrowed material is original to a Wolters Kluwer imprint (Adis, Lippincott-Raven Publishers, Williams & Wilkins, Lea & Febiger, Harwal, Igaku-Shoin, Rapid Science, Little Brown & Company, Harper & Row Medical, American Journal of Nursing Co, and Urban & Schwarzenberg - English Language).
8. If you opt not to use the material requested above, please notify Rightslink within 90 days of the original invoice date.
9. Please note that articles in the ahead-of-print stage of publication can be cited and the content may be re-used by including the date of access and the unique DOI number. Any final changes in manuscripts will be made at the time of print publication and will be reflected in the final electronic version of the issue. Disclaimer: Articles appearing in the Published Ahead-of-Print section have been peer-reviewed and accepted for publication in the relevant journal and posted online before print publication. Articles appearing as publish ahead-of-print may contain statements, opinions, and information that have errors in facts, figures, or interpretation. Accordingly, Lippincott Williams & Wilkins, the editors and authors and their respective employees are not responsible or liable for the use of any such inaccurate or misleading data, opinion or information contained in the articles in this section.
10. Other Terms and Conditions:

v1.1

If you would like to pay for this license now, please remit this license along with your payment made payable to "COPYRIGHT CLEARANCE CENTER" otherwise you will be invoiced within 48 hours of the license date. Payment should be in the form of a check or money order referencing your account number and this invoice number RLNK500638742.
Once you receive your invoice for this order, you may pay your invoice by credit card. Please follow instructions provided at that time.

Make Payment To:
Copyright Clearance Center
Dept 001
P.O. Box 843006
Boston, MA 02284-3006

For suggestions or comments regarding this order, contact RightsLink Customer Support: customercare@copyright.com or +1-877-622-5543 (toll free in the US) or +1-978-646-2777.

Gratis licenses (referencing $0 in the Total field) are free. Please retain this printable license for your reference. No payment is required.